SRPSKO HEMIJSKO DRUŠTVO (BEOGRAD)

BULLETIN OF THE CHEMICAL SOCIETY Belgrade

(Glasnik Hemijskog društva — Beograd)

Vol. 35, No. 1, 1970

Published by
SRPSKO HEMIJSKO DRUŠTVO (BEOGRAD)
1970

Translated and published for U.S. Department of Commerce and
the National Science Foundation, Washington, D.C., by
The NOLIT Publishing House, Terazije 27/II, Belgrade, Yugoslavia
1970

Edited by
PAUL PIGNON

Printed in "Prosveta", Belgrade

15th MEETING OF THE CHEMISTS OF THE SOCIALIST REPUBLIC OF SERBIA AND SYMPOSIUM ON CHEMISTRY AND FOOD TECHNOLOGY

and

ANNUAL CONVENTION OF THE SERBIAN CHEMICAL SOCIETY

January 21—23, 1970

HELD AT THE UNIVERSITY SCHOOL OF AGRICULTURE,
UNIVERSITY OF NOVI SAD

CONTENTS

I. FOOD CHEMISTRY AND TECHNOLOGY

II. GENERAL AND ANALYTICAL CHEMISTRY

III. PHYSICAL CHEMISTRY

IV. ORGANIC CHEMISTRY

Page

Page

V. METALLURGY

VI. CHEMICAL ENGINEERING

ABSTRACTS OF PAPERS

I. FOOD CHEMISTRY AND TECHNOLOGY

METHODS FOR THE REMOVAL OF WAXES FROM SUNFLOWER OIL

B. OŠTRIĆ-MATIJAŠEVIĆ, **J. TURKULOV** and I. MEZEI

School of Technology, Novi Sad

Though present in raw sunflower oil in very small quantities (0.01 to 0.1%) waxes cause difficulties in refining and very often diminish the quality of the final oil. The methods used nowdays in practice for removal of waxes from oils and the results obtained by applying them to raw sunflower oil are reviewed. Although the value of the conventional method is not diminished — removal to waxes by winterisation (cooling to 4—8°C) and subsequent filtration) — we point out the advantages of a newer method in which the waxes are separated from the oil during the prerefining. This method uses a "low" temperature ($<30°C$) and substances which accelerate sedimentation of waxes utilizing their property that at these temperatures they loose their lipophilic characteristics and can be very easily removed from the oil in the presence of an emulsifier. Additives in prerefining were phosphates and detergents and some others.

The results show that it is possible, under given conditions, to remove most waxes contained in oil in the course of prerefining. As the prerefining is normally used in practice in order to remove phosphatides and other undesirable components, simultaneous removal of waxes has great advantages.

Removal of waxes was checked by determining oil clarity by means of the Cold Test.

MICROELECTROPHORETIC STUDY OF CASEIN

M. CARIĆ and J. ĐORĐEVIĆ

School of Technology, Novi Sad and Faculty of Agriculture, Beograd

The composition of casein isolated from sheep's milk during the lactation period was analyzed by boundary electrophoresis after Tiselius, in veronal buffer at pH 8.6 and at an ionic strength $\mu = 0.1$ after dialysis of the casein solution against the same buffer. α_s-, $\varkappa$-, β — and γ — casein were registered quantitively (in descending order of mobility in the electrical field). Their mutual ratios and ratio to total casein were calculated.

Total protein and casein content of the milk were also determined and the variation of casein's participation in the total proteins during the lactation period was studied.

The results are statistically analyzed.

STUDY ON SEPARATION DYNAMICS OF STRAWBERRY JUICE AROMA

D. ŠULC and R. NIKOLAJEVIĆ

School of Technology, Novi Sad

The separation of strawberry juice aroma by concentrating of juice in a special apparatus under high vacuum and low temperature was studied. Practically complete dearomatization was obtained in seven runs by which a coefficient of juice evaporation of 84.5% was achieved and the concentrated juice contained 51.7% solids.

The aromatic condensates obtained from each run were analyzed by gas chromatography (Beckman GC—2A apparatus). Nineteen volatile components were resolved, of which 14 were identified. From planimetry of the chromatograms, graphs were drawn showing the dynamics of aroma separation (volatile components) relative to the rate of juice evaporation. The plots obtained illustrate that the rate of aroma separation is highest during the early stage of juice concentration, i. e. after 10 to 35% evaporation, falling off gradually until the end of condensation when it again increases slightly. The presence of poorly soluble and poorly volatile compounds (geraniol, fatty oils, terpenelike compounds) certainly tend heavily to delay the separation of some volatile components, and it is therefore necessary to apply a very high evaporation (85%) to get complete dearomatization.

AROMATICITY STUDIES OF SOME PAPRIKA VARIETIES

D. ĆIRIĆ and D. ŠULC

School of Technology, Novi Sad

The aromaticity of some paprika varieties that are widely cultivated and processed into various food articles was studied. The varieties were Rotunda Green, Californian Wonder, Pazardžijska Kapija, Kurtovska Kapija and Horgoška Slatka I. The paprikas were ground and depectinized and samples of the pulp were distilled in a special apparatus under high vacuum and low temperature. The aromatic condensates obtained were examined by gas chromatography: 42 to 57 components were resolved in different samples, of which 12 were identified. The total surface areas of the chromatograms obtained were calculated by triangulation and taken as a measure of aroma intensity.

The highest aromaticity was found in the variety Rotunda Green. Taking its value as 100% the other varieties had the following aroma intensities: Californian Wonder 45.17%, Horgoška Slatka 44.17%, Pazardžijska Kapija 14.45 and Kurtovska Kapija only 5.19%.

The result indicate that aromaticity is variety-specific under the same conditions.

AN INVESTIGATION OF THE COMPOSITION AND CHEMICAL CHARACTERISTICS OF WALNUT OIL

M. D. DŽAMIĆ

School of Agriculture, Beograd

The results of many-year investigations of characteristics of the oil of a great many walnut varieties (Juglands regia, L) are presented. By application of gas chromatography individual free fatty acids and the acid composition of triglycerides was determined. On basis of the results the varieties examined are classified according to their technological values.

PROTEIN PREPARATIONS AS EMULSIFIERS IN MEAT INDUSTRY

P. MITIĆ and D. IBROČIĆ

Yugoslav Food Industry Institute, Novi Sad

The protein preparations used as fat and tallow emulsifiers in meat products are important additives in the production of sausages, canned meat and other meat products. Due to the great number of preparations on the market and also to different and often contradictory reports on their application, the necessity arises for quality determination and testing. The basic methods for quality examination of these preparations are presented. As their use is regulated by law the basic legal requirements are also given.

APPLICATION OF POLYPHOSPHATES IN THE MEAT INDUSTRY

D. IBROČIĆ, Đ. DRLJEVIĆ und P. MITIĆ

Yugoslav Food Industry Institute, Novi Sad

The use of phosphates in the meat industry is relatively new. These are available on the market in the form of various polyphosphate preparations and are used to preserve juices in meat canning. They are also used in processing of blood, production of meat paste, preparation of emulsions, etc. In this paper the fundamental characteristics of polyphosphates are reviewed from the aspects of hygiene and technology of meat, some analytical methods are described and the main reasons for studying and checking the quality of polyphosphate preparations are put forward.

ECONOMIC PROBLEMS OF FUNCTIONAL INTERNAL TRANSPORT IN THE MEAT INDUSTRY SOLVED BY INTRODUCTION OF MODERN EQUIPMENT

R. KARAKAŠ und B. GAĆEŠA

Yugoslav Food Industry Institute, Novi Sad

Internal transport in the Yugoslav meat industry is a vital problem whose solution is becoming more and more pressing. Manual handling is still predominant in our slaughterhouses and has to be eliminated, not only because of the principles of productivity, economy and profitability but also for hygienic reasons. A comparative analysis of the system and mode of internal transport in Yugoslav and some other European slaughterhouse is made.

DETERMINATION OF SUGAR-BEET SAPONIN BY MEANS OF $FeCl_3$ REAGENT

S. VOLF and **K. ŠEREŠ**

School of Technology, Novi Sad

The Zak reaction between triterpene and $FeCl_3$ reagent was investigated for analytic determination of beet saponin. Contrary to the findings of former investigators, a significant influence of saccharide on the extinction of the colored complex was observed. Glucose and sapogenin of sugar-beet in equimolecular proportions give approx. 10% greater extinction than the colored complex from chromatographed pure sapogenin. By an analysis of the influence of saccharide on the extinction of mixtures of saccharide and pure sapogenin, a correction factor for spectrophotometric determination of saponin using $FeCl_3$ reagent has been determined.

PROTEINS OF SUGAR-BEET I. PRESERVATION OF CELL JUICE

K. ŠEREŠ

School of Technology, Novi Sad

Because of the different physiological roles of proteins and pectins, it is not probable that in plant juices these ingredients are complexed as found by former investigators in isolating them. To prove that the creation of protein-pectin complex is only a result of the isolation procedure required the preparation of permanently stable cell juice. The various available methods of preserving sugar-beet juice for the examination of protein structure and chemical composition did not ensure sufficient long-term stability. Therefore we prepared a concentrate of pressed beet juice by evaporation in a moderate vacuum. The concentrate was then submitted to molecular distillation. By this procedure a stable dry powder was obtained, which on resolution gave practically unaltered cell juice for systematic examination.

OPTIMUM CONDITIONS OF THERMAL ACTIVATION OF BAUXITES USED AS COLOR ADSORBENTS IN THE SUGAR INDUSTRY

I. J. VAVRA and **LJ. M. PETROV**

School of Technology, Novi Sad

The conditions of thermal activation of five different kinds of Yugoslav bauxite were investigated with a view to their application as adsorbents of colored substances in the sugar industry. Granulated samples were heated in the temperature interval from 200—900°C, with different bauxite bed thicknesses and heating time. Activity was determined by adsorption of colored substances from model solutions of molasses and sugar.

All the samples showed an adsorption optimum in the temperature interval 450—500°C. Up to this temperature a correlation was found between adsorption capacity and ignition loss.

Unlike La Land we found that red bauxites possess greater adsorptivity than white.

THE APPLICATION OF GEL FILTRATION IN THE DETERMINATION OF DISTRIBUTION OF MOLECULAR WEIGHTS OF PECTINS FROM SUGAR-BEET

S. I. PETROV

School of Technology, Novi Sad

Pectin from sugar-beet, isolated and refined, with 65% of polygalacturonic acid and a mean molecular weight of 60,000, determined by Deuel and Henglein's method, was separated in aqueous solution on sephadex G—25, G—50 and G—75.

In the fractions polygalacturonic acid, galactan, and araban were detected after Schneider *et al.* by measuring extinction at 215,275 and 340 nm. Galacturonic acid was determined by McComb and Mc Cready's method and the conductivity was measured.

The results show that gel filtration can be used to determine the distribution of molecular weights in pectin.

PRODUCTION OF UNIFORM CRYSTALS OF SUCROSE BY PLANNED GRAINING

J. VIKTOROVIĆ, LJ. TEREK and R. MILETIĆ

Yugoslav Food Industry Institute, Novi Sad

Yugoslav beet sugar factories recently introduced a new technique of massecuite seeding using a suspensions of finelyground granulated sugar in isopropanol. Studying this technique in some sugar plants and comparing the results with the graining method using castor sugar, the following was concluded:

1. The texture of the white table sugar produced by the new procedure is more uniform;
2. The crystals of sucrose contain less dust;
3. The percentage of adhering crystals is considerably smaller;

The last massecuites show a more uniform structure and contain less microcrystals.

STUDY OF THE CONDITIONS FOR FORMATION OF ANTICORROSIVE INCRUSTATIONS IN THE EVAPORATORS OF BEET SUGAR PLANTS

J. VIKTOROVIĆ, LJ. TEREK, V. KARADŽIĆ and S. OBRADOVIĆ
Yugoslav Food Industry Institute, Novi Sad

In the evaporators of beet sugar plants the heated tubes with free metal surfaces corrode. The conditions under which they are protected by an anticorrosive incrustation were studied and the following conclusions drawn:

1. The quantity of Ca-salts in the sugar juices depends on both the anion composition and pH of the juices being less in the pH interval 9.0 to 9.5. than in the interval pH 8.0 to 8.5.
2. The aggressiveness of juice in the evaporators towards incrusted $CaCO_3$ depends on the thermal stability of the juice i. e., on the decrease of pH due to formation of organic compounds yielding soluble calcium salts.
3. The aggressiveness of the juice is lower at higher pH values where its buffering power is more evident.

CAUSES OF CORROSION OF THE HEATING TUBES IN THE EVAPORATORS OF BEET SUGAR PLANTS

J. VIKTOROVIĆ, LJ. TEREK, V. KARADŽIĆ and S. OBRADOVIĆ

Yugoslav Food Industry Institute, Novi Sad

From a study of the incidence of corrosion in the heating tubes in evaporator unite under both laboratory and plant conditions, the following conclusions were drawn:

1. Corrosion occurs in the tubes without incrustation where the free metal surface comes into direct contact with the juice.
2. Oxygen in the juice is not the only cause of spot corrosion as confirmed by the fact that the iron content of the solution many times exceeds the stoichiometric ratio relative to the dissolved oxygen.
3. The free metal surface of the heating tubes is divided into anode and cathode zones because of different energetic conditions.
4. In the sugar juices copper coatings are formed over the anode fields, favoring corrosion of the hydrogen cathode.
5. The potential of the iron electrode under the conditions existing in evaporator batteries is very high about 700 mV, and is not essentially affected by various juice ingredients.
6. The rate of corrosion in the alkaline medium depends upon pH and increases with decreasing OH-ion concentration.

ESTIMATION OF SUGAR QUALITY BY THE SCORE SYSTEM

J. VIKTOROVIĆ, LJ. TEREK and R. MILETIĆ

Yugoslav Food Industry Institute, Novi Sad

A method has been developed for sugar quality evaluation based on the analysis of 117 samples from the 1968/69 production from which the statistical distribution of various indices was used to the following metrics:

1. each 0.5 degrees of the given sugar type is allocated 1 point,
2. each 0.0015% conductometrically determined and is allocated 1 point,
3. each extinction measured on a Lange colorimeter up to 0.0066 is allocated 1 point

By the proposed method refined sugar can have at most 26.9 points and white table sugar at most 53.7 points. If the score exceeds the maximum limit the grade is altered and refined becomes white table sugar, and the latter into raw sugar which cannot be used as a food article.

FRACTIONATION OF SOLUBLE PROTEINS FROM WHEAT LEAVES

S. LAJŠIĆ, B. GRUJIĆ-INJAC, Đ. JELENIĆ and R. SIMIĆ

School of Sciences, Beograd and Institute for Application of Nuclear Energy in Agriculture, Veterinary Medicine and Forestry, Beograd

Soluble proteins from wheat leaves were extracted by TRIS—HCl buffer (pH—8.3) and fractionated on sephadex G—200 column. The amino acid composition of the fractions was determined.

CHEMICAL ANALYSIS OF ANIMAL FODDER. V. FRACTIONATION OF SOLUBLE PROTEINS IN ALFALFA

B. GRUJIĆ-INJAC and D. KOLARSKI

School of Sciences, Beograd and Faculty of Agriculture, Beograd

Soluble proteins of the domestic alfalfa variety K_1 were isolated with water, 10% NaCl and 0.2% NaOH. After dialysis, proteins were fractionated on G—200 Sephadex columns. The fractions obtained were analysed by a modification of the Lowrey method. The extinction was read at 750 mμ and in the ultraviolet at 260 mμ and 280 mμ.

INFLUENCE OF PECTOLYTIC PREPARATIONS ON CHERRY PULP AROMA

D. ŠULC and R. NIKOLAJEVIĆ

School of Technology, Novi Sad

The effect of pectolytic preparations on cherry pulp was studied to determine whether these preparations lead to the formation of volatile components and the increase aroma of depectinized pulp. Samples of original cherry pulp and samples previously treated with 0.3% of "Pectinol K" 0.3% of "Rohament P" (Röhm and Haas, Darmstadt, West Germany) at 45°C for 2 hours, were distilled in a special apparatus under high vacuum and low temperatures. The aromatic condensates obtained were examined by gas chromatography (Beckman GC—2A): 19 aromatic components were resolved, of which 11 were identified. The chromatograms were planimetered and the total area was calculated, as a measure of the aroma intensity of the sample.

The sample treated with Rohament P had a 1.2 times higher aroma intensity than the original cherry pulp, while that treated with Pectinol K a 1.6 times higher intensity. The samples treated with the pectolytic preparations contained more fruit esters and carbonyl compounds and the pulp treated with Pectinol K exhibited a considerable increase of methanol due to de-esterification of pectic substances.

INVESTIGATION OF LIPOID SUBSTANCES AND PROTEINS FROM YELLOW CORN GLUTENE

B. GRUJIĆ-INJAC, **M. JOVANOVIĆ**, Đ. STEFANOVIĆ and S. LAJŠIĆ

School of Sciences, Beograd

The lipoid substances obtained from yellow corn glutene by extraction with petroleum ether, were separated and identified. Acids, phytosterols and carotenoids were determined. We also investigated proteins obtained from the same glutene.

THIN-BOILING STARCHES

O. JANČIĆ, O. RIŠKOVIĆ, A. ĐORĐEVIĆ and I. VORGIĆ

Institute of Chemistry, Technology and Metallurgy, Beograd

The basic characteristics of thin-boiling starches produced at the Institute and a great number of starch modifications are reviewed.

PARTIALLY HYDROLIZED STARCHES

O. JANČIĆ, A. ĐORĐEVIĆ and I. VORGIĆ

Institute of Chemistry, Technology and Metallurgy, Beograd

The best depolymerization was achieved by the action of a mineral acid and its salt. Under certain precisely determined conditions neither excessive swelling of the starch granule nor the formation of gel occurs. The product is specified by viscosity and ease of paste formation and is suitable for use in the textile and paper industries.

DRY MODIFICATION OF STARCHES

O JANČIĆ, **I. VORGIĆ** and A. ĐORĐEVIĆ

Institute of Chemistry, Technology and Metallurgy, Beograd

By dry treatment of commercial starch in a model reactor, depolymerised products of different viscosity without reducing materials were obtained. This method where the starch granule is only swelled in the semi-dry state, but not suspended, represents an ecconomical and simple procedure for modifying native starch applicable in the textile industry.

THE INFLUENCE OF ADDING HYDROGEN PEROXIDE TO STEEPING WATER ON BARLEY MALTING

V. KRAJOVAN, **S. GAĆEŠA**, D. PEJIN and S. CINCAR

School of Technology, Novi Sad

By adding H_2O_2 to steeping water in quantities of 125—1000 mg per kg barley, malt solution was to some degree accelerated, while malting losses were only insignificantly greater. However, adding H_2O_2 greatly reduced anthocyanogens in the kiln malt compared with control malt, and the other criteria of malt quality were practically the same. Anthocyanogen level in the malt was especially decreased if H_2O_2 (500 mg/kg of barley) was added in several portions at every water change, or only in the first water: the anthocyanogen level of these malts was only 26 or 28% of that in the control malt. Adding the same quantities of H_2O_2 at once in the later phases of steeping gave poorer results and the malting losses were greater. Considering all these findings, it may be expected that by using H_2O_2 during steeping, malting time can be reduced, and malt of superior quality suitable for the production of beers with greater stability, can be produced.

EFFECT OF TEMPERATURE ON FRACTIONATION OF "CRUDE FIBER" BY VAN SOEST'S METHOD

D. KOLARSKI and D. ZEREMSKI

School of Agriculture, Beograd

In comparative investigations of corn silage, sugar beet pulp silage, dry sugar beet and alfalfa hay the presence of soluble and insoluble fractions of "crude fiber" was determined. Neutral and acid detergents were used after Van Soest and the influence of drying temperatures of the feed samples on the seperation of various fractions was studied.

PREPARATION OF THIN-BOILING STARCHES BY HYPOCHLORITE OXIDATION METHOD

O. JANČIĆ and **A. ĐORĐEVIĆ**

Institute of Chemistry, Technology and Metallurgy, Beograd

Calcium hypochlorite acting on aqueous starch suspension at 30° yields thin-boiling starch. Basic properties of this product, viscosity, solubility and percentage of carboxyl were determined. Compared with the parent, the viscosity of the hot paste is reduced, transparency and solubility are increased and gel-strength appreciablly reduced. This product is especially suitable for the paper industry.

PREPARATION AND PROPERTIES OF MONOSTARCH PHOSPHATES

O. RIŠKOVIĆ

Institute of Chemistry, Technology and Metallurgy, Beograd

Action of monosodium phosphate solution on commercial starch at room temperature yields the monostarch phosphate. The basic properties of the product, viscosity, solubility, percentage of phosphorus, degree of depolymerization and swelling were investigated. This is a thin-boiling starch of high quality for use in the textile, paper and food industries.

OPTIMIZATION OF "DRY MODIFICATION" PROCESS OF NATIVE STARCH AND MODELING OF REACTOR FOR THIS PROCESS

B. PEROVIĆ, O. JANČIĆ, **D. LEKOVIĆ** and I. VORGIĆ

Institute of Chemistry, Technology and Metallurgy, Beograd

As part of a program of research on starch derivates and modified starches the Institute has developed a new "dry modification" process for native starches. The optimization of the basic chemical reaction in this process is described.

The second part of the paper presents a qualitatively new approach to the design of a chemical reactor for this reaction. The principle of this approach is modeling on the basis of optimization and semiindustrial trials.

THE SORPTION PROPERTIES OF STARCHES DEPENDING ON THEIR ORIGIN AND PRETREATMENT

P. S. PUTANOV, D. SMILJANIĆ, M. JURANJI and M. BALAĆ

School of Technology, Novi Sad and Institute of Chemistry, Technology and Metallurgy, Beograd

The sorption properties of unmodified corn starch and its two modifications, and of wheat, rice and potato starches were investigated by McBain's method with benzene, diethylether and methanol as sorbates.

The sorption of benzene and diethylether appeared to be negligible. The sorbed quantity of methanol was not appreciably influenced by the origin of the starch, except that on potato starch it was somewhat less.

The quantity of methanol sorbed decreased linearty with increasing temperature on all starches. The sorption properties of these starches, measured at room temperature, were not affected by the heat pretreatment.

Differences in the sorption of methanol on unmodified starch and its modifications were most apparent at room temperature, decreasing with increasing temperature.

CONCENTRATION RATIOS OF Fe, Cu, Mn AND Mo AND THEIR INFLUENCE ON SOME REDOX-SYSTEMS IN APPLE

M. D. DŽAMIĆ and **R. DŽAMIĆ**

School of Agriculture, Beograd

Mn, Cu and Mo were determined in a large number of apple varieties during technological ripeness. Their concentration rations were determined and the possibility of an interrelationship of their catalytic functions in apple metabolism is considered. The relationship between these elements and some redox-systems in the fruit which are of importance for apple technology was also examined.

SEPARATION OF WATER-SOLUBLE VITAMINS ON CELLULOSE LAYERS

S. E. PETROVIĆ and B. E. BELIA

Department of Chemistry, University of Novi Sad

The separation of water-soluble vitamins on a thin layer of cellulose was investigated. The best of the solvent systems tested was n-butanol: $CH_3COOH : H_2O$ (70 : 7 : 23). Eight water-soluble vitamins which separated very well in this were investigated. They were identified under UV light at 254 m μ using 0.5% solution of ninhydrine in 96% ethanol.

THE INFLUENCE OF COMBINED X-RAY AND PLANT HORMONE OF SOYBEAN YIELD AND THE QUANTITY AND QUALITY OF OIL IN GENERATIONS R_1, R_2, R_3°, AND R_4

E. CERKOVNIKOV, **M. KIRIGIN** and A. STEINER

School of Medicine, University of Zagreb, Rijeka Section, Institute of Chemistry and Biochemistry, and Institute of Physics

Szürkebàrat soybean seeds were treated before planting with 2 kr X-rays from a 100 kV_p X-ray tube with a 0.16 mm Cu + 0.6 mm Al filter at a dose rate of 1.5 kr/h. During the growth period at definite time intervals the plants were sprayed with phenylmercapto acetic acid ($C_6H_5—S—CH_2COOH$) in concentrations of 0.1 μg and 0.01 μg per seed. The tests were carried out from 1963 to 1968, seeds from the previous harvest being used the following year. The first year tests were denoted R_1 in second year R_2 and the third R_3. In the fourth year, to see how the newly acquired properties were transmitted, the plants were sprayed during the growth period only with water (R_3°) and in the fifth year too (R_4).

The quantity and weight of beans, pods and stems was determined as the growth index:

$$J = \frac{p}{a} 100\%$$

p = the number or weight of given part of treated plant

a = the same for nontreated plant

Harvested beans were crushed and a mean sample was analysed by standard chemical methods.

The results indicate that some hormone concentrations in some cases not only inhibit X-ray action but even increase the yield. This was especially seen in the R_3 generation.

Treatment of 2 kr X-rays followed by plant hormone during the growth period increased the calorific value of crude oil from generation to generation.

The results are shown in tables and diagrams.

THE INFLUENCE OF SOME FACTORS ON THE QUALITY OF PROTEIN AND AMINO ACID COMPOSITION IN TECHNOLOGICALLY IMPORTANT APPLE VARIETIES

M. D. DŽAMIĆ and D. VELIČKOVIĆ

School of Agriculture, Beograd

Extensive investigations have been carried out on the amino acid composition of apples in order to study the influence of some factors (variety, ecological conditions, etc.) on their ratios. The ratio of amino acids to the protein fraction and their ranges of variation were also examined. Differences between varieties regarding their protein quality were determined, their being of essential interest in their technological processing. Special reference is made to the biochemical aspects and function of these amino acids which primarily influence the fermentative activity of the fruit tissue and the metabolitic balance.

CONCENTRATION RATIO OF SOME ORGANIC ACIDS IN APPLES AT TECHNOLOGICAL RIPENESS

R. DŽAMIĆ and **M. D. DŽAMIĆ**

School of Agriculture, Beograd

The quantitative metabolism of malic, quinic, citric, citro-malic and other organic acids was investigated in a large number of apple varieties from different regions of Serbia. The dependence of their concentrations on some factors of technological importance was investigated. Their concentration ratios were examined and the metabolitic interrelationship of concentration changes with regard to the positions of the acids in the oxidation reduction processes in the fruit is discussed theoretically.

II. GENERAL AND ANALYTICAL CHEMISTRY

BINDING POWER OF HYDROLIZED ETHYL SILICATE AS A FUNCTION OF PROPERTIES OF THE SILICA FILLER

S. STEVIĆ-TRIVUNAC, M. DRAGOJEVIĆ and S. RADOSAVLJEVIĆ

School of Technology and Metallurgy, Beograd and Institute of Chemistry, Technology and Metallurgy, Beograd

It is found that the mechanical strength of ceramic investments, used in casting, which are made with hydrolized ethyl silicate binder and silica filler, is affected not only by grain size but also by the mineralogical characteristics of the silica. The influence of these factors on the binding power of mixtures of hydrolized ethyl silicate and characteristic forms of silica was studied. It was found that the form of the silica considerably affects the properties of the fired ceramic investments.

THE INFLUENCE OF GELATINE ON A MIXTURE OF GYPSUM AND 5% PORTLAND CEMENT

S. STOJADINOVIĆ

School of Civil Engineering, Sarajevo

Adding gelatine to a mixture of gypsum + 5% portland cement profonds the time of hydratation, which is very important in civil engineering. The reason is that the ion of calcium causes a hydrate to be formed. Calcium ion is produced by:

— the dissolution of solid gypsum
— the hydrolysis of solid clinker of the cement

Since the latter process is more rapid, the clinker calcium ions and the gelatine attract water first which produces the same effect as an insufficient quantity of water in the hydratation of gypsum $CaSO_4$, i.e. the rate of gypsum hydratation is slowed down.

INFLUENCE OF VARIOUS FLUXES ON THE SINTERING OF MAGNESIUM SILICATE WITH A VARIABLE $MgO:SiO_2$ RATIO

R. NIKOLIĆ

Ceramic Insulators, Aranđelovac

Previous investigations concerning the improvement of sintering synthetic magnesium silicate for the production of steatite have been concerned with the influence of temperature and mineralizers on magnesium metasilicate. This paper reports a study of the influence of some fluxes on the sintering of magnesium silicate in a wide range of $MgO:SiO_2$ ratios. A number of products of practical interest were obtained. Free MgO content, which has a strong influence on the plastification capacity, is practically constant at the given firing temperature within of protoenstatite and forsterite region. Sintering is the most intensive in a region close to forsterite.

MICROHARDNESS OF SILICON CONTAINING PYROLITIC CARBON

A. TUKOVIĆ and S. MARINKOVIĆ

Boris Kidrič Institute of Nuclear Sciences, Vinča, Beograd

The Vickers microhardness of silicon-containing pyrolytic carbon cross-sections was measured. The carbon was prepared by chemical vapor codeposition from a $CH_4 — SiCl_4$ gas mixture at 1150—1600°C; its Si content varied over the range 0—13 wt %. Pure pyrocarbon, having a microstructure characterized by narrow growth cones, has a low microhardness (80 kg/mm²). A small Si addition (up to 0.2 %) hardly affects the microstructure and the hardness values (100—150 kg/mm²). Samples with a higher Si content (1—13%) are composed of large cones, usually growing from lenticular inclusions, and of the narrow cones typical of low-silicon pyrocarbon. Microhardness of the narrow cones corresponds to the low-silicon pyrocarbon, but the microhardness of the lenses corresponds to that of pure SiC and drops abruptly at the boundary with the rest of the large cone, though still above the hardness of the narrow cones.

These results show that in samples with a high Si content the SiC is preferentially deposited in the large cones. The lenticular inclusions are nearly pure β-SiC and are probably formed by carbidization of pure Si droplets, which, in turn, might be formed by $SiCl_4$ decomposition; the lenses then serve as nuclei on which SiC is preferentially deposited together with pyrocarbon. This hypotesis can explain: a. — absence of lenses in samples deposited at low temperatures, at which Si is no longer liquid; b. — abrupt drop of the microhardness at the boundary between a lens and the rest of the large cone.

THE INFLUENCE OF SOME ADMIXTURES ON THE SPECIFIC SURFACE AREA OF CARBON MADE BY CARBONISATION OF ORGANIC MATERIALS

D. BRACILOVIĆ, M. DRAGOJEVIĆ and S. RADOSAVLJEVIĆ

School of Technology, Beograd and Institute of Chemistry, Technology and Metallurgy, Beograd

Admixtures were added in the form of organic salts to the initial organic material before carbonisation. Carbonisation was carried out either by heating alone or by heating in the presence of some inorganic acids.

The majority of additives had a somewhat similar effect on specific surface area. Increasing quantity of the salt increased the specific surface area up to maximum after which further addition decreased it.

POSSIBILITIES OF ACTIVATED SLUDGE PURIFICATION OF BEOGRAD WASTE WATER

G. GAJIĆ, J. MILOVANOVIĆ-NIKOLIĆ and V. TRIFUNOVIĆ

Institute of Chemistry, Technology and Metallurgy, Beograd

Conditions and efficiency of activated sludge purification of waste water from Novi Beograd and Zemun were investigated by batch and continuous methods. The Novi Beograd waste water consists mainly of household and office waste water while of Zemun includes industrial waste water.

The recirculation ratio for the continuous activated sludge process was 1:1 and it was a high rate process.

The 5-day BOD value of effluent steadied at below 10 mg/lit after 30 days.

TECHNOLOGICAL DEVELOPMENT OF LABORATORY METHOD FOR REMOVAL OF ^{60}Co FROM RADIOACTIVE EFFLUENTS

A. ŠVABIĆ and LJ. KNEŽEVIĆ

Boris Kidrič Institute of Nuclear Sciences, Vinča

A laboratory method removal of ^{60}Co from effluents by coprecipitation, reduction and ion-exchange has been developed.

Earlier methods were studied and modified so as to be applicable in the same installation. By reducing the number of operations and the consumption of chemicals and other materials the procedure has been adapted to industrial conditions.

DEVICE FOR MEASURING AIR POLLUTION WITH SOME NOXIOUS GASES AND VAPORS BY INTERFEROMETRY

S. PONGRAC

School of Sciences, Beograd

An experimental procedure using Rayeigh—Löwe's gas interferometer has been developed into a practical and reliable method for monitoring air pollution by some noxious gases and vapors (e. g. CO_2, CH_4, $C_6H_5NH_2$, etc). The discussion of the results so obtained gives data on the precision and accuracy obtained under the given conditions.

CHEMICAL BEHAVIOR OF RADIOPHOSPHORUS OBTAINED BY NEUTRON IRRADIATION OF SODIUM TETRAPOLYPHOSPHATE

O. Ž. JOVANOVIĆ-KOVAČEVIĆ

Boris Kidrič Institute of Nuclear Sciences, Beograd

To study the nature of the chemical changes induced by the exposure of different target materials to mixed pile irradiation, the behavior of radiophosphorus in neutron-irradiated and isothermaly annealed sodium tetrapolyphosphate $Na_6P_4O_{13}$ was investigated. By highvoltage paper electrophoresis twelve ^{32}P-labelled anions of oxyphosphorous acids, mostly degradation products of the initial polyphosphate, were separated and identified. The principal chemical changes following the n, gamma reaction and isothermal annealing are described.

EXTRACTION OF ACTINIDES BY TRI-n-BUTYL PHOSPHATE AND 4-NITRO PHENOL 2-SULPHONIC ACID

Z. B. MAKSIMOVIĆ, M. BERAN and M. M. KOPEČNI

Boris Kidrič Institute of Nuclear Sciences, Vinča, Beograd

The extraction of uranium and plutonium from acid nitrate and chloride solutions with tri-n-butylphosphate in n-dodecane and 4-nitrophenol 2-sulphonic acid as the complexing agent has been studied. The composition of chelates of uranium and plutonium with 4-nitrophenol 2-sulphonic acid in the organic phase was also investigated. The distribution coefficients obtained in the extraction of plutonium in the presence of the comlexing agent are much higher than those obtained in extraction by TBP alone ($D_{ext} \backsim 20$).

SOLVENT EXTRACTION OF NEPTUNIUM Np (V) AND SOME FISSION PRODUCTS BY MIXTURE OF TRIBUTYL PHOSPHATE AND ALKYLAMMONIUM NITRATES FROM NITRIC ACID SOLUTIONS

R. G. PUZIĆ and Z. B. MAKSIMOVIĆ

Boris Kidrič Institute of Nuclear Sciences, Vinča, Beograd

The extraction of Np (V), Eu (III) and Nb (V) from 3M nitric acid with tributyl phosphate and trilaurylammonium nitrate or trilaurylmethylammonium nitrate in n-hexane or toluene as diluents was investigated. A small synergic effect was observed.

EXTRACTION OF ACTINIDES AND FISSION PRODUCTS BY TRILAURYLAMMONIUM OXIDE

Z. B. MAKSIMOVIĆ and R. G. PUZIĆ

Boris Kidrič Institute of Nuclear Sciences, Vinča, Beograd

The extraction of Pu(IV), Pu(VI), U(VI), Np(V) and (Zr/Nb) from nitric acid solution with trilaurylammonium oxide (TLAO) in hylene as diluent was investigated. The extraction of nitric acid as a function of its concentration and the concentration of TLAO was also examined. The extraction of Pu(IV), Pu(VI), U(VI) and (Zr/Nb) from 3M HNO_3 and Np(V) from 1M HNO_3+2M $NaNO_3$+0.025M $NaNO_2$ was examined in detail. In the extraction of U(VI) with TLAO from very weak solutions of HNO_3 ($C_{HNO_3}<0.1$ M) high distribution coefficients were obtained, being much higher than in the case with TLA.

THE SYNTHESIS OF MONOCHLOROTRIFLUOROETHYLENE

M. S. JAĆOVIĆ and **J. Đ. RADOVIĆ-ADŽIĆ**

Institute of Chemistry, Technology and Metallurgy, Beograd

Monochlorotrifluoroethylene, a monomer for polychlorotrifluoroethylene known as Kel-F, was prepared.

The synthesis consists of dehalogenation of 1,1,2-trichloro-1,2,2-trifluoroethane with metallic zinc in ethanol. The investigation covered the influence of the ratio of reactants, the content of water and ethanol in the reaction mixture, the zinc grain size and the temperature on yield and purity of products.

Monochlorotrifluoroethylene was purified by low-temperature fractional distillation and analysed by gas chromatography.

Working conditions for getting chromatographically pure monomer in a 90% yield were found.

POLYMERISATION OF MONOCHLOROTRIFLUOROETHYLENE

M. S. JAĆOVIĆ, **M. D. JANIĆ** and J. Đ. RADOVIĆ-ADŽIĆ

Institute of Chemistry, Technology and Metallurgy, Beograd

The polymerisation of monochlorotrifluoroethylene in contact with water containing a redox system consisting of potassium persulfate and sodium bisulfite was studied.

A set of experiments was made under different conditions varying the ratio of elementorganic and water phase, concentration of the redox system, temperature and time of polymerisation. The experiments were done to explain the nature of this polymerisation and to determine the influence of each factor on molecular weight and yield of the polymer.

SPECTROCHEMICAL ANALYSIS OF HIGH PURITY TELLURIUM

B. ZMBOVA

Boris Kidrič Institute of Nuclear Sciences, Beograd — Vinča

Two procedures have been developed for spectrographic determination of impurities in tellurium: a direct procedure and one using preconcentration of the impurities on a graphite matrix.

The direct procedure consists in exciting the tellurium sample in a DC arc with an NaCl—KCl mixture as a spectrochemical buffer. The following elements have been determined by this method: Al, Mn, Mg, Cu, Be, In, Ga, Pb, Sn, Ni, Co, Bi, Cr and Ag in the concentration range 1×10^{-4} to $1\times10^{-2}\%$. The precision of the method, expressed by the standard deviation, is 5—25%.

In the other procedure the impurities are pre-concentrated on a graphite matrix by distillation of tellurium in vacuum. The concentrate is mixed with a buffer mixture consisting of graphite+NaCl+KCl+GeO_2, and excited in a DC arc. The following elements and concentration ranges are covered by this method: Ga, In, Be, Mn, Pd, Zr, Rh and Ti from 5×10^{-6} to $1\times10^{-4}\%$, Ni, Co, Cr, Pb, Bi from 1×10^{-5} to $1\times10^{-3}\%$, Ag, Al and Cu from 10^{-6} to $2\times10^{-5}\%$ and Pt from 5×10^{-5} to $1\times10^{-3}\%$. This sensitivity was achieved with 1 g samples of tellurium.

HIGH-TEMPERATURE REACTIONS BETWEEN BORN CARBIDE AND SOME FLUORIDES AND OXIDES IN THE GRAPHITE BASE AND THEIR APPLICATION IN THE SPECTROCHEMICAL ANALYSIS OF GRAPHITE

S. RAJIĆ

Institute for Technology of Nuclear and Other Raw Materials, Beograd

Reactions taking place in systems of graphite-boron carbide+a third component in the controlled temperature range of 1000—2000°C were investigated by spectrochemical and X-ray diffraction methods. It was found that boron evaporated at 1200°C when NaF or LiF were added, at 1600°C when ZnF_2 was added and at 1900°C when CaF_2 was added as the third component.

In the boron carbide — graphite — magnesium oxide system, magnesium borate $Mg_3(BO_3)_2$ was found to be formed at high temperatures. A new phase, aluminum borate $9Al_2O_3 \cdot 2B_2O_3$, was also found on addition of aluminum trioxide as the third component. Added vanadium pentoxide formed vanadium boride, VB_2. In the graphite—boron carbide—silicon dioxide system several phases were found but not identified. With calcium fluoride as the third component no changes occurred up to 1900°C, while at 2000°C there was a just detectable amount of calcium hexaboride. In the case of sodium fluoride new phases were sometimes found, but not identified.

These results are discussed from the spectrochemical point of view. It is shown that the spectrochemical behavior of trace elements depends on high-temperature reactions in the graphite base.

SPECTROGRAPHIC DETERMINATION OF HYDROGEN IN METALS BY A HOLLOW-CATHODE TECHNIQUE

J. S. MATIĆ-DOBROSAVLJEVIĆ and D. S. PEŠIĆ

Boris Kidrič Institute of Nuclear Sciences, Beograd

Hydrogen was determined in metals by the method of isotopic equilibrium with deuterium. Discharge in a low pressure tube with a hot hollow-cathode was used to liberate trace H_2 from the metal. The intensity ratio of hydrogen and deuterium lines was measured on a 3 m Eagle spectrograph. The dependence of line intensity on discharge conditions was studied and is discussed. The method has been developed for routine analysis of titanium and copper.

DETERMINATION OF GASES IN METALS BY VACUUM FUSION METHOD

V. VRGA and M. TOMAŠEVIĆ

Institute for Technology of Nuclear and Other Raw Materials, Beograd

The vacuum fusion method was applied for the determination of microamounts of oxygen, hydrogen and nitrogen in metals. Methods are given for uranium, zirconium, titanium, magnezinum and molybdenum. The results given here were obtained on a Ströhlein apparatus in a vacuum down to 10^{-4} Torr. The fusion was carried out in a graphite resistance furnace and the analysis was done in a Feichtinger micro gas analyser. The limits of error of determination are: for oxygen ± 6%, hydrogen ± 12%, nitrogen ± 17%.

SPECTROPHOTOMETRIC DETERMINATION OF LEAD IN PRESENCE OF OXALYLDIHYDRAZIDE

M. M. JOVANOVIĆ and V. J. REKALIĆ

School of Technology and Metallurgy, Beograd

The possibility of spectrophotometric determination of lead-ion in the presence of oxalyldihydrazide has been examined. It is shown that lead-ion in the presence of 0.2 M KOH gives a complex with oxalyldihydrazide having an absorption maximum at 370 μ. Concentrations of 0.06 to 0.60 mM/lit obey Beer's law. Color stability is established after two hours and remains constant for next two hours, during which the lead-ion determination can be made.

SPECTROPHOTOMETRIC INVESTIGATION OF REAGENT Az-p-NO_2 AND ITS REACTION WITH La

N. **PERIŠIĆ-JANJIĆ**, A. MUK and V. CANIĆ

Department of Chemistry, University of Novi Sad and Boris Kidrič Institute of Nuclear Sciences, Vinča, Beograd

The reagent Az-p-NO_2 was investigated by spectrophotometry, its spectra in different media recorded, and its dissociation investigated. The dissociation constant has been determined. The spectra of complex formation with La were investigated. The molar ratio and stability constant of the complex have been determined. The reagent can be used to determine La in quantities greater than $1.4\ 10^{-6}$ M/lit.

DETERMINATION OF Al, Ca, Li AND Sr IN URANIUM

M. KLISKA-MATIĆ, M. MARINKOVIĆ and V. ANTONIJEVIĆ

Boris Kidrič Institute of Nuclear Sciences, Vinča, Beograd

A quantitative spectrometric method for determination of Al, Ca, Li and Sr in uranium has been developed. The procedure involves the separation of these elements from uranium by ether extraction in nitric acid solutions and the use of low-temperature arc for their determination.

RADIOMETRIC ANALYSIS OF MIXED PRECIPITATES

R. DESPOTOVIĆ

Ruđer Bošković Institute, Zagreb

A radionuclide of the same chemical form as the stable nuclide is spontaneously and homogeneously distributed in the phases of a polycomponent system. The total composition of polycomponent systems can be determined by radiometric analysis. The principle of this application of radionuclides is described.

CONDUCTOMETRIC DETERMINATION MICRO AMOUNTS OF CARBON IN URANIUM DIOXIDE

M. TOMAŠEVIĆ

Institute for Technology of Nuclear and Other Row Materials, Beograd

A conductometric method for determining carbon uranium dioxide has been developed. Samples are burned in an oxygen stream at 1200°C in an induction furnace, and the gases are conducted through a conductometer absorption cell which contains a very dilute solution of barium hydroxide. If the samples contain fluorine, lead oxide should be added, which reacts with it giving stable lead fluoride. This eliminates trouble from fluorine. The errors of determination are +5.4 to —4.0% for the carbon concentration range 25—200 μg C. The standard deviation for 50 μg C is 1.15 μg, and the lower limit of determination is 5 ppm.

NEUTRALIZATION COULOMETRY DETERMINATION OF HYDROXYLAMMONIUM SALTS

M. S. JOVANOVIĆ and **B. D. VUČUROVIĆ**

School of Technology and Metallurgy, Beograd

As a further step in the examination of neutralization determinations of hydroxylammonium salts, the electrolytically generated titrant was coulometrically added.

The coulometric cell consisted of a vessel containing two platinum electrodes separated by a sintered-glass diaphragm. Internal generation of the titrant took place in 1 m sodium sulfate solution.

The end-point was detected by either a potentiometric or a biamperometric technique. In the second case, a bismuth-bismuth electrode pair was used as the indicator system. The results are satisfactorily consistent.

DETERMINATION OF SOME TWO-COMPONENT MIXTURES OF ORGANIC SUBSTANCES BY KINETIC METHODS

V. VAJGAND, T. PASTOR, T. TODOROVSKI, D. POCKOVA-NIKOLOSKA, M. ARSIĆ-MICIĆ and N. PUTIĆ

School of Sciences, Beograd, Faculty of Tecnohology and Sciences, Skoplje, and Faculty of Liberal Arts, Priština

The best kinetic methods for determining components in mixtures without their previous separation are those in which the components are taken in large excess compared to the common reagent (the Roberts and Regan method), or vice versa, since the reaction can then be considered of the first order. The possibility of applying such methods depends on getting a suitable ratio between the rate constants of the chemical reactions of the components (depending to a large extent on steric factors), the composition and temperature of the solution and the choice of an appropriate technique for measuring the reaction rate.

The paper describes the conductometric determination of mixtures of isoamyl methyl ketone and acetophenone via hydroxylamine hydrochloride in aqueous media, of isopropyl amine and benzyl amine by phthalic anhydride in acetic acid, the determination of mixtures of formaldehyde and acetone via the rate of formation of the bisulfite compound using polarography, and the determination of acetic and propionic anhydrides in mixture following the hydrolysis rate by interferometry.

NEW KINETIC TITRATION METHOD FOR THE DETERMINATION OF SILVER AND PALLADIUM IN SOLUTION

V. VAJGAND, V. NIKOLIĆ, **D. STOJANOVIĆ** and LJ. ĐORĐEVIĆ

School of Sciences, Beograd and Institute for the Application of Nuclear Energy in Agriculture, Zemun

The slow reaction between hydrogen peroxide and potassium iodide is catalyzed by traces molybdate in the acid medium. If to a solution containing all these components except iodide, Ag^+ or Pd^{2+} is added, then on titrating with iodide the catalytic reaction only begins practically after all the silver or palladium has precipitated. During the titration the potential is followed, i. e. read always at the same interval after the addition of the titrant (e. g. 1 minute). The precipitation curves exhibit very pronounced changes at the end-point, those in case of palladium titration being much higher than in ordinary potentiometric titration.

On a similar principle, the end-point can be detected by other catalytic chemical reactions of the Landolt type, catalyzed by traces of iodide. For example, by making use of the reaction Ce(IV)—As(III) it is possible to determine Ag^+, Hg^{2+}, Pd^{2+} etc., as already partly reported in the literature.

Apart from the catalytic indicator reaction mentioned above, we were also able to determine Ag+ and Pd^{2+} by applying the non-catalytic reaction Cr(IV)—As(III) in the presence of iodide as mediator for the potentiometric measurement of redox potential. The titration is performed in 3N sulfuric acid with an excess of As(III) present. The method is accurate and precise.

DETERMINATION OF WEAK ORGANIC BASES AND ACIDS USING VARIOUS CATALYTIC INDICATOR REACTIONS

V. VAJGAND, F. F. GAÀL, LJ. ZRNIĆ and R. KRIZSÀN

School of Sciences, Beograd and Faculty of Sciences, Novi Sad

Coulometric titrations of tertiary amines in mixtures of nitrobenzene, acetic anhydride (4 : 1) and sodium perchlorate (O.1 M) with hydroquinone added to the solution titrated were performed by generation of hydrogen ion at a platinum anode. The determination of bases by coulometric titration based on the generation of hydrogen ion from hydroquinone also permits the application of yet another indicator reaction for the end-point detection: addition reaction of acetic anhydride to the quinoid system, also an exothermal process, extending the method to very weak bases, e.g., caffeine, since it is possible to avoid even traces of water in the system. The end-point was determined by photometric, catalytic thermometric and potentiometric methods. The samples taken were 0.7—2.5 mg and the average deviation amounted to less than 1%.

A new visual catalytic titration method for the determination of macro amounts of tertiary amines and salts of organic acids is described. It is based on the reaction of dehydratation of formic acid in acetic anhydride solution. Hydrogen ion catalyses the dehydratation of formic acid so the titration end-point can be observed by violent liberation of gasses from the solution titrated.

The latest results in catalytic thermometric determination of acids in a mixture of acetone, diacetone alcohol and sodium perchlorate (0.5 M) as supporting electrolyte by generating the titrant at a platinum cathode are presented.

CATALYTIC THERMOMETRIC END-POINT DETECTION OF CHELATOMETRIC AND PRECIPITATION TITRATIONS IN WATER AND NON-AQUEOUS SOLVENTS

F. KISS

School of Sciences and Department of Chemistry, University of Novi Sad

The application of catalytic thermometry to the end-point detection of chelatometric and precipitation titrations in water and non-aqueous solvents is discussed. Direct, inverse, substitutional and back titration methods for determination of ultramicro amounts of several anions and cations have been developed. The decomposition of hydrogen peroxide and the reactions between cerium(IV) and arsenic(III), cerium(IV) and antimony(III), and hydrogen peroxide and several organic substances were used as exothermic indicator reactions.

REVERSED-PHASE PARTITION CHROMATOGRAPHY OF AMERICIUM, URANIUM AND THORIUM WITH A MIXTURE OF ORGANIC SOLVENTS

M. CVJETIĆANIN

Boris Kidrič Institute of Nuclear Sciences, Vinča

The synergistic effect of a mixture of thenoyltrifluoroacetone (HTTA) and trioctylphosphine oxide (TOPO) was investigated for U(VI), Th(IV) and ^{241}Am(III) by reversed-phase partition chromatography. The composition of the metallic species formed in the organic phase was determined. The results obtained are interpreted in terms of a simple partition equilibrium by analogy with the distribution of species in solvent extraction. The conditions for the separation of the ions are also given.

SEPARATION OF IRON II AND IRON III LABELLED WITH RADIOISOTOPE ^{59}Fe BY COLUMN CHROMATOGRAPHY

S. KOZOMARA and F. KRLEŽA

Boris Kidrič Institute of Nuclear Sciences, Vinča, Beograd
and Faculty of Sciences, Sarajevo

Iron II and iron III (labelled with ^{59}Fe) can be separated by column chromatography with basic aluminum oxide and determined by radiometric analysis: iron III is masked with glycerin and iron II converted into potassium

ferrocyanide with potassium cyanide. After masking iron III with glycerine (in the ratio of about 1 : 1000) glycocol buffer solution (pH=9) and a small excess of 1% solution of potassium cyanide are added. The solution is then passed through the column with basic aluminum oxide. After washing the column with water all the potassium ferrocyanide is present in the effluent. Iron III is then eluted with 0.1 N hydrochloric acid.

SEPARATION OF ALDEHYDES BY THIN LAYER CHROMATOGRAPHY

V. D. CANIĆ and **M. B. VOJINOVIĆ**

Department of Chemistry, University of Novi Sad

A method for separation of C_1—C_{10} aldehydes on rice starch-silica gel (7 : 3) layers with the solvent mixture benzen-petroleumether (4 : 1) is described. 2,4-Dinitrophenylhydrazone derivatives have been separated.

The method was used to identify acetaldehyde, propylaldehyde, butyraldehyde and benzylaldehyde in wine distillate. Organic acids need not to be removed from the wine by ion-exchange before separation.

INFLUENCE OF SOLVENT VAPOR IN THIN LAYER CHROMATOGRAPHY ON STARCH

S. M. PETROVIĆ and V. D. CANIĆ

The rate of sorption of solvent vapors on starch thin layers and the influence of atmosphere saturation in the chromatographic chamber on R_f-values and H. E. T. P. were observed.

III. PHYSICAL CHEMISTRY

SEPARATION OF FREONS BY CHROMATOGRAPHY ON $BaTiO_3$

M. V. ŠUŠIĆ, D. R. VUČELIĆ, S. V. MENTUS, **V. J. VUČELIĆ-MILAKOVIĆ**
and B. D. KARAULIĆ

*School of Sciences, and Institute of Chemistry, Technology
and Metallurgy, Beograd*

Sorption of several freons on the ferroelectric salt $BaTiO_3$ was studied. The results are applied in a method for chromatographic separation of the mixture gaseous freon-air-liquid freon at room temperature and low pressure. Qualitative and quantitative analysis was carried out. Retention times and basic kinetic and thermodynamic parameters for the gas/solid system were determined.

THE ION-EXCHANGE OF SOME DIVALENT CATIONS ON LINDE 4A ZEOLITE

O. M. GAČINOVIĆ, P. D. RADOVANOV, M. TODOROVIĆ AND I. J. GAL

Boris Kidrič Institute of Nuclear Sciences, Beograd

The preparation and chemical and physical characteristics of the Cd, Zn, Ni, Ca forms of 4A zeolite are described. These divalent cations reversibly replace sodium in the zeolite by up to 80—100%. The new zeolite forms, if not dehydrated, retain the basic zeolite crystalline structure. Some typical ion-exchange isotherms are presented.

Li-Na ION-EXCHANGE IN MIXED SOLVENTS ON SYNTHETIC ZEOLITES

Z. DIZDAR and P. POPOVIČ

Boris Kidrič Institute of Nuclear Sciences, Vinča, and Institute of Nuclear and Other Raw Materials, Beograd

Ion-exchange Li-Na on synthetic zeolites Linde 4A and Linde 13X in mixed solvents is investigated within the framework of a systematic study on ion-exchange in mixed solvents. Solvents used were methyl alcohol, aceton, dioxan and dimethylsulfoxide, with water as the second component. The results indicate some specific properties of dimethylsulfoxide in ion-exchange process, owing especially to its relatively high dielectric constant and high dipole moment.

THE SORPTION OF NON-POLAR MOLECULES ON LINDE 5A ZEOLITE

V. M. ŠUŠIĆ, **R. D. VUČELIĆ**, I. ZUPANČIĆ and A. M. HUTER

School of Sciences, Institute of Chemistry, Technology and Metallurgy, Boris Kidrič Institute of Nuclear Sciences, Beograd and J. Štefan Nuclear Institute, Ljubljana

Methane and ethane sorption was studied by spin-echo and wide-line NMR methods. From the concentration dependence of longitudinal relaxation time the specific surface area was determined and is in agreement with the BET results. The mechanism of the longitudinal relaxation depends on the concentration of paramagnetic impurities which show in the EPR spectrum of the original sieve specimen. The activation energy of surface mobility was determined. An increase of this energy with the degree of surface covering was established. An analysis of the wide-line spectra shows a deformation of the spherical methane molecule. At concentrations where the molecules are sufficiently close together intermolecular interactions change the isotropic rotations into anisotropic rotations about an axis normal to the surface. The activation energy is about 0.015 eV.

Behavior of the ethane molecule is almost the same except for a conformal transition at 153—154 K°.

WATER SORPTION ON ALUMINOSILICATE CRYSTALS
I. NMR STUDIES

M. V. ŠUŠIĆ, **D. R. VUČELIĆ**, M. A. HUTER, S. V. MENTUS,
D. B. KARAULIĆ and V. J. VUČELIĆ-MILAKOVIĆ

*School of Sciences, Institute of Chemistry, Technology and Metallurgy,
Beograd, and Boris Kidrič Institute of Nuclear Sciences, Beograd*

An NMR method was used to examine water sorption on the synthetic zeolite Linde 5A. The correlation times and activation energies of hindered rotation of molecules for different degrees of coverage were determined. A significant temperature dependence of molecular local magnetic fields was found. From the parameters derived from the NMR spectra, an anisotropic model of the water with a strictly defined axis of rotation is proposed. A method for calculation of moments is applied to the spectra of sorbed molecules, and gives good agreement with the theoretical results derived from the proposed model.

SORPTION OF WATER ON ALUMINOSILICATE CRYSTALS
II. PROBING A SURFACE COVERED BY SMALL MOLECULES

V. M. ŠUŠIĆ, R. D. VELEČIĆ, **V. S. MENTUS**, J. V. VUČELIĆ-MILAKOVIĆ
and D. B. KARAULIĆ

*School of Sciences, Beograd and Institute of Chemistry,
Technology and Metallurgy, Beograd*

The state of water on the surface of Linde 5A zeolite was studied by probing the covered surface with molecules of methane and deuterium. With change of water concentration on the surface there is also a change in the character of the surface on which small molecules are sorbed. The nature of this change was examined by chromatographic determination of the heat of sorption of methane and deuterium. In the concentration range where water molecules interact and closed structures are formed, methane and deuterium are sorbed practically on the monomolecular water layer. This results in an appreciable decrease in the heat of sorption. The existence of two sorption regions was proved by DTA. Corresponding studies with methyl alcohol did not reveal different sorption region. The results confirm the model proposed from NMR measurements of anisotropic rotation of the water molecules about a single axis.

WATER SORPTION ON ALUMINOSILICATE CRYSTALS
III. THERMAL AND CALORIC EFFECTS

M. V. ŠUŠIĆ, D. R. VUČELIĆ, **D. B. KARAULIĆ**, V. J. VUČELIĆ-MILAKOVIĆ
and S. V. MENTUS

*School of Sciences and Institute of Chemistry, Technology
and Metallurgy, Beograd*

A DTA and TG analysis of sorbed water and methyl alcohol on the molecular sieve Linde 5A at different degrees of coverage was made. It was found that depending on the concentration of sorbed water there are two energetically different states. For the case of methyl alcohol no such phenomenon was detected. The results obtained are not consistent with the hypothesis of the existence of two types of sorption center: cationic and anionic (with hydrogen bond formation). The proposed model of water sorption involving mutual hydrogen bonds starting with a degree of coverage of 0.5 is on the other hand in good agreement with the quantitative and qualitative results of DTA and TG analysis.

CRYSTAL STRUCTURE ANALYSIS OF U_2O_5

R. HERAK and **B. PRELESNIK**

Boris Kidrič Institute of Nuclear Sciences, Vinča, Beograd

Uranium oxide U_2O_5 is obtained as an insoluble residue after treating U_3O_8 with hot H_2SO_4. The powder oxidizes easily in air. X-ray and neutron powder diffraction methods were used to determine the crystal structure model of U_2O_5. The crystal chemistry of uranium oxides existing in the UO_2—$UO_{2.67}$ stoichiometric range is discussed.

THE DISSOCIATION CONSTANTS OF NITRILOTRIACETIC ACID AND THE STABILITY CONSTANTS OF ITS CHELATES WITH ALKALINE EARTH METALS IN ETHANOL-WATER MIXED SOLVENTS

I. ZSIGRAI and T. KISS

School of Sciences and Department of Chemistry, University of Novi Sad

The dissociation constants of nitrilotriacetic acid (NTA) and the stability constants of its chelates with barium, calcium and magnesium in 30 percent and in 60 percent ethanol at 20°C were determined. All solutions were made 0.1 M in potassium chloride. The determinations were performed by pH-metric titration with a potassium hydroxide standard solution using a glass electrode

and a saturated calomel electrode. The negative logarithms of the acid dissociation constants (pK) of NTA in 30 percent ethanol were found to be 1.93, 3.08 and 10.04 and in 60 percent ethanol 2.30, 3.28 and 10.73 respectively. The stability constants of NTA-chelates of barium, calcium and magnesium in 30 percent ethanol were found to be $10^{5}:^{47}$, $10^{7}:^{21}$, and $10^{6}:^{28}$, and in 60 percent ethanol $10^{6}:^{19}$, $10^{6}:^{89}$, and $10^{7}:^{62}$, respectively. The stability constants are about 100 times greater in 60 percent ethanol than in water.

THE FORMATION OF HALIDE COMPLEXES OF SOME DIVALENT CATIONS IN MOLTEN $NH_4NO_3.2H_2O$

R. M. NIKOLIĆ and I. J. GAL

Boris Kidrič Institute of Nuclear Sciences, Vinča, Beograd

Using solvent-extraction combined with the radioactive tracer technique, the formation of chloride and bromide complexes of $Hg^{2}+$, $Zn^{2}+$ and $Cu^{2}+$ in molten $NH_4NO_3.2H_2O$ was investigated in the temperature range 50—90°C. Consecutive stability constants and the standard thermodynamic functions are computed and interpreted in terms of a quasi-crystalline model of the molten electrolyte.

POLAROGRAPHIC BEHAVIOR OF URANIUM IN SOLUTIONS OF HIDROQUINONE

G. EL INANY and D. S. VESELINOVIĆ

School of Sciences, Beograd and Institute of Chemistry, Technology and Metallurgy, Beograd

During the reduction of uranium in solutions of hydroquinone at the dropping mercury electrode (D. M. E.) we obtained different waves depending on solution pH and concentration of hydroquinone. In alkaline and weak acid media uranium gives stable complexes which are not reducible at the D. M. E. The complex formed in a weak acid medium (pH 5—7) is insoluble, while the complexes in alkaline media are soluble. In acid medium (pH<5) two waves appear. Their half-wave potentials depend on the pH of the solution and on the concentration of hydroquinone. Both waves are due to one electron reductions (VI→V) an (V→IV). With increasing solution pH $E_1/_2$ of the first wave becomes more negative but the change is small, maybe due to the low stability of the complex. For the second wave the change in $E_1/_2$ is more pronounced; it shifts to more positive, showing that the processes in solution are more complicated. It was found that the wave height is a linear function of the concentration of uranium.

REACTIONS OF ZIRCONIUM AND THORIUM WITH ARSENAZO III IN STRONGLY ACID MEDIA

A. MUK and S. B. SAVVIN

Boris Kidrič Institute of Nuclear Sciences, Beograd and V. I. Vernadsky Institute of Geochemistry and Analytical Chemistry, Moscow

Reactions of zirconium and thorium with the reagent arsenazo III were investigated by spectrophotometry. Changes of molar ratio and molar absorptivity with medium acidity were investigated. The composition of the complex, metal-ion binding in the complex and the nature of the chemical bond in strongly acid media are discussed.

COMPLEXATION OF SCANDIUM WITH REAGENTS OF THE ARSENAZO GROUP

V. NIKOLIĆ and A. MUK

Boris Kidrič Institute of Nuclear Sciences, Vinča, Beograd

Scandium complexes with arsenazo reagents were investigated by spectrophotometry. Molar ratios of the complexes were determined. The bonding of the scandium with the reagents is discussed. Selectivity and sensitivity of the color reactions are compared.

INVESTIGATION OF INSOLUBLE COMPOUNDS FORMED BY ETHYLENEDISULPHURDIACETIC ACID AND COPPER (II), MERCURY (II) AND SILVER (I)

D. VESELINOVIĆ, **LJ. RAJKOVIĆ** and D. SUŽNJEVIĆ

School of Sciences, Beograd and Institute of Chemistry, Technology and Metallurgy, Beograd

Ethylenedisulphurdiacetic (H_2Z) with Cu(II) and Hg(II) forms both soluble chelates and insoluble compounds. We investigated the insoluble compounds with Cu(II), Hg(II) and Ag(I). Copper and mercury form compounds of the type Mez and silver AgHZ and Ag_2Z. The solubility products of the compounds were determined. Mainly electrochemical methods and IR-spectrometry were used.

SYNTHESIS AND STUDY OF THE CONFIGURATION OF DINITROBIS(AMINO-ACIDATO)-COBALTATES(III) CONTAINING TWO DIFFERENT AMINO ACIDS AS LIGANDS

M. B. ĆELAP, G. S. **STOJANOVIĆ** and T. J. JANJIĆ

School of Sciences, Beograd and Institute of Chemistry, Technology and Metallurgy, Beograd

The syntheses of dinitrobis (amino-acidato)-cobaltates(III) containing two different amino acids as ligands are described. The complexes with the following amino acid pairs were prepared: glycine/alanine, glycine/α-aminobutyric acid, glycine/valine, alanine/α-aminobutyric acid, alanine/valine and α-aminobutyric acid/valine. In addition, the configuration of the complexes was studied using the electron absorption spectra. It was found that the nitro-groups occupy the *cis*-position. The infrared spectra of the compounds were also analysed.

PREPARATION AND STUDY OF COBALT(III) COMPOUNDS WITH L-ARGININE AND L-HISTIDINE

M. B. ĆELAP, **B. A. KAMBERI** and T. J. JANJIĆ

School of Sciences, Beograd and Institute of Chemistry, Technology and Metallurgy, Beograd and Faculty of Liberal Arts, Priština

The syntesis and configuration study of cobalt(III) octahedral coordination compounds with L-arginine and L-histidine are described.

The dinitrobis (L-argininato) cobalt(III) complex ion $[Co(L\text{-}arg)_2(NO_2)_2]^+$ was obtained both by the direct method from the corresponding components and by the action of L-arginine on alkali hexanitrocobaltates(III). It was established by means of electron absorption spectroscopy that the nitro groups are coordinated in the *cis*-position, which is in agreement with the number of optical isomers isolated.

The complex compound with L-histidine, i. e. nitrobis(L-histidinato)cobalt(III), $[Co(L\text{-}his)_2NO_2]$. $1/2H_2O$, was obtained in analogous ways. Its structure was also investigated by means of the electron absorption spectra.

An other complex with L-histidine, the trinitro(L-histidinato)cobaltate(III) ion, $[Co(L\text{-}his)(NO_2)_3]^-$, was obtained by the action of sodium histidinate on sodium hexanitrocobaltate(III). The tentatively assigned facial configuration of this complex is in agreement with its electron absorption spectra.

The infrared absorption spectra of the obtained complexes were also analyzed.

ELECTRONIC SPECTRUM OF THE $^{12}C^{18}O$ MOLECULE. II

J. D. JANJIĆ, D. S. PEŠIĆ and D. S. JANKOVIĆ

School of Technology, University of Novi Sad, B. Kidrič Institute of Nuclear Sciences, Vinča, Beograd

The emission Herzberg band system of the $^{12}C^{18}O$ molecule was recorded in a hollow carbon cathode discharge tube and oxygen-18. Vibrational constants and isotope shifts have been determined.

MASS SPECTRA, IONIZATION POTENTIALS AND BOND DISSOCIATION ENERGIES OF CALCIUM AND BARIUM CHLORIDES

K. ZMBOV

Boris Kidrič Institute of Nuclear Sciences, Vinča, Beograd

Ionization and dissociation of gaseous $BaCl_2$ and $CaCl_2$ under electron impact have been studied by mass spectrometry. Mass spectra and appearance potentials of molecular and fragment ions were determined.

Equilibria of the type $MCl_2(g) + M(g) = 2\ MCl(g)$ were investigated at high temperatures and their enthalpies were measured. The results are used to determine stepwise bond dissociation energies of $BaCl_2$ and $CaCl_2$ molecules.

DETERMINATION OF SOME TRANSITION ELEMENTS IN SYNTHETIC BERYL BY ATOMIC ABSORPTION MEASUREMENT

S. RISTIĆ and V. BOJOVIĆ

School of Sciences, Beograd, and Institute of Chemistry, Technology and Metallurgy, Beograd

This communication describes an atomic absorptiometric method for the determination of chromium, nickel and cobalt in synthetic beryl samples. For rapid decomposition of this alumosilicate mineral ($Be_3Al_2Si_6O_{18}$) we used

an appropriate mixture of fluoro-boric acid which gave good results in some recently published investigations on similar (silicate) materials.

The experimental procedure is here described. The clear solution to be analyzed was blown through an atomizer into an appropriate flame burner and the radiation of the analytical flame evaluated by atomic absorption measurement using standard techniques (the atomic absorption setup was a Hilger attachment for the Hilger H707 Uvyspek Spectrophotometer and hollow cathode lamps for Cr, Ni and Co).

The interference of the main stoichiometric elements is not excessive so that fairly good results for the determination of Cr, Ni and Co can be obtained under well-specified conditions. The concentration range of the solutions employed and the experimental error are well within the limits usually given for standard determinations by atomic absorptiometry.

ABSORPTION SPECTRA AND CHEMICAL TRANSFORMATIONS OF FLAVYLIUM PERCHLORATE IN AQUEOUS AND NON-AQUEOUS MEDIA

S. RISTIĆ and J. BARANAC

School of Sciences, Beograd and Institute of Chemistry, Technology and Metallurgy, Beograd

The process of chalcone cyclization, which under well-defined conditions may lead to the formation of the basic skeleton of the antyocyanidine chromophoric system, has been studied by many authors. The interpretation of the mechanism of this process has given rise, however, to a discussion of the number and nature of the intermediate compounds and the role of water and incident light in the process. Continuing our previosly published investigations od 2-hydroxychalcone, we took the inverse route going from a cyclized chalcone, i.e. flavylium perchlorate to study its spectrochemical and chemical behavior.

We studied the absorption spectra of flavylium perclorate in hydroxylic, non-hydroxylic and buffered solutions, to try and get more precision in defining the molecular species involved. The behavior of the flavylium perchlorate salt was especially interesting in conc. sulfuric acid (37 N) and a buffered solution (pH = 12.40), where intensive fluorescence phenomena were observed.

An interpretation of the results is given, involving an attempt to correlate the absorption and fluorescence spectra.

EFFECT OF ANOMALOUS DISPERSION IN INFRARED SPECTRA OF LIQUIDS IN BINARY MIXTURES WITH SOLIDS

D. MIOČ, U. MIOČ and S. ANIĆ

School of Sciences, Beograd, and Institute of Chemistry, Technology and Metallurgy, Beograd

The effect of anomalous dispersion on absorption bands in infrared spectra of binary liquid-solid mixtures was studied. The mixtures were prepared from liquids with strong absorption bands in the investigated spectral range, and solid with no absorption in this range. The effect on the absorption bands of the liquids was examined. The magnitude of the effect was investigated as a function of the difference of the refractive indices of the components on the linear part of dispersion curve in the vicinity of the absorption bands. Change of sign of the difference leads to an inversion of the effect.

UNUSUAL THERMOANALYTICAL BEHAVIOR OF SOME BERYLS (SHOWN BY THE TG, DTG AND DTA CURVES)

S. M. RISTIĆ

School of Sciences, Beograd

The published analytical data on the total ignition loss (IL), i.e. the water content (in %) of various natural beryls vary within wide limits. Since some recent investigations established that the IL of beryl often shows two distinct maxima ($t_{M_1} \backsim 350$°C and $t_{M_2} \backsim 1000$°C), there persists a basic misunderstanding among various authors in quoting IL data for this mineral.

About thirty samples of natural beryl where investigated on a modern thermoanalytical instrument (Paulik-Paulik's Derivatograph-Hungary) recording simultaneously the TG, DTG and DTA curves, plus a control temperature curve.

Some beryl samples, especially these of the "non-stoney" type, showed an unusual behavior namely a negative IL and a characteristic DTA-curve. The results obtained are discussed, in an attempt to interpret the phenomena observed.

SURFACE CHARGE ON LOW-TEMPERATURE $ZnO—Cr_2O_3—CuO$ CATALYST DURING OXYGEN CHEMISORPTION

P. S. PUTANOV, M. JOVANOVIĆ, **J. NOVOTNY*** and Ž. JOVANOVIĆ

Institute of Chemistry, Technology and Metallurgy, Beograd
**Institute of Physical Chemistry, Polish Academy of Sciences, Krakow*

As part of the systematic study of the low-temperature $ZnO—Cr_2O_3—CuO$ catalyst, the work function of several samples in vacuum and oxygen atmosphere was investigated by the dynamic condenser method for contact potential difference determination. The influence of oxygen chemisorption on the catalyst surface charge at 300°C was examined and kinetic data about work function changes during the process of chemisorption have been analyzed.

STUDY OF ZINC—COPPER—CHROMIUM CATALYST FOR THE SYNTHESIS OF METHANOL. II. INVESTIGATION OF BINARY MIXTURES

P. S. PUTANOV, **A. TERLECKI-BARIČEVIĆ** and B. ALEKSIĆ

Institute of Chemistry, Technology and Metallurgy, Beograd

Some characteristics of the binary mixtures $Zn(OH)_2—Cr(OH)_3$ $ZnO—$ $—CrO_3$, $Cu(OH)_2—Cr(OH)_3$ and $CuO—CrO_3$ with the stoichiometric ratios for zinc and copperchromate and chromite formation were investigated. Processes which take place as a result of individual transformations or interactions of the components during the thermal treatment of the catalyst were studied by DTA, TG and electrical conductivity measurements.

INVESTIGATION OF SOME POSSIBLE CAUSES OF DETERIORATION OF CATALYSTS FOR STEAM REFORMING OF NATURAL GAS. II. THE INFLUENCE OF CARBON DEPOSITION

P. S. PUTANOV and B. ALEKSIĆ

Institute of Chemistry, Technology and Metallurgy, Beograd

To establish possible causes of catalyst deterioration the influence of water vapor/gas ratio and its variations during a proces, and of prolonged operation under unfavorable conditions on carbon deposition and consequently on the mechanical strength of the catalyst were investigated.

THE EFFECT OF THERMAL TREATMENT ON THE POROUS STRUCTURE OF VANADIUM CATALYSTS FOR H_2SO_4 PRODUCTION

P. S. PUTANOV, N. JOVANOVIĆ, D. SMILJANIĆ and B. MILISAVLJEVIĆ

Institute of Chemistry, Technology and Metallurgy, Beograd

Commercial vanadium catalyst samples were exposed to temperatures considerably higher than their maximum working temperatures for different times, to evaluate their thermal stability. Changes of total porosity and the shifting of the maximum in the pore volume against pore radius distribution curve were observed by the mercury penetration method.

INVESTIGATION OF VANADIUM CATALYSTS FOR H_2SO_4 PRODUCTION: PHYSICAL AND CHEMICAL PROPERTIES AND ACTIVITY

P. S. PUTANOV, B. MILISAVLJEVIĆ and D. SMILJANIĆ

Institute of Chemistry, Technology and Metallurgy, Beograd

A number of commercial vanadium catalyst samples were investigated to establish a criterium characterizing their performance in an industrial plant. The chemical composition, textural properties, effective diffusivity and activity were determined under laboratory conditions.

REACTIVE DIFFUSION IN THE MAGNESIUM-GERMANIUM SYSTEM

M. JANČIĆ and **LJ. RADONJIĆ**

School of Technology and Metallurgy, Beograd and Institute of Chemistry, Technology and Metallurgy, Beograd

The phenomena of the formation of new magnesium — germanium phases in the reaction between magnesium and single-crystal germanium was studied. The kinetic curves of the process have been plotted and the diffusion parameters evaluated. A mechanism of the formation of the new phases is given.

REACTIVE DIFFUSION IN THE STRONTIUM-SILICON SYSTEM

M. JANČIĆ and LJ. RADONJIĆ

School of Technology and Metallurgy, Beograd and Institute of Chemistry, Technology and Metallurgy, Beograd

The reaction between strontium and single-crystal silicon yields new phases. The kinetics of the formation of new phases on a single crystalline substrate is examined. The constitution of the phases was examined using a micro electron probe.

THE INFLUENCE OF THE CRYSTALIZATION RATE ON GRAIN GROWTH AND THE APPEARANCE OF NEW PHASES IN THE SYSTEM Bi-Sb-Te-Se

M. JANČIĆ and LJ. RADONJIĆ

School of Technology and Metallurgy, Beograd and Institute of Chemistry, Technology and Metallurgy, Beograd

The crystalization of thermoelectric materials based on solid solutions of Bi-Sb-Te-Se was examined. Crystalization was performed by zonal melting of samples with a changing rate of zone withdrawal. The relation between grain size and withdrawal rate was established. The appearance of the secondary tellurium phase as a function of the crystalization rate is considered.

THE FORMATION OF PHASES IN THE MAGNESIUM-SILICON SYSTEM BY REACTION DIFFUSION

M. JANČIĆ

School of Technology and Metallurgy, Beograd

The conditions for the formation of the intermediate compounds Mg_2Si and MgSi by the reactive diffusion of magnesium and single-crystal silicon were examined. The stability range of Mg_2Si and the conditions for the formation of MgSi were determined. The diffusion coefficients of the reaction components are evaluated and kinetic curves for the process given.

DETERMINATION OF BOILING DIAGRAM OF BENZENE-FURFURAL MIXTURE

Ž. ŽIVANOV, D. MIŠKOVIĆ, S. RADOSAVLJEVIĆ and A. CVEJIĆ

Department of Chemistry, University of Novi Sad

The extract phase obtained by the extraction of furfural with benzene from aqueous solution contains benzene, furfural and some water. In order to examine the possibility of separating benzene by distillation the boiling diagram of benzene-furfural mixture was experimental determined. The diagram shows that the system has no azeotrope. Since with water benzene forms a low boiling point azeotrope, it is possible to get water-free furtural by distillation of benzene from the extract phase.

KINETICS OF HYDROLYSIS OF ZIRCONYL CHLORIDE SOLUTION

R. ĆOSOVIĆ

Institute for Technology of Nuclear and Other Raw Materials, Beograd

The kinetics of hydrolysis of water solution of zirconyl chloride, with and without free hidrochloric acid, was investigated. We found that the reaction is a complicated one: its beginning exhibits an induction period; later on it follows a first-order rate law. The specific reaction rate and an approximate value of the activation energy were determined.

This work represents a preliminary phase of a more profound study of this reaction which could be of a great practical importance.

ELECTROCHEMICAL EQUILIBRIA IN THE REDOX SYSTEM FERROIN/FERRIIN

D. JOVANOVIĆ and T. RAKIĆ

School of Technology and Metallurgy, Beograd

Studying kinetics of the electrochemical redox system ferroin/ferriin, two electrochemical equilibria whose potentials differ by a few hundred millivolts were established. It is considered that this behavior of the system is due to the chemical transformations of one form of the iron (III) with 1, 10-phenantroline (ferriin) into another, more stable form.

Potentiometric titration with $KMnO_4$ solution was applied to measure the standard potentials of the two equilibria and their pH dependence.

KINETICS OF ELECTROCHEMICAL DISSOLUTION AND DEPOSITION OF ZINC IN ACID SOLUTIONS OF ZINC SULPHATE

D. M. DRAŽIĆ and S. HADŽI-JORDANOV

School of Technology and Metallurgy, Beograd

The kinetics of anodic dissolution and cathodic deposition of zinc was studied by a galvanostatic method. The measurements were done in zinc sulphate solutions (0.01-1 M) containing sodium sulphate (1 M) and suitable amounts of sulphuric acid to keep the pH in the range 0.5 to 5. The kinetics of hydrogen evolution was examined independently corresponding solutions without zinc sulphate. The experimentally determined relations between the electrode potentials and current densities are taken as a basis for the discussion of the electrochemical reaction mechanism.

HULL'S CELL WITH A DEFINED DIFFUSION LAYER THICKNESS

A. R. DESPIĆ and **C. R. MILOVANOVIĆ**

Institute of Chemistry, Technology and Metallurgy, Beograd

The Hull's cell has found wide application in determining conditions of practical electroplating. However, in cases where diffusion of some species affects the process (e.g. leveling, electropolishing) reproducibility of results is not easily attained because of undefined hydrodynamic conditions in the electrolyte.

A Hull-type cell was made with a rotating cone as the cathode. Hydrodynamic boundary layer and diffusion layer thickness are determined solely by the rate of rotation of the electrode. In order to determine the diffusion layer thickness as a function of the distance from the tip of the cone at various rates of rotation, a multilayer conical electrode was made and the limiting diffusion current of ferricyanide ions was measured. Results are also reported of the application of this cell to the investigation of the leveling affect of dodecylbenzene sulphonate on copper.

SOME PROBLEMS IN Pb AND Cd AMALGAM CORROSION

A. R. DESPIĆ and **O. S. VITOROVIĆ**

School of Technology and Metallurgy, Beograd
and Institute of Chemistry, Technology and Metallurgy, Beograd

Electrode potentials were measured of Pb and Cd amalgams dropping into aqueous solutions of (a) corresponding simple ions, (b) corresponding complexes with EDTA and (c) more electropositive ionic species.

The results obtained indicate reversible behavior of the Pb(Hg) electrode down to a concentration of 2.5×10^{-4} M $Pb^{2}+$ and that of Cd(Hg) down to 5×10^{-4} M $Cd^{2}+$ in acid solutions. The potentials are pH independent up to pH 5 and 6, respectively.

One could conclude that in this concentration range the hydrogen corrosion of the amalgams is negligibly slow, and hence does not affect the electrode potential.

In the presence of excess EDTA, the potentials are considerably more negative than those in simple salt solutions. They are found to be determined primarily by the hydrogen corrosion current, with the expected dependence of the mixed potential on pH.

In solutions of more electropositive ionic species, these amalgam electrodes exibit the pseudo-Nernstian behavior of potential as a function of concentration of the species involved, down to 10^{-4} M. At lower concentrations, this dependence is lost because of an increasing influence of the reduction of impurities in solution, primarily traces of dissolved oxygen.

CORROSION OF VEHICLE COOLING SYSTEM BY VARIOUS COOLANTS

ZOROVIĆ, CVIRN and RADEKA

Army Technical High School, Zagreb

This paper deals with corrosion of the multicomponent metal system constituting the cooling system of motor vehicles. The coolants examined were: tap water, rain water, distilled water, demineralized water, and deionized water containing inhibitors. The negative properties of hard water have been demonstrated. Laboratory results favor the use of electrochemically deactivated water.

CORROSION OF VEHICLE FUEL TANKS DUE TO WATER IN FUEL

ZOROVIĆ, RADEKA and CVIRN

Army Technical High School, Zagreb

This work continues research reported earlier (1st Congress on Industrial Chemistry, Beograd, June 1969). First a discrimination of possible reasons for the corrosion was attempted. It was found that the most agressive component of fuel was water, which either falls to the bottom of the tank or adheres to the walls, because of the dipolar character of its molecule.

The possibilities for inhibiting corrosion of iron fuel tank by means of several inhibitors acting from the aqueous phase have been examined. Optimum concentrations of inhibitors are given and they are classified according to protective efficiency.

CORROSION OF ZINC IN SULFURIC ACID SOLUTIONS

S. MLADENOVIĆ and Z. RADOVANOVIĆ

School of Technology and Metallurgy, Beograd

In sulfuric acid solutions with low germanium concentration the corrosion of zinc increases with increase of both sulfuric acid and germanium concentration. The corrosion is increased by the presence of antimony, arsenic, copper, cobalt and iron. Lead and cadmium ions inhibit it.

The content of germanium, which activates zinc corrosion in sulfuric acid solutions, does not decrease during the process of corrosion.

THE CORROSION OF LEAD IN CHROMIUM PLATING SOLUTION

S. N. MLADENOVIĆ, M. VUJAČIĆ and S. NEDELJKOVIĆ

School of Technology and Metallurgy, Beograd

The chemical stability of lead containing 0.04% Cu in a chromium plating solution depends on its composition and temperature, and on the previous treatment of its surface. The corrosion of the lead increases with increase of (VI) oxide, and decreases with increase in sulfuric acid concentration. The corrosion rate depends very much on the fluorosilicic acid concentration. With increasing fluorosilicic acid concentration it first decreases and than increases. If the lead is previously passivated in a sulfuric acid solution its corrosion is low at low concentrations of fluorosilicic acid in the plating bath, but appreciable at higher concentrations.

IV. ORGANIC CHEMISTRY

THE CONDENSATION REACTION BETWEEN 2—QUINOLINECARBOXYLIC ACID AND 2—PHENYL 4—QUINOLINECARBOXYLIC ACID AND AROMATIC AMINES

P. DŽADŽIĆ, M. PILETIĆ and B. BASTIĆ

School of Technology Novi Sad, Faculty of Technology and Metallurgy, Beograd and Institute of Chemistry, Technology and Metallurgy, Beograd

The condensation reactions between 2-quinolinecarboxylic acid and 2-phenyl-4quinolinecarboxylic acid and o-phenylenediamine, o-aminophenol, o-aminothiophenol, 1,2-naphthalenediamine and 1,8-naphthalenediamine have been carried out. The reaction conditions were determined, the products were isolated and their structures verified by elemental analysis.

DETERMINATION OF IONIZATION AND EXTRACTION CONSTANTS OF 4-NITRO-1-PHENOL-2-SULPHONIC ACID

M. M. KOPEČNI, M. D. ŠEĆEROV, M. BERAN and Z. B. MAKSIMOVIĆ

Boris Kidrič Institute of Nuclear Sciences, Vinča, Beograd

The second ionization constant of 4-nitro-1-phenol-2-sulphonic acid was determined ($K_2=9.33 \pm 1,00 \times 10^{-7}$; $K_1 = 1$) by spectrophotometry and potentiometry.

The composition of the complex was determined after the extraction of 4-nitrophenol-2-sulphonic acid with TBP in n-dodecane in the organic phase; a ratio 3:1 was found. Also the extraction constant ($K_{ex}=4.06$) was found.

The composition of chelates of uranium and thorium with 4-nitrophenol-2-sulphonic acid in aqueous phase was investigated by spectrophotometry: a ratio 1:1 was found. The stability constants of the chelates in the aqueous phase were also determined.

DETERMINATION OF IONIZATION AND EXTRACTION CONSTANTS OF 3,5-DINITRO SALICYLIC ACID

M. D. ŠEĆEROV, M. M. KOPEČNI, M. BERAN and Z. B. MAKSIMOVIĆ

Boris Kidrič Institute of Nuclear Sciences, Vinča, Beograd

Ionization constants ($K_1=1.11\times10^{-3}$ and $K_2=1.58\times10^{-7}$) of 3,5-dinitro salicylic acid were determined by potentiometry and spectrophotometry. The composition of the complex in the organic phase was determined by spectrophotometry after the extraction of 3,5-dinitro salicylic acid with TBP in n-dodecane; the ratio 2:1 was found. Also the extraction constant K_{Ext} was determined. The composition of the chelate of uranium with 3,5 dinitro salicylic acid in the aqueous phase was also investigated by spectrophotometry and a 1 : 1 ratio was found. The stability constant of the chelate complex of uranium and plutonium in the aqueous and the organic phase was determined.

STUDIES OF THE REACTIVITY OF IMIDAZOLCARBOXYLIC ACIDS

Đ. M. DIMITRIJEVIĆ, Ž. TADIĆ and **M. RADOJKOVIĆ-VELIČKOVIĆ**

School of Technology and Metallurgy, Beograd, and Institute of Chemistry, Technology and Metallurgy, Beograd

In order to investigate the effect of nitrogen atoms on the activity of the carboxylic groups in the imidazolcarboxylic acids, imidazolmonocarboxylic and some imidazoldicarboxylic acids and methyl and phenyl substituted imidazolmonocarboxylic and imidazoldicarboxylic acids were investigated by measuring the second-order rate constants of their reactions with diphenyldiazomethane. Theoretical interpretation of the results obtained considers the electrical effects and steric hindrances as a function of the position and interaction of nitrogen atoms and carboxylic groups.

REACTION OF 3-NITROPHTHALIC ACID ANHYDRIDE WITH NAPHTHYLAMINES

Đ. M. DIMITRIJEVIĆ, **O. A. ĐURKOVIĆ**, I. J. VUJIĆ
and Z. M. JAKOVLJEV

School of Technology and Metallurgy, Beograd

The orientation of the ring-opening reaction of 3-nitrophthalic acid anhydride with naphthylamines has been investigated. It has been established that in the reaction with ethyl-α-naphthylamine the ring of the 3-nitrophthalic acid anhydride, like in the previously studied reaction of 3-nitrophthalic acid anhydride with diphenylamine, opens in the β-position with respect to the nitro group, which proves that in this reaction the steric dominates over the inductive effect.

The constitution of the nitro-N-naphthylamic acids obtained by the action of α- and β-naphthylamines on 3-nitrophthalic acid anhydride could not be established, and therefore it was also impossible to deduce the orientation of the reaction in this case: in an attempt to esterify these acids with diazomethane, the reaction used in our method for demonstrating the constitution, closure of an N-substituted imide ring occurred instead of formation of the corresponding methylester.

ULTRAVIOLET ABSORPTION STUDIES AND SOLUTION EQUILIBRIA OF SOME PYRIDINE DERIVATIVES

V. HANKONYI, V. KARAS-GAŠPAREC and Z. BINENFELD

Department of Chemistry and Biochemistry, School of Medicine, and Army Technical High School, Zagreb

The ultraviolet absorption spectra of a number of known and some new compounds of the formula

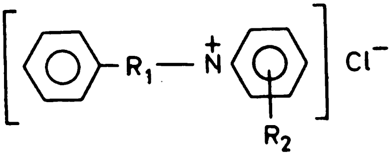

where R_1 = $—CH_2—$, $—COCH_2—$, $—C(NOH)CH_2—$

R_2 = Ø, 2-methyl, 4-methyl, 2-hydroxyiminomethyl, 4-hydroxyiminomethyl

were measured at various pH values and constant ionic strength (O.1) within a temperature range of 24.5 to 26°.

The spectrophotometric data were used to calculate the dissociation constants. Some correlations between the absorption spectra and the structure of the compounds have been studied.

THE REACTIVITY OF PYRIDINE — AND PYRIDINE-1-OXIDE ACETIC ACIDS IN REACTION WITH DIPHENYLDIAZOMETHANE

Đ. DIMITRIJEVIĆ, Ž. TADIĆ, M. MIŠIĆ-VUKOVIĆ, and B. JOVANOVIĆ

School of Technology and Metallurgy, Beograd

The dependence of the acidity of pyridine- and pyridine-1-oxide acetic acids on electrical and steric effects in the corresponding molecules was studied through the rate constants of the reaction with diphenyldiazomethane as a measure of the acidity. The rate constants were determined spectrophotometrically by measuring the decrease of diphenyldiazomethane concentration. For comparison the rate constant for phenylacetic acid was determined.

It was established that electrical and steric effects in the pyridine-and pyridine-1-oxide molecule, give these acids higher acidity then phenylacetic acid. The measured rate constants were also compared with the previously determined corresponding rate constants for pyridinemonocarboxylic acids and pyridine-1-oxide monocarboxylic acids and the differences in acidity are discussed.

RATES OF REACTION OF DIAZINE MONOCARBOXYLIC ACIDS WITH DIPHENYLDIAZOMETHANE

Đ. DIMITRIJEVIĆ, Ž. TADIĆ and **V. JEZDIĆ**

School of Technology and Metallurgy, Beograd and Boris Kidrič Institute of Nuclear Sciences, Vinča, Beograd

The reactivities of diazine monocarboxylic acids towards diphenyldiazomethane in absolute ethyl alcohol were measured at several temperatures. Rate coefficients were determined and the activation energies calculated.

EXAMINATION OF POSSIBILITIES OF EXTRACTING FURFURAL FROM AQUEOUS SOLUTIONS WITH SOLVENTS

Ž. ŽIVANOV, A. CVEJIĆ and **N. VULEKOVIĆ**

Department of Chemistry, University of Novi Sad

In order to find a suitable solvent for the extraction of furfural from aqueous solutions the distribution coefficients of furfural for different solvents were determined. The dependence of the distribution coefficient on furfural concentration for some solvents was also examined.

THE INVESTIGATION OF SOME FORMS OF PHOSPHOROUS AND NUCLEIC ACIDS IN BULL SEMEN OF DIFFERENT QUALITY

S. GRUJIĆ, M. MIŠKOVIĆ, R. PERKUČIN and S. KEVREŠAN

Chemistry Department, University of Novi Sad, School of Agriculture, University of Novi Sad and Veterinary Institute, Novi Sad

Soluble and lipid phosphorous, deoxyribonucleic and ribonucleic acid were investigated in bull semen of differing motility and fertility. The results show that sperm motility was very highly correlated with DNA, and soluble and lipid phosphorous. The correlation between sperm motility and RNA content was low.

As has been shown previously, the correlation between fertility and motility is high. Therefore, since the correlations in this study between motility and DNA, soluble and lipid phosphorous levels are high, it is likely that these factors can be used to assess fertility.

SOLUBILITY OF ERGOSTEROL ESTERS IN MIXTURES OF SOME ORGANIC SOLVENTS

S. N. RAŠAJSKI and **D. M. PETROVIĆ**

Faculty of Technology and Metallurgy, Beograd

Earlier data on the solubility of ergosterol esters acetate, caprylate, laurate and palmitate are completed with data on the solubility of ergosteryl butyrate, valerate, caprate and caproate. The solubility in five solvents (ethyl—, n-butyl—, and n-octylalcohol, benzene, cyclohexane) and mixtures of them has been determined in the temperature range 15—65°C. All the esters exhibit a solubility maximum in mixtures of two non-polar solvents. As the number of carbon atoms in the acid part of the ester molecule increases the solubility parameter decreases. The results are presented in graphs showing the effect of the number of carbon atoms in the ester molecule on the solubility, with the position of the solubility maximum if any and the solubility parameter.

THIN-LAYER CHROMATOGRAPHY OF ERGOSTEROL AND ERGOSTEROL ESTERS

S. N. RAŠAJSKI and **D. M. PETROVIĆ**

School of Technology and Metallurgy, Beograd

Studying the solubility of ergosterol esters of fatty acids, R_f values of ergosteryl acetate, butyrate, valerate, caprate, caprylate, caproate, laurate and palmitate have been determined. Except for acetate and palmitate, R_f values for these esters are published now for the first time. Silica gel G(Kemica Zagreb and Laphoma, Skopje) and five solvent mixtures were used. The dependence of R_f on the number of carbon atoms in the acid part of the ester molecule is exhibited.

OLEANOLIC ACID FROM APPLE LEAVES

N. VUKOJEVIĆ, M. PERGAL, R. PETKOVIĆ, **O. GAŠIĆ** and B. BELIA

School of Sciences, Faculty of Technology, Faculty of Agriculture and Chemistry Department, University of Novi Sad

Oleanolic acid was isolated from various varieties of apple (Jonathan, Red Delicious and Golden Delicious). For analysis we took the first, third and fourth leaves. Oleanolic acid was demonstrated and determined in petroleum ether and ether extract of dried leaves. The course of isolation was followed by thin layer chromatography on silicagel G (Stahl) in the solvent system chloroform: acetone (8 : 2). The oleanolic acid from apple was compared with that from *Eugenia cariophilate.*

CHEMICAL ANALYSIS OF LICHEN PROTEINS. II. FRACTIONATION OF SOLUBLE PROTEINS FROM *EVERNIA PRUNASTRI* AND *CETRARIA ISLANDICA*

Đ. STEFANOVIĆ, B. GRUJIĆ-INJAC and **D. KOLARSKI**

School of Sciences, Beograd and Faculty of Agriculture, Beograd

Soluble proteins of *Evernia prunastri* and *Cetraria islandica* were isolated by successive extraction with water, 10% NaCl and 0.2% NaOH. After dialysis, proteins were fractionated on G—200 Sephadex columns. The fractions obtained were analysed by a modification of the Lowrey method. The extinction was read at 750 mμ, and in the ultraviolet at 260 mμ and 280 mμ.

CYANO-BROMINE CLEAVAGE OF A BACTERIAL PROTEASE FROM SORANGIUM SP.

V. LESKOVAC and D. R. WHITAKER

Division of Biochemistry, National Research Council, Ottawa, Canada

As an initial step in the elucidation of the primary structure of β-lytic enzyme from *Sorangium sp.*, its cyano-bromine cleavage has been investigated. The kinetics of cleavage was determined. The enzyme contains 4 methionyl residues (M. W. 19,100) which quantitatively transform into homoserine. Four CNBr-fragments were obtained, and separated by a salting-out procedure at neutral pH into three smaller soluble peptides and a large insoluble polypeptide chain. Further separation of soluble peptides and purification of the insoluble residue were done by gel-filtration on Sephadex G columns in 5% acetic acid.

The smaller fragments contain 5, 14 and 31 amino acids, respectively, and the large one 127 amino acids. The amino acid composition, N- and C-terminal amino acids, tryptophan and cystine content of each fragment have been determined. Further fractionation of the large fragment was carried out by reduction and amino-ethylation of its disulfide bridges.

THE SYNTHESIS OF A DERIVATIVE OF STREPTOMYCIN

M. MILOSAVLJEVIĆ and A. ĐELINEO

Institute of Chemistry, Technology and Metallurgy, Beograd and Institute for Antibiotics, Galenika, Beograd

Many attempts have been made to obtain new less toxic forms of streptomycin. Synthesis of such a derivative and its properties are described.

FURFURAL PRODUCTION AND OUR POSSIBILITIES

Ž. ŽIVANOV and N. ČAKAN

Department of Chemistry, University of Novi Sad

The methods of production, factors affecting the yield and the endeavors to improve production and to make it cheaper are presented. It is pointed out that there are possibilities for coordination of furfural production with sulfuric acid and superphosphate fertilizer production, for which there are good conditions in Yugoslavia. A continuous process could be achieved by this coordination.

ANALYSIS OF GASOLINES BY GAS CHROMATOGRAPHY

K. PETROVIĆ and **M. KAPOR**

Oil Rafinery, Pančevo

Fractions of straight-run naphta and reformate were analyzed by gas chromatography. The obtained results shown the composition of gasolines produced at Pančevo. The same results can be used for determination of some physical parameters of gasoline.

CHARACTERISTICS OF CRUDE OILS FROM VOJVODINA

D. STEVANČEVIĆ, J. JOVANOVIĆ, S. PROTIĆ and **M. SOKIĆ**

Institute of Chemistry, Technology and Metallurgy, Beograd

Preliminary analysis of 9 crudes from the fields "Kikinda", "Palić", "Velebit", "Mokrin", and "Elemir" was carried out. The bases of the crudes, the structural indexes and the yields of base fractions are shown in tables. On the basis of the data obtained, the oils are compared.

THE IMPORTANCE OF THE KEROGEN ISOLATION PROCEDURE IN INVESTIGATING OIL-SHALE ORGANIC SUBSTANCE

M. ĐURIČIĆ and D. VITOROVIĆ

School of Agriculture and Faculty of Sciences, Beograd, Institute of Chemistry, Technology and Metallurgy, Beograd

Geochemical studies of kerogen are usually preceded by isolation, i. e. its separation from the associated mineral constituents. For this purpose, many procedures have been suggested and used. However, not enough attention has been paid to possible changes in the composition of the organic material.

Chemical methods of demineralizing oil-shales to get low-ash kerogen were studied. It was found that even by treatment of the shale with water, dilute acids or diluted alkalies, small amounts of complex mixtures of organic substances were dissolved, a fact not noted before. The knowledge of the composition and structure of these substances is of interest for organic geochemical studies of old sediments, and then should not be disregarded as before.

An enrichment procedure giving good results is described. Data are given on the examination of organic components dissolved during enrichment of

Aleksinac oil-shale. Acidic components were identified with a system consisting of a gas chromatograph (Varian Aerograph Model 600), a mase sprectrometer (Hitachi-Perkin-Elmer RMU 6—D) and a computer (IBM 1800). The results obtained are discussed in the light of degradation studies on the same oil-shale kerogen.

ISOLATION AND IDENTIFICATION OF n-PARAFFINS OF ALEKSINAC OIL-SHALE BITUMEN

D. VITOROVIĆ and **M. ŠABAN**

School of Sciences, Beograd, and Institute of Chemistry, Technology and Metallurgy, Beograd

Various components of the soluble part of oil-shale organic substance (i. e. of the bitumen) are of considerable importance for the geochemical interpretation of the origin of these sediments. For this interpretation the composition of the n-paraffin fraction has often been used. In this paper, results are presented for the n-paraffin fraction of Aleksinac oil-shale bitumen.

The bituminous part of the shale organic substance, isolated by benzene Soxhlet extraction for 100 hours, was separated into acidic, basic and neutral constituents by the usual chemical procedure. The neutral portion was treated with n-pentane and the hydrocarbon fraction isolated from the pentanesoluble part by means of Al_2O_3. The paraffins were isolated on silica gel and then separated into the n-paraffin and the iso- and cycloparaffin fractions by means of molecular sieves. By GLC techniques the n-paraffin fraction was found to consist of a C_{13}—C_{32} series.

An organic geochemical interpretation of the paraffin fraction composition is given.

THE INVESTIGATION OF COMPOSITION HETEROGENEITY OF STYRENE-DIBUTYLITACONATE COPOLYMERS BY LIGHT SCATTERING IN DIFFERENT SOLVENTS

J. VELIČKOVIĆ and **J. VUKAJLOVIĆ**

School of Technology and Metallurgy, Beograd, and Institute of Chemistry, Technology and Metallurgy, Beograd

Apparent average molecular weights of several samples of styrene-dibutylitaconate copolymers of different average composition, determined in a series of 5—7 selected solvents with significantly different refractive indices, were extrapolated to true M_w values. By treatment of the results according to the theory of Benoit *et al.* on light scattering of copolymers, the P and Q parameters of chemical inhomogeneity, and $M_w{}^A$ and $M_w{}^B$, the molecular weights of component A and B in the sample, were calculated statistically. The observed chemical inhomogeneities are discussed in terms of degrees of conversion and monomer ratios in synthesis. Radii of rotation and second virial coefficients determined from Zimm extrapolation diagrams are correlated with copolymer solubilities in the selected solvents.

HYDROLYSIS OF CELLULOSE

S. N. **RAŠAJSKI** and **LJ. P. VRHOVAC**

School of Technology and Metallurgy, Beograd

Hydrolysis of cotton cellulose and of regenerated cellulose from cadoxen solution has been investigated. Hydrolysis was carried out with 5N HCl at 0°, 20° and 60°C, for different periods of time. We determined the change in degree of polymerisation of the cellulose by measuring the viscosity of cellulose solutions, and the change of the crystallinity ratio by X-rays. From the experimental results the rate constants and the crystallinity ratio in unhydrolized residue have been calculated for each temperature. The dependence of the change in degree of polymerisation and crystallinity ratio on the time of hydrolysis is shown graphically.

Data are also given for hydrolysis at 20°C of a regenerated mixture of cellulose fraction (DP about 4000) and leveling off cellulose (DP about 250).

ELECTROCHEMICAL OXIDATION OF ß-DIKETONES

M. LAČAN, M. VUKIČEVIĆ and **I. TABAKOVIĆ**

School of Technology, Zagreb, Army Technical High School, Zagreb and Institute of Food Science and Technology, Zagreb

The conditions for the synthesis of 3,4-diacyl-2,5-hexanedione, 3,4-diaroyl-2,5-hexanedione and 2,3-diaroyl-1,4-diaroyl-1,4-butandione by electrochemical oxidation of some β-diketones were studied.

The oxidative dimerization products were obtained in the best yield when the reactions were carried out in 10% solution of potassium hydroxide in 70—90% methanol using a platinum gauze electrode and nickel cathode. The cell was without diaphragm.

Liquid and gas products of electrochemical oxidation were analyzed by gas chromatography.

METHYLENE SULFIDES AND POLYSULFIDE POLYMERS

S. RADOSAVLJEVIĆ, LJ. STAŠIĆ, V. REKALIĆ and M. TENC-POPOVIĆ

Institute of Chemistry, Technology and Metallurgy, Beograd
and Faculty of Technology and Metallurgy, Beograd

Several kinds of methylene sulfide and polysulfide polymers were prepared using formaldehyde and sodium hydrogen sulfide, sodium sulfide, disulfide or tetrasulfide, with and without carbon disulfide, as starting materials. Final products were white, pale yellow and yellow powders, except in two cases when rubbery substances were obtained. Tetrasulfide polymers were desulfurized and then treated with a mixture of sodium hydrogen sulfide and sulfite, in order to strip -S-S- bonding. With increasing molar ratio of formaldehyde, the polymer yield increases.

SOME NEW POLYCHLOROPHENYL POLYSULFIDES

A. ŠAKIĆ, D. RAKIN and Z. BINENFELD

Institute of Chemistry, Technology and Metallurgy, Beograd

Using 1, 2, 3 trichloro-, 1, 2, 4, 5- and 1, 3, 4, 5- tetrachlorobenzene as starting material some new polychlorophenyl polysulfides were obtained as result of the reaction between them and S_2Cl_2 in the presence of Al, Sn and Cu as catalysts. Their structures were determined by elemental analysis, molecular weight and IR spectroscopy.

SOLUBILITIES AND SOLUBILITY PARAMETERS OF (POLY DI-n-ALKYLITACONATES)

J. VELIČKOVIĆ, V. JURANIČEVÀ and **J. VUKAJLOVIĆ**

Institute of Chemistry, Technology and Metallurgy, Faculty of Technology
and Metallurgy, Beograd and Polymer Institute, Slovakian Academy
of Science, Bratislava, Czechoslovakia

The Hildebrandt polymer solubility parameters δ_p of poly (di-n-alkylitaconates) with 1 to 11 carbon atoms in the ester substituents were estimated from solubility tests in more than 30 polar and nonpolar organic solvents, The rather narrow δ_p solubility range of about 9.3 ± 0.2 for poly(dimethylitaconate) expands to 8.5—12 for the next polymer in the series and then contracts gradually, with a pronounced shift towards the region of poorly associa-

ted solvents with low δ_H values. More exact values of solubility parameters were obtained from cloudpoint titrations of dilute polymer solutions after Suh and Clarke (J. Polymer Sci. A-1,5: 1671, 1967) in marginal solvents of the solubility region. All polymers investigated are more soluble in solvents with poor hydrogen bonding; the narrow solubility range of poly(dimethylitaconate) is possibly a consequence of the nonamorphous state of this polymer at ambient temperature.

THE DETERMINATION OF Θ — COMPOSITIONS OF BINARY SOLVENT/NONSOLVENT MIXTURES OF POLY(DI-n-ALKYLITACONATE) SOLUTIONS

V. JURANIČEVÀ and **J. VELIČKOVIĆ**

Polymer Institute, Slovakian Academy of Science, Bratislava, Szechoslovakia,
Institute of Chemistry, Technology and Metallurgy and Faculty
of Technology and Metallurgy, Beograd

Elial's method of extrapolating turbidometric titration results (Makromol.Chem. 78: 58, 1964) was applied to the determination of the Θ — compositions of solutions of poly(dimethyl-), poly(diethy-l), poly(dipropyl-) and higher (di-n-alkylitaconate) polymers in systems with benzene, chloroform, ethyl acetate and butanone as solvent and methanol as nonsolvent. Experiments were performed at 30° in an instrument with automatic registration of the transmitted light and some in a specially adapted octagonal cell for measuring scattered light on a Brice Phoenix photometer. φ_{crit}, the volume fraction of nonsolvent under Θ — conditions, passes through an indeterminate maximum for poly (diethylitaconate) ($\varphi_{crit} > 1$); for polymers of higher diesters the critical volume decreases monotonically: ethyl acetate and butanone change into nonsolvents, while from the φ_{crit} values in systems with benzene and chloroform the solubility of polymers with up to more than 15 C-atoms in the pendant substituents of the poly(methylene) chain can be predicted.

ON THE POSSIBILITY OF PMMA FRACTIONATION BY FRACTIONAL ELUTION OF A COLUMN WITH INERT CARRIER

S. JOVANOVIĆ and S. STANKOVIĆ

School of Technology and Metallurgy, Beograd and Institute of Chemistry,
Technology and Metallurgy, Beograd

Fractionation of PMMA on columns with standard carrier (glass beads, 0.1 mm diam). does not give reliable distribution curves of molecular weights, due to irreversible adsorption of PMMA on the beads. A teflon powder (particles of approximately the same dimensions) was used as a carrier instead of glass beads. Three samples of PMMA (obtained by suspension polymerization) of different molecular weights were fractionated by fractional elution. The distribution curves obtained prove that with this carrier fractionation is successful. This technique, with teflon carrier, can also be used for fractionating polymers which have not so far been successfully fractionated.

ELECTROCHEMICAL INITIATION OF METHYLMETHACRYLATE POLYMERIZATION

S. JOVANOVIĆ, D. ŠEPA, M. VOJNOVIĆ, LJ. ILIĆ
and N. STEVANOV

School of Technology and Metallurgy, Beograd

The electrochemical initiation of methylmethacrylate polymerization was studied in order to find out the mechanism of initiation and obtain a high degree of conversion. The supporting electrolyte was 0.25 N HCl solution and the cathodes were of Hg, Pb, Pt, Ta, Au, Fe, Al or Zn. The influence of temperature, rate of mixing and amount of Fe^{3+} ion in the supporting electrolyte on the rate of polymerization and the molecular weight of the polymer was investigated.

The mechanism of initiation of polymerization is discussed.

THE CONDENSATION REACTIONS BETWEEN 2-FURAN CARBOXYLIC ACID AND 2-BENZOFURANCARBOXYLIC ACID AND AROMATIC AMINES

J. ODAVIĆ-JOSIĆ, B. BASTIĆ and M. PILETIĆ

*School of Technology, Novi Sad, Faculty of Technology and Metallurgy,
Beograd, and Institute of Chemistry, Technology
and Metallurgy, Beograd*

In the condensation reactions of 2-furancarboxylic acid and o-phenylenediamine, o-aminophenol, o-aminothiophenol, 1,2-naphthalenediamine and 1,8-naphtalenediamine, satisfactory results were not obtained and for that reason instead of the free acid its chloride was used for reactions with these amines. The corresponding products were isolated and their structures verified by elemental analysis.

Free 2-benzofurancarboxylic acid did react with the mentioned amines, the reaction products were isolated and their structures verified by elemental analysis.

THE SOLVOLYTIC CYCLIZATIONS OF CYCLODECENYL SYSTEMS

M. LJ. MIHAILOVIĆ, M. GAŠIĆ, M. DABOVIĆ and LJ. LORENC

School of Sciences, Beograd

The solvolytic reactions of stereoisomeric *cis* and *trans* 3β-acetoxy, 10-seco-1(10)-cholesten-5 — p-nitrobenzoate in 90% aqueous acetone at 125° were investigated. It was found that the reactions are stereospecific and result in transannular bond formation between C_1 and C_5, giving, in both cases, 5(10→1βH)*abeo*-5β-cholest-10(19)-en-3β-acetate. Rate measurements show that the *trans* isomer solvolyzes about 15 times faster than the *cis* isomer. These results indicate that solvolysis involves transannular participation of the double bond, and that this interaction, probably due to the conformation, is more pronounced in the *trans* than in the *cis* isomer.

INTRAMOLECULAR CYCLIZATION OF 16-PICOLINYLIDENE-5-ANDROSTEN-17-ONE BY CATALYTIC HYDROGENATION

M. STEFANOVIĆ, **I. V. MIĆOVIĆ**, D. JEREMIĆ and D. MILJKOVIĆ

School of Sciences, Beograd and Institute of Chemistry, Technology and Metallurgy, Beograd

By catalytic hydrogenation of 16-picolinylidene-5-androsten-17-one (80° and 50—60 atm. hydrogen pressure over Pd/C as catalyst) two new isomeric steroid alkaloids were obtained. They are structurally related to the naturally occurring alkaloid solanidine.

THE REDUCTION OF Δ^4-ANDROSTENE-3, 17-DIONE-11 β-OL BY METAL HYDRIDES

M. STEFANOVIĆ, **R. JANKOV** and M. GAŠIĆ

School of Sciences, Beograd and Institute of Chemistry, Technology and Metallurgy, Beograd

The stereochemistry of the reduction of Δ^4-androstene-3, 17-dione-11 β-ol by various reducing agents was investigated. Contrary to earlier results, it was found that both epimeric Δ^4-adrostene-3, 11β, 17 β-triol and Δ^4-androstene-3α, 11β, 17 β-triol are formed, the ratio depending upon the reducing agent. The thermodynamic stabilities of the epimers was investigated.

SULPHONATION OF α-OLEFINES WITH SODIUM BISULPHITE SOLUTION IN THE MIXTURES OF WATER AND ALCOHOLS

S. N. RAŠAJSKI, **S. S. FILIPOVIĆ** and D. U. SKALA

School of Technology and Metallurgy, Beograd and Institute of Chemistry, Technology and Metallurgy, Beograd

α-olefines in water-methyl alcohol, water-ethyl alcohol or water-propyl alcohol solution react with sodium bisulphite in the presence of catalysts which give free radical: oxygen from the air and sodium hypochlorite. The reaction was studied in the temperature range 40—80°C. The concentration of α-olefines in the reaction mixture has no influence on the reaction rate if the concentration of sodium bisulphite is low and constant. It has been proved that the reaction rate has a maximum for a given amount of sodium hypochlorite, which is temperature dependent. The reaction is very fast at low temperature if it is catalysed by air oxygen. Mixtures of the olefines were sulphonated both discontinuously and continuously.

INFRARED SPECTRA OF PRODUCTS COUPLING BETWEEN DIAZONIUM ION AND SOME SYMMETRIC TRIKETONES

D. ŠKARE and **Z. MEIĆ**

Army Technical High School, Zagreb and Ruđer Bošković Institute, Zagreb

Products obtained by coupling diazonium ion with active methylene groups of sym-diaroylacetones (Ar = phenyl, p-tolyl, 2-thienyl) were investigated by means of infrared spectroscopy. The results show that these compounds are rather in hydrazone than in azo-form, as is seen from the positions and intensities of the C=O and C=N stretching absorption bands.

ISOMERISATION OF PERHYDROACENAPTHENE AND TRIMETHYLENE NORBORNANE TO ADAMANTAN AND ITS HOMOLOGUES

D. STEVANČEVIĆ, B. BASTIĆ and B. STEVANČEVIĆ

School of Sciences, Beograd and Institute of Chemistry, Technology and Metallurgy, Beograd

The effect of temperature and catalyst on the isomerisation of trimethylenenorbornane into adamantan was investigated. The most suitable catalyst for this reaction was found to be $AlCl_3$+t-butilbromide giving a maximum content of adamantan of nearly 35% after 60 min at 80°C.

The isomerisation of perhydroacenaphthene into 1,3-dimethyladamantan in the presence of aluminum halogenide catalysts was also studied. By gas chromatography on a 50 m polyphenylether column it was established that the final products of the reaction are 1-ethyladamantan isomerising into 1,3-dimethyladamantan and that in certain phases of the reaction about 15 intermediates are present, changing successively into one another.

SCALED MAXIMUM OVERLAP CALCULATIONS ON NORBORNENE AND SOME RELATED MOLECULES

M. ECKERT-MAKSIĆ, Z. B. MAKSIĆ and M. RANDIĆ

Boris Kidrič Institute of Nuclear Sciences, Vinča, Beograd

Electronic structure of norbornene and some related molecules was studied by the scaled maximum overlap method. The parameters of the resulting localised orbitals were correlated with available experimental data. Very close agreement with experimental data was obtained for J_{C-H} spin-spin coupling constants, chemical shifts and molecule geometry.

THE COUPLING OF DIAZONIUM ION WITH SYMMETRIC TRIKETONES

M. LAČAN and D. ŠKARE

Army Technical High School, Zagreb

Continuing research on reactions of diazonium salts with compounds containing active methylene groups, we have carried out the coupling of benzenediazonium cloride with symmetric triketones Ar—CO—CH_2—CO——CH_2—CO—Ar (Ar = phenyl, p-tolyl, 2-thienyl) in methanolic sodium hydroxide solution buffered with sodium acetate. Under these conditions derivatives of 1,5-diaryl-1, 2, 3, 4, 5-pentanpentones were obtained, because azo-tohydrazone conversion occurred during the coupling. Compounds not previously described were identified on the grounds of the elemental analysis and IR, UV and VIS spectra.

HYBRIDIZATION OF SOME DERIVATIVES OF CYCLOBUTENE

M. RANDIĆ and LJ. VUJISIĆ

Ruđer Bošković Institute, Zagreb and Boris Kidrič Institute of Nuclear Sciences, Beograd

The electronic structure of some derivates of cyclobutene was studied by the metod of maximum overlap using Clementi atomic orbitals, under the assumption that the bond energies are proportional to the corresponding overlap integrals. The bending of bonds in the ring was confirmed in all molecules. By comparing the results for cyclobutene and those for its derivatives with exocyclic double bonds, rehybridization of the carbon skeleton was proved.

V. METALLURGY

SELECTIVE Mn REDUCTION IN CAST IRON

R. ŠOTRA and D. MITKOV

Motor and Tractor Factory, Novi Beograd

Direct production of ferittic nodular iron requires basic metal with low Mn (less than 0.30%). To examine possible alternatives for special low Mn pig iron, selective reduction of Mn in cupola metal in ladle was studied.

Pyrite in quantities of 0.5%—1.7% provided an efficiency of Mn reduction from 26 to 60%. Carbon and silicon contents were practically not influenced by the treatment. Increase in S was substantial, but S is normally reduced during the later phases of nodular iron production. It is further planned to examine the influence of possible inhibitors on spheroidal graphite formation.

MAGNETIC ANNEALING PHENOMENA IN METASTABLE Fe—Cu SOLID SOLUTIONS

R. M. SOFRENOVIĆ

Boris Kidrič Institute of Nuclear Sciences, Vinča, Beograd

An electron transmission study of metastable Fe—Cu solid solutions prepared by "quenching" from the vapor phase provided strong evidence that the decomposition process at elevated temperatures is significantly decreased by the presence of a magnetic field. The precipitation of copper was decreased by about three times probably due to an increase of the collision frequency factor. The latter was caused by the magnetic field being perpendicular to the main direction of diffusion of iron and copper atoms, in the direction of film thickness.

MICROSTRUCTURE AND MICROHARDNESS OF PLASMA-SPRAYED TUNGSTEN CARBIDE COATINGS ON GRAY CAST IRON

M. J. PAVLOVIĆ and I. M. KLEJN

Boris Kidrič Institute of Nuclear Sciences, Vinča, Beograd

Tungsten carbide coatings were plasma-sprayed on graw cast iron. The microstructure and microhardness of three types coating of different initial chemical composition were studied. From the results obtained, the possibilities for application of these coatings are analysed.

$BaSO_4$ IN THE PRESENCE OF BASIC BLAST FURNACE BURDEN COMPONENTS

A. MARKOTIĆ

School of Technology, University of Zagreb, Metallurgical Department, Sisak

The presence of $BaSO_4$ in burden ore cause trouble in blast furnace operation and complicates the procedure of smelting.

The breakdown temperature of $BaSO_4$, i.e. the temperature of its crystallographic transformation, has been investigated, and the results provides basis for the detailed explanation of the behavior of $BaSO_4$ in the presence of the basic burden components, primarly C (coke), Fe_2O_3, SiO_2, MgO, CaO, Al_3O_3 . . . .

The experiments involved the destruction of $BaSO_4$ outside the blast furnace, and the results have been applied to $BaSO_4$ — containing iron ore from Vareš, on which the destruction of $BaSO_4$ was directly observed.

STABILITY OF BODY-CENTERED CUBIC STRUCTURE IN METALS AND ALLOYS

M. JOVANOVIĆ

Boris Kidrič Institute of Nuclear Sciences, Vinča, Beograd

The effect of solute substitution in 52.5 at % Au-Cd alloy at an electron concentration of 1.475 has been studied to determine the stability of the β-phase in the presence of elements of various atomic and ionic size, valency and electronegativity. It is shown that a simple explanation of β-phase stability in terms of readily available parameters is not possible.

The elastic constants of some single-crystal β-phase alloys were also measured, to correlate them with β-phase stability. A relationship has been discovered between β-phase stability (measured in terms of the M temperature) and the shear resistance [110] [110].

SYNTHESIS OF WÜSTITE (FeO)

M. PRELOŠČAN

Institute of Metallurgy, Sisak

In order to get pure wüstite, which is necessary in the quantitative determination of iron oxides by X-ray diffraction, three types of laboratory experiment were conducted:

1 hydrogen reduction of pure hematite at 800°C.

2. heating a stoichiometric mixture of iron and magnetite powder at 900°C in a neutral atmosphere and rapid cooling

3. heating Fe_2O_3 and Fe mixture at 900°C in a nitrogen atmosphere

Insufficiently rapid cooling is the difficulty of the first method, and because of which some wüstite decomposes into Fe_3O_4 and Fe.

By the second method wüstite of satisfactory punity was obtained (99,6% FeO; 0,4% Fe) but because magnetite first has to be produced in the laboratory, the process is rather difficult.

The third method is the most economical, since hematite and iron powder are easily obtained, the procedure is rather quick and it gives the best results.

CHARACTERISTIC OF THE LAYER ADHERING TO THE DECANTED SOLID-LIQUID INTERFACE

Đ. MILOSAVLJEVIĆ

Boris Kidrič Institute of Nuclear Sciences, Vinča, Beograd

In the study of the morphology of the solid-liquid interface decanting is still the most widely used technique. However a layer of the melt adheres to the decanted interface and masks the finer details. Up to now, endeavors have been focussed mostly on getting the adherent layer as thin as possible, neglecting its characteristics.

In this work the structure of the adherent layer as a function of some solidification parameters (temperature gradient at the interface and rate of interface advance) has been studied. It was found that the structure of this layer depends upon cooling conditions but also upon the width of the interface. With increase of the ratio G/R, the boundary between the specimen and the frozen adherent layer becomes sharper.

QUANTITATIVE DETERMINATION OF IRON OXIDE BY X-RAY DIFFRACTION

V. NOVOSEL — RADOVIĆ

Institute of Metallurgy, Sisak

By quantitative analytical chemistry it is usually very difficult to distinguishing the chemical indentity of various phases in a mixture and determine them. X-ray diffraction analysis is much more convenient, since each component of the mixture produces its characteristic pattern independent of the others. The intensity of each component's pattern is proportional to the amount present, so that quantitative analysis can be developed. For example, analytical determination of iron oxides in the presence of other components becomes routine by diffraction, but difficult or impossible by chemical methods.

A method of quantitative iron oxide analysis on a scintillation counter X-ray diffraction spectrometer has been developed. It eliminates many of the difficulties of the chemical methods and is appliciable to a wide variety of mineral powders over a range of a few percent. The method is particularly suited to rapid analysis required in monitoring reduction processes, plant output or desired for research.

The method in non-destructive.

Calcium fluoride is employed as an internal standard. The accuracy of the analysis is affected by the following factors:

a) reproducibility

b) particle size of iron oxides

c) line coincidences

These factors are discussed and it is concluded that the major shortcoming is lack of reproducibility, probably due to inhomogenity of the mixture of sample ore, sinter, scale and internal standard.

THE APPLICATION OF DOMESTIC PRODUCTS IN METALLOGRAPHY

B. LUKIĆ and Đ. MILOSAVLJEVIĆ

Boris Kidrič Institute of Nuclear Sciences, Vinča, Beograd

The possibility of metallographic preparation of some metals and alloys (copper, tin, zinc, brass, bronze, new silver, stainless steel, gray cast iron and aluminum alloys) with materials produced in Yugoslavia has been studied. It was found that some domestic polishing pastes can be used in metallography. The polishing effects of these pastes were compared and optimum conditions for their use are suggested.

It is shown that by using selected domestic products (mounting resin, cloths, felts and polishing pastes) and foreign products which are always available on the market (emery papers), one can get specimens quite satisfactory for metallografic analysis. Therefore there is no need to import the expensive materials for metallography.

TEMPERATURE DEPENDENCE OF MODULS OF ELASTICITY OF ZIRCALLOY-4

Ž. SPASIĆ and G. SIMIĆ

Boris Kidrič Institute of Nuclear Sciences, Vinča, Beograd

This research was necessary for the development and testing of nuclear fuel elements. The temperature law of the moduls of elasticity of Zircalloy-4 is determined and described. The results obtained for the temperature range 27°—400°C are compared with similar data from the literature.

EFFECT OF FATIGUE ON MICROSTRUCTURE OF Zr-1.5 WT% Sn

V. M. STEFANOVIĆ, O. NEŠIĆ and Ž. SPASIĆ

Boris Kidrič Institute of Nuclear Sciences, Vinča, Beograd

The effect of pure one-direction cyclic loading on the tensile properties and microstructure of Zr-1,5 wt.% Sn alloy (Zircalloy-2) was examined. The loading was in the range of elastic and plastic strains. The results of tensile testing indicate that the alloy is only slightly hardened by low or high cycling fatigue. Microstructural changes were studied by optical and transmission electron microscopy. An increase of dislocation density in the alloy was observed.

PHYSICO-CHEMICAL PROPERTIES OF ELECTROLYTE FOR ELECTROLYTIC COPPER REFINING

S. ĐORĐEVIĆ, M. PJEŠČIĆ, Z. STANKOVIĆ and V. DUNJIĆ

School of Technology and Metallurgy, Beograd, Faculty of Mining and Metallurgy, Bor and Copper Institute, Bor

In order to find out the optimum conditions for electrolytic copper refining the following properties of the electrolyte were determined: 1. — conductivity; 2. — density; 3. — viscosity; and 4. — vapor pressure. All

these parameters were measured in the temperature range 45 to 75°C, a copper concentration range 0.5 to 1.0 moles per liter and a sulphuric acid concentration between 1.5 and 2.5 moles per liter. From the results the temperature dependences of the conductivity, density, viscosity and vapor pressure are derived.

CELL VOLTAGE DISTRIBUTION ON TANKS FOR ELECROLYTIC COPPER REFINING

V. DUNJIĆ, M. JUŠČEK and S. ĐORĐEVIĆ

Copper Institute, Bor and Faculty of Technology and Metallurgy, Beograd

The cell voltage on tanks for electrolytic cooper refining in Bor was measured over one year and its distribution on counter e.m.f., electrolyte, electrodes, bas-bars and various sorts of contacts was determined. The results are discussed regarding electric power economization.

VACUUM COPPER — PRODUCTION METHODS AND PROPERTIES

I. STOJŠIĆ, S. TODOROVIČ and Lj. GLIŠOVIĆ

Institute for Technology of Nuclear and Other Mineral Raw Materials, Beograd and Cable Factory, Svetozarevo

The metallurgy laboratory of the Institute for Technology of Nuclear and Other Mineral Raw Materials is carrying out research concerning the refining effect of vacuum remelting of copper cathodes from RTV—Bor as a function of parameters of induction, arc and electron beam melting. Simultaneously, the Metallurgy laboratory of the Research and Development Center of the Moša Pijade Cable Factory is carrying out a program of determination of the range of characteristics of vacuum-melted copper.

The report gives the first results concerning the refining effects of the methods of copper vacuum melting tested and some measurements of physical, mechanical and metallurgical properties of vacuum-melted cathode copper.

THE EFFECT OF ANODE COPPER ON THE PROPERTIES OF ELECTROLYTIC COPPER POWDER

J. DIMITRIJEVIĆ and S. ĐORĐEVIĆ

Copper Institute, Bor and Faculty of Technology and Metallurgy, Beograd

Anode copper for electrolytic production of copper powder is cathode copper from electrolytic copper refining or wirebars. Electrolytic copper includes surface active substances which are added during electrolytic refining. During annodic dissolution of the copper all these substances are released into the electrolyte. By titration with potassium permanganate it was found out that the quantity of organic substances in the electrolyte increases with the time of electrolysis.

Particle size distribution, apparent density and fluidity were different for copper powder obtained under the same conditions from anode copper of various origins.

REFINING SULFURIC ACID AND AMMONICAL SOLUTIONS OF NICKEL FROM COPPER

V. KNEŽEVIĆ and M. TOMAŠEVIĆ

Institute for Technology of Nuclear and Other Mineral Raw Materials, Beograd

Leaching laterite ore of nickel with sulphuric acid and leaching nickel concentrate with ammonia yield solutions which contain some cooper. To remove copper from the acid solutions we studied both the method of cementation by active nickel powder and precipitation with hydrogen sulphide. We also studied the possibility of cementing copper from ammonical solutions of nickel.

The concentration of copper in solutions after cementation is 7—8 mg/lit and when doing the cementation from ammonical solutions it is necessary to use a closed system at 80°C.

The removal of copper from sulphuric acid solutions of nickel by precipitation with hydrogen sulphide is more effective than cementation by active nickel powder. The concentration of copper in solution after precipitation is 0.02 mg/lit. The process can be readily monitored via the potential change of an indicator platinum electrode conected with a saturated calomel reference electrode.

EQUILIBRIUM DISTRIBUTION OF COBALT AND NICKEL WITH ALKYLPHOSPHORIC ACID AND α-HYDROXYOXIMES IN LIQUID EXTRACTION OF METALS FROM SULPHATE SOLUTIONS

V. ŽIVANOVIĆ

Institute for Technology of Nuclear and Other Mineral Raw Materials,
Beograd

Liquid-liquid equilibrium data have been obtained for the distribution of cobalt and nickel between aqueous sulphate solutions and kerosene solutions of D_2EHPA and Lix 63. The efficiency of cobalt and nickel extraction was examined as a function of: pH, organic solvent composition, phase ratio, contact time and other parameters.

It was found out that nickel and cobalt could be separated with a suitable mixture of these two extractants in kerosene. The best separation coefficient was obtained at pH 1.5.

The investigations were performed with leach liquors of nickel ore from Goleš.

DETERMINATION OF THE EFFECTIVE DISTRIBUTION COEFFICIENTS OF IMPURITIES IN LEAD REFINING BY ZONE MELTING

D. ĐURKOVIĆ and S. PETROVIĆ

Institute for Technology of Nuclear and Other Mineral Raw Materials,
Beograd

Using the transition point method the effective distribution coefficients of a number of impurities in lead during its refining by zone melting have been determined. Refining was done at travel rates of 0.8; 0.6 and 0.4 mm/min. By extrapolation to zero rate the equilibrium distribution coefficients were determined. For analysis of impurity distribution the spectrographic method was used. We also determined the maximum possible errors of the effective distribution coefficients.

THERMAL DECOMPOSITION OF MOLYBDENUM PENTACHLORIDE

D. ĐURKOVIĆ

Institute for Technology of Nuclear and Other Mineral Raw Materials, Beograd

The rate of thermal decomposition of molybdenum pentachloride was investigated. Solid molybdenum pentachloride was evaporated at 100 to 150°C and decomposed on a resistance-heated molybdenum filament and graphite ring with removal of chlorine.

From the test results, the order and specific rate of the decomposition reaction in the kinetic range and the energy of dissociation of molybdenum pentachloride have been determined.

The refinement of molybdenum obtained by this method is analysed.

LEACHING OF URANIUM DURING ORE GRINDING

N. VRAČAR and **D. MILIĆ**

Institute for Technology of Nuclear and Other Mineral Raw Materials, Beograd

Uranium ore grinding with a "pebble" grinding charge in the presence of sulphuric acid solution was investigated. During this procedure simultaneous leaching of uranium takes place. The first series of experiments was done using 1 kg of the ore, 2.5 kg of "pebble" grinding charge and a solid: liquid ratio of 2 : 1 in a laboratory porcelain mill. Subsequent experiments were done in an iron mill lined with acid-resistant hard rubber. The feed was 5 kg ore with 10 kg "pebble" and a solid: liquid ratio 2 : 1.

The dependence of uranium solubility on grinding time and the sulphuric acid concentration was studied. Under the conditions investigated a 60—90% yield of uranium was obtained.

A STUDY OF THE POSSIBILITY OF SEPARATING URANIUM FROM INDUSTRIAL PHOSPHORIC ACID

M. LAZAREVIĆ and A. DELEON

Institute for Technology of Nuclear and Other Mineral Raw Materials, Beograd

The aim of this was to investigate the possibility of separating uranium from the phosphoric acid produced by wet sulphuric acid dissolution of phosphate bearing rocks. This acid with 28—32 mgr/lit P_2O_5 is a potential reservoir of uranium. Uranium was extracted from it by liquid-liquid extraction with organo-phosphorous compounds. Special attention was devoted to the influence of fluorine and the EMF on the uranium distribution coefficient.

So far the following extracting media have been tried: DDPA, MBPA, DBRA, DZEHPA, and kerosene. Under the optimum extraction conditions best results were obtained with DDPA. The uranium was separated from the organic phase with concentrated sulphuric acid.

VI. CHEMICAL ENGINEERING

A SURVEY OF AND PROPOSALS FOR BASIS TERMS IN CHEMICAL ENGINEERING

S. KONČAR-ĐURĐEVIĆ, A. TASIĆ and B. ĐORĐEVIĆ

School of Technology and Metallurgy, Beograd and Institute of Chemistry, Technology and Metallurgy, Beograd

Some important new basic terms with corresponding definitions are proposed. The terms aim to achieve exactness of concept while being in spirit of the language. Most of the technical and chemical engineering terms at present used in Yugoslavia are accepted without discussion.

METHODS OF CALCULATING DIFFUSION COEFFICIENTS FOR BINARY AND TERNARY NON-ELECTROLYTIC SOLUTIONS

I. JUSTINIJANOVIĆ, B. ĐORĐEVIĆ, A. TASIĆ and D. SIMOVIĆ

Institute of Chemistry, Technology and Metallurgy, Beograd, and Faculty of Technology and Metallurgy, Beograd

The knowledge of the mutual diffussion coefficients and ternary diffusion coefficients at all concentrations is very important for determination of binary and ternary three dimensional graphs of diffusion coefficient against concentration.

The applicability of some methods for calculating binary and ternary diffusion coefficents has been examined. The results are compared and are found to agree with experiment.

ANALYSIS OF BINARY DIFFUSION MEASUREMENTS IRREVERSIBLE THERMODYNAMICS

B. ĐORĐEVIĆ, A. TASIĆ, N. AFGAN and D. MALIĆ

*School of Technology and Metallurgy, Beograd, Institute of Chemistry,
Technology and Metallurgy, Beograd, and Boris Kidrič Institute
of Nuclear Sciences, Vinča*

Diffusion in binary non-electrolytic solutions has been studied by the method of linear nonequilibrium thermodynamics.

It is shown that the phenomenological coefficients can give information about both ideal and non ideal systems and also about systems with associating polymers and compound formation.

The thermodynamic treatment is based on our experimental investigation of ideal and non ideal binary systems.

THE ONSAGER RECIPROCAL RELATION FOR TERNARY ISOTHERMAL DIFFUSION IN NON-ELECTROLYTIC LIQUID SYSTEMS

B. DIMITRIJEVIĆ, A. TASIĆ, D. NASTOVIĆ, N. AFGAN and D. MALIĆ

*School of Technology and Metallurgy, Beograd, Institute of Chemistry,
Technology and Metallurgy, Beograd, and Boris Kidrič Institute
of Nuclear Sciences, Vinča*

Onsager's reciprocal relation for the ternary diffusion of nonassociating systems is discussed. It is shown that coefficients of ternary diffusion and the phenomenological coefficients may be determined from experimental measurements of the friction coefficients. It can be concluded that the hydrodynamic approach should play an important role in describing multicomponent diffusion.

APPLICATION OF SIGNAL FLOW GRAPH TO ANALYSIS OF ABSORPTION DYNAMICS

M. BOGOSAVLJEVIĆ and M. POPOVIĆ

School of Technology, Novi Sad

This paper presents a topological method using a signal flow graph for the dynamic characteristics of absorption. Using a mathematical model it is possible to give a simplified representation of the dynamic pattern in a multistage absorption column.

POSSIBILITIES OF APPLYING ZIGZAG SYSTEM FOR SIMULTANEOUS DRYING AND GRADING

B. PEROVIĆ

Institute of Chemistry, Technology and Metallurgy, Beograd

One of the main disadvantages of conventional drying is unequal final moisture distribution. Many attempts have been made to overcome this disadvantage, mainly based on the discovery that the larger and wetter, (i. e. heavier) particles stay longer in the gaseous fluid flow of the mass and heat carrier.

Analyzing the kinetics of particle motion in a zigzag system the author arrives at the conclusion that such a system could be satifactory for pneumatic drying. This application gains in significance when combined simultaneously with grading for which zigzag systems are already applied. This would offer the possibility of using one apparatus, based on the zigzag principle instead of two as up to now.

EFFECT OF JET DISTRIBUTION ON THE STATE OF GAS-SOLID SPOUTED BED

D. V. VUKOVIĆ and R. MILJKOVIĆ-NAPESKA

School of Technology and Metallurgy, Beograd and Institute of Chemistry, Technology and Metallurgy, Beograd

In a gas-solid spouted bed of monodispersed glass beads the influence of air jet distribution on the pressure drop in the bed, spouting velocity and the mixing of solid particles was investigated. Correlations between the characteristic parameters of the system are presented.

FLOW PATTERN OF A LIQUID-SOLID SPOUTED BED

D. V. VUKOVIĆ and **F. POPOVSKA**

School of Technology and Metallurgy, Beograd and Faculty of Technology and Metallurgy, Skopje

The hydrodynamics of a water spouted bed with spherical glass beads was determined. The influence of packed bed depth on the pressure drop, spouting and mixing of the beads was investigated.

Correlations for the spouting velocities are derived.

HYDRODYNAMIC INVESTIGATIONS OF SCALED UP PUMP-MIX EXTRACTOR. POWER NUMBER AND HOLD UP OF DISPERSED PHASE

M. PERUNIČIĆ, V. PAVASOVIĆ, A. TOLIĆ and A. ČERMAK

Boris Kidrič Institute of Nuclear Sciences, Vinča, Beograd
and UJV Rež, Prague, Czechoslovakia

Hydrodynamic tests on three unit stages of the mixer settler made it possible to analyze a dimensional equation for the power number of the form.

$$N_p = f(Re, Er, L/D)$$

Using the above equation, experimental relationships were derived enabling calculation of the power for different operating conditions.

Preliminary hydrodynamic investigations of the mixer settler showed that the hold-up of dispersed phase in the mixing chamber depends on the geometry and hydrodynamic parameters, so that it can be represented in the form:

$$\frac{V_d}{V_o} = f(V_d, \; 1/V_o, \; D, \; L, \; n, \; p, \; Q)$$

Dimensional analysis of this dependence yields a dimensional equation of the form

$$\frac{V_d}{V_o} = g\left(\frac{p\,Q\,L}{V_o\,n\,D}\right)$$

By using the experimental results it is shown that the above equation has the simple form

$$\frac{V_d}{V_o} = A_o\left(\frac{p\,Q\,L}{V_o\,n\,D}\right)^{K_o}$$

The constant A_o and the exponent K_o were determined for operating conditions requiring a uniformity of mixing of over 90% since this is the sort of value needed for practical applications.

HYDRODYNAMIC INVESTIGATIONS OF SCALED-UP PUMP-MIX MIXED SETTLERS. UNIFORMITY OF MIXING AND MIXING INDEX

V. PAVASOVIĆ, M. PERUNIČIĆ, A. TOLIĆ and A. ČERMAK

Boris Kidrič Institute of Nuclear Sciences, Vinča, Beograd
and UJV Rež, Prague, Czechoslovakia

Scale-up of the laboratory Pump Mix mixer settler was performed according to the principles of similarity. Parameters obtained by a theoretical study of the scale-up made it possible to construct and build the unit stages of extractor on which comparative hydrodynamic investigations were made.

This paper gives the results of some hydrodynamic experiments relating to the uniformity of mixing which was experimentally determined by the homogeneity method for a two-phase liquid system. The results are shown in dependence on geometrical characteristics of the extractor, r. p. m. of the agitator, dispersed to continuous phase flow rate ratio and total volumetric flow rate.

From an analysis of the results a dimensional correlation dependence between the uniformity of mixing and the above geometrical and hydrodynamic parameters has been derived.

DETERMINATION OF DENSITY OF VOLATILE LIQUID MIXTURES BY THE MAGNETIC FLOAT METHOD

A. TASIĆ, **P. PAVLOVIĆ** and B. ĐORĐEVIĆ

School of Technology and Metallurgy, Beograd, Boris Kidrič Institute
of Nuclear Sciences, Vinča, and Institute of Chemistry,
Technology and Metallurgy, Beograd

A magnetic float apparatus for the determining the density of volatile liquid mixtures has been constructed, and tested on the binary mixtures acetone-benzene, benzene-carbon tetrachloride and acetone-carbon tetrachloride. It is possible to measure densities in the range 0.75—1.6 g/cm^3 using two floats. The sample necessary for measurement is 10 cm^3. The overall maximum error of measurement is $\pm$ 1.1 × 10^{-3} g/cm^3.

DETERMINATION OF THE VAPOR-LIQUID EQUILIBRIUM DATA FOR THREE-COMPONENT SYSTEMS

A. TASIĆ, B. ĐORĐEVIĆ, **D. BUKUR** and D. SIMONOVIĆ

School of Technology and Metallurgy, Beograd and Institute of Chemistry, Technology and Metallurgy, Beograd

The isobaric vapor-liquid equilibrium data were determined experimentally for three binary systems whose components are constituents of a ternary system. The data obtained are thermodynamically verified. From them the vapor-liquid equilibrium parameters for the corresponding ternary system are derived by a graphical-analytical method.

TEMPERATURE FLUCTUATION MEASUREMENT IN TWO-PHASE BOUNDARY LAYER

LJ. JOVANOVIĆ, V. PIŠLAR, M. STEFANOVIĆ and N. AFGAN

Boris Kidrič Institute of Nuclear Sciences, Vinča, Beograd

The temperature fluctuation in a two-phase boundary layer was measured with a low-inertia thermocouple. By statistical processing of the thermocouple signal temperature distribution functions in the two-phase steam-water mixture were obtained. From the distribution the most probable temperatures of each phase at different distances from the heated surface in a pool boiling of water are calculated. Frequency analysis of the signal yields the spectral power density as a function of frequency for different locations of the thermocouple.

GASEOUS CURTAINS FOR PREVENTING OIL FILM SPREADING ON LIQUID SURFACE

F. ZDANSKI, S. KONČAR-ĐURKOVIĆ and V. VUČKOVIĆ

School of Technology and Metallurgy, Beograd and Institute of Chemistry, Technology and Metallurgy, Beograd

Investigations were conducted to evalute ways of preventing an oil film spreading on the surface of water. The oil film was compressed by means of an air curtain. This barrier allows free passage of objects and free flow of the bulk liquid.

THE ROLE OF PROFESSIONAL ASSOCIATIONS, SOCIETIES AND UNIONS IN THE APPLICATION AND PREPARATIONS OF LEGAL REGULATIONS IN THE FIELD OF INDUSTRIAL PROPERTY PROTECTION

V. KOPTA

Yugoslav building center, Beograd

Laws and Rules from the field of industrial property protection regulate relations ruling in economy. These relations change according to the degree of development both in economy and in society as a whole. Therefore, it is necessary for professional quorums from industry to give their own judgement about the development and to suggest adequate measures which will characterize this phase of the development, so that the laws brought against these judgements could represent real relationships between the working capacities in our society.

To illustrate this, several characteristic examples of such actions in the world practice of industrial property protection have been given.

Izdavač:
IZDAVAČKO PREDUZEĆE "NOLIT", BEOGRAD, TERAZIJE 27/II

*

Štampa:
GRAFIČKO PREDUZEĆE "PROSVETA", BEOGRAD
ĐURE ĐAKOVIĆA 21

SRPSKO HEMIJSKO DRUŠTVO (BEOGRAD)

BULLETIN OF THE CHEMICAL SOCIETY
Belgrade

(Glasnik Hemijskog društva — Beograd)

Vol. 35, No. 2-3, 1970

Editor:
ALEKSANDAR DESPIĆ

Published by
SRPSKO HEMIJSKO DRUŠTVO (BEOGRAD)
1970

Translated and published for U.S. Department of Commerce and
the National Science Foundation, Washington, D.C., by
the NOLIT Publishing House, Terazije 27/II, Belgrade, Yugoslavia
1971

Translated bv
PAVEL ČMELIK

Edited by
PAUL PIGNON

Printed in "Prosveta", Beograd

CONTENTS

GLASNIK HEMIJSKOG DRUŠTVA, Vol. 35, No. 2-3, 1970, pp. 203—207

GHDB-93 535.34-1:547.869

Original Scientific Paper

INFRARED SPECTRA OF 2-THIONOTHIAZOLIDINE-4-ONES. THE EFFECT OF THE THIONO GROUP ON THE AMIDE CARBONYL FREQUENCY

by

ALEKSANDRA M. STOJILJKOVIĆ, RUŽICA M. TASOVAC
and ALEKSANDAR M. JOKIĆ

In the course of an investigation on thiazolidine chemistry⁽¹⁾ we have studied the infrared spectra of a series of 2-thionothiazolidine-4-ones, and in this paper we report on the position of the thiono and the amide carbonyl frequency in the spectra of these compounds. We have also carried out a correlation of the infrared spectra of thiazolidine-4-ones and imidazolidine-4-ones, based on the literature data.

Published data on the position of the thiono (C = S) stretching frequency in various systems show that it is not precisely localized and that it depends greatly on the structural environment; it can vary within the range 1550—850 *cm*$^{-1}$ (2). According to C.N.R. Rao and R. Venkataraghavan(3) it seems necessary to distinguish two groups of thiono derivatives: one in which the thiono group is linked to atoms such as carbon, sulphur and oxygen, and the other in which it is linked to one or two nitrogens. However, in 2-thionothiazolidine-4-ones the thiono group is linked to a sulphur atom on one side and to nitrogen on the other.

In the spectra of the 3,5-disubstituted and 3,5,5-trisubstituted 2-thionothiazolidine-4-ones listed in Table I we observed strong absorption bands in the 1300—1100 *cm*$^{-1}$ region. Regardless of the substituent all these compounds exibited very intense absorption (comparable to that of a carbonyl) in the 1250—1200 *cm*$^{-1}$ region, and a second much weaker absorption in the 1150—1100 *cm*$^{-1}$ region. The corresponding thiazolidine-4-ones, obtained by Raney nickel desulphurization of the thiono group(1), exhibited no intense bands in these regions, but comparatively weak absorptions which are probably due to different deformation vibrations. No other bands characteristic of the thiono group and absent from the spectra of thiazolidine-4-ones were observed. On the basis of this evidence, the bands appearing in the 1250—1200 *cm*$^{-1}$ and in the 1150—1100 *cm*$^{-1}$ regions may be assigned to the stretching frequency of the thiono group in 2-thionothiazolidine--4-ones.

On the other hand inspection of the spectra of 2-thionothiazolidine--4-ones revealed a rather high frequency for the amide carbonyl. All 3,5-disubstituted and 3,5,5-trisubstituted derivatives listed in Table I showed an intense amide carbonyl absorption in the 1750—1700 *cm*$^{-1}$ region, loca-

TABLE 1

2-Thionothiazolidine-4-ones Whose Infrared Spectra Were Studied

A.

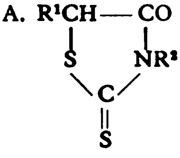

R^1:	R^2:
CH_3—	C_6H_5—
C_2H_5—	C_6H_5—
C_3H_7—	C_6H_5—
CH_3—	p-$CH_3C_6H_4$—
C_2H_5—	p-$CH_3C_6H_4$—
C_3H_7—	p-$CH_3C_6H_4$—

3,5-Disubstituted 2-thionothiazolidine-4-ones

B.

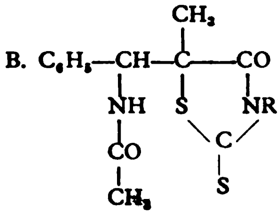

R^2: C_6H_5—
p-$CH_3C_6H_4$-
p-$CH_3CONHC_6H_4$—

(both diastereoisomers in each case)

3,5,5-Trisubstituted 2-thionothiazolidine-4-ones

lized at 1735 *cm*$^{-1}$ in the most of the derivatives (normal-chain amide band usually appears below 1700 *cm*$^{-1}$). At first glance this high amide carbonyl could be ascribed to strain effects of the five-membered ring. If this were true, the corresponding thiazolidine-4-ones would also be expected to exhibit a high amide carbonyl. However, the products obtained by desulphuration of the thiono group of compounds listed in Table I (1) showed normal amide carbonyl absorptions in the 1670—1640 *cm*$^{-1}$ region. Valuable evidence was obtained from 3,5,5-trisubstituted derivatives in which one substituent possessed an open-chain amide carbonyl (compounds B in Table I): the spectra of these compounds showed two amide carbonyl peaks, one above and the other below 1700 *cm*$^{-1}$. In the spectra of the corresponding 2-methylene compounds the latter frequency remained unchanged and was therefore assigned to open-chain amide carbonyl, and the former was replaced by a new peak which was close to the open-chain amide carbonyl but always appeared at a somewhat higher frequency, probably due to some steric effects.

The observed values of the amide carbonyl frequency of the compounds listed in Table I are in agreement with the spectra of 2-thionothiazolidine-4-ones reported by other authors⁽⁴⁾. Reviewing the spectra of 2-alkylthiazolidine-4-ones we found that the amide carbonyl frequency in these derivatives appears below 1700 *cm*$^{-1}$, in the 1680—1660 *cm*$^{-1}$ region⁽⁵⁾. In the case of pseudothiohydantoin, in which the thiono group is replaced by an imino group, the amide carbonyl appears at 1655 *cm*$^{-1}$ ⁽⁶⁾. These findings suggest that not strain but the thiono group is responsible for shifting the amide carbonyl to above 1700 *cm*$^{-1}$.

To get evidence about whether the effect of the thiono group on the position of the amide carbonyl is specific for the thiazolidine ring or not, we tried to correlate our results with those reported for other azolidine-4-ones. Unfortunately the only available data were those referring to imidazolidine-4-one derivatives. In the spectra of 2-thionoimidazolidine-4-ones the amide carbonyl was found to be high, in the 1770—1740 cm^{-1} region (7), whereas the corresponding 2-methylene derivatives display a strong amide carbonyl at lower wave numbers 1710—1690 cm^{-1} (8).

On the basis of the above data it is evident that the thiono group is the main factor shifting the amide carbonyl to higher frequencies. A possible explanation would be as follows: the position of the amide carbonyl is primarily governed by the polarity of the carbonyl. In thiazolidine-4-ones and imidazolidine-4-ones the polarity of the carbonyl is decreased by the presence of nitrogen, as in all amides. However, where there is a thiono group adjacent to the nitrogen it interacts with nitrogen, inhibiting the conjugation of carbonyl with nitrogen, increasing the polarity of the carbonyl and shifting it to a higher frequency. The increased polarity of the carbonyl due to the presence of a thiono group in the 2-position is also manifested in the increased chemical reactivity of hydrogens of the 5-methylene group in different azolidine-4-ones, as established by S. N. Baranov(9).

One can postulate resonance stabilization between the main resonance structures:

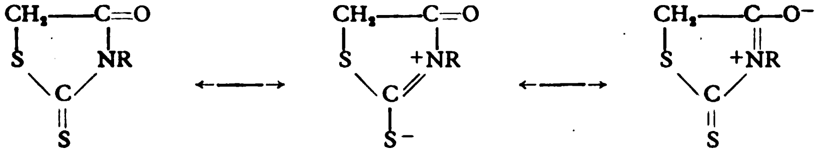

(a) (b)

Since sulphur is a third period element it forms double bonds less readily than oxygen*, which is a second period element, and the C = S bond has a greater tendency towards a partial single bond character. Therefore the contribution of the resonance structure (a), which increases the polarity of carbonyl, is greater than that of the resonance structure (b). This contribution is manifested in a shift of the amide carbonyl of 2-thionothiazolidine-4-ones and 2-thionoimidazolidine-4-ones to higher frequencies in comparison with the amide carbonyl of the corresponding 2-methylene derivatives.

EXPERIMENTAL

3,5-disubstituted and 3,5,5-trisubstituted 2-thionothiazolidine-4-ones (Table I) were prepared according to procedures described in previous publications(1). The corresponding thiazolidine-4-ones were obtained by Raney-nickel desulphurization of the thiono group(1).

Infrared spectra were recorded in KBr pellets on a Perkin-Elmer Infracord Model 137.

---

* It should be noted that a carbon-sulphur double bond results from the less favorable $2p$—$3d$ overlap.

SUMMARY

Characteristic absorptions in the 1250—1200 cm^{-1} and in the 1150—1100 cm^{-1} region in the spectra of 2-thionothiazolidine-4-ones are assigned to stretching frequencies of the thiono group. The assignment is based on the disappearance of these bands in the spectra of the corresponding 2-methylene derivatives.

The amide carbonyl absorption in the spectra of 2-thionothiazolidine--4-ones and 2-thionoimidazolidine-4-ones is found at a rather high frequency considering its position in the spectra of thiazolidine-4-ones and imidazolidine-4-ones. The shift to higher frequencies is ascribed to the presence of the thiono group, and is explained by the nature of the carbon--sulphur double bond.

Department of Chemistry,
School of Sciences, Belgrade University,
and Institute of Chemistry, Technology
and Metallurgy, Belgrade, Yugoslavia

Received 24 November, 1969

REFERENCES

1. Stojiljković, A. M., M. M. Stefanović and R. M. Tasovac. "Kondenzacione reakcije 2-tionotiazolidin-4-ona(rodanina) sa aromatičnim N,N-bisamidima u prisustvu bortrifluorideterata" (Condensation Reactions of 2-Thionothiazolidine-4-one(Rhodanine) with Aromatic N,N-Bisamides in the Presence of Borontrifluoride Etherate) — *Glasnik hemijskog društva* (Beograd) 28:* 27, 1963.

   Stojiljković, A. M., M. M. Stefanović and A. Jokić. "A Novel Route to 3,5,5-Trisubstituted Thiazolidine-4-ones" — *Tetrahedron* 21: 831—834, 1965.

   Stefanović, M. M., A. M. Stojiljković and A. M. Jokić. "Separation of Diastereoisomeric 3,5,5-Trisubstituted 2-Thionothiazolidine-4-ones" — *Glasnik hemijskog društva* (Beograd) 31*(2): 95—101, 1966.
2. Bellamy, L. J. *The Infrared Spectra of Complex Molecules* — London: Methuen, 1957.
3. Rao, C. N. and R. Venkataraghavan. "The C=S Stretching Frequency and the —N—C=S Bands in the Infrared" — *Spectrochimica Acta* 18: 541—547, 1962, and references therein.
4. Brown, F. C., C. K. Bradsher, B. F. Moser and S. Forester. "Structure and Antimicrobial Activity of 3-Aminorhodanines" — *Journal of Organic Chemistry* 24: 1056, 1959.
5. Pennigton, F. C., W. D. Celmer, W. U. McLamore, V. V. Boggert and J. A. Soloms. "Microbiologically Active 4-Thiazolidones" — *Journal of the American Chemical Society* 75: 109—114, 1953.
6. Durden, J. A., H. A. Shansbury and W. A. Catlette. "The Reaction of Glycidic Esters with Thiourea in Aqueous Sulphuric Acid Solution" — *Journal of American Chemical Society* 81: 1943, 1959.
7. Epp, A. "Infrared Spectra of 3-Phenyl-2-Thiohydantoins" — *Analytical Chemistry* 29: 1283, 1957.
8. Zehavi, U. and Ben Ishai. "The Reactions of Carbobenzoxy-amino Acids with Carbonyl Compounds" — *Journal of Organic Chemistry* 26: 1097, 1961.
9. Baranov, S. N. "Issledovanie reakt͡sionnoĭ sposobnosti vodorodnykh atomov metilenovoĭ gruppy nekotorykh azolidinov" (Investigation of the Reactivity of Hydrogen Atoms of the Metyhlene Group of Some Azolidines) — *Zhurnal obshcheĭ khimii* (Moskva): 1230, 1962.

---

* Available in English translation from the National Technical Information Service, Springfield, Virginia, 22151.

GLASNIK HEMIJSKOG DRUŠTVA, Vol. 35, No. 2-3, 1970, pp. 209—216

GHDB-94 541.124:547.584

Original Scientific Paper

THE REFORMATSKY REACTION WITH SOME CYCLIC IMIDES. I.

PREPARATION OF 3-SUBSTITUTED PHTALIMIDINES

by

LUCIJA Š. ARSENIJEVIĆ and DANICA Dj. STEFANOVIĆ

Heterocyclic nitrogen compounds can be obtained by the Reformatsky reaction starting with a cyanoester or halonitrile, yielding compounds with a pyridine(1, 2), pyrrole(3), pyrrolidine(3, 4), isoquioline(5), Δ^1-pyrroline(7), Δ^1-piperideine(7), or isoindoline(6) ring. The last was obtained by the Reformatsky reaction from cyanoester I, the intermediate cyclic acylimine II being isomerised into enamide III. On introducing α-bromoester with a tertiary bromine atom into this reaction in order to prevent the isomerisation, instead of acylimine IV its reduced product V was obtained:

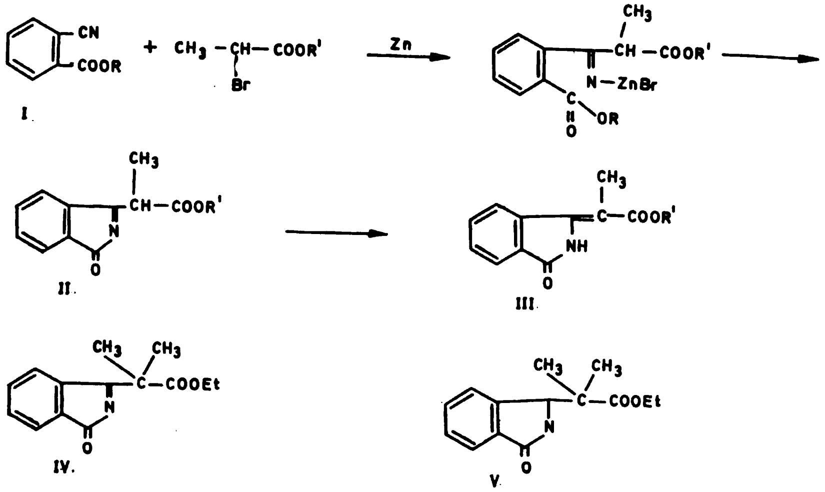

The unexpected fromation of phtalimidine V instead of acylimine prompted us to try the synthesis of the latter in another way. The Reformatsky reaction of phtalimide with α-bromoisobutyrate offered an opportunity, provided the reaction was carried out in the same way as with the N-substituted phtalimide*, and the β-hydroxyester VIIIc could be dehydrated by the elimination of the hydroxyl group and hydrogen from the NH-group.

The reactions of phtalimide with bromoacetic and α-bromopropionic acid esters are also described.

When the Reformatsky reaction with phtalimide was carried out in ether or benzol the yields were very poor because the presence of active hydrogen made the N-zinc bromide complex precipitate which hindered the reaction of the carbonyl group. This difficulty was overcome by using tetrahydrofurane as the solvent.

When phtalimide reacted with an excess (1 : 3) of bromoacetic ester and zinc, β-hydroxy ester VIIIa was obtained; its infrared spectrum (of a diluted solution in $CHCl_3$) showed characteristic absorptions at 3590 cm^{-1} (OH-group), 3445 cm^{-1} (NH-group), 1735 cm^{-1} (CO ester) and 1710 cm^{-1} (lactam CO group). This compound readily gave up a molecule of water on heating with xylene in a Dean-Starck apparatus to yield α, β nonsaturated ester IXa. The infrared spectrum of this compound (i.e. of its dilute solution in CCl_4) did not show an absorption at 3600 cm^{-1} but only at 3390, 1727, 1684 and 1645 cm^{-1} (NH-group, Co-group of α, β nonsaturated ester, CO-group of γ-lactam and the olefine double bond). If this nonsaturated ester was heated to boiling point with dilute solution of potassium hydroxide in methanol, the potassium salt of the α, β nonsaturated acid precipitated almost quantitatively even after a short heating. The molecular weight of this acid, determined by acidimetry, agreed with formula Xa (found: 188.2; calculated: 189.1).

The compounds IXa and Xa are enamides; this was proved by heating them with hydrochloric acid, giving *o*-acetylbenzoic acid (XIIa). The transformation of cyclic enamides into keto-acids under the influence of acids has already been described in references (3) and (6).

The reaction of phtalimide with ethyl α-bromopropionate and zinc was carried out in the same way as with bromoacetic ester, giving compound VIIIb, whose IR-spectrum (of a dilute solution in $CHCl_3$) had absorption bands similar to β-hydroxy ester VIIIa, i.e. 3590 cm^{-1} (OH-group), 3440 cm^{-1} (NH-group) 1732 cm^{-1} (CO ester) and 1715 cm^{-1} (lactam CO). By dehydrating with xylene or heating at 150—160°C, 3-/1′-carbethoxy-ethylidene/-phtalimidine (IXb) was obtained, this being identical with the product obtained by the Reformatsky reaction of *o*-cyano-ethyl-benzoate(6). By heating this ester with a solution of alkalis in methanol saponification soon occurred and monocarbonic acid Xb was obtained, this giving the above described 3-ethylidene-phtalimidine on thermal decarboxylation(6). When this ester or acid Xb was heated with dilute hydrochloric acid for 3—4 hours *o*-propionyl-benzoic acid (XIIb) was formed.

The reaction of phtalimidine with ester of α-bromoisobutyric acid gave β-hydroxy-ester VIIIc in as good a yield (84%) as in the above described examples. The IR-spectrum of this compound (1% solution in CCl_4) had a narrow absorption band at 3605 cm^{-1} (OH-group), and a wide band (3300—3460 cm^{-1}), with peaks at 3420 and 3460 cm^{-1}, in the region of

---

* The reaction of N-methylphtalimide with bromoacetic ester has been described by Lukeš(8) and Michael(9). N-methyl-3-hydroxy-3-carbethoxymethyl-phtalimidine was obtained in a yield of 24 and 31%, respectively.

the NH-group. The ester carbonyl absorbs at 1735 *cm*$^{-1}$ and the lactam carbonyl at 1708 *cm*$^{-1}$.

In order to obtain acylimine IV the elimination of a molecule of water from β-hydroxy-ester VIIIc by azeotropic distillation was attempted. However, when using toluene or xylene it always split into phtalimide and ethyl isobutyrate. The attempt to saponificate this compound into β-hydroxy acid was fruitless because a diluted base transformed it into the alkaline phtalimidine salt even without heating; on acidifying the phtalimide precipitated almost quantitatively.

On the basis of the IR-spectra and the chemical transformations giving known compounds it is clear that the above reactions proceeded according to the following scheme:

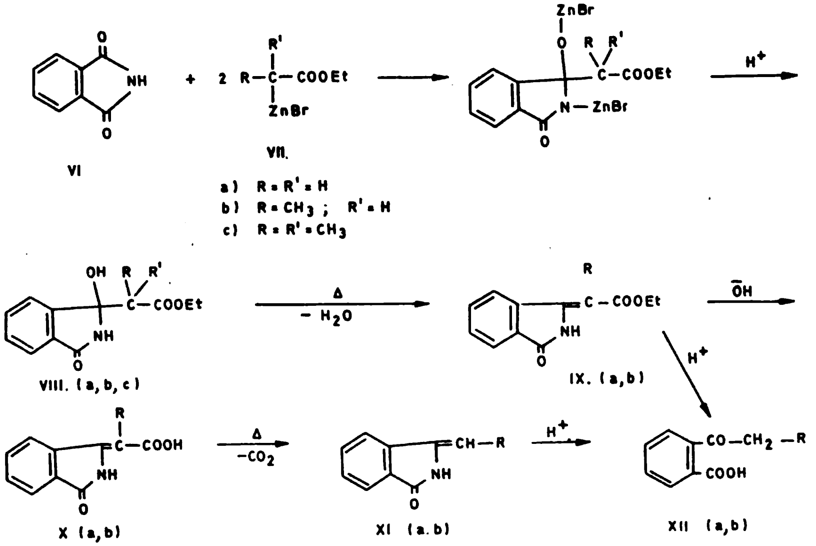

Only two moles of the Reformatsky reactant (VII) took part in the reaction with phtalimide, one of these reacting with the active hydrogen of the NH-group and the other with the carbonyl group. Although the reactant was in excess, the other carbonyl group did not react; the same has already been observed in the reaction with N-methyl-phtalimide$^{(8, 9)}$. The cyclic structure of hydroxyl compound VIII, unlike the alternative structure XIII, was proved by analysis of its IR-spectrum.

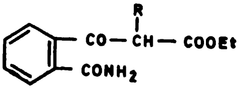

XIII.

However, it must be pointed out that Linstead$^{(10)}$ synthesized compound VIII by another method, and structure XIII ascribed it as the more probable.

In the present and earlier studies(6) cyclic enamides were found to hydrolyze into the corresponding keto-acids relatively easily. In this reaction the bond between carbon in the carbonyl group and nitrogen was probably broken first, giving (e.g. with compound IX) the carboxyl and the β-ketimino-ester group (XIV). On further hydrolysis the intermediate compound XV was formed, which then undergoes the ketonic decomposition.

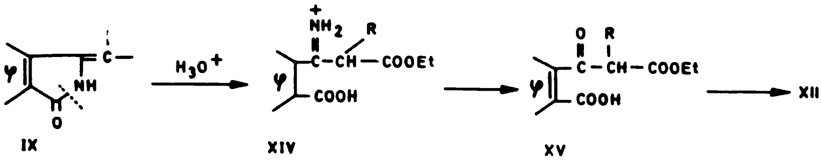

In order to explain the mechanism opening the five-membered ring the point at which enamide is protonised must be known, bearing in mind that a compound of this type has three centers susceptible to the influence of an electrophylic reactant(11, 12): nitrogen, oxygen and the nonsaturated carbon in the β-position relative to nitrogen. There are few data in the literature on the acid hydrolysis of enamide; only one paper(13) dealing with the mechanism of this reaction was known to us and that was for an open-chain enamide. According to this mechanism the proton from the acid binds to the β-carbon atom and then water is bound to carbon in the α-position relative to the amino-group:

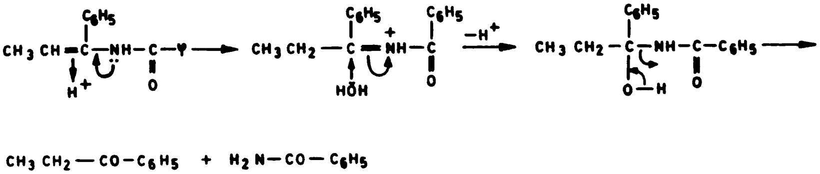

The fact that this hydrolysis yielded benzamide indicated that the N-alkyl bond was broken, but not the N-acyl one. However, as *o*-acyl-benzoic acid, but not *o*-acyl-benzamide, was obtained by hydrolysis of compounds IX, X and XI, it is clear that in the cyclic enamides the N-acyl bond* was broken, and therefore the mechanism of hydrolysis differed from that with the open-chain enamide:

---

* By heating 2-alkyliden-pyrrolidone or 2-alkyliden-piperid-one(3) (on the enamide structure of these compounds see ref.(5)) for half an hour with 10% hydrochlorie acid a keto-acid was formed, but no amide, this giving proof that the ring gets broken between nitrogen and the carbonyl group:

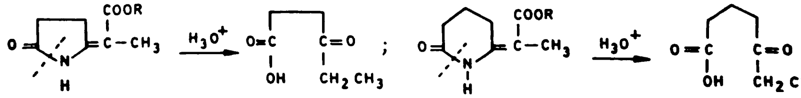

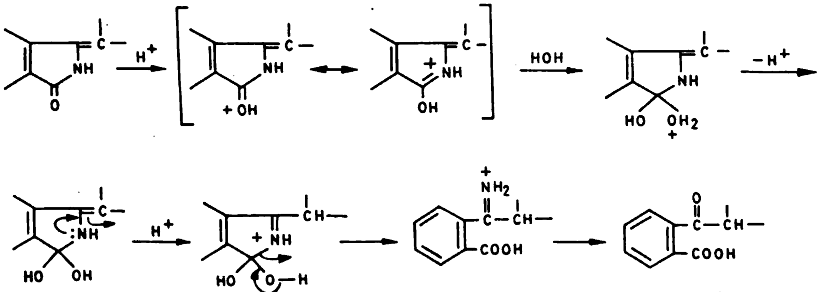

XII. (a, b)

Most probably the cyclic enamide (like the amides⁽¹⁴⁾) binds a proton to the oxygen in the carbonyl group, after which water is bound and the proton from the oxonium ion released. The enamine thus formed binds a proton to the β-carbon atom, this resulting in breaking of the ring and on further hydrolysis the ketimine obtained is transformed into keto-acid XII.

EXPERIMENTAL

IR-spectra were taken on a Perkin-Elmer model 237 spectrophotometer and the melting points were determined on a Kofler microscope.

3-Hydroxy-3-Carbethoxymethyl-phtalimidine (*VIIIa*)

9.8 *g* (0.066 mole) phtalimide, 13 *g* (0.2 *g* at) zinc filings, 33.4 *g* (0.2 mole) ethyl-ester of α-bromoacetic acid, a few *mg* $HgCl_2$ and 80 *ml* dry tetrahydrofurane were placed in a 500 *ml* flask. A vigorous reaction lasting about 15 minutes was induced by the initial heating; gentle simmering of the solution was maintained by cooling the flask from time to time. After the reaction had calmed down the mixture was simmered gently for another half hour. After this it was cooled and 100 *ml* 20% acetic acid saturated with sodium chloride added. After an hour stirring the organic layer was separated, cooled with ice and, while stirring, a 50% potassium carbonate solution added until a weak alkaline reaction was achieved. The organic layer was separated again, then washed twice with saturated sodium chloride and dried with magnesium sulphate. The solvent was removed by distillation and a small amount of *n*-hexane added to the residue, this resulting in crystalisation. The crystals were filtered and washed with *n*-hexane. The yield was 16 *g* (86%), m.p. = 130°C. On recrystallisation from benzol-ethanol mixture (9 : 1) m.p. was 134°C.

Analysis for $C_{12}H_{13}O_4N$.	C	H	N
— *Calculated:*	61.27%	5.57%	5.96%
— *Found:*	61.51	5.32	6.20

3-Carbethoxymethylene-Phtalimidine (*IXa*)

In a flask fitted with a Dean-Starck extension 23.5 *g* ester VIIIa and 60 *ml* xylene were heated until the precipitation of water droplets ceased.

Then xylene was removed by distillation and the residue recrystallised from ethanol. The crystals obtained had m.p. 99°C [According to ref. (10) m.p. = 99°C].

3-Carboxymethylene-phtalimidine (Xa)

1.8 *g* ester IXa was dissolved in 30 *ml* 2.5% potassium hydroxide solution in methanol and the solution boiled for 30 minutes. After this methanol was removed by vacuum distillation and the residue dissolved in water, then filtered and washed with ether. The aqueous solution was decolored with active carbon, filtered, acidified with hydrochloric acid and the crystals thus obtained were filtered and dried. The yield was 0.95 *g* (82%), m.p. = 222°C [according to ref. (10, 15, 17) m.p. = 200 and 228°C].

O-Acetyl-Benzoic Acid (XIIa)

0.2 *g* acid Xa or 0.25 *g* ester IXa were heated at boiling point for three hours with 6 *ml* 10% hydrochloric acid. The solution was then cooled and extracted with ether, the ether extract being then washed and dried with magnesium sulphate. Ether was removed by distillation and the residue recrystallised from aqueous solution. The crystals melted at 114—115°C [according to ref. (16, 18) m.p. = 114—115°C].

3-Hydroxy-3-(1'-Carbethoxyethyl)-Phtalimidine (VIIIb)

14.7 *g* (0.1 mole) phtalimidine, 54.3 *g* (0.3 mole) ethyl ester of α-bromopropionic acid, 19.5 *g* (0.3 *g* at) zinc, a few *mg* mercuric chloride, 100 *ml* dry tetrahydrofurane were placed in a flask and heated until the beginning of the reaction. The reaction ceased after 10—15 minutes and the reaction mixture was heated for another half hour. The product was treated in the same way as compound VIIIa, except that 300 *ml* 20% acetic acid was used for decomposing the organo-metallic complex. The yield was 23 *g* (83%) of crystalline substance with m.p. = 170°C. On recrystallisation from ethanol-water mixture (1: 1) m.p. was 173°C.

Analysis for $C_{13}H_{15}O_4N$.	— *Calculated:*	C 62.64%	H 6.07%	N 5.62%
	— *Found:*	62.88	6.28	5.86

3-(1'-Carbethoxylethylidene)-Phtalimidine (IXb)

By dehydrating hydroxy-ester VIIIb, according to the same technique as for VIIIa, a product was obtained which recrystalled from ethanol melted at 127°C [according to ref. (6) m.p. = 127°C].

3-(1'-Carboxyethylidene)-Phtalimidine (Xb)

Ester IXb was saponified in the same way as IXa. The crystals obtained by recrystallisation from ethanol melted at 231—232°C [according to ref. (6) m.p. = 231—232°C].

3-Ethylidene-Phtalimidine (XIb)

This product was obtained by decarbonisation of acid Xb as described in ref. (6).

IR-spectrum (KBr pellets): 3413 *cm*$^{-1}$ (NH), 1695 *cm*$^{-1}$ (COγ-lactam), 1621 *cm*$^{-1}$ (C=C bond).

O-Propionyl-Benzoic Acid (XIIb)

0.35 *g* ester IXb or 0.3 *g* acid Xb and 10 *ml* 10% hydrochloric acid were heated at boiling 4 hours. The solution was cooled and extracted with ether. The extract was washed and then ether evaporated. On adding a small amount of benzol to the residue crystals melting at 93°C [according to ref. (18, 19) m.p. = 91°C and 93°C] were obtained.

The same product was obtained by heating 3-ethylidene-phtalimidine (XIa) with 10% hydrochloric acid for 4 hours⁽⁶⁾.

3-Hydroxy-(1'-Carbethoxy-1'-Methyl-Ethyl)-Phtalimidine (VIIIc)

This compound was obtained in the same way as described under hydroxy-ester VIIIb by taking 14.7 *g* (0.1 mole) phtalimide, 19.5 *g* (0.3 *g* at) zinc and 58. *g* (0.3 mole) ethyl-ester of α.bromo-isobutyric acid. The yield was 22 *g* (84%), m.p. = 114°C. On recrystallisation from 50% ethanol m.p. was 115°C.

Analysis for $C_{14}H_{17}O_4N$	— *Calculated:*	C 63.87%	H 6.51%	N 5.32%
	— *Found:*	63.57	6.28	5.20

NMR-spectrum (VARIAN 60 A, solution in CCl_4, with TMS as the internal standard): 5.21 ppm singlet (O—H), 5.78 ppm singlet (N—H).

Laboratory of Organic Chemistry
School of Pharmacy, Belgrade University

Received 8 September, 1969

REFERENCES

1. Arsenijević, V., H. Lapin and A. Horeau. "Nouvelle méthode de synthèse des pyridines α, α'-disubstituèes" — *Comptes rendus des séances de l'Académie des Sciences* (Paris) 248: 3309—3310, 1959.
2. Lapin, H., V. Arsenijević and A. Horeau. "Action des α-bromo-esters en présence de zinc sur les nitriles esters. I. Synthèses de pyridines α, α'-disubstituèes" — *Bulletin de la Société chimique de France* (Paris) 247: 1700—1703, 1960.
3. Lapin, H. and A. Horeau. "Action des α-bromo-esters en présence de zinc sur les nitriles-esters. II. — Synthèses de pyrroles α, α'-disubstituèes, de dihydropyrrolénones et de dihydropyridones" — *Bulletin de la Société Chimique de France* (Paris) 275: 1703—1707, 1960.
4. Lapin, H. and A. Horeau. "Nouvelle action du réactif de Réformatsky sur les nitriles esters et les diesters" — *Chimia* (Aarau, Switzerland): 551—552, 1961.
5. Arsenijević, L. and V. Arsenijević. "Réaction de Réformatsky sur les nitriles-esters aromatiques. I. — Synthèse des hydroxy -1 isoquinoléines et des hydroxy -3 isoquinoléines substituées" — *Bulletin de la Société Chimique de France* (Paris) 526: 3403—3407, 1968.

6. Arsenijević, L. and V. Arsenijević. "Réaction de Réformatsky sur les nitriles-esters aromatiques. II. — Synthèse des phtalimidines substituées" — *Bulletin de la Société Chimique de France* (Paris) 792: 4943—4946, 1968.
7. Arsenijević, L. and V. Arsenijević. "The Reformatsky Reaction with Aliphatic γ- and σ-Halonitriles. The Synthesis of Some 2-Substituted Δ^1-Pyrrolines and Δ^1-Piperideines" — *Croatica Chemica Acta* (Zagreb) 528: 1—7, 1969.
8. Lukeš, R. "Sur la stabilité des Pyrrolones vis-a-vis de l'eau" — *Collection* (Praha) 4: 81—86, 1932. Lukeš, R. and F. Šorm. "Action du réactif de Réformatsky sur les méthylimides de certains acides dicarboxyliques. II^e partie. Action des réactif organométalliques sur le groupe amide. Partie XIII." — *Collection* (Praha) 12: 637—640, 1947.
9. Micheel, F. and W. Flitsch. "Synthesen mit 3,4-Dioxo-pyrrolizidin" — *Chemische Berichte* (Berlin) 94: 1749—1756, 1961.
10. Linstead, R. P. and H. G. Rowe. "Phtalocyanines and Related Compounds. Part XVII. Intermediates for the Preparation of Tetrabenzoporphyrins: Acids Derived from Phtalimidine" — *Journal of the Chemical Society* (London): 1070—1076, 1940.
11. Kagan, H. B., A. Horeau and Y. S. Heng. "Iminomagnésiens. II. — Action sur les esters" — *Bulletin de la Société Chimique de France* (Paris) 217: 1457—1459, 1965.
12. Heng, Y. S. and H. B. Kagan. "Iminomagnésiens. III. — Propriétés d'acylimines et acylenamines" — *Bulletin de la Société Chimique de France* (Paris) 217: 1460—1463, 1965.
13. Heng, Y. S. "*Action des iminomagnésiens sur les esters. Contribution à l'étude de la réaction de Réformatsky sur les nitriles* (thesis), Paris, 1963.
14. Sigdwick, N. V. *The Organic Chemistry of Nitrogen* — Oxford: Clarendon Press, 1966, p. 232.
15. Gabriel, S. and M. Micheel. "Über die Einwirkung von waserentziehenden Mitteln auf Saureanhydride" — *Berichte der Deutschen Chemischen Gesellschaft* (Berlin): 1551—1562, 1877.
16. Gabriel, S. "Zur Kentniss des Methylenphtalids" — *Berichte der Deutschen Chemischen Gesellschaft* (Berlin) 486: 2451—2458, 1885.
17. Dent, C. E. "Preparation of Phtalocyanine-like Pigments Related to the Porphyrins" — *Journal of the Chemical Society* (London): 1—6, 1938.
18. De Benneville, P. "The Synthesis of Keto Acids and Ketones by the Reaction of Acid Anhydrides with Cadmium Alkyls" — *Journal of Organic Chemistry* 6: 462—466, 1941.
19. Anwers, K. and A. Heinze. "Über die Konstitution der aliphatischen γ-Ketonsäuren und der aromatischen o-Aldehyde und o-Ketocarbonsauren sowie deren Derivate" — *Berichte der Deutschen Chemischen Gesellschaft* (Berlin) 72: 584—601, 1919.

GLASNIK HEMIJSKOG DRUŠTVA, Vol. 35, No. 2-3, 1970, pp. 217—222

GHDB-95

581.4:543.82 + 543.842/.843

Original Scientific Paper

THE CORRELATION OF CARBON, HYDROGEN AND MINERALS IN PLANTS

by

ZAGORKA FILIPOVIĆ

According to data in ref.(1) the average carbon content of plant leaf is 45 *g*, hydrogen 6 *g* and ash(2, 3) about 5 *g* per 100 *g* dry vegetable material. However, in our studies the deviations from this average were found to be considerable. In the present work changes of leaf carbon and hydrogen content in relation to changes of the mineral content will be considered.

MATERIAL AND METHOD

The concentration of carbon, hydrogen and pure ash in the leaf of maize, wheat, barley, soybean, sunflower, potato, cabbage, bean, tomato, paprika, pea, lettuce, strawberry, blackberry, tobacco, sugarbeet, grass, clover and foxglove were determined by elementary analysis (Pregl). The samples were collected from various parts of the country in two years. The environmental factors affecting the growth of the plant, e.g. soil, climate, etc., were very diverse. The number of the samples studied was 126.

A number of leaves of the same plant were washed with double distilled water, dried at 105°C and homogenized. Carbon, hydrogen and ash were expressed as grams per 100 *g* of dry material.

RESULTS AND DISCUSSION

The concentration of carbon in the material ranged from 27 to 48 *g*, hydrogen from 4 to 7 *g*, and ash from 2 to 20 g (occasionally up to 25 and once 32 *g*).

In Fig. 1 and Fig. 2 carbon and hydrogen concentrations are plotted against ash.

Discussion of Fig. 1. First attention is drawn to the interesting information given by Fig. 1: the concentration of carbon in plant leaf can be deduced from the ash content. Instead of a complicated organic analysis, it is sufficient to ignite the material and from the amount of ash find the carbon content. The equation of the straight line in Fig. 1 is

$$C = \frac{6}{8.8} \cdot (70.5 - M) \qquad (1)$$

where C and M are weight of carbon and ash (*g*) per 100 *g* dry vegetable material.

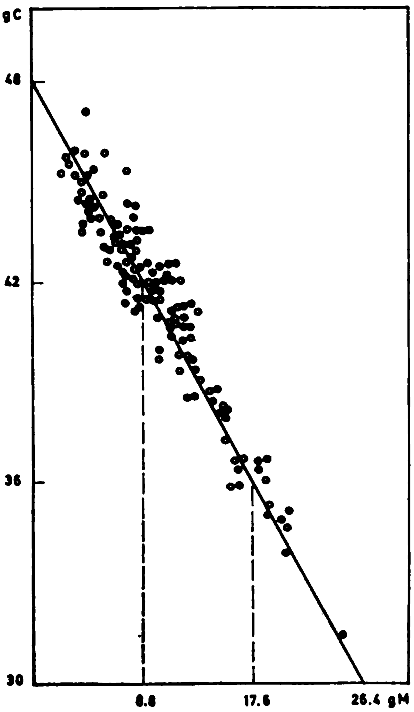

Fig. 1

Carbon content (C) as a function of ash (M).

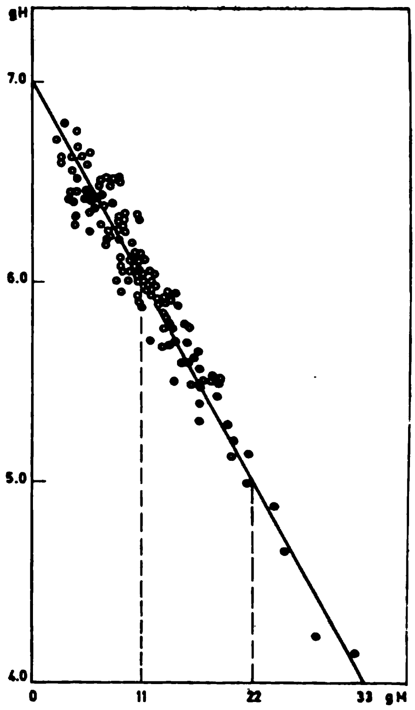

Fig. 2

Hydrogen content (H) as a function of ash (M).

The coefficients 6 and 8.8 in equation (1) mean that carbon and ash were found in the ratio

$$6\,g\ C : 8.8\,g\ M,$$

i.e. with an increase in the amount of ash by 8.8 *g*, the amount of carbon in the plant leaf decreases by 6 g, or 0.5 gram-atom of this element.

Equation (1) may be transformed into:

$$C + 0.68\,M = 48, \tag{2}$$

expressing that carbon plus 68% ash make up a constant weight of 48 *g* (per 100 *g* dry vegetable material).

The accuracy of equation (2) is demonstrated for several experimental results chosen at random in Table 1.

Discussion of Fig. 2. From this figure, as in the case of carbon, it may be seen that the amount of hydrogen in plant leaf can be deduced from

TABLE 1

Analytical data

No.	Plant	C g	M g	C + 0.68 M − 48
1	Wheat Vrčin	45.35	4.08	48.12
2	Barley Plitvice	44.11	6.33	48.41
3	Strawberry Crepaja	43.19	7.12	48.03
4	Maize Kosovo	42.40	8.72	48.33
5	Clover Igman	41.65	9.11	47.84
6	Soybean Jajinci	40.88	10.33	47.90
7	Cabbage Ruma	40.80	10.02	47.61
8	Bean Mali M. Lug	41.28	10.67	48.53
9	Wheat Čačak	40.02	12.99	48.17
10	Soybean Čačak	39.66	12.96	48.47
11	Tobacco Samoš	40.28	12.54	48.80
12	Sunflower Osijek	36.70	16.27	47.76
13	Tomato Despotovac	38.20	14.90	48.33
14	Potato Vlasinsko Jezero	39.65	13.00	48.49
15	Sugarbeet Petrovac na Mlavi	37.51	15.98	48.37
16	Tomato Petrovac na Mlavi	35.39	18.61	48.04
17	Lettuce Mali M. Lug	35.40	20.04	49.03
18	Cabbage Hvar	34.20	19.64	47.56
19	Cabbage Crepaja	31.65	24.28	48.16
20	Maize Ljubičevo	27.03	32.03	48.81

TABLE 2

Analytical data

No.	Plant	H g	M g	$H+\frac{M}{11}=7$
1	Maize Ljubičevo	4.14	32.03	7.1
2	Cabbage Crepaja	4.84	24.28	7.0
3	Sunflower Jajinci	5.42	18.56	7.1
4	Tomato Zrenjanin	5.47	16.90	7.0
5	Sugarbeet Petrovac na Ml.	5.55	15.98	7.0
6	Tomato Karlovac	5.71	14.14	7.0
7	Potato Melenci	5.79	13.80	7.0
8	Paprika Petrovac na Ml.	5.89	13.05	7.1
9	Potato Vlasinsko jez.	5.84	13.00	7.0
10	Tobacco Samoš	5.90	12.54	7.0
11	Bean Delibl. peščara	6.00	12.00	7.1
12	Wheat Čačak	5.89	11.99	7.0
13	Pea Novi Sad	6.09	11.62	7.1
14	Soybean Jajinci	6.14	10.33	7.1
15	Clover Vršac	6.04	9.42	6.9
16	Sunflower, Tuzla	6.34	7.43	7.0
17	Barley Plitvice	6.43	6.33	7.0
18	Strawberry Crepaja	6.44	7.12	7.1
19	Soybean Osijek	6.50	6.42	7.1
20	Wheat Mali M. Lug	6.71	2.80	7.0

the known amount of ash. The equation of the straight line in Fig. 2 is:

$$H = \frac{1}{11}(77 - M) \tag{3}$$

where *H* and *M* are weights of hydrogen and ash (in *g*) per 100 *g* dry vegetable material.

According to equation (3) hydrogen and plant ash were found to be in the ratio

$$1\,g\,H : 11\,g\,M.$$

This ratio (see Fig. 2) means that for an increase of the amount of ash by 11 *g* the amount of hydrogen decreases by 1 *g* or 1 gram-atom.

The accuracy of equation (3), or its simpler form

$$H + \frac{M}{11} = 7 \tag{4}$$

is checked on experimental data chosen at random in Table 2.

In conclusion, let us reiterate that equations (2) and (4) were derived from analysis of 126 different plant samples. The development stage and the environmental conditions of the plant (e.g. the soil type, humidity and pH, illumination, etc.) were very different. In spite of this, allowing for analytical error (±4% for *C* and ±5% for H), equations (2) and (4) were valid for all samples.

Department of Inorganic Chemistry,
School of Pharmacy, Belgrade University

Received 20 December, 1969

REFERENCES

1. Maksimov, N. A. *Fiziologija bilja* (Plant Physiology) — Novi Sad: Dnevnik, 1961.
2. *Handbuch der Pflanzenphysiologie, Band IV.* — Berlin: Springer Verlag, 1958, pp. 7—11.
3. Bonner, J. and J. Varner. *Plant Biochemistry* — New York-London: Academic Press, 1965, p. 440.

GLASNIK HEMIJSKOG DRUŠTVA, Vol. 35, No. 2-3, 1970, pp. 223—236

GHDB-96 541.124:546.15:546.215

Original Scientific Paper

NEW POSSIBILITIES FOR THE APPLICATION OF LANDOLT'S EFFECT IN KINETIC METHODS OF CHEMICAL ANALYSIS

by

VILIM J. VAJGAND, DIMITRIJE DJ. STOJANOVIĆ and
DJURDJE B. JELENIĆ

The reaction between potassium iodide and hydrogen peroxide

$$H_2O_2 + 2\,I^- + 2\,H^+ \longrightarrow I_2 + 2\,H_2O$$

in which the Landolt effect appears(1), has been investigated by a number of researchers(2, 3, 4, 5). At room temperature this reaction proceeds slowly with precipitation of iodine. However, it is sped up by the presence of very small amounts of a catalyst such as molybdenum, tungsten or some other metals. The reaction rate may be observed by the change in color intensity of the solution to which starch has been added. I͡atsimirskiĭ(6) utilized this possibility and worked out a method for determination of very small amounts of molybdenum from the acceleration of the reaction in the presence of this catalyst.

According to data in ref. (6), amounts of molybdenum greater than $2 \cdot 10^{-8}$ *g/ml* were determined by this reaction. As far as the determination of lower concentrations is concerned, it is only mentioned that it was very difficult due to the influence of impurities mainly silicates, in whose presence no precipitation of iodine at all could be observed in very dilute solutions of molybdenum.

In the study of this reaction our aim was, above all, to investigate the possibility of determining molybdenum in concentrations smaller than those determined hitherto, and also of determining certain inhibitors of the components in the above reaction(7).

EXPERIMENTAL

The rate of the reaction was registered by photometry and potentiometry.

A. Photometric Determinations

1. Determination of very small amounts of molybdenum by means of a calibration curve

The data required for the construction of a calibration curve were obtained by direct measurement of differences of photocurrent between the molybdenum-catalyzed and non-catalyzed reactions. For this differential technique a Lange colorimeter connected to a Zeiss galvanometer with a sensitivity of 10^{-10} A per scale division was found suitable.

Standard solutions of molybdenum were made up from Merck p.a. ammonium molybdate. The molybdenum content of the ammonium molybdate was determined by heating it to constant weight at 300 to 400°C and measuring the MoO_3 residue. The water used in the experiment was deionized twice and then distilled in quartz vessels. Vessels were washed in a mixture of HNO_3 and HCl (1 : 1) and a saturated solution of KOH in ethanol. Before use the solutions were stored in a thermostat at 20°C; they were prepared for analysis in the following way:

3 *ml* 0.01 M KI previously twice recrystallised from ethanol, 2 *ml* 2 M HCl and 2 *ml* 0.2% starch were weighed out in two volumetric 50 *ml* flasks. Then a predetermined volume of the standard molybdate solution was added to one of the flasks. Finally 3 *ml* of 0.01 M hydrogen peroxide solution was added simultaneously to both flasks. The time was measured by stopwatch from the addition of peroxide. The solutions were made up to the mark and stirred thoroughly, and 10 *ml* of each solution was put into the colorimeter cells. The difference in photocurrent between the catalyzed and non-catalyzed reactions were measured every 15 seconds. The results were plotted on a graph of photocurrrent against time (Fig. 1).

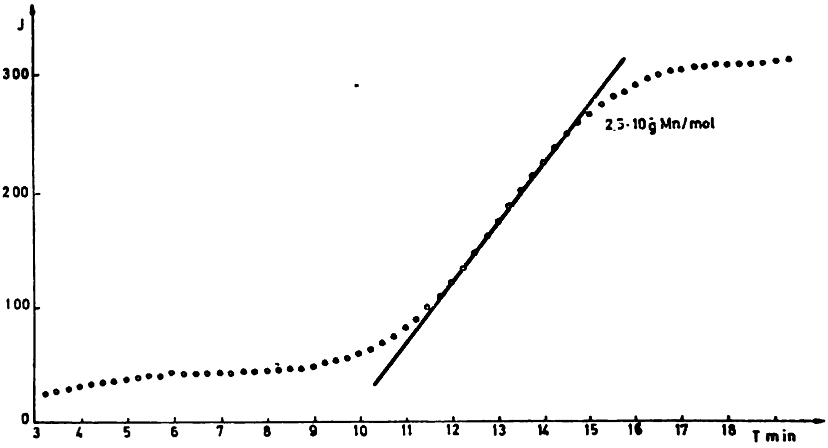

Fig. 1
Shape of "catalytic wave" shown from the reaction start

The curve obtained in this way, called a "catalytic wave", resembles a polarographic curve and consists of three parts: the initial, almost horizontal part corresponding to the incubation (induction) period t_{ind} and lasting up to the beginning of precipitation of iodine (Landolt's effect), the ascending part corresponding to an increasing difference in the photocurrent, and again a horizontal part after completion of the Mo-catalyzed reaction. If the non-catalytic reaction is fast enough the end of the curve begins to fall drop.

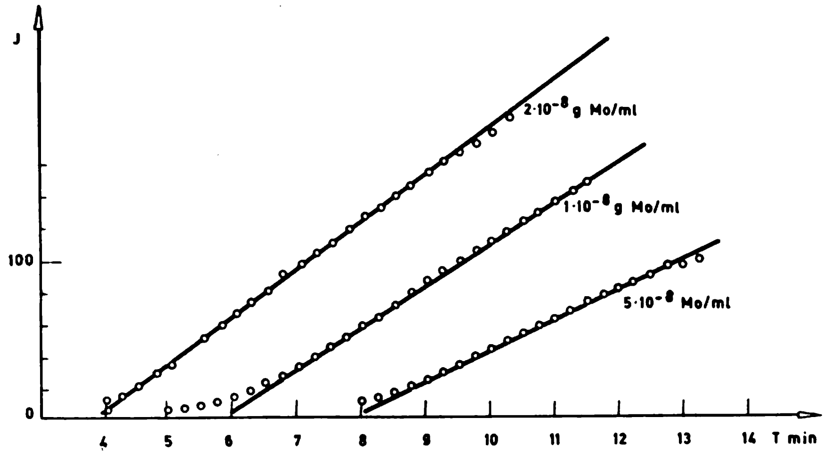

Fig. 2

Difference in photocurrent between catalytic and non-catalytic reaction plotted against time

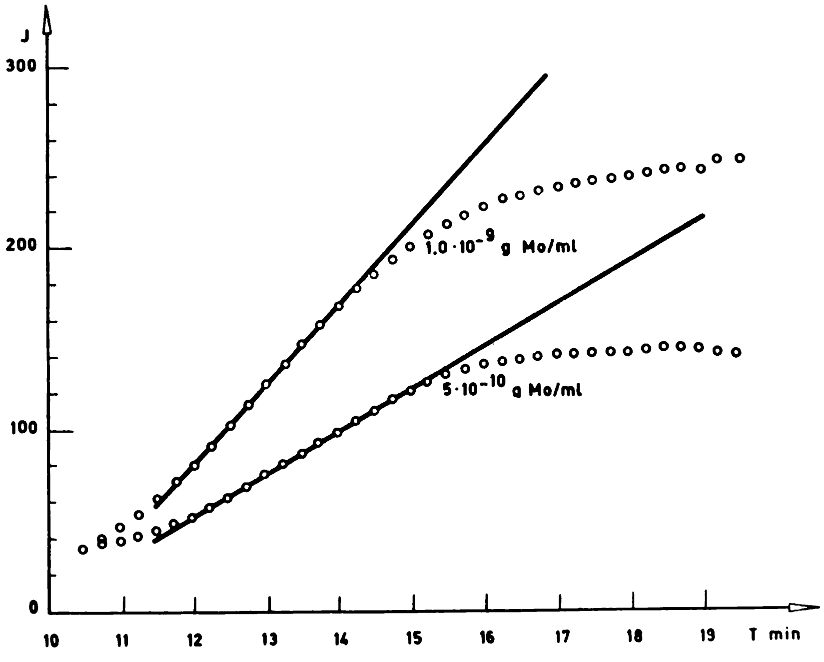

Fig. 3

Shape of curves for minimum (limiting) concentrations

With a catalyst concentration of about 10^{-8} *g* Mo/*ml* the induction period was 4 to 6 minutes (Fig. 2), with concentrations of 10^{-9} or lower it was about 10 minutes (Fig. 3). The exact end of the induction period was determined from the intersection of the horizontal and the ascending part of the curve. Plotting the function $1/t_{ind} \propto C_{Mo}$ gives a straight line (line A in Fig. 4) and this can be used as a calibration curve for the determination of molybdenum.

The concentration of molybdenum may also be determined from the gradient of the ascending part of the wave. If the tangent of the angle made by the straight lines extrapolation of the ascending part of the wave and the abscissa is plotted against the molybdenum concentration a straight line is obtained (curve B in Fig. 4).

The results obtained for concentrations between $5 \,.\, 10^{-9}$ and $2 \,.\, 10^{-8}$ *g* Mo/*ml* were analyzed statistically and the error of determination found to be ±6%.

By increasing the sensitivity of the multiflex-galvanometer to the maximum, determinations of concentrations between $1 \,.\, 10^{-9}$ and $5 \,.\, 10^{-10}$ *g* Mo/*ml* were successfull, this being the lower limit of sensitivity of the method. A slow transition from the induction period to the "catalytic" part of the curve may be seen in Fig. 3.

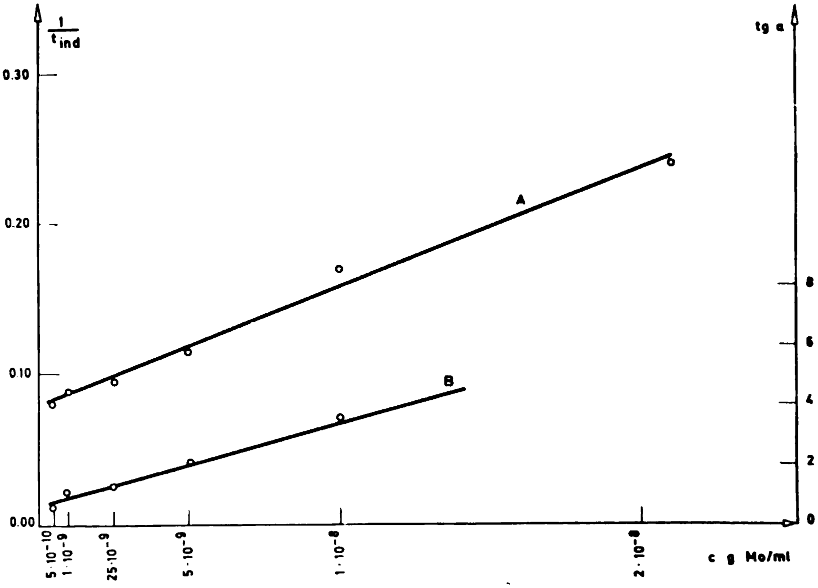

Fig. 4

Calibration curve for molybdenum:
A — the function $1/t_{ind} \propto c$; B — function $\tan \alpha \propto c$

These measurements were also analyzed statistically. The average deviation from the mean value for 5 measurements was ±10%.

2. *Determination of Lead*

As lead ion inhibits for the molybdate ion (Pb^{2+} forms insoluble $PbMoO_4$ with MoO_4^{2-}), this effect was tried as the principle of a method for the determination of lead.

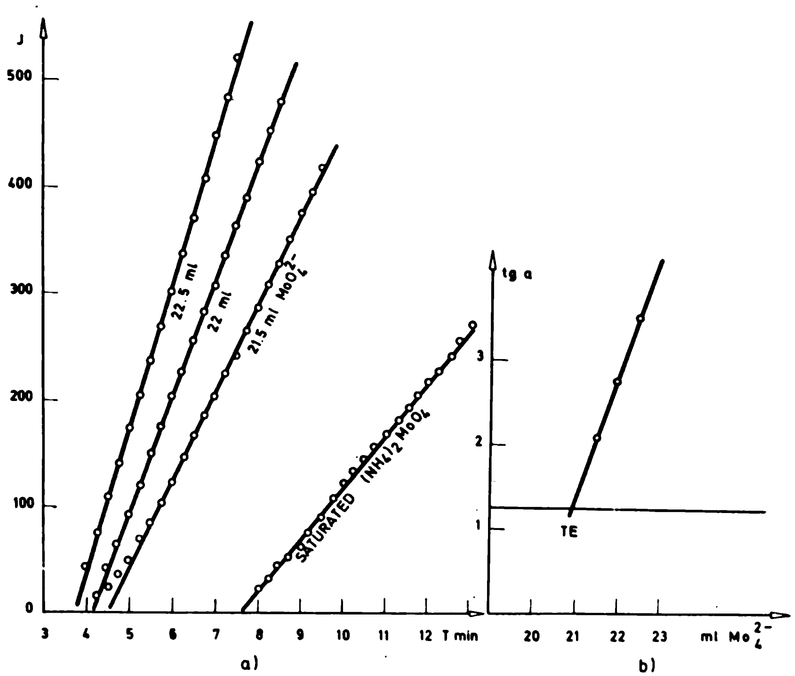

Fig. 5

Catalymetric titration of lead with molybdate:

(a) Time dependence of difference in photocurrent, for samples containing different volumes of titrant (molybdate) added in excess;

(b) Calculated slopes of the above curves against volume of the titrant added.

Twenty *ml* $1.08 \cdot 10^{-4}$ M lead nitrate solution was weighed out into each of three dry 50 *ml* flasks, and then various volumes (21.5, 22.0 and 23.5 *ml*) of 1.04 M ammonium molybdate solution were added to each sample so that molybdate ion was in excess.

The lead molybdate precipitated and settled on the bottom of the vessel or was separated by centrifuge (in the case of smaller samples). The clear supernatant was analyzed. 5 *ml* of it was pipetted into a 50 *ml* flask. 2 *ml* glacial acetic acid, 5 *ml* 0.01 M solution of KI and 2 *ml* 0.2% starch solution were added. The solution for a non-catalyzed reaction was made in the same way. After adding 3 *ml* 0.01 M hydrogen peroxide and diluting the solution with water up to 50 *ml*, differences in photocurrent were measured in the same way as in the determination of molybdenum. As lead molybdate has a solubility factor of 2.5 . 10^{-11}(8), in order to compensate for catalysis due to molybdate ions from lead molybdate the rate of the reaction with the same volume (5 *ml*) of saturated solution of lead molybdate was determined first. From the results the equivalence point was found graphically in the following way:

The dependence of the photocurrent on the time is first plotted in the coordinate system shown in Fig. 5a for the corresponding volumes of added molybdate solution and for saturated molybdate. The slope of the straight line corresponding to the saturated molybdate solution is plotted on the ordinate of another coordinate system (Fig. 5b) and a line parallel to the abscissa drawn through this point. The number of milliliters of standard molybdate solution is plotted on the abscissa. The slopes found from graph *a* for every added volume of standard molybdate solution are plotted on the ordinate and a line drawn through these points. The equivalence point EP is found as the interesection of the normal to the abscissa through the poinr where this line cuts the line corresponding to the saturated molybdate solution (Fig. 5b).

For this method of determination of an inhibitor from the change in the rate of reaction during titration (this being done by measuring the tangent of the angle) the term "catalymetric titration" has been proposed by I͡at͡simirskiĭ(9). Table 1 shows the results of determination of lead by this method.

TABLE 1

Results of Determination of Lead with Ammonium Molybdate by Catalymetric Titration

Taken *ml* 1.08 · 10^{-4} M $Pb(NO_3)_2$	Theor. necess. *ml* 1.04 · 10^{-4} M $(NH_4)_2MoO_4$	Consumed *ml* 1.04 · 10^{-4} M $(NH_4)_2MoO_4$	Pb found in %	Average deviation in %
10.00	10.38	10.45 10.35 10.35	100.7 99.7 99.7	—0.4
15.00	15.60	15.45 15.75 15.40	99.0 101.0 99.4	—0.8
20.00	20.80	20.95 20.60 20.65	100.7 99.0 99.3	—0.7

Lead in more dilute solutions was determined in the same way. In the titration of 5 . 10^{-5} M lead nitrate the error of determination was 6%, and 18% with 1 . 10^{-5} M lead nitrate.

Plotting the error of determination E against the concentration of lead nitrate gives the exponential curve shown in Fig. 6.

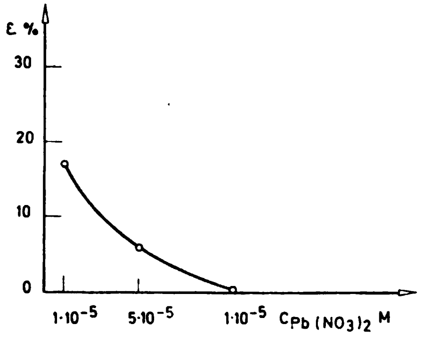

Fig. 6

Percentage error in determination of lead depending on its concentration in catalymetric titration

3. *Determination of Bases and Hydrogen Peroxide*

As the reaction between potassium iodide, hydrogen peroxide and molybdenum has a catalytic character only in an acid medium, bases may be determined by photometric titration. A base inhibits the Landolt reaction up to the equivalence point, and after this the first appearance of an excess of H^+ ions catalyses the reaction between potassium iodide and hydrogen peroxide. Because of this the titration must be carried out slowly near the equivalence point.

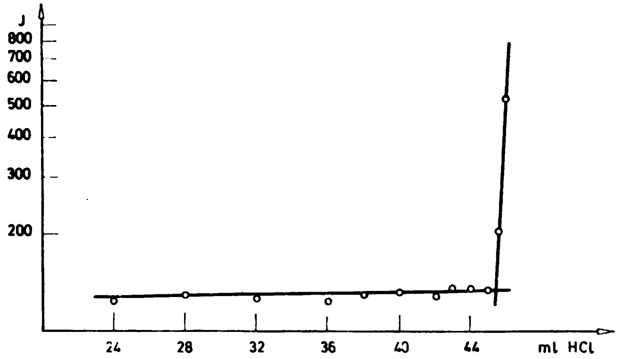

Fig. 7

Catalytic photometric titration of 5.00 *ml* of 0.1919 N $SnCl_2$ with 0.1391 N H_2O_2. Equivalence point (EP) 6.90 *ml*, titration end point (TEP) 6.96 *ml*.

5 *ml* 0.1 *M* NaOH was titrated in the cell of the Lange colorimeter with a 0.1 *N* solution of HCl. Before the titration 3 *ml* 0.01 *M* KI, 2 *ml* molybdate solution (10 *μg Mo/ml*), 3 *ml* 0.01 *M* hydrogen peroxide and 2 *ml* 0.2% starch solution were added to the solution of the base.

During the titration the solution was stirred with a magnetic mixer, and the titrant was added at equal time intervals (every 2 minutes). After this time the difference in photocurrent was measured. Figure 7 shows the dependence of photocurrent on the volume of titrant added. Until the equivalence point the photocurrent changed only negligibly, the line being almost horizontal, while after it it rose rapidly. If the function $\log i \propto V_{ml}$ is plotted on a graph, the end point of the titration is found at the intersection of the two straight lines.

Hydrogen peroxide may be determined in a similar way. When a very acid solution of standard $SnCl_2$ (to which a small amount of sodium bicarbonate was added in order to prevent oxidation of divalent tin by oxygen from the air) was titrated with hydrogen peroxide, no change of photocurrent was observed until the equivalence point. At the equivalence point a rapid increase was obtained (Fig. 8).

Only 0.1 *N* and 0.01 *N* hydrogen peroxide were determined, but even more dilute solutions may be titrated by this method.

Tin may also be determined in this way if titrated with a standard solution of hydrogen peroxide.

4. *Determination of Palladium*

The determination of palladium on the basis of its inhibiting effect on the reaction between Ce(IV) and As(III) in an acid medium was described by Fedorova and I͡at͡simirskiĭ(10).

In order to investigate the possibility of determining palladium on the basis of its inhibitory effect on the reaction between hydrogen peroxide and iodide in acid medium, a standard solution of potassium iodide was added to a specified volume of a standard solution of palladium salt, taking care that iodide was in excess. The precipitate of palladium iodide was separated by centrifuging 5 minutes at 4000 r.p.m. After this 5 *ml* of the clear supernatant was pipetted into a 50 *ml* flask. To this aliquot 1 *ml* molybdate solution having a concentration of 5 *μg Mo/ml*, 2 *ml* 0.2% solution of starch and 3 *ml* 0.01 M hydrogen peroxide were added. As the solution of palladium salt alredy contained 0.6 M acid (to prevent hydrolysis), it was not acidified. After making up the solution to the mark, the difference in photocurrent between this solution and water in the other cell was measured. The equivalence point was found in the same way as in the determination of lead (Fig. 9), the only difference being that in this case the catalysis due to the solubility of palladium iodide was not allawed for because this compound was very insoluble.

The errors in the determination of palladium as palladium nitrate were very big (10—15%), and may be ascribed to the influence of nitrite being formed during dissolving of palladium in nitric acid, this releasing iodine from the iodide. This method produced better results if palladium chloride was used instead of nitrate.

B. **Potentiometric Determinations**

The photometric method for determining lead and palladium involves difficulties with the separation of precipitate. The precipitate must be separated because the size of the particles changes and therefore also the absorptivity of the solution with the time. In the case of palladium iodide a black

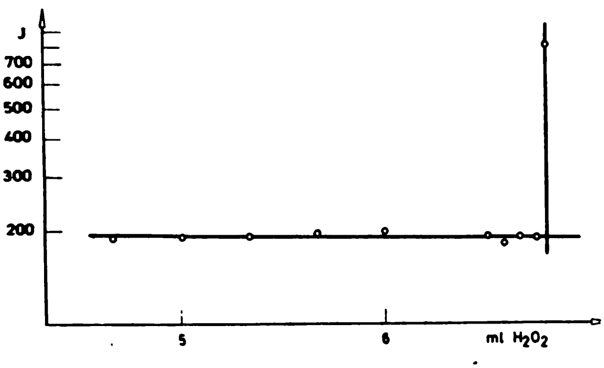

Fig. 8

Catalytic photometric titration of 5.00 *ml* of 0.1040 N NaOH with 0.1157 N HCl. EP 4.50 *ml*, TEP 4.54 *ml*.

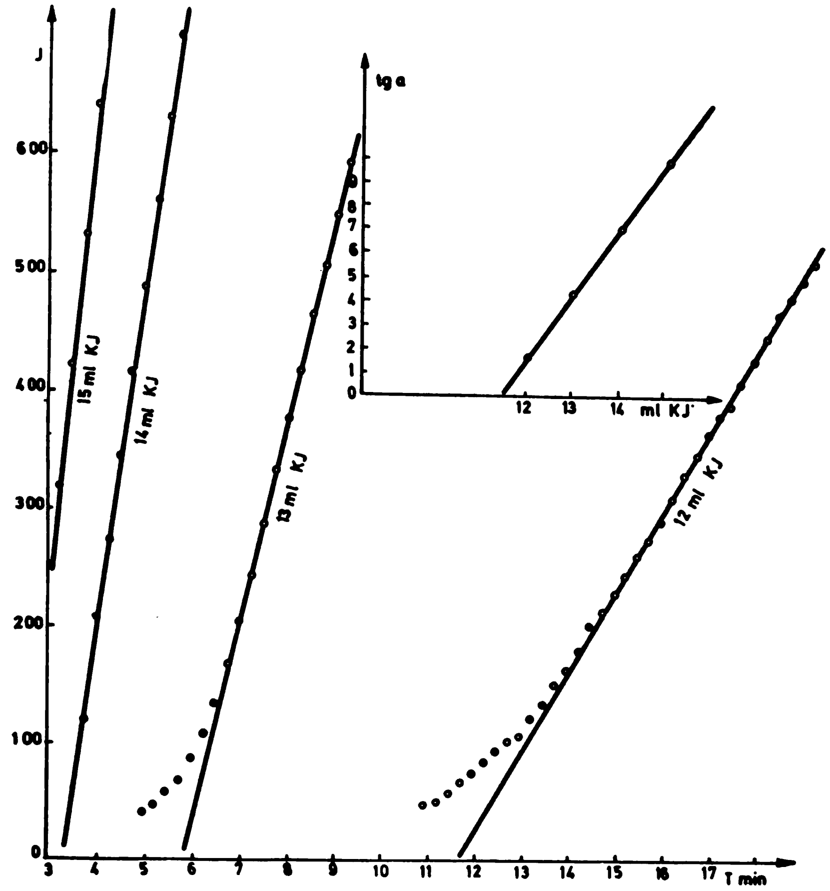

Fig. 9

Catalymetric titration of 10.00 *ml* of 4.7. 10 ^{3} M $Pd(NO_3)_2$ with 9.66 . 10^{-3} M KI. EP 9.76 *ml*, TEP 11.48 *ml*.

precipitate was also formed, this making impossible the observation of the blue color appearing after the equivalence point. In order to avoid these difficulties, determinations were also tried by potentiometric titration.

Determination of Palladium

Palladium was titrated potentiometrically by adding 10 *ml* water, 2 *ml* molybdate having a concentration of 100 *μg Mo/ml*, and 3 *ml* 0.1 M hydrogen peroxide to a specified volume of nitric-acid solution of palladium nitrate in a beaker containing a platinum and a saturated calomel electrode. One minute after the addition of hydrogen peroxide a standard solution of 0.1 N potassium iodide was added from a burette at equal time intervals (1 minute) and the potential measured immediately with a Radiometer 22 pH meter. During the titration the solution was stirred with a magnetic mixer.

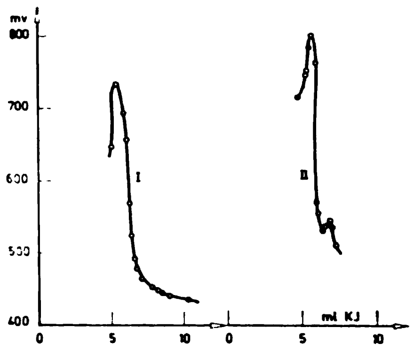

Fig. 10

Catalytic potentiometric titration of 3.00 *ml* of 0.1012 M $Pd(NO_3)_2$ with 0.1003 M KI. Curve *a:* without catalyst; *b:* in the presence of 100 *μg/ml* of molybdenum.

From the results the number of *ml* of potassium iodide added was plotted against the potential (Fig. 10, curve No. II.). Curve No I. in the same figure shows the dependence obtained by potentiometric titration of palladium with potassium iodide under the same conditions but with no molybdenum or hydrogen peroxide present. Up to the equivalence point the shape of the curve depends on the acid used; it changed least extent in titrating in a hydrochloric acid solution. In sulphuric or nitric acid solution the curve first rises then slowly falls, and near the end point of titration drops rapidly. After the addition of the least excess of iodide the Landolt effect was identified by the rising potential, this being as much as 100 *mV* per minute.

As seen from the curves, in the case of the catalytic reaction a much bigger increase and a steeper slope was obtained for the same volume of 0.1 N potassium iodide solution than in the case of the non-catalytic one. Consequently, by this reaction palladium may be determined with much greater sensitivity than by a classical potentiometric titration. Determinations of palladium by potentiometric titration based on the catalytic effect of molybdenum on the reaction of iodide and peroxide in acid medium are given in Table 2.

TABLE 2

Results of Determination of Palladium by Potentiometric Titration in the Presence of Mo as Catalyst for the Reaction $H_2O_2 + 2I + 2H^+ \rightarrow I_2 + 2H_2O$

Taken *ml* 0.1012 M $Pd(NO_3)_2$	Theoretically necessary *ml* 0.1003 M KI	Consumed 0.1003 M KI	Palladium found in %	Relative error in %
0.5	1.01	1.05	103.9	3.9
2.0	4.04	3.96	98.0	—2.0
3.0	6.04	5.95	98.5	—1.5
5.0	10.08	10.15	100.7	0.7

These titrations were performed with by the deap-stop method using a pair of Radiometer PP1311 platinum electrodes at a potential difference of 50 *mV*. Current was measured with a multiflex galvanometer (10^{-10} A /scale division). During titration the current rose slowly to the equivalence point and then rapidly. In this way 1 to 2 *mg* of palladium was determined with a relative error of 3%.

Determination of Silver

The potentiometric titration of silver was done with a platinum and a saturated calomel electrode. The changes of potential were read on the pH meter in millivolts. The titration was done in the following way: 2 *ml* 4 M sulphuric acid, 2 *ml* molybdate with a concentration of 100 *μg Mo/ml*, 3 *ml*

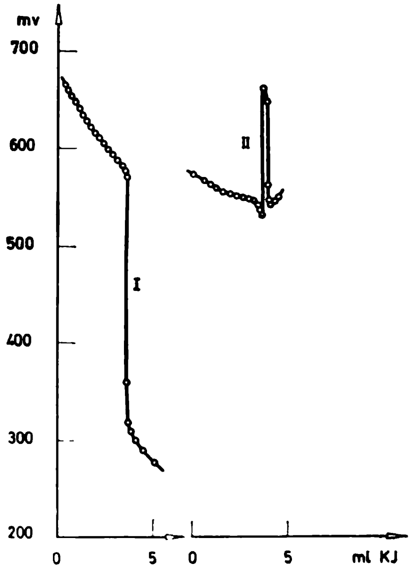

Fig. 11

Catalytic potentiometric titration of 3.00 *ml* of 0.1239 N $AgNO_3$ with 0.1003 M KI. Curve *a:* without catalyst; *b:* in the presence of 100 *μg/ml* of molybdenum

0.1 M hydrogen peroxide solution and 10 *ml* water were added to a known volume of a standard solution of silver nitrate. This solution was stirred with a magnetic mixer and titrated with 0.1 M potassium iodide solution at equal time intervals (1 minute) from a microburette. The potential was also read one minute after the addition of iodide.

From the results a graph was constructed of the dependence of the added volume of potassium iodide on the potential change (Fig. 11, curve No. II).

In this case the classical potentiometric titration was also performed for comparison: the curve obtained is shown in the same figure (curve No I). In this case silver was determined more precisely by the classical method.

TABLE 3

Results of Determination of Silver by Potentiometric Titration in the Presence of Mo as Catalyst for the Reaction $H_2O_2 + 2I + 2H^+ \rightarrow I_2 + 2H_2O$

Taken *ml* 0.1239 N $AgNO_3$	Theoret. necessary *ml* of 0.1003 N KI	Consumed *ml* of 0.1003 N KI	Silver found in %	Relative error in %
0.5	0.02	0.60	96.8	—3.2
3.0	3.70	3.66	98.4	—1.6
5.0	6.17	6.12	99.2	—0.8
10.0	12.35	12.30	99.6	—0.4

Although the potentiometric determination of silver on the basis of the Landolt effect, shown in Table 3, gave relatively big errors, the curves in this and in the previous case (determination of palladium) show an interesting feature. If silver was titrated in the classical way, the potential at the platinum electrode first decreased slowly, and then rapidly at the equivalence point. However, if the solution also contained hydrogen peroxide and molybdate, the potential again decreased up to the equivalence point but rose rapidly on reaching it, due to the oxidation of iodide. The end point of the titration could be seen visually by adding starch to the titrated solution.

All the methods, conditions of determination and results are summarized in Table 4.

Institute of Chemistry,
School of Sciences,
University of Belgrade
Institute for the Application of Nuclear
Energy in Agriculture, Veterinary Medicine
and Forestry, Belgrade

Received 7 November, 1969

TABLE 4

Experimental Conditions and Results

Component determined	Concentration range *g*-ion/*lit*	Role in reaction	Technique used for determin.	Conditions of determination				Amount of determ. compon. in *mg*	Relative error in %
				[H+] *g*-ion/*lit*	$[I^-]$ *g*-ion/*lit*	$[H_2O_2]$ *mol*/*lit*	[Mo] *μg*/*ml*		
Mo	$2 \cdot 10^{-7}$ $5 \cdot 10^{-9}$	Catalyst	Photometry	$8 \cdot 10^{-2}$ HCl	$6 \cdot 10^{-4}$	$6 \cdot 10^{-4}$		0.025—1 μg	6—10
Pb	$1 \cdot 10^{-4}$ $1 \cdot 10^{-5}$	Inhibitor for MoO_4^{2-}	„	$7 \cdot 10^{-1}$	$1 \cdot 10^{-3}$	$6 \cdot 10^{-4}$	0.05—0.005	0.2—0.4	1
OH^-	10^{-1}	Inhibitor for H	„		$2 \cdot 10^{-3}$	$2 \cdot 10^{-3}$	1.3	20	0.8
Sn^2+	10^{-1}	Inhibitor for H_2O_2	„	5.5	$2 \cdot 10^{-3}$		0.4	57	1.2
Pd	$5 \cdot 10^{-3}$ „ „	Inhibitor for I^-	„ Potentiom. Biamperom.	0.6 HNO_3 or HCl		$6 \cdot 10^{-4}$ $2 \cdot 10^{-2}$ $2 \cdot 10^{-3}$	0.1 6—11 0.3	10 5—50 1—2	0.7—4 3
Ag	$5 \cdot 10^{-2}$	Inhibitor for I^-	Potentiom.	$4 \cdot 10^{-1}$ H_2SO_4		$1 \cdot 10^{-2}$ $2 \cdot 10^{-2}$	7—12	7—130	0.4—3.2

REFERENCES

1. Svehla, G. "The Application of Landolt Reactions in Quantitative Catalytic Analysis" — *The Analyst* (London) 94(1120): 513—521, 1969.
2. Sharipov, R. K. and O. A. Songina. "Elektrokhimicheskoe opredelenie molibdena po kataliticheskoĭ reakt͡sii okislenii͡a iodida perekis'i͡u vodoroda" (Electrochemical Determination of Molybdenum by Catalytic Oxidation Reaction of Iodide with Hydrogen Peroxide) — *Zavodskai͡a laboratorii͡a* (Moskva) 29(11): 1293—1296, 1963.
3. Jedrzejewski, W. "Application of Amperometry in Kinetic Methods of Quantitative Analysis. I. Catalytic Determination of Small Amounts of Molybdenum" — *Chemia analyticzna* (Warszawa) 4(3): 647—653, 1959.
4. Hadjiioannou, T. P. "Microdetermination of Molybdenum by an Automatic Reaction Rate Method" — *Analytica Chimica Acta* (Amsterdam) 35(3): 360—364, 1966.
5. Malmstadt, H. V. and S. I. Hadjiioannou. "A New Automatic Spectrophotometric Rate Method for Selective Determination of Glucose in Serum Plasma, or Blood" — *Analytical Chemistry* (Washington) 34(4): 452—455, 1962.
6. I͡at͡simirskiĭ, B. K. and P. L. Afanaseva. "Opredelenie malykh kolichestv molibdena" (Determination of Small Amounts of Molybdenum) — *Zhurnal analiticheskoĭ khimii* (Moskva) 11(3): 319—323, 1956.
7. I͡at͡simirskiĭ, B. K. *Kinetic Methods of Analysis* — Oxford: Pergamon Press, 1966, p. 52.
8. Busev, A. I. *Analiticheskai͡a khimia͡i molibdena* (Analytical Chemistry of Molybdenum) — Moskva: Izdatel'stvo Akademii nauk SSSR, 1962, p. 15.
9. Iatsimirskii, B. K. and T. I. Fedorova. "Katalimetricheskoe titrirovanie" (Catalymetric Titration) — *Zhurnal analiticheskoĭ khimii* (Moskva) 18(11): 1300—1305, 1963.
10. Fedorova, T. I. and K. B. I͡at͡simirskiĭ. "Opredelenie malykh kolichestv paladii͡a metodom katalimetricheskogo titrirovanii͡a" (Determination of Small Amounts of Palladium by Catalymetric Titration) — *Zhurnal analiticheskoĭ khimii* (Moskva) 22(2): 283—285, 1967.

GLASNIK HEMIJSKOG DRUŠTVA, Vol. 35, No. 2-3, 1970, pp. 237—243

GHDB-97 543.253:546.47:546.74 + 546.73

Original Scientific Paper

POLAROGRAPHIC DETERMINATION OF ZINC IN THE PRESENCE OF NICKEL AND COBALT*

by

SRETEN N. MLADENOVIĆ and MILIVOJE ISAKOVIĆ

INTRODUCTION

In the reduction of the divalent cobalt ion at the dropping mercury electrode the half-wave potential against saturated calomel electrode is for the majority of supporting electrolytes more negative than —1.0 *V*. In a supporting electrolyte consisting of ammonium hydroxide and ammonium chloride, depending on their concentration the half-wave potential of divalent cobalt against SCE varies from —1.30 to —1.45 *V*(1–3).

In the majority of supporting electrolytes the half-wave potential of divalent nickel ion being reduced at the dropping mercury electrode is somewhat more positive than that potentials of divalent cobalt. In the electrolyte 1 M NH_3 + 0.2 M NH_4Cl it is —1.06 *V* against SCE.

In the reduction of zinc at the dropping mercury electrode the half-wave potential in the majority of supporting electrolytes is not more positive than —1.0 *V* against SCE. In the electrolyte 1 M NH_3 + 0.2 M NH_4Cl it is —1.33 *V*.

From these values it may be concluded that in solutions of ammonium hydroxide and ammonium chloride zinc is difficult to determine by polarography in the presence of nickel and especially in the presence of cobalt(1–5).

In present work the possibilities of polarographic determination of zinc in the presence of nickel and cobalt in a supporting electrolyte containing complexon I, ammonium chloride and ammonium hydroxide were investigated.

EXPERIMENTAL

Polarographic determinations were made on a Radiometer PO4 polarograph. All chemicals were of the highest purity.

In the polarographic determination of cobalt and zinc in the supporting electrolyte 2 M NH_4Cl + 4 M NH_4OH + 0.01% gelatine, the polarographic waves of cobalt, nickel and zinc were superimposed and could not be resolved. The superimposition of the cobalt and zinc waves excluded any possibility of polarographic determination of these metals.

---

* Communicated at 12th Conference of Chemists of the SR of Serbia, Belgrade, 1968.

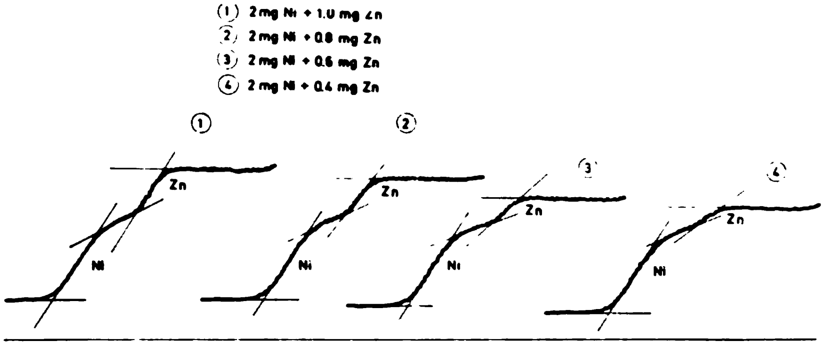

Fig. 1

Polarographic curves from determination of zinc in the presence of nickel in the supporting electrolyte 2 M NH_4Cl + 4 M NH_4OH + 0.01% gelatine.

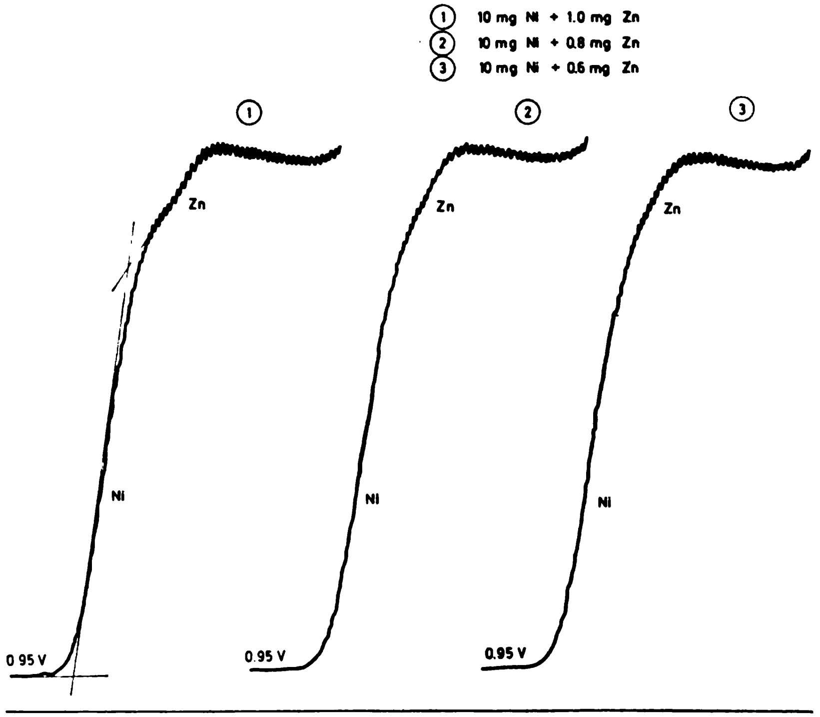

Fig. 2

Polarographic curves from determination of zinc in the presence of large amounts of nickel in the supporting electrolyte 2 M NH_4Cl + 4 M NH_4OH + 0.01% gelatine

The polarographic determination of zinc in the presence of nickel from the solutions containing nickel in ten times greater quantity was possible in the supporting electrolyte 2 M NH_4Cl + 4 M NH_4OH + 0.01% gelatine. This may be seen from the polarogram in Fig. 1.

As seen in Fig. 2, the polarographic determination of zinc in the above electrolyte was impossible above a tenfold greater concentration of nickel than to zinc.

From the polarogram in Fig. 3 it may be concluded that the polarographic determination of zinc in the presence of cobalt was possible in the supporting electrolyte: 0.1 M NH_4Cl + 0.1 M NH_4OH + 0.01 M complexon I + 0.6% Na_2SO_3 + 0.01% gelatine. In this electrolyte zinc produced two waves, one having a half-wave potential of about —1.37 *V* and the other of about —1.61 *V* against SCE (Fig. 3). As seen in Fig. 4, the first wave disappeared in the supported electrolyte 0.2 M NH_4Cl + 1 M NH_4OH + + 0.1 M complexon I + 0.6% Na_2SO_3 + 0.18% gelatine.

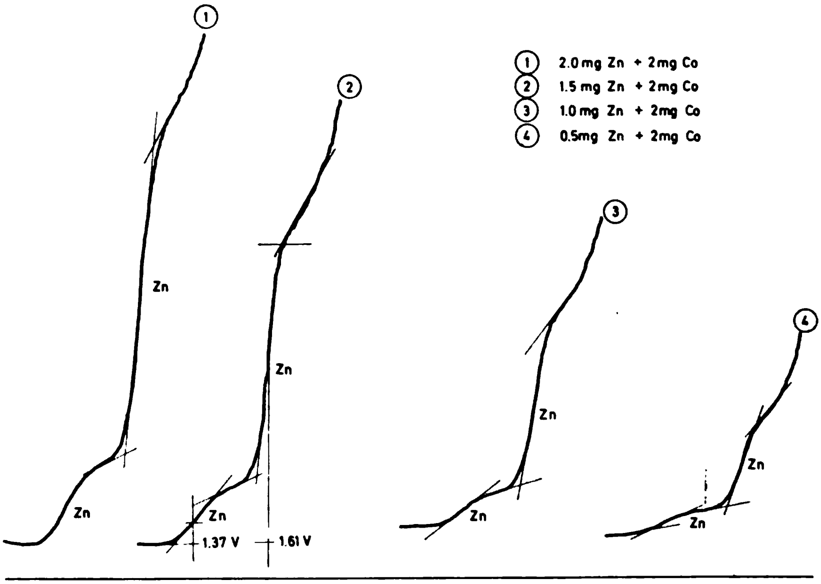

Fig. 3

Polarographic curves from determination of zinc in the presence of cobalt in the supporting electrolyte 0.1 M NH_4Cl + 0.1 M NH_4OH + 0.01 M complexon I + + 0.6% Na_2SO_3 + 0.01% gelatine

According to data in Table 1 it may be concluded that there the step height is a linear function of the amount of zinc. This linearity indicates that in the solution of ammonium hydroxide, ammonium chloride and complexon I cobalt did not interfere with the polarographic determination of zinc.

In ammoniacal solution the wave of nickel usually appeared before that of zinc, this not being the case in the solution of ammonium hydroxide, ammonium chloride and complexon I.

TABLE 1

Supporting electrolyte: 25 ml ($0.2\ M\ NH_4Cl + 1\ M\ NH_4OH + 0.1\ M$ *complexon I* $+ 0.6\%$ $Na_2SO_3 + 0.18\%$ *gelatine*)

Wave height *mm*	Zinc *mg*	Cobalt *mg*
69.0	2.0	2.0
52.0	1.5	2.0
33.0	1.0	2.0
17.0	0.50	2.0
8.0	0.25	2.0

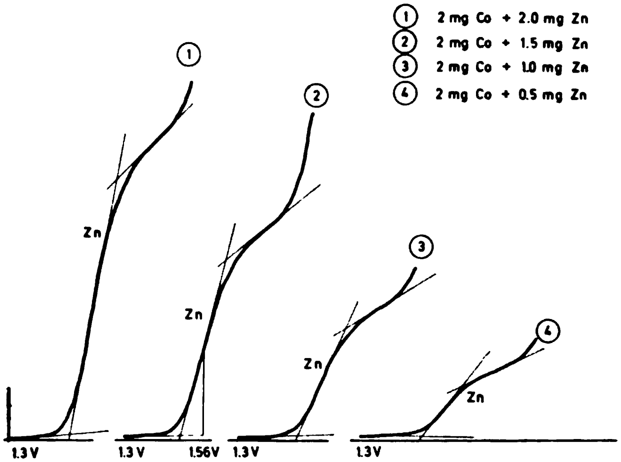

Fig. 4

Polarographic curves from determination of zinc in the supporting electrolyte $0.2\ M\ NH_4Cl + 1\ M\ NH_4OH + 0.1\ M$ complexon I $+ 0.6\%\ Na_2SO_3 + 0.18\%$ gelatine

TABLE 2

Supporting electrolyte: 25 ml ($0.2\ M\ NH_4Cl + 1\ M\ NH_4OH + 1\ M$ *complexon I* $+ 0.6\%$ $Na_2SO_3 + 0.18\%$ *gelatine*)

Wave height (*mm*)	Zinc *mg*	Nickel *mg*
102.0	2.0	2.0
74.0	1.5	2.0
49.0	1.0	2.0
25.0	0.50	2.0
13.0	0.25	2.0

From the data in Table 2 it may be concluded that there is a linear relationship between wave height and the amount of zinc in this polarographic determination in the presence of nickel in a solution consisting of ammonium chloride, ammonium hydroxide and complexon I.

In the polarographic determination of zinc in the presence of nickel and cobalt in a solution consisting of ammonium chloride, ammonium hydroxide and complexon I there was again a linear relationship between wave height and the amount of zinc (Table 3).

TABLE 3

Supporting electrolyte: 25 ml (0.2 M NH_4Cl + *1 M* NH_4OH + *0.1 M complexon I* + *0.6%* Na_2SO_3 + *0.18% gelatine)*

Wave height *mm*	Zinc *mg*	Nickel *mg*	Cobalt *mg*
75.0	2.0	2.0	2.0
54.0	1.5	2.0	2.0
35.0	1.0	2.0	2.0
18.0	0.50	2.0	2.0
9.0	0.25	2.0	2.0

CONCLUSION

Zinc in metals and alloys containing cobalt is usually determined by polarography in a supporting electrolyte based on ammonium hydroxide and ammonium chloride after preliminary removal of cobalt with α-nitroso--β-naphtol from hydrochloric acid solution(1).

The polarographic determination of zinc in the presence of cobalt and nickel in a solution of ammonium hydroxide, ammonium chloride and complexon I is simple and does not require preliminary precipitation of cobalt. The possibility of determining zinc in the presence of cobalt and nickel in this solution may be explained by the formation of stable nickel and cobalt complexes, these being reduced at more negative potentials than the zinc complex.

Institute of Physical Chemistry
and Electrochemistry
School of Technology and
Metallurgy, Belgrade University

Received 17 June, 1969

REFERENCES

1. Kovalenko, P. N. and L. S. Nadezhdina. "Elektrodnai͡a poli͡arizat͡sii͡a pri elektrolize nikelia i kobal'ta na kapel'nom rtut'nom katode. I. " (Electrode Polarization in Electrolysis of Nickel and Cobalt at Dropping Mercury Cathode. I.) — *Zhurnal obshcheĭ khimii* (Moskva-Leningrad) 22: 740, 1952.
2. Lingane, J. J. and H. Kerlinger. "Polarographic Determination of Nickel and Cobalt" — *Industrial and Engineering Chemistry, Analytical Edition* (Washington) 13: 77, 1941.
3. Voříšková, M. "Polarographische Studien mit der tropfenden Quecksilberkathode — LXXXIV — Abscheidungs- und Reduktions-Potentiale der Metallionen in ammoniakalischer Lösung" — *Collection of Czechoslovak Chemical Communications* (Praha) 11: 580, 1939.
4. Přibil, R., Z. Roubel and E. Svátek. "Nové komplexotvorné látky v polarografii. I. Kyselina 1, 2-diaminocyklohexan-N, N, N', N'-tetraoctová" (New Complexing Agents in Polarography. I. 1,2-Diaminocyclohexane-N, N, N', N'-Tetraacetic Acid) — *Chemické listy* (Praha) 46: 396, 1952.
5. Lingane, J. J. "Systematic Polarographic Metal Analysis. Determination of Tin, Lead, Nickel and Zinc in Copper-Base Alloys" — *Industrial and Engineering Chemistry. Analytical Edition* (Washington) 18: 429, 1946.

GLASNIK HEMIJSKOG DRUŠTVA, Vol. 35, No. 2-3, 1970, pp. 245—254

GHDB-98

543.253:547.417:546.621-31

Original Scientific Paper

POLAROGRAPHIC BEHAVIOR OF OXALYLDIHYDRAZIDE AND OF ALUMINUM ION IN ITS PRESENCE AT VARIOUS pH's*

by

VLADIMIR J. REKALIĆ and MILENA M. JOVANOVIĆ

Hydrazone obtained from oxalyldihydrazide (ODH) gives a very sensitive color reaction with copper, and has recently been proposed as a reagent for determination of copper. This prompted us to investigate the polarographic behavior of ODH and of some cations in its presence.

EXPERIMENTAL

Polarographic determinations were made on a PO4 polarograph. The half-wave potentials were measured against a saturated calomel electrode. The mercury drop rate was 1.8 *mg* sec^{-1} and the drop period 3.5 sec^{-1}. All solutions were made immediately before the measurements by diluting equal volumes of 0.01 M ODH, 0.02 M $AlCl_3$, 2.5 M KCl and 0.5% gelatine. The reagents used were p.a., B.D.H. Determinations were carried out in the presence of 0.5 M KCl as supporting electrolyte and 0.01% gelatine. The solution pH was measured with a Radiometer 22 glass electrode immediately before the polarographic determination. The pH was adjusted with 0.01 to 0.1 M hydrochloric acid or NaOH solution.

RESULTS AND DISCUSSION

At pH values between 4 and 9 ODH 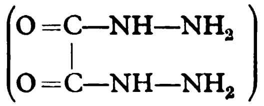 $\left(\begin{array}{l} O{=}C{-}NH{-}NH_2 \\ \quad\;| \\ O{=}C{-}NH{-}NH_2 \end{array}\right)$ produced a well-defined wave, its half-wave potential in chloride solution at a concentration of 0.1 to 8.0 mM being between —1.625 and —1.765 *V* (Table 1 and Fig. 1a). There was a linear relation between the concentration and the diffusion current at the above concentrations. At pH above 9 the wave height decreased by 2—6% and shifted towards more negative values, in 0.5 M KOH becoming equal to the wave of the supporting electrolyte (Table 2).

Decreasing the pH of the solution to below 4.0 also decreased the wave height and at pH = 2.6 it was half the original. Below pH = 2.4 the wave

---

* Extracts from this paper published on the ocasion of the 13th and 14th Meeting of Chemists of Serbia held 1968 and 1969 in Belgrade.

began to flatten out and at pH = 2.2 its height could no longer be determined. For pH values between 2.6 and 9 the half-wave potential of 4 mM ODH solution remained constant at —1.725 ± 0.02 *V*. This wave was irreversible and may be ascribed to the reduction of ODH.

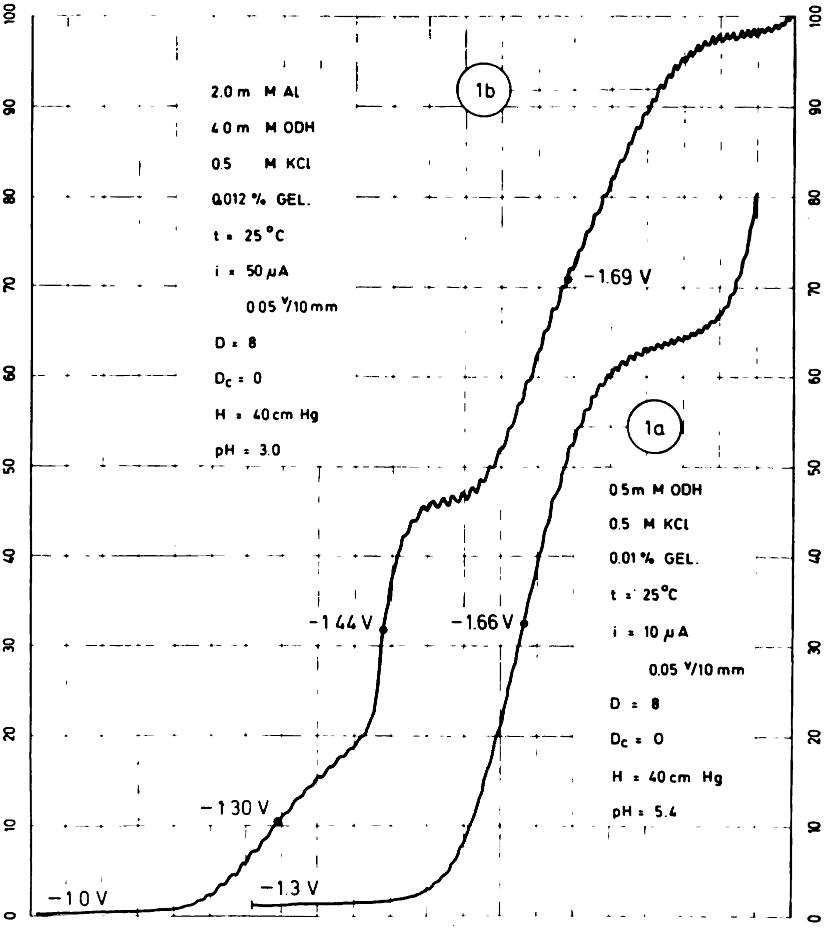

Fig. 1

Polarographic waves of ODH and its compound with Aluminum

In a solution having pH below 4 ODH produced an additional irreversible wave at positive potentials (Fig. 1b). Its height was considerably influenced by the pH. Moreover, even at approximately the same pH (e.g. 3.4), there was no linear relation between wave height and the concentration of the solution. For concentrations of ODH between 0.5 and 8 mM and pH = = 3.4 the half-wave potential was between —1.30 and —1.40 *V*. For a 4 mM solution and pH 2.6 to 3.8 it was —1.28 *V*.

TABLE 1

Wave Height and Half-Wave Potential at Various ODH Concentrations

ODH concentration (*mM/lit*)	Height of polarographic wave at I - 10 μA ($h_{1/2}$*cm*)	Half-wave potential ($E_{1/2}$ *V*)	pH
0.01	0.72	—1.625	5—6
0.05	1.96	—1.650	
0.10	3.46	—1.660	
0.30	9.72	—1.660	
0.50	15.65	—1.660	
0.80	25.20	—1.670	
1.00	30.90	—1.675	
2.00	61.8	—1.700	
4.00	122.0	—1.725	
6.00	188.0	—1.750	
8.00	249.5	—1.765	

At certain concentrations of ODH (e.g. 4.0 mM) the wave height increased with decreasing pH. If the concentration was below 0.5 mM no reproducible waves could be obtained.

In a supporting electrolyte of 0.5 M KCl at pH = 3.4 the hydrogen ion produced a pronounced wave with a half-wave potential of —1.5 *V*. However, this wave was not the same on the V/I curve in ODH solution. Instead a wave appeared with a half-wave potential of —1.30 *V*, this probably originating from a compound containing a hydrogen ion.

As already mentioned, the height of the wave at a half-wave potential of about —1.3 *V* (the first wave of ODH) increased with decreasing pH while that at about —1.7 *V* (the second wave) decreased. From Fig. 2 it may be seen that the sum of the two waves, measured at the same solution pH, corresponded to the height of the second polarographic wave of ODH measured in a solution whose pH was between 4 and 9.

TABLE 2

ODH Wave Height and Half-Wave Potential at Different pH Values

Concentration ODH solution *mM/lit*	Height of polarographic wave at I - 10 μA ($h_{1/2}$*cm*)	Half-wave potential ($E_{1/2}$ *V*)	pH
4.0	122.0	—1.725	4.2
4.0	122.0	—1.725	5.6
4.0	122.0	—1.725	7.0
4.0	122.0	—1.725	8.0
4.0	122.0	—1.730	9.0
4.0	120.5	—1.770	9.9
4.0	117.5	—1.790	11.0
4.0	118.5	—1.820	13.0

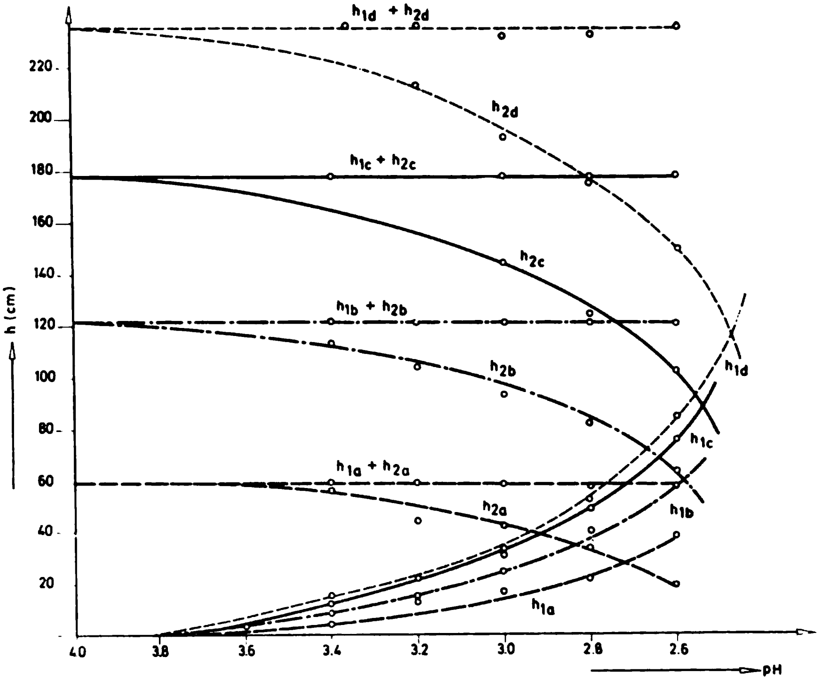

Fig. 2

Dependence of the height of ODH waves 1 and 2 on pH

h_{1a} and h_{2a} — 2 mM ODH
h_{1b} and h_{2b} — 4 mM ODH
h_{1c} and h_{2c} — 6 mM ODH
h_{1d} and h_{2d} — 8 mM ODH

2. Polarographic Wave of Aluminum in the Presence of ODH

The behavior of lead, zinc, cadmium, indium, aluminum and magnesium ions in the presence of ODH was also examined. Only aluminum cation was found to produce a polarographic wave from reaction with ODH. Other cations produced only the waves originating from their own reduction.

The first studies on polarographic behavior of aluminum ion date back to the early days of polarography and were made by Prazler(3). As the supporting electrolyte Prazler used 0.05 N $BaCl_2$ and obtained a wave with a half-wave potential of —1.75 *V*, this corresponding to the reduction of aluminum ion. More or less pronounced waves originating from the reduction of aluminum ion may be obtained in 0.1 M $BaCl_2$, 1 M and 0.5 M KCl or LiCl and even in a solution of magnesium chloride at certain pH values. The precise control of pH is indispensable for obtaining the polarographic waves of aluminum in aqueous electrolytes. It must correspond to the hydrolysis of aluminum ion. Precipitation of hydrated aluminum oxide occurs at too high a pH, while at too low pH overlapping with the wave of hydrogen ion occurs, this being more or less equal to the wave of aluminum. Because of this fact, regulators cannot bo used for adjusting the pH to get coincidence of the aluminum waves because even weak acids contain hydrogen ions(8).

The procedure of Willard and Dean(4) is based on quite a different principle. They found that the complex formed by aluminum ion with Pentachrome violet SW (Di-o-hydroxyazo dye) is suitable for determination of small amounts of aluminum. The dye containing the azo-group reduces at $pH = 4.7$ producing a polarographic wave with a half-wave potential of —0.3 *V*. On addition of aluminum ion the diffusion current, i.e. height of the wave, remains unchanged but part of the wave is shifted down by 0.2 *V*, so that two waves are produced of which the second, with a half-wave potential of —0.5 *V*, depends on the concentration of aluminum ion. The authors consider that this is due to the fact that the dye occurs only in the *trans*-form, while the complex is in the *cis*-form. The *cis*-form is reduced with more difficulty, its wave appearing at a more negative potential. Therefore both waves originate from the dye but the height of the second depends on the amount of dye bound with aluminum.

A similar phenomenon occured on the introduction of aluminum ions into the solution of ODH. As already mentioned, ODH produced a polarographic wave with a half-wave potential of —1.725 *V* at a concentration of 4 mM/*lit* in 0.5 M KCl. On the addition of aluminum ions to the solution of ODH the diffusion current, i.e. the wave height, remained unchanged, but a part of the wave was shifted down by about 0.4 *V*. giving two waves of which the second, with a half-wave potential —1.35 *V*, depended on the concentration of aluminum ions. If this concentration was 0.6 to 6 mM/*lit*, the concentration of ODH 4 mM/*l*, the pH of the solution 4.2 to 4.4 and the supporting electrolyte 0.5 M KCl with 0.01% gelatine, then there was a linear relationship between the concentration of aluminum ion and the diffusion current (Fig. 3, curve h_{Al-ODH}).

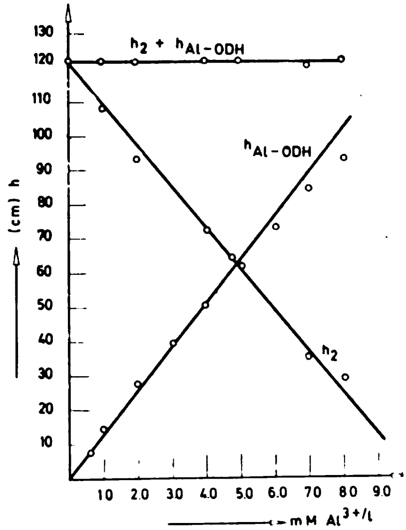

Fig. 3

Dependence of the polarographic wave height on the concentration of $Al^{3}+$ in 4 mM ODH solution

$h_{Al\text{-}ODH}$ — Height of the wave of the compound of $Al^{3}+$ and ODH
h_2 — Height of the wave of ODH
$h_2 + h_{Al\text{-}ODH}$ — Sum of the ODH and $Al^{3}+$ + ODH waves

The height of the wave corresponding to the aluminum ions did not change with decreasing pH down to 2.6, but at pH below 4 the first wave of ODH appeared and it was shifted up by 0.05 *V* ($E_{1/2}$ = —1.25 *V*) in the presence of aluminum ions, this making determination of the height of the wave of the compound formed by aluminum and ODH considerably more difficult.

If pH of the solution was increased above 4.5, then opalescence occurred and the height of the wave corresponding to the compound of aluminum and ODH decreased.

TABLE 3

Heights of Waves of ODH and Its Compound with Aluminum at Various Solution pH's: $[Al^{3+}] = 2$ *mM/lit*; $[ODH] = 4$ *mM/lit*

Height of polarographic wave at I = 10 μ*A* (*cm*)				Half-wave potential *V*			pH
h_1	$h_{Al—ODH}$	h_2	$h_1 + h_2 + h_{Al—ODH}$	E_1	$E_{Al—ODH}$	E_2	
		122.0	122.0			—1.725	4.2—9.0
	28.5	93.5	122.0		—1.35	—1.665	4.2—4.4
1.40	28.5	92.0	121.9	—1.28	—1.37	—1.70	4.0
2.5	28.5	91.0	122.0	—1.30	—1.39	—1.70	3.8
9.3	28.5	84.0	121.8	—1.30	—1.40	—1.70	3.4
13.5	28.8	78.5	121.8	—1.28	—1.41	—1.69	3.2
24.5	28.0	69.0	121.5	—1.30	—1.44	—1.69	3.0
40.5	28.0	51.5	120.0	—1.28	—1.46	—1.70	2.8
64.5	28.0	deform.		—1.28	—1.50		2.6

If the concentration of aluminum ions in the ODH solution of a definite concentration (e.g. 4 m*M*/*lit*) and pH 4.2 to 4.4 was increased, up to certain level (8 m*M*/*lit*), the wave of the compound of aluminum and ODH also increased, while the second wave of ODH decreased. At the same time, the sum of these two waves, at the same pH, was equal to the height of the second wave of ODH measured without aluminum ion present (Fig. 3). On decreasing the solution pH at a fixed concentration of ODH (e.g. 4 m*M*/*lit*) and aluminum ions (e.g. 2 m*M*/*lit*) to below 4.2, the height of the first wave of ODH increased and that of the second decreased, while the wave corresponding to their compound remained unchanged. As seen from Table 3, the sum of these three waves corresponds to the height of the second wave of ODH (h_2) measured without aluminum at pH 4.2 to 4.4.

From the above results it may be concluded that the concentration of ODH can be determined by polarography in KCl supporting electrolyte at a solution pH between 4 and 9. Aluminum can be best determined at pH 4.2 to 4.4 because at these values the first wave of ODH does not appear, although the relationship between the concentration of aluminum ions and the wave height is linear for pH between 2.8 and 4.2.

Aluminum can also be determined in 2.4 mM or 8 mM ODH solution. The higher the concentration of this compound the higher the range of aluminum concentrations which can be determined. Concentrations of aluminum up to 10 mM/*lit* may be determined in 8 mM dihydrazide solution.

Apart from KCl, solutions of hydrochloric acid, and sodium, barium, calcium and ammonium chloride of various concentrations were treid as the supporting electrolyte. NaCl, $CaCl_2$ and $BaCl_2$ could be used but the critical current of the compound of aluminum with ODH was less. In hydrochloric acid and ammonium chloride this wave did not appear.

TABLE 4

Heights of the Wave of the Compound of Aluminum with ODH and the Wave of Trivalent Aluminum Measured in 10 mM Aluminum Chloride Solution

ODH concentration *mM/lit*	Concentration of Al-Ion *mM/lit*	Height of polarographic wave at $I = 10\,\mu A$ (cm)			Half-wave potential (*V*)		pH
		h_{Al-ODH}	h_{Al}	$h_{Al-ODH} + h_{Al}$	E_{Al-ODH}	E_{Al}	
	10.0		183.0			—1.78	4.2
0.10	10.0	7.05	167.0	174.0	—1.44	—1.77	
0.50	10.0	29.5	137.5	167.0	—1.43	—1.75	
1.00	10.0	53.5	105.0	163.5	—1.41	—1.75	
2.00	10.0	105.0	45.0	150.0	—1.41	—1.70	
3.00	10.0	112.5	27.0	139.5	—1.41	—1.68	

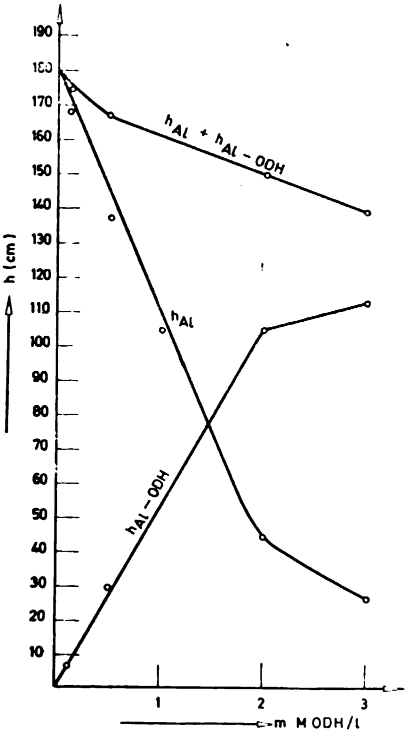

Fig. 4

Dependence of the polarographic wave height on concentration of ODH in 10 mM Al^{3+} solution

h_{Al-ODH} — Height of the wave of the compound of Al^{3+} and ODH

h_{Al} — Height of the wave of Al^{3+}

$h_{Al-ODH} + h_{Al}$ — Sum of the two waves

The experiments so for described refer to aluminum ion in the presence of an excess of oxalyldihydrazide. On the other hand, if there was an excess of aluminum ions, at $pH = 4.2$ the wave of the compound of aluminum and ODH was accompanied by another wave originating from the reduction of trivalent aluminum. In this case the wave with a half-wave potential about —1.725 *V* originating from the reduction of ODH did not appear.

According to the data in Table 4, at concentrations of ODH of 0.10 to 3.0 mM in 10 mM solution of aluminum chloride and in the presence of 0.5 M KCl and 0.01% gelatine, there appeared a wave originating from the compound of aluminum and ODH at a half-wave potential —1.44 to —1.41 *V* and also a wave corresponding to the reduction of trivalent aluminum at —1.77 to —1.68 *V*.

From Fig. 4 it may be seen that there was a linear relation between the concentration of ODH completely bound with aluminum (h_{Al-ODH}) and the diffusion current for concentrations of ODH up to 2 mM and an aluminum concentration of 10 mM. It may also be seen that the height of the wave corresponding to trivalent aluminum decreased linearly with increasing ODH concentration above 2 mM/*lit*.

School of Technology and Metallurgy, Belgrade University
Institute of Analytical Chemistry, Belgrade

Received 17 October, 1969

REFERENCES

1. Gran, G. "The Use of Oxalyldihydrazide in a New Reaction for the Spectrophotometric Microdetermination of Copper" — *Analytica Chimica Acta* (Amsterdam) 14: 150—152, 1956.
2. Vallon, I. I. and A. Badinaud. "Etude des chelates oxalylhydrazidoniques du cuivre" — *Bulletin des Traveaux de la Societe de Pharmacie de Lyon* 7: 163—177, 1963.
3. Stevančević, B. D. "Direct Spectrophotometric Determination of Microgram Quantities of Copper in High-Purity Uranium with Oxalyldihydrazide" — *Zeitschrift für Analytische Chemie* 165: 348—354, 1959.
4. Golubović, V. and M. Jovanović. "Spektrofotometrijsko određivanje mikrogramskih količina bakra u nekim mineralnim vodama SR Srbije" (Spectrophotometric Determination of Microgram Quantities of Copper in Some Mineral Waters of Serbia) — *Hemijska industrija* (Beograd) 10: 274—275, 1968.
5. Kolthoff, I. M. and J. J. Lingane. *Polarography* (2nd ed.) — New York-London: Interscience Publishers, 1952.
6. Willard, H. H. and A. J. Dean. "Polarographic Determination of Aluminium" — *Analytical Chemistry* 22: 1264—1267, 1950.

GLASNIK HEMIJSKOG DRUŠTVA, Vol. 35, No. 2-3, 1970, pp. 255—258

GHDB-99 531.715.1:546.289

Original Scientific Paper

DETERMINATION OF ORIENTATION OF GERMANIUM CRYSTALS BY INTERFEROMETRY

by

MILAN G. BREKIĆ and DRAGANA V. GLOJER

INTRODUCTION

For the determination of crystal orientation the X-ray method and reflectometry are mainly used$^{(1,\ 2)}$.

A new method for determination of the orientation of germanium crystal from the interference patterns obtained from alloy pits on the crystal surface and from the crystal surface itself was proposed by R. Dreiner and R. Garnache$^{(3)}$. In order to obtain alloy pits whose bottom is the (111) plane, they used the method given by K. Lehovec and co-workers$^{(4)}$. This method requires a fairly expensive and complicated apparatus. For the measurement of misorientation the following well-known relations are used:

$$\sin V = \sin M \cos \gamma$$

$$\sin H = \sin M \sin \gamma$$

where V is the angle of misorientation in the vertical direction from the direction [111], and H is the angle of misorientation in the horizontal direction. M is the angle formed by the direction [111] and a line normal to the direction of cutting, and γ is the angle between the interference fringes of the pit and the reference edge. The reference edge is obtained by slanting the surface whose orientation is being determined by an angle of 2—3° and it represents one of the axes.

PREPARATION OF SAMPLES AND DETERMINATION OF ORIENTATION

A slab with as near as possible (111) orientation is cut from the single crystal whose orientation is to be determined. A section of the slab surface is slanted by 2—3° in order to obtain the reference edge. The whole slab surface is first ground with carborundum powder No. 600 and then with No. 1200. During this treatment care must be taken to apply even pressure over the slab in order to avoid irregular working of the surface. A layer of 20 to 30 μ is removed from the surface by grinding.

The alloying is very complicated and depends upon many parameters, particularly if a pit with well-defined boundaries, small depth and an absolutely flat bottom is desired.

In the present work a simple method for obtaining alloy pits was used. An indium pellet about 100 μ in diameter is placed on the slanted surface near the edge being alloyed. The pellet is fixed by pressing it gently into the surface of germanium. The slab is carefully placed on a quartz base and put into a hydrogen-atmosphere alloying furnace. After a number of experiments the best results were obtained at an alloying temperature of 500 ± ± 10°C for 8 minutes. In order to obtain a sufficiently thin layer of recrystallised germanium in the alloy pit, the cooling rate had to be about 20°C/min. Indium was removed from the alloy pit by dissolving in warm hydrochloric acid for 2 minutes.

All studies were made on an N-type germanium single crystal obtained by extrusion in a horizontal vessel. The number of dislocations was 20000 per cm^2 and the specific resistance 2 Ohm cm.

Figure 1 shows the interference pattern of a germanium slab with a cavity on the slanted surface.

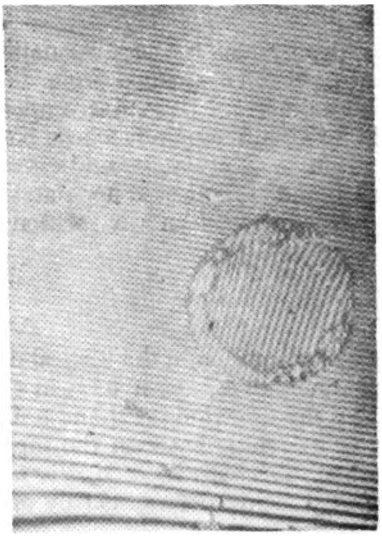

Fig. 1

Interference picture on (111) surface of a germanium crystal (× 100)

For determination of the correction angles the angles γ and M have to be found. The angle γ is determined by measuring the angle between the interference fringes appearing on the slanted part and those on the pit bottom (see Fig. 1). The expression for calculating the angle M is obtained from the relations for interference:

$$\tan M = \frac{(x-1)\frac{\lambda}{2}}{L}$$

where x is the number of fringes per unit length L, and λ the wavelength of the sodium light.

The correction angles V and H are either negative or positive, depending on the orientation of the (111) plane to the cutting surface. If H is positive, then the fringes on the bottom of the pit are inclined to the left relative to the normal to the fringes on the slanted surface, and conversely. V is positive if the fringes turn upwards and negative if they turn downwards.

TABLE 1

Experimental results

No.	Direction of measurement	Misorientation		
		Interfer.	X-ray	reflect.
1.	Horizontal direction	—2° 25’	—1° 56’	—2° 20’
	Vertical direction	+18’	+25’	+27’
2.	» »	+20’	+17’	+24’
	» »	+20’	+25’	+18’
3.	» »	+14’	+10’	+13’
	» »	+1°	+48’	+1° 10’
4.	» »	—2’	0	—10’
	» »	+20’	+8’	+15’
5.	» »	0	+10’	+8’
	» »	0	+18’	+10’
6.	» »	0	+7’	+8’
	» »	0	+15’	+5’

The measurements of orientation by intererfometry are compared with those obtained by the X-ray and reflectometry methods in Table 1. It may be concluded that the error in the determination by interferometry relative to the reflectometry and X-ray methods was less than ± 20 minutes.

School of Technology,
Institute of Mechanical Technology,
Belgrade University

Received 6 June, 1969

REFERENCES

1. Schwuttke, G. H. "Determination of Crystal Orientation by High Intensity Reflectograms" — *Journal of the Electrochemical Society* 106: 315—317, 1959.
2. Valčić, A. and M. Brekić. "Reflektometrijsko određivanje orijentacije kod monokristala germanijuma i silicijuma" (Determination of Orientation of Germanium and Silicon Single Crystals by Reflectometry) — *Glasnik hemijskog društva* (Beograd) 31 (7—8)*, 1966.
3. Drenier, R. and R. Garnache. "Precision Orientation of Germanium Crystals in the [111] Direction, Using Alloy Pits" — *Journal of Applied Physics* 33 (3).
4. Lehovec, K. and K. Busen. "Capillary Alloying: An Improved Alloying Method" — *Journal of the Electrochemical Society* 108 (3), 1961.

---

* Available in English translation from National Technical Information Service, Springfield, Virginia, 22151.

Izdavač

IZDAVAČKO PREDUZEĆE "NOLIT", BEOGRAD, TERAZIJE 27/II

*

Štampa

GRAFIČKO PREDUZEĆE "PROSVETA", BEOGRAD,
ĐURE ĐAKOVIĆA 21

SRPSKO HEMIJSKO DRUŠTVO (BEOGRAD)

BULLETIN OF THE CHEMICAL SOCIETY

Belgrade

(Glasnik Hemijskog društva — Beograd)

Vol. 35, No. 4-5-6, 1970

Editor:
ALEKSANDAR DESPIĆ

Published by
SRPSKO HEMIJSKO DRUŠTVO (BEOGRAD)
1970

**Translated and published for U.S. Department of Commerce and
the National Science Foundation, Washington, D.C., by
the NOLIT Publishing House, Terazije 27/II, Belgrade, Yugoslavia
1971**

Translated by
PAVEL ČMELIK

Edited by
PAUL PIGNON

Printed in "Prosveta", Beograd

CONTENTS

GLASNIK HEMIJSKOG DRUŠTVA, Vol. 35, No. 4-5-6, 1970, pp. 261—269

GHDB-100 539.16:628.112—628.113

Original Scientific Paper

AN INVESTIGATION OF NATURAL RADIOACTIVITY OF SPRING AND WELL WATER IN BELGRADE AND ITS SURROUNDINGS

by

DRAGICA M. KIRIĆ

This paper represents a continuation of earlier investigations on the radioactivity of spring and well water in Belgrade and its surroundings.

The presence of radon in a spring water lacking dissolved radium salts may be explained by its dissolution during the flow of water through the upper layers of the soil to where radon, a decay product of radium, has migrated from the lower layers. As a result radon may sometimes be found far away from its place of origin. This migration of radon and its dissolution in flowing groundwater results in the phenomenon that the radon percentage in many radioactive waters exceeds the equilibrium quantity corresponding to the content of radium in the water by several times. As far as medical practice is concerned, only waters containing radon without radium, i.e. radon waters, are of interest.

GEOLOGY

Almost all springs in Belgrade and its immediate surroundings rise in terrain which, according to J. Cvijić⁽²⁾, used to be two lakes or their banks (i.e. the orosional terraces of the Pannonian lake from the Pliocene): The Belgrade area (altitude 120—140 m) and the Pinosava area (210—240 m), except for Kumodraž and the foot of Avala, which, according to their altitude, belong to the Rtanj plateau (310—330 m).

This terrain is built mainly by beds of Sarmatian limestone, flysch and argillaceous schist. The merokarst (green karst) of the surroundings of Belgrade begins in the village of Žarkovo (5 km southwest of Belgrade), may be found near Kneževac and Sremčica, and extends through Makiš to the river Sava. There are also beds of blue Urgonic limestone overlain by the Neogene, mostly the Sarmatian, represented by marlstone and marly limestone at top and compact Sarmatian limestone at the bottom. In same places beach sand and gravel overlie the strata of Sarmatian limestone, as between Repište and Žarkovo. Further to the north, at Železnik and Sremčica, the Sarmatian limestone overlies flysch sandstone and shale.

The karst in the Sarmatian limestone is rich in subterranean watercourses, caves, uvalas and sinkholes; the last are found in loose material originating from weathering of the limestone (seldom in the rock itself) and consisting of clay and sandy clay detritus. Atmospheric water is often retained for a long time in these sinkholes. The drainage of the water absorbed by sinkholes gives rise to springs. J. Cvijić describes Bele Vode and Repište as examples of the most powerful springs, and Debela Voda and

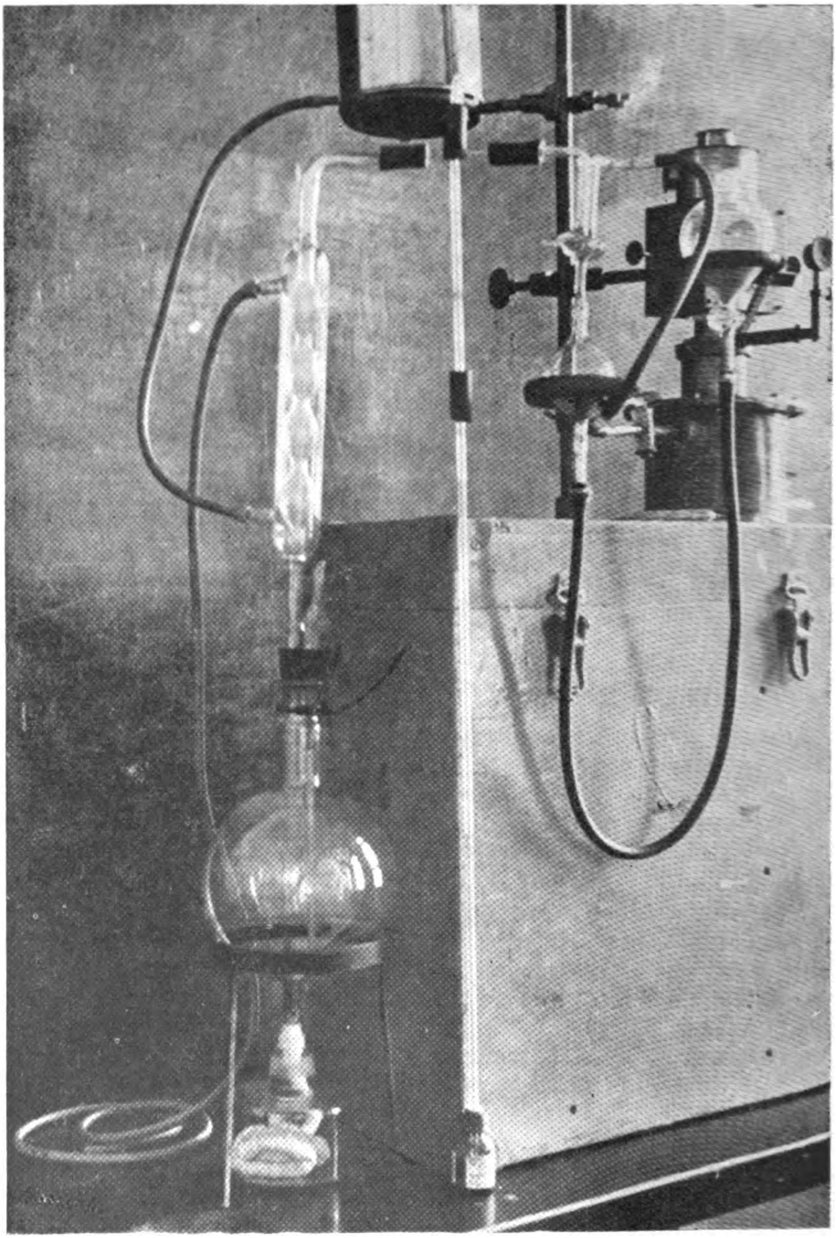

Fig. 1.
Radioactivity measuring apparatus

Turski Točak at the village of Sremčica as karstic springs. He considered the first to be in hydrographic connection with the neighboring sinkholes.

METHOD

Radioactivity was measured with an apparatus made by the author representing a portable modification of the stationary setup constructed by Professor D. K. Jovanović (Fig. 1), based on the ionization chamber method. From the water sealed in an evacuated flask radon was extracted by boiling under reduced pressure and transferred to an evacuated previously calibrated ionization chamber(3). The measured ionization current was extrapolated to the value which would correspond to the time when water sample was taken from the spring.

RESULTS AND DISCUSSION

The results of all investigations on the radioactivity of water in the area shown by Fig. 2 are summarized in Table 1, those of the present study being labelled(.). Measurements were made during the period from 1963

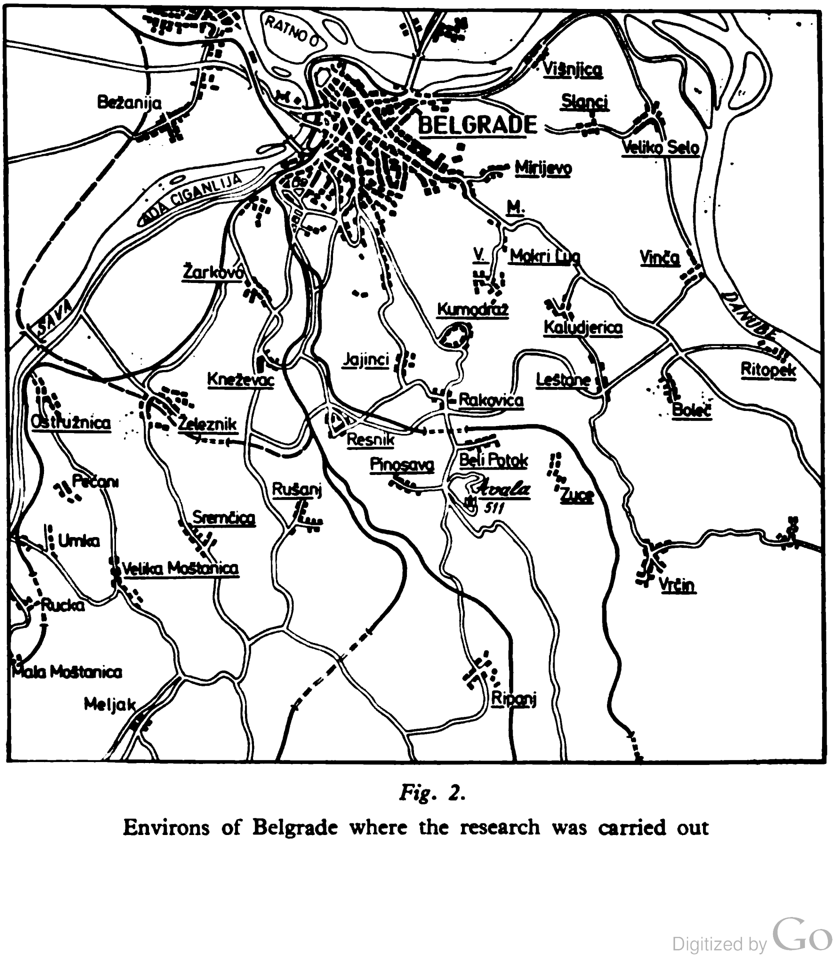

Fig. 2.

Environs of Belgrade where the research was carried out to 1968. The results represent the mean values obtained during the summer (May-September). In most waters the variations were not large. A more detailed study on changes of spring water radioactivity with season will be reported in a separate paper.

TABLE 1

Radioactivity of Spring and Well Water in the Belgrade Area

Location and site	Temperature (°C)	Spec. yield *lit/min*	Radioactivity per liter	
			Eman	Mache
I Belgrade				
(1) Izvor u crkvi Sv. Petke (Kalemegdan) (S)*	12	—	3.2	0.90
(2) Turska česma (Kalemegdan) (DF)*	12	3	4.1	1.15
(3) Rimski bunar (Kalemegdan) (W)*	—	—	0.0	0.00
(4) Čukur-česma (DF)	—	—	3.4	0.94
(5) Spomen-česma kod Gradske bolnice (DF)	12.2	70	7.9	2.18
(6) Izvor u ulici Velizara Kosanovića (S)	14.4	60	5.3	1.46
(7) Pašina česma (DF)	11.2	24	7.2	2.00
(8) Česma u Davidovićevoj ulici (DF)	12.8	30	5.4	1.49
(9) Izvor Delkova bara u Dubokom potoku (S)	12.4	48	6.4	1.79
(10) Česma u Sinjskoj ulici (Marinkova bara) (DF)	12.6	20	6.0	1.68
(11) Paun-česma u selu Banjici (DF)	12.8	40	5.3	1.47
(12) Česma Potklenje u selu Banjici (DF)	12.4	40	4.9	1.35
(13) Česma u Lisičjem potoku (DF)	11.6	24	7.7	2.13
(14) Česma Banja u podnožju Kanarevog brda (DF)	11.8	24	5.3	1.47
(15) Česma Zelenjak u Rakovici (DF)	14.4	40	1.2	0.34
(16) Bunar Sv. Petka u manastiru Rakovica (W)	—	—	1.5	0.43
(17) Spomen-česma u Rakovici (DF)	11.8	24	6.5	1.81
(18) Hajdučka česma (Košutnjak) (DF)	11.8	23	9.4	2.61
(19) Miloševa česma (Košutnjak) (DF)	11.2	5	1.8	0.49
(20) Česma pred crkvom u Topčideru (DF)	13.0	—	7.7	2.12
(21) Topčiderska česma (DF)	13.8	65	1.2	0.33
(22) Izvor u Radničkoj ulici (S) (.)	—	—	2.5	0.69
(23) Subterranean water near church in Topčider (.)	—	—	1.3	0.38
(24) Izvor ispod Avale (ka Ripnju) (S) (.)	15.6	2	3.1	0.87
II Višnjica				
(1) Česma Drvar (DF)	—	—	0.0	0.00
(2) Izvor sumporovite vode u "banji" (sulphuric S)	17.8	3	4.3	1.19
(3) Izvor na obali Dunava ispred "banje" (S)	14.8	8	4.9	1.35
(4) Izvor "banja" (S)	16.2	3	10.1	2.79
(5) Izvor iza "banje" (uncaptured S)	17.0	—	10.6	2.93
(6) Česma u Gornjoj mali (DF)	13.8	30	6.1	1.70
(7) Česma pred školom (DF)	18.6	15	2.2	0.62
(8) Česma Belo brdo (DF)	15.6	18	6.8	1.89
(9) Česmica (DF)	13.8	12	6.9	1.91
(10) Česma Graca (DF)	13.0	8	4.2	1.16
(11) Česma Ramadan (DF)	12.8	20	7.5	2.07

Location and site	Temperature (°C)	Spec. yield *lit/min*	Radioactivity per liter	
			Eman	Mache
III Slanci				
(1) Izvor na putu ka rezervoaru (uncaptured S)	—	—	6.2	1.73
(2) Česma kraj puta za Slance (DF)	16.4	12	5.3	1.48
(3) Spomen-česma (DF)	19.6	60	8.2	2.28
(4) Donja česma (DF)	20.2	60	7.5	2.07
IV Veliko Selo				
(1) Česma Čagljanac (DF)	13.8	—	5.2	1.45
(2) Izvor na desnoj obali potočića (S) (.)	9.8	—	8.8	2.42
(3) Izvor Hladna voda (S) (.)	12.0	—	1.8	0.51
V Mirijevo				
(1) Gornja česma (DF)	12.4	8	4.4	1.22
(2) Spomen-česma (DF)	10.8	40	8.2	2.26
VI Mali Mokri Lug				
(1) Česma Ekmeluk (DF)	12.8	15	2.7	0.77
VII Veliki Mokri Lug				
(1) Stojićeva česma (Veličkov kraj) (DF)	12.2	8	5.3	1.47
(2) Petrov kladenac (W)	13.6	30	2.8	0.79
VIII Kaluđerica				
(1) Česma I (DF)	17.0	24	2.2	0.61
(2) Česma II (DF)	14.2	12	4.4	1.23
(3) Česma Bunarče (DF)	14.3	15	6.6	1.82
(4) Suva česma (DF)	14.8	12	4.0	1.10
(5) Mala česma (kod pumpe) (DF)	12.8	12	5.4	1.50
(6) Velika česma (kod pumpe) (DF)	11.4	5	8.4	2.33
(7) Barutanska česma (DF)	11.8	12	6.7	1.87
(8) Divlji izvor u drugoj jaruzi (uncaptured S) (.)	—	—	3.3	0.91
IX Vinča (Gornja)				
(1) Česma Kuvanluk (DF)	13.6	15	2.1	0.60
X Leštane				
(1) Česma Krečanac (DF)	14.0	15	5.0	1.39
(2) Izvor Bunarče (S) (.)	13.2	—	2.2	0.62
XI Boleč				
(1) Spomen-česma (DF)	14.0	12	1.8	0.51
(2) Česma (DF) (.)	12.0	1	2.8	0.78
XII Ritopek				
(1) Mandin bunar (W)	—	—	3.2	0.90
(2) Česma kod crkve (DF)	16.8	8	4.0	1.12
XIII Avala				
(1) Česma kod šumske uprave (DF)	10.2	1	2.5	0.70
XIV Resnik				
(1) Stara česma (DF) (.)	14.4	—	2.9	0.80

Location and site	Temperature (°C)	Spec. yield *lit/min*	Radioactivity per liter	
			Eman	Mache
XV Pinosava				
(1) Česma kraj Avalskog puta (DF)	18.2	1	1.0	0.29
(2) Velika česma (DF)	13.6	20	5.5	1.54
(3) Mala česma (DF)	12.0	6	7.4	2.05
XVI Beli Potok				
(1) Česma Karabunar (DF)	13.2	24	1.6	0.46
(2) Česmica (DF)	15.9	8	1.4	0.39
(3) Spomen-česma (DF)	15.4	20	1.7	0.49
(4) Čarapićeva česma (DF)	13.2	30	2.7	0.75
(5) Izvor Kamenac (S)	14.0	4	0.9	0.26
(6) Jerska česma (DF)	13.4	24	0.7	0.21
(7) Izvorčić u jaruzi (uncaptured S)	13.7	—	6.5	1.79
(8) Česma u čairu (DF) (.)	14.5	3	6.8	1.88
(9) Radojkina česma (u Zavojcu) (.)	—	4	5.9	1.63
XVII Jajinci				
(1) Česma (DF)	13.6	30	2.5	0.70
(2) Izvor Bunarče (S) (.)	11.0	—	5.7	1.58
XVIII Rakovica selo				
(1) Spomen-česma (DF)	15.0	12	0.0	0.00
(2) Česma Čubura (Railovac) (DF)	13.0	20	4.0	1.11
(3) Izvor Bukovica (S)	14.4	15	1.7	0.47
XIX Kumodraž				
(1) Izvor Vodica (S)	11.6	—	1.7	0.47
(2) Česma Bubanj (DF)	13.6	7	3.3	0.92
(3) Spomen-česma (DF)	14.4	5	2.9	0.80
XX Kneževac				
(1) Česma kod škole (DF)	13.5	15	2.6	0.73
XXI Rušanj				
(1) Bunar (bivša pumpa) (W)	14.0	—	3.5	0.98
(2) Bunar Radušnja (W)	12.6	—	6.6	1.80
XXII Sremčica				
(1) Česma (DF)	13.8	22	2.3	0.65
(2) Izvor Debela voda (DF)	13.6	30	0.0	0.00
(3) Izvor Bukvar (S)	13.0	4	2.1	0.58
(4) Izvor Turski točak (S)	12.8	15	0.0	0.00
XXIII Železnik				
(1) Izvor Sv. Petka (S)	12.4	—	6.4	1.77
(2) Česma (DF)	12.3	20	9.0	2.48
XXIV Ostružnica				
(1) Velika česma (DF)	15.0	45	4.7	1.30
(2) Skeledžina česma (DF)	14.2	27	4.6	1.28
(3) Barudžina česma (DF)	14.8	12	0.0	0.00

Location and site	Temperature (°C)	Spec. yield *lit/min*	Radioactivity per liter	
			Eman	Mache
XXV Žarkovo				
(1) Česma Bele vode (DF)	13.4	250	1.3	0.37
(2) Česma Zmajevac (DF)	13.6	110	5.9	1.65
(3) Česma Provalija (DF)	13.4	300	2.8	0.78
(4) Mala česma (DF)	13.8	30	10.0	2.76
(5) Velika česma (DF)	13.2	64	5.8	1.60
(6) Česma Repište (DF)	13.2	250	2.1	0.60
XXVI Kijevo				
(1) Česma ispod puta (DF) (.)	15.6	5	4.6	1.27
(2) Česma Vrelo (DF) (.)	12.0	24	2.9	0.79
XXVII Velika Moštanica				
(1) Česma Točak (DF) (.)	13.2	2	2.1	0.59
XXVIII Vrčin				
(1) Izvor u Kasapovcu (S) (.)	13.5	—	0.9	0.27
(2) Sičkov izvor (uncaptured S) (.)	13.5	—	7.2	1.98
XXIX Ripanj				
(1) Španska česma (DF) (.)	12.6	4	27.6	7.60
(2) Izvor u jaruzi (S) (.)	14.0	—	2.8	0.78
XXX Zuce				
(1) Česma Točak (DF) (.)	13.2	24	45.2	12.43
(2) Česma Točić (DF) (.)	11.8	—	3.8	1.06
(3) Izvor Bunarče (S) (.)	11.5	—	19.8	5.66
(4) Velika česma — Zuce 1930 (DF) (.)	12.2	15	1.7	0.47
(5) Razvaljena česma (DF) (.)	12.5	—	26.2	7.22
(6) Izvor Cigansko Bunarče (S) (.)	12.5	—	18.4	5.07
(7) Izvor Radušin Bunar (S) (.)	11.0	—	0.8	0.22
(8) Izvor u Vranovcu (S) (.)	11.0	—	0.9	0.24
(9) Česma ispod Avale (DF) (.)	10.8	4	15.7	4.33
(10) Izvor ispod kamenoloma (S) (.)	11.5	—	6.5	1.79
(11) Izvor Bačvica (S) (.)	14.0	—	38.5	10.60
(12) Izvor Radučin bunar (Močila) (S) (.)	11.0	2	104.6	28.79
(13) Mali izvor u Močilima (uncaptured S) (.)	11.8	—	8.3	2.29
(14) Izvor iznad razvaljene česme (S) (.)	12.5	—	20.6	5.67
(15) Izvor Mastirina (S) (.)	12.5	—	8.8	2.42
(16) Izvor u Brdanima (uncaptured S) (.)	18.0	—	1.8	0.51
(17) Bunar br. 15 (W) (.)	13.0	—	44.4	12.22
(18) Bunar br. 11 (W) (.)	—	—	30.6	8.42
(19) Bunar br. 17 (W) (.)	—	—	3.7	1.04
(20) Bunar br. 13 (W) (.)	—	—	34.4	9.46
(21) Bunar br. 10 (W) (.)	—	—	11.3	3.12

---

* Abbreviations used in the table: (S) — spring, (DF) — drinking-fountain, (W) — well. For (.) see the text.

From the results obtained in 30 localities with a total of 130 sites — springs and wells — the area of Belgrade may be described as very rich in radioactive waters. It is noteworthy that radioactive water may be found on the whole stretch from Kalemegdan to the mountain of Avala.

Considering that all these waters are free from radium and contain only radon, they could all be used in balneology as drinking water, without any danger from their radioactivity.

From Table 1 it may be seen that in certain waters the radioactivity is appreciable, i.e. exceeding 3.5 M.U. which is usually taken as a criterion for using radioactive water in balneology.

CONCLUSION

The natural radioactivity of spring and well water from a total 30 localities in Belgrade and its close vicinity covering an area of about 400 km^2 was investigated. The results showed that only 6 out of the 130 waters were not radioactive; others showed radioactivity from 0.22 to 2.93 M.U. per liter, and 13 over 3 M.U. per liter (from 3.12 to 28.79 M.U.).

Radioactivity was measured by the ionization method. From the content of radon it may be concluded that the Belgrade area is rich in radioactive springs.

Department of Physics,
School of Medicine, Belgrade Univ.

Received 29 December, 1969

REFERENCES

1. Kirić, D. M. "Radioaktivnost izvora u Beogradu i njegovoj okolini" (Radioactivity of Springs in Belgrade and Its Surroundings) — *Zbornik radova Medicinskog fakulteta* (Beograd): (to be published).
2. Cvijić, J. *Geomorfologija I i II knj.* (Geomorphology. Vol. I & II) — Beograd: Državna štamparija, 1924.
3. Yovanovitch, D. K., and C. Chamié. "Préparation du sel étalon radiofèfe" — *Compt. rend. Acad. sci.* (Paris) 175: 266, 1922.
4. Jovanović, D. K. "O radioaktivnim vodama Jugoslavije" (Radioactive Waters in Yugoslavia) — *Glas srpske kraljevske akademije* (Beograd) 145: 1931.
5. Vučić, V. *Radioaktivnost vode i gasova Niške banje i njihovo aktiviranje* (Radioactivity of Water and Gas in the Spa Niška Banja and Their Activation) — Beograd: SAN, 1950, p. 162.
6. Baranov, V. I. *Radiometrii͡a* (Radiometry) — Moskva: Akademii͡a nauk SSSR, 1955.
7. Schreiber, H. *Biophysikalische Strahlkunde. Band I. Röntgenstrahlen und Radioaktivität* — Berlin: 1957.
8. Pećinar, M. "Hidrologija termalnih vrela Niške banje i njihova zaštita od rashlađivanja i mućenja" (Hydrology of Thermal Springs in the Spa Niška Banja and Their Protection from Cooling and Clouding) — *Glas SAN* (Beograd) 247: 1961.

GLASNIK HEMIJSKOG DRUŠTVA, Vol. 35, No. 4-5-6, 1970, pp. 271—278

GHDB-101

543.422.8:541.123.1/.2

Original Scientific Paper

A NEW METHOD OF PREPARING SAMPLES FOR QUANTITATIVE X-RAY DIFFRACTION ANALYSIS

by

JELICA D. MIŠOVIĆ and VERICA D. RAJKOVIĆ

Quantitative X-ray diffraction analysis of powders still requires study. A number of papers deal with the errors of this method. Nearly all authors agree that errors most frequently occur due to the mode of preparing the sample.

The methods of preparing samples may be divided into two main groups, viz. dry and wet. In wet methods the powder is allowed to fall freely onto the carrier, which is usually a small mould or a microscope slide with a hollow. The powder is then gently pressed in order to keep it in place. Finally the sample is treated in such way as to eliminate any orientation of the crystals, which in these experiments appears to be undesirable. A method like this was proposed by McCreery(1, 2), and was later employed (with minor alterations) by a number of other authors.

The first wet method was described in 1947 and was designed by Redmond(3). Toluene and ethyl acetate were employed as a dispersion agent, and tungsten oxide and carbide were determined with the addition of molybdenum carbide. This method was further investigated by Kay(4) who proposed its modification for determination of quartz. As the dispersion agent he used isoamyl acetate, both alone and with the addition of collodion. Simić and Rajković(5) modified the method to a considerable extent for the analysis of copper compounds and some antimony compounds. They used a mixture of isoamyl acetate, ethanol and collodion as the dispersion agent. A precisely determined quantity of the suspension was applied by pipette onto slides.

A new modification of the wet method is proposed in this paper. Its advantages are that it requires less material and skill.

EXPERIMENTAL

The following is required for preparing the samples:

Specimen — The substance to be studied should be ground to the required grade and have a homogeneous composition.

Slides — These are obtained by cutting ordinary microscope slides into three parts. They have an area of approx. 6 *cm*^{2}.

Pipette — A 1 milliliter graduated pipette.

Platinum needle — 2—3 *cm* long.

Dispersion agent — A 2 : 1 mixture of isoamyl acetate and ethanol is first prepared. The dispersion agent is then made with collodion to the desired concentration by making up the above mixture to a volume of 15 *ml* with 0.5—3 milliliter of 4% solution of collodion in ether.

Preparation technique

Since the method proposed here was compared with those given by Kay and by Simić & Rajković, the procedure for all three wet methods is given below. All possible deviations of the X-ray measurements are also mentioned.

(a) *Kay's method*$^{(4)}$. — 0.1 *g* pulverized material is placed in an agate mortar, soaked with 0.4 *ml* dispersion agent and mixed without pressing for about 2 minutes. After this the whole suspension is poured onto a slide and dried. The sample is then ready for measuring the diffraction maximums.

Diffraction maximums are given in *mm*. Every result represent the average of the values measured in three positions on two or three samples, depending upon the properties of the material studied. The average values measured on different samples can differ by as much as ±20% if the material sticks to the walls of the vessel in which suspension is made, and if there is any selective sedimentation within the sample the results may be high or low by a factor of two.

(b) *Simić & Rajković's method*$^{(5)}$. — Exactly 0.4 *g* pulverized material is measured into an agate mortar, soaked with the dispersion agent and mixed gently until a homogeneous suspension is obtained. A quantity of 0.08, 0.16 or 0.24 *ml* suspension is transfered with the 1 *ml* pipette onto the slide and spread over it. The sample is then dried and the diffraction maximum measured in the dry state.

Diffraction maxima are given in *mm*. Every result represents the average of the values measured in three positions on three different samples. The average values measured on different samples may differ by as much as ±5 *mm*, if any condition for controlling selective sedimentation within the sample as required by the method has not been satisfied. Hence the method requires extreme precision and skillful manipulation.

(c) *New method*. — 0.025—0.36 *g* pulverized material is measured on a slide. The quanity depends upon the properties of material, but mostly upon its grain size distribution and specific weight. The smaller the particles and specific weight of the material the smaller the quantity required to evenly cover the slide, which appears to be necessary for obtaining reproducible diffraction maxima.

After measuring an experimentally determined quantity of the material, 0.08—0.24 *ml* of the chosen dispersion agent is added with the 1 *ml* pipette. Small deviations in the volume of agent do not have much influence, this not being the case with the above methods. However, it must be kept in mind that selective sedimentation within the sample may occur during drying, a longer time is required for the evaporation of larger amounts of dispersion agent, this leading to an increased sedimentation.

The pulverized material and dispersion agent are mixed together with a platinum needle and poured over the slide, which is tilted about at the same time. The sample is then dried and X-rayed. Certain materials were found to give a glossy film in the presence of more concentrated collodion, which peeled off the slide on drying. In such cases the concentration of collodion in the dispersion agent must be decreased in order to avoid this but at the same time not so much as to cause crumbling of the film on drying.

The diffraction maxima, representing the average of values measured in three positions on one sample, are reproducible. The average values measured on different samples prepared from the same material and under identical conditions deviate by a maximum of ± 1 mm. The method does not require either high precision or skillful manipulation.

RESULTS AND DISCUSSION

In order to ascertain the advantages and disadvantages of the proposed method as compared with the earlier wet techniques, it was tested both on one and two-component samples. X-ray measurement on samples prepared according to all the above methods are given in Tables 1—4; they represent averages of nine measurements, i.e. on three samples in three different positions.

Certain effects during preparing the samples may change the magnitude of the diffraction maximum i.e. different results may be obtained for two samples prepared from the same material and equal amounts of suspension. On analyzing the earlier wet techniques, it is found that the magnitude of the diffraction maximum depends on:

(a) rapid selective sedimentation of particles during the transfer of suspension onto the slide;

(b) selective sedimentation during drying.

The deviations induced by (a) may be checked on samples prepared from only one component, those induced by (b) on multi-component samples.

The results in Tables 1—4 clearly show how much these effects and the corresponding deviations have been reduced.

One-component samples

One-component samples were made with pulverized Sb_2O_3, Sb and Cu_2O. From these materials, having a particle size of below 7 μ, samples were prepared according to method (b) and the new method. The diffraction maxima measured on them were very close; values are given in Table 1.

These samples were prepared with quantities of 0.0005—0.0053 g per slide. The layer was such as to cause a change of the diffraction maximum with change of thickness Selective sedimentation (a) would cause a change of the diffraction maximum in these samples. However, the results in Table 1 show that this was not the case, and also that the change of the maximum in multi-component samples was only due to selective sedimentation (b).

It was found that the proposed method of preparing samples had the following advantages:

— Far less material is required, and therefore also the time and work involved in grinding is less.

TABLE 1

Diffraction Maxima of Sb_2O_3, Sb and Cu_2O (in mm)

Quantity of material on the slide (*g*)	Mode of preparation					
	By method b)			By new method		
	Sb_2O_3	Sb	Cu_2O	Sb_2O_3	Sb	Cu_2O
0.0005	22.63	7.67	4.23	24.27	7.40	4.60
0.0027	74.43	36.07	17.80	71.60	36.25	18.80
0.0053	99.51	65.13	33.37	88.30	71.20	36.77

— By measuring the pulverized material on the slide itself is no danger of error in the quantity as in the case of its transfer in a suspension.

— Pouring the suspension, i.e. spreading out the powder with a platinum needle is far simpler and therefore no great skill and care are required.

— Selective sedimentation within the sample during drying may be avoided by adjusting the amount of dispersion agent.

— By adjusting the collodion component in the dispersion agent a film which does not peel off but also daes not crumble during the measurement may be obtained.

In conclusion it must be pointed out that besides the above advantages the cost of preparing samples by the new method was 10—20 times lower because of the smaller quantity of pulverized material and dispersion agent used and less time and work spent on grinding.

Comparative tests were also made on Sb powder of the following grades: (1) < 7 μ, (2) 5—20 μ, and (3) 20—40 μ. The samples were prepared according to all three methods (a, b, c).

Kay's method, in which the whole suspension prepared from 0.1 *g* pulverized material is transfered onto the slide, appeared to be more successful with coarse than with finely ground material, since with the latter the suspension stuck to the walls of the agate mortar.

Samples of grades (2) and (3) could not be made by the method of Simić & Rajković due to rapid sedimentation of coarse particles during preparation of the suspension in the mortar.

Testing the new method on the same grade antimony powder showed that with increasing particle size the amount of powder on the slide also had to be increased. The minimum quantity of antimony on the slide giving maximum intensity of the diffraction maximum was found experimentally:

— < 7 μ — over 0.02 *g*
— 5—20 μ — over 0.05 *g*
— 20—40 μ — over 0.1 *g*

Two-component samples

These samples were prepared by mixing together equal weights of the following materials:

$Sb_2O_3 : Sb = 1 : 1$,
$Sb_2O_3 : Cu_2O = 1 : 1$, and
$Sb_2O_3 : SiO_2$ (amorphous) $= 1 : 1$

In these mixtures Sb_2O_3 was the measured component. The particles were below 7 μ in diameter. Samples were prepared by all three methods. X-ray measurements on these samples are given in Table 2.

TABLE 2

Diffraction Maxima of Sb_2O_3 Measured on Two-Component Samples (in mm)

Un-measured component	Mode of preparation						
	(a)	(b)			(c)		
	Quantity of sample (*g*) or of suspension (*ml*) on the slide						
	0.1 *g* 0.4 *ml*	0.0213 *g* 0.08 *ml*	0.0426 *g* 0.16 *ml*	0.0639 *g* 0.24 *ml*	0.0213 *g* —	0.0426 *g* —	0.0639 *g* —
Sb	82.29	51.75	85.05	94.25	42.85	38.97	45.62
Cu_2O	94.17	59.03	84.37	89.02	53.70	55.37	53.65
SiO_2 (amorphous)	90.64	78.67	89.55	88.90	72.75	68.02	72.42

The new method was also tested on samples prepared by mixing together equal parts of Sb_2O_3 and Sb with different grades of powdered antimony: (1) < 7 μ, (2) 5—20 μ, and (3) 20—40 μ. In all three cases the Sb_2O_3 pow-

TABLE 3

Diffraction Maxima of 1 : 1 Mixture of Sb_2O_3 and Various Grades of Sb

Size of Sb particles (μ)	Mode of preparation						
	(a)	(b)			(c)		
	Quantity of sample (*g*) or suspension (*ml*) on the slide						
	0.1 *g* 0.4 *ml*	0.0213 *g* 0.08 *ml*	0.0426 *g* 0.16 *ml*	0.0639 *g* 0.24 *ml*	0.0213 *g* —	0.0426 *g* —	0.0639 *g* —
<7	82.29	51.75	85.05	94.25	42.85	38.97	45.62
5—20	80.53	57.95	85.95	89.50	43.25	52.94	55.10
20—40	80.21	70.73	72.22	79.29	42.33	34.48	48.65

der grade was the same (< 5 μ). The Sb_2O_3 diffraction maxima measured on these samples (Table 3) showed that with changing grade of the unmeasured component the reproducibility decreased. However, it must be pointed out that the samples prepared by the older methods gave appreciably higher maxima due to very pronounced selective sedimentation, while with those prepared by the new method random deviations were more frequent and pronounced.

It may be concluded that fine grinding both of the sample and the standard, i.e. the determined and the secondary components, is essential for the new method too.

The method was also tested on mixtures prepared by blending together equal parts of one- and two-component samples used in original state as for the measurements in Tables 1 and 2) and amorphous SiO_2. The results are given in Table 4. It may be seen that the addition of solid diluent considerably decreased deviations originating from selective sedimentation and those characteristic of the new method (Table 3).

TABLE 4

Diffraction Maxima of Equal Parts of Sb_2O_3 and Sb in 1 : 1 Mixture with Amourphous SiO_2 (in mm)

Size of Sb particles (μ)	Mode of preparation						
	(a)	(b)			(c)		
	Quantity of sample (*g*) or suspension (*ml*) on the slide						
	0.1 *g* 0.4 *ml*	0.0213 *g* 0.08 *ml*	0.0426 *g* 0.16 *ml*	0.0639 *g* 0.24 *ml*	0.0213 *g* —	0.0426 *g* —	0.0639 *g* —
<7	41.15	34.48	33.30	33.30	32.28	32.28	33.55
5—20	75.70	50.92	63.82	72.75	66.35	68.57	70.59
20—40	82.10	58.57	72.60	74.29	70.12	73.40	73.14
<5 Cu_2O	62.15	58.63	55.37	61.50	55.07	53.50	55.39

The results show that the advantage of the proposed method is in the always constant quantity of sample and of individual components, and in that selective sedimentation can be minimized by decreasing the amount of dispersion agent or altering the concentration of collodion in it.

SUMMARY

A new method of preparing samples for quantitative X-ray analysis of pulverized material is proposed. The method was tested on one and two-component samples and compared with the wet methods of Kay⁽⁴⁾ and Simić & Rajković⁽⁵⁾.

The method has the advantage of always using a constant quantity of sample and the same ratio of components in the specimen and the sample. Selective sedimentation within the sample can be reduced to a minimum by: (a) decreasing the quantity of dispersion agent, (b) altering the quantity of collodion in the agent, or (c) adding solid diluent. Then any errors are random.

School of Technology, Belgrade University,
and Department of Analytical Chemistry,
Institute of Chemistry, Technology
and Metallurgy, Belgrade

Received 20 February, 1969

REFERENCES

1. McCreery, G. L. "Improved Method for Powdered Specimen Used on the Geiger Counter X-Ray Spectrometer" — *Journal of the American Ceramical Society* 32: 141—143, 1949.
2. Klug, H. P., and L. E. Alexander. *X-Ray Diffraction Procedures* — New York: John Wiley & Sons, Inc., 1959, pp. 300.
3. Redmond, J. C. "Quantitative Analysis with X-Ray Spectrometer" — *Analytical Chemistry* 19: 773—775, 1947.
4. Kay, K. "Rapid Quartz Analysis by X-Ray Spectrometry" — *American Industrial Hygiene Association Quarterly* 11: 185—194, 1950.
5. Simić, V. and V. Rajković. — (Unpublished manuscript).

GLASNIK HEMIJSKOG DRUŠTVA, Vol. 35, No. 4-5-6, 1970, pp. 279—284

GHDB-102

54-44:536.3/.9-31:546.262.3

Original Scientific Paper

THE EFFECT OF ADDITIVES ON CATALYST PROPERTIES IN LOW-TEMPERATURE CARBON MONOXIDE CONVERSION

by

PAULA S. PUTANOV and ŽARKO D. JOVANOVIĆ

Catalytic conversion of carbon monoxide with water vapor into carbon dioxide and hydrogen is a part of the process of hydrogen production from natural gas(1, 2). The increasing production of hydrogen, used primarily for ammonium synthesis, makes this reaction increasingly important in the chemical industry. Demands on it are becoming evermore rigorous because in many cases high-purity hydrogen (99.5% or more) with a low content of carbon monoxide is needed.

Two types of catalyst are employed today for the industrial catalytic conversion of carbon monoxide. Ferric oxide containing a small amount of chromium oxide is used in so-called high-temperature conversion, performed at temperatures of 400—500°C, with a 3—4% residue of unconverted carbon monoxide. Combinations of zinc and chromium and, since recently, also copper allow conversion at low temperatures, i.e. at 180—250°C, or 280—350°C depending on the type of catalyst; the carbon monoxide residue in the converted gas is reduced to 0.2—0.6. Another advantage of this second type of catalyst is that at high pressure no lateral reactions(3—6) occur as is the case with iron-chromium catalysts(7—9).

As such complex catalytic systems are both industrially important and interesting from the theoretical point of view, catalysts for low-temperature carbon monoxide conversion have been investigated in many laboratories. The main aim of most studies has been that of increasing the activity or of thermal stability of the catalyst(10, 11).

EXPERIMENTAL

A basic type of catalyst was chosen for the present investigations, in which the sequence of components is: zinc-copper-chromium. Varieties of this type are rarely employed in industry. However, under appropriate conditions they give good results and are particularly interesting with regard to the role of each component.

In order to determine the effect of different promotors on the properties of this type of catalyst, investigations were made of the textural properties, catalytic activity and thermal stability of an unpromoted catalyst, and a catalyst to which potassium, calcium, magnesium, titanium, aluminum and manganese oxide promoters were added by mechanical stirring and coprecipitation.

The basic catalytic substance was synthesized from aqueous solutions of zinc, copper and chromium nitrates mixed in fixed ratios. The solution was first heated to 90°C and then precipitated with 5% ammonia. The solution was mixed by bubbling air. The precipitation temperature was maintained around 80°C. After quantitative precipitation, the precipitate was washed with distilled water until nitrate ions were completely removed. It was then pressed and dried at 105°C for a period of 48 hours. Annealing was performed at 300—340°C. Binding materials and graphite flakes were added, the mass was well homogenized and then formed in 5 × 5 mm tablets. Tablets were gradually heated up to 340°C and kept at this temperature for 5 hours.

Promotors were added to the catalyst in amounts from 1 to 1.5% by mechanically stirring the metal oxides with the pulverized catalyst and also by precipitating them together with the basic components from the nitrate salt solutions.

The textural properties of the catalyst were observed by comparing the specific surface area, total porosity and pore structure. The specific surface area of the catalyst was determined by the BET method using low-temperature adsorption of nitrogen. The total porosity was determined from the ratio of apparent to actual density, and the pore size distribution was determined by mercury porosimeter(12).

The catalytic activity was studied by determining the degree of conversion in an integral reactor which represented a scaled-down model of an industrial reactor. The ratio between the amount of catalyst (100 *ml*) and of the reactant (flow rate: 400—1200 *ml/min*) was chosen so as to give a difference in concentration of the reacting components at the gas inlet and outlet of the reactor sufficient for adequate determination of the efficiency of the process and the decrease of the catalytic activity. The grain size of the catalyst was 5 × 5 *mm*, reactor temperature 200—300°C, gas mixture composition: 60—62% hydrogen, 31—33% carbon monoxide and 5—10% nitrogen, the vapor-gas ratio 1.3—1.0.

Industrial conditions require that overheating the catalyst by 50—100°C above the normal temperature of the process should not permanently deactivate it. We investigated thermal stability increasing the temperature to above 250°C, i.e. 10°C in each test, and then after 45—60 minutes reducing it back to experimental conditions. The thermal stability was investigated with the same flow rate, gas mixture composition and vapor-to-gas ratio as under experimental conditions at which the catalyst has the highest activity.

RESULTS

Experimental results for the activity and textural properties of non-promoted catalyst samples are shown in Table 1. Samples I—V represent varieties of the basic type of catalyst in which the proportions of components varied as follows: 68—73% zinc oxide, 15—20% copper oxide and 9—14% chromium oxide.

TABLE 1

Textural Properties of Nonpromoted Catalysts having Different Ratios of the Basic Components

Sample	Density g/cm^3		Total porosity	Spec. surf. m^2/g	Pore diam. Å	Conversion %
	Apparent	Actual				
I	1.92	3.48	0.453	36.1	270	99.2
II	1.49	4.87	0.694	32.5	285	99.1
III	1.40	4.30	0.675	39.4	480	98.5
IV	1.68	4.21	0.601	35.8	210	98.5
V	1.36	4.73	0.713	37.9	275	98.5

The results show that the basic catalysts possess high activity at temperatures suitable for carbon monoxide conversion (180—250°C).

Investigations of the thermal stability of nonpromoted catalytic samples showed that overheating to 260—280°C decreased the activity, while on returning to experimental conditions (180—250°C) the initial activity was immediately reestablished. The activity decrease caused by heating to 290—310°C was recuperated after 2 or 3-day use of the catalyst in experimental conditions. After overheating to 320—350°C, the activity was reestablished in experimental conditions when air was bubbled over the catalyst. On overheating to 360°C or above the catalyst permanently lost its activity.

Our earlier investigations of a high-temperature catalyst for carbon monoxide conversion showed that mechanically added promotors improved the thermal stability of the catalyst(13). For this reason, the first step in the present work was to investigate the effect of different metallic oxide promoters mixed with the basic components. Textural properties and activities of promoted zinc-copper-chromium catalysts are shown in Table 2. The basic mass composition corresponds to that of catalyst III in Table 1.

TABLE 2

Textural Properties and Activity of Zinc-Copper-Chromium Catalysts Mixed with Metallic Oxide Promoters

Sample	Density g/cm^3		Total porosity	Specif. surface m^2/g	Conversion %
	Apparent	Actual			
1	1.73	4.09	0.587	38.4	98.5
2	1.42	4.39	0.677	37.6	97.8
3	1.53	4.48	0.659	36.7	97.5
4	1.63	4.63	0.648	35.9	97.7
5	1.69	4.62	0.635	35.9	95.6
6	1.78	4.52	0.607	37.6	98.2
7	1.65	4.27	0.614	40.6	96.6

The first sample in a nonpromoted catalyst, the second one contains magnesium oxide, the third aluminum trioxide, the fourth calcium oxide, the fifth titanium dioxide, the sixth magnesium oxide and aluminum trioxide, and the seventh a mixture of magnesium oxide, aluminum trioxide, calcium oxide and titanium dioxide.

As may be seen from Table 2 there is no essential difference in textural properties between nonpromoted and promoted catalysts. The slight differences in the porosity and the specific surface area are within the sensitivity limits of the method used, and they cannot considerably affect the catalytic activity. The catalytic activity of promoted samples in the optimum temperature range is within the same limits or lower than before adding oxides.

The results obtained for promoted catalysts at temperatures exceeding 350°C do not indicate any shift of the limit of activity loss. These catalysts seemed only to be more resistant to sudden temperature changes under experimental conditions and when first used. This is not particularly advantageous taking into account the poor results obtained for catalytic activity.

From these investigations it may be concluded that metallic oxides added by mixing did not have any particular effect on the catalyst properties. This is due to the fact that these metallic oxides do not react chemically with the basic components, nor do they show any peptizing effect on the basic catalytic mass, i.e. they do not form solid solutions and therefore, as was seen, do not prevent thermal sintering of the catalyst, nor do they make for a larger contact surface. This conclusion has been confirmed by differential thermal analysis(14).

Activity and textural properties of catalysts promoted by coprecipitation of additives with the basic components are shown in Table 3.

TABLE 3

Activity and Textural Properties of Low-Temperature Catalyst with Coprecipitated Promoters

Catalyst	Basic components	Promoters	Porosity %		Spec. surf. m^2/g		CO outlet %	Conversion
			reduced	nonreduced	nonreduced	reduced		
I	Zn-Cu-Cr	—	72.6	76.6	35.1	27.4	0.4	98.5
II	Zn-Cu-Cr	Mg	74.5	76.3	37.0	26.7	0.6	97.5
III	Zn-Cu-Cr	Al	79.6	77.4	53.0	54.5	3.5	86.3
IV	Zn-Cu-Cr	K	74.4	65.6	33.6	28.0	0.4	98.3
V	Zn-Cu-Cr	Ca	75.9	77.6	38.9	28.6	0.4	98.5
VI	Zn-Cu-Cr	Al Mg Ca K	74.8	68.5	48.9	54.3	5.2	80.4
VII	Zn-Cu-Cr	Mn	66.7	69.5	32.8	25.3	0.4—0.2	98.9

From Table 3 it is seen that oxides of magnesium, potassium and calcium did not influence catalytic activity. In these samples, after activity reduction, the porosity increased, while the specific surface was reduced. The catalyst with aluminum oxide promotor had a much reduced activity and its textural properties changed, unlike the samples containing magnesium, potassium and calcium oxides. In the catalyst containing aluminum the porosity decreased while the specific surface increased. From the experimental results for sample VI in Table 3 it may be concluded that the structure and activity of the catalyst and its textural properties were predominantly affected by aluminum irrespective of the presence of three other elements.

Overheating of catalyst samples with these promoters showed that their thermal stability had not improved and their activity was already reduced at temperatures above 250°C, while at temperatures above 350°C it was completely lost. However, sample VII, promoted with manganese, showed high activity. Its textural properties are similar to these of nonpromoted catalyst and samples with magnesium, potassium and calcium. Overheating of this sample showed that it was the most stable of all samples so far investigated in our laboratory. Even after overheating to 350—400°C its activity could be reestablished in experimental conditions.

From these investigations it may be concluded that magnesium, potassium and calcium oxides promoters do not affect the properties of the catalyst irrespective of the mode of addition. Aluminum oxide added by coprecipitation acts as an inhibitor. Manganese oxide added by coprecipitation acts as a structural promoter and improves the catalytic activity and the thermal stability of the catalyst.

SUMMARY

The effect of several metallic oxides on catalytic activity and thermal stability of a three-component low-temperature catalyst for carbon monoxide conversion has been studied.

Promotors were added by mechanical mixing and by coprecipitation with the basic components of the catalyst.

Metallic oxides added by mechanical mixing did not have any noticable effect on the activity or thermal stability of the catalyst; textural properties depend on the kind and amount of oxides added.

When promotors were coprecipitated with the basic components, it was found that aluminum oxide acted as an inhibitor, while manganese improved the thermal stability of the catalyst. The textural properties o the inhibited and promoted catalysts showed considerable differences.

REFERENCES

1. Blasiak, E. K. Laindler, S. Pawlikowski, and J. Sobolewski. *Tehnologia związkow azotowych. Tom I.* (Technology of Nitrogen Compounds) — Warszawa: Państwowe widawnictwa techniczne, 1955.
2. Goodridge, F., and H. A. Quazi. "The Water-Gas Shift Reaction: A Comparison of Industrial Catalysis" — *The Chemical Engineer* (211), *Transactions of the Institution of Chemical Engineers* 45(7): T274, 1967.
3. Atroshchenko, V. I., and B. Bibr. "Issledovanie konversii okisi ugleroda vodi͡anym parom pri povyshënnom davlenii" (Conversion of Carbon Monoxide by High-Pressure Steam) — *Zhurnal prikladnoi khimii* 32(5): 997, 1959.
4. Atroshchenko, V. I., and G. N. Ivanova. "Kinetika reakt͡sii konversii okisi ugleroda parami vody na t͡sink-khromovom katalizatore pod povyshënnym davleniem" (The Kinetics of Carbon Monoxide Conversion by High-Pressure Steam over a Zinc-Chrome Catalyst) — *Zhurnal prikladnoĭ khimii* 37(3): 517, 1964.

5. Ivanovskiĭ, F. P., G. E. Braude, and T. A. Semënova. "Izuchenie prot͡sessa konversii i podbor katalizatorov dli͡a konversii okisi ugleroda pri povyshënnom davlenii" (High Pressure Carbon Monoxide Conversion: A Study of the Process and Choice of Catalyst), in: *Trudy Gossudarstvennogo nauchno-issledovatel'skogo i proektnogo instituta azotnoĭ promyshlennosti* (Collected Papers of the State Nitrogen Industry Research and Design Center) — Moskva-Leningrad: Izdatel'stvo khimicheskoĭ literatury, 1957.

6. *Spravochnik azotechika* (Nitrogen Engineering Manual) — Moskva: Izdatel'stvo khimii͡a, 1967.

7. Ivanovskiĭ, F. P., G. E. Braude, and T. A. Semënova. "Sposob poluchenii͡a niskotemperaturnogo katalizatora konversii okisi ugleroda" (Production of Low-Temperature Catalyst for Carbon Monoxide Conversion) — *Avtorskoe svidetel'stvo USSR, klass 12g, 401, No 123523. Zai͡avlennoe 6 fevrali͡a 1959 g za No 618528/23*) USSR Patent No 123523, Application Registered on February 6, 1959, No. 618528(23) — published in: *Bi͡ulleten' izobreteniĭ* (21): 1959.

8. Ivanovskiĭ, F. P., G. E. Braude, I. A. Semënova, and B. G. Li͡udkovskai͡a. "Issledovanie katalizatora konversii okisi ugleroda na osnove okislov t͡sinka, khroma i medi" (Carbon Monoxide Conversion Catalysts Based on Zinc, Chrome and Copper Oxides) — *Sbornik Problemy kinetiki i kataliza — fizika i fiziko khimii͡a kataliza* (Collected Papers: Problems of Kinetics and Catalysis. Physics and Physical Chemistry of Catalysis) — Moskva: Izdatel'stvo Akademii nauk USSR, 1960.

9. Semënova, I. A., M. I. Markina, B. I. Steĭnberg, L. I. Kozlov, and N. K. Maiorov. "Niskotemperaturnyĭ katalizator dli͡a prot͡sessa konversii okisi ugleroda" (A Low-Temperature Catalyst for Carbon Monoxide Conversion) — *Khimecheskai͡a promyshlennost'* 2(4): 277—280, 1966.

10. Kostrov, V. V., I. P. Kirillov, and A. M. Alekseev. "Izuchenie prot͡sessa formirovanii͡a t͡sinkkhrommednykh katalizatorov konversii okisi ugleroda" (Formation of Zinc-Chrome-Copper Catalysts for Carbon Monoxide Conversion) — *Izvestii͡a vysshikh uchebnykh zavedeniĭ USSR "Khimii͡a i khimicheskai͡a tekhnologii͡a"* (9): 1027—1030, 1967.

11. Markina, M. I., G. K. Boreskov, F. P. Ivanovskiĭ, and B. G. Liudkovskai͡a. "Issledovanie kataliticheskoĭ aktivnosti zhelezokhromovykh katalizatorov v prot͡sesse vzaimodeistvii͡a okisi ugleroda s vodi͡anym parom" (Catalytic Activity of Iron-Chrome Catalyst in the Reaction of Carbon Monoxide and Steam) — *Kinetika i kataliz* 2(6): 867, 1961.

12. Putanov, P. "Porous Materials Structure Investigation" — *Hemijska industrija*(1): 141—147, 1969.

13. Atroshchenko, V. I., A. M. Alekseev, A. P. Zasorin, I. P. Kirillov, V. I. Konvisar, and A. R. I͡astrebeneckiĭ. *Tekhnologii͡a svi͡azannogo azota* (Bound Nitrogen Technology) — Khar'kov: Izdatel'stvo Khar'kovskogo Universiteta, 1962.

14. Putanov, P., Ž. Jovanović, and Bj. Aleksić. "The Influence of Certain Chemical Structure Changes of the Low-Temperature Carbon Monoxide Shift Catalyst on Its Behavior in Heat Treatment" — *Glasnik hemijskog društva* (Beograd): (this issue).

GLASNIK HEMIJSKOG DRUŠTVA, Vol. 35, No. 4-5-6, 1970, pp. 285—294

GHDB-104 54.02:54-44:546.262.3:66.04

Original Scientific Paper

THE INFLUENCE OF CERTAIN CHEMICAL STRUCTURE CHANGES IN LOW-TEMPERATURE CARBON MONOXIDE SHIFT CATALYST ON ITS BEHAVIOR IN HEAT TREATMENT*

by

PAULA S. PUTANOV, ŽARKO D. JOVANOVIĆ and BOJANA D. ALEKSIĆ

A relatively small number of published works gives information about processes which ensue during heat treatment of the zinc hydroxide-chromic hydroxide-copper hydroxide system which represents the basis for a low temperature CO-shift catalyst. There are data regarding the thermal analysis of low — temperature catalysts, but in these cases neither chromium nor zinc are found in the form of their hydroxides, the former appearing as chromic acid anhydride and the latter as zinc oxide(8, 9). Certain papers deal with the zinc oxide-chromium trioxide system, which corresponds to the catalyst used in the synthesis of methanol, in which chromic acid and zinc oxide are the initial components(7, 12). However, the derivation of an analogy for the CO-shift catalyst meets with difficulties since the form of the initial components affects the kind of intermediates or products of their reaction.

The formation of chromate or chromite, the building up ot spinels or the formation of solid solutions can take place at different temperatures in the zinc-chromium-copper system. These differences become more obvious if the mixture is heated in various atmospheres (hydrogen, carbon monoxide, etc. (3, 7, 8). When promoters are added the processes become *even more complex*. It is known that the chemical form of the added components and the mode of addition affect the chemical and structural form of the promoter in the catalyst following heat treatment and activation. A promoter precipitated together with the basis catalyst will not be distributed in it in the same way as one put into a partially or completely heat-treated catalyst by melting, or one mixed into a pasty base catalyst.

Our aim was to define the processes which take place in the low — temperature CO-shift catalyst while it is undergoing heat treatment, reduction and activation, and when it is placed in reactive surroundings. For that purpose, we carried out differential thermal analysis of catalyst samples without promoters, and for samples promoted by salts of potassium, calcium, aluminum, manganese and magnesium, by a mixture of salts of potassium, magnesium, aluminum and calcium (mixture I), and by a mixture of salts of magnesium, aluminum and manganese (mixture II).

---

* Communicated at the 14th Conference of Chemists of the SR of Serbia, Belgrade, January 1969.

The basic catalyst was obtained by precipitating zinc, cupric and chromic hydroxides from 10% solutions of the corresponding nitrates of these metals, purity p.a., with 5% solutions of hydroxides by rapid dropping. All promoters were precipitated from the corresponding nitrates together with the basic catalyst. The precipitate was rinsed with distilled water until the nitrate reaction ceased and dried at 105° for 48 hours.

By precipitation of zinc, chromium and cupric by ammonium hydroxide from a solution of the nitrates also containing potassium, magnesium and calcium nitrate, a distribution of potassium, magnesium and calcium in the form ot nitrates, which are converted into oxides during subsequent heat treatment, was obtained in the basic hydrophylic gel⁽⁵⁾. This was confirmed by the appearance of nitrous vapors on high-temperature treatment of catalyst containing one of these promoters.

Since the ammonium nitrate was completely removed by rinsing, the initial systems in this research contained zinc, cupric and chromic hydroxide, aluminum and magnesium hydroxide, and potassium, magnesium and calcium nitrate.

The differential thermal analysis was carried out in an apparatus with an automatic heating recorder and an automatic temperature recorder (Stanton Standat 6—25) with aluminum oxide as the inert reference substance. In all experiments the heating rate was 10°C/min. The weight of each sample was about 80 *mg*. The experiments were carried out in the temperature range from room temperature to 600°C. The recording principle of this apparatus is such that endothermic processes are plotted above the base line and exothermic below.

To examine the effect of the atmosphere in which heat treatment takes place we carried out DTA in air, nitrogen, hydrogen, vacuum, in a mixture of nitrogen and carbon monoxide (the CO concentration being 30%), and in a reaction mixture consisting of 60% hydrogen, 33% carbon monoxide and 7% nitrogen.

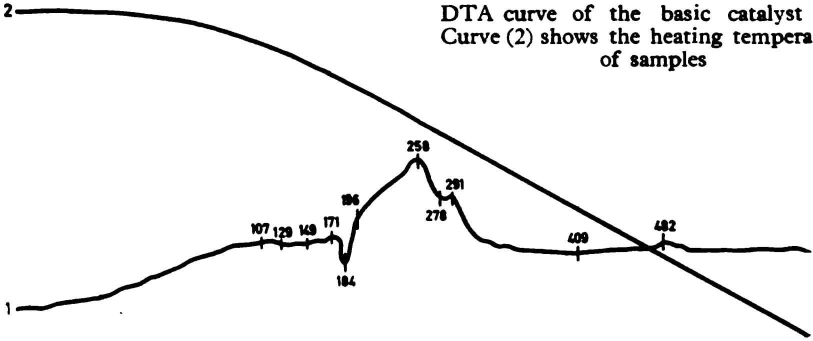

Fig. 1.

DTA curve of the basic catalyst (1). Curve (2) shows the heating temperature of samples

The catalyst without promoters (basic catalyst) contained zinc, cupric and chromic hydroxide as initial components. The process of its decomposition in air is shown in Fig. 1. Explanations of the effects seen on the DTA curve are given in Table 1⁽²˒ ¹⁰˒ ¹¹⁾.

TABLE 1

Effect no.	Type	Nature	Temp. of initiation °C	Temp. of maximum, °C
I	endothermic	release of weakly-bound water from hydroxides	room temperature	107
II	endothermic	decomposition of $Zn(OH)_2$ into ZnO; decomposition of Cu(OH); release of weakly-bound water from hydroxides	149	171
III	endothermic	complete dehydration of ZnO; further dehydration of chromium hydroxide	184 (a jump at 196)	258
IV	endothermic	regrouping inside chromium oxides — decomposition of higher valency chromium oxides produced in preceding processes	278	291
V	endothermic	release of oxygen, which usually precedes the crystallization of chromium trioxide	409	482

Up to 620°C there was no exothermic peak of the chromium trioxide crystallization, which in air takes place in the chromic hydroxide itself at temperatures ranging from 350° to 400°C. This is the usual phenomenon of "protective" action of other oxides present in the mixture. The effect of the formation of copper chromate, which accompanies chromium trioxide crystallization, was not noticed either(4).

DTA of samples of catalyst precipitated with a single promoter is shown in Fig. 2. In addition to the similar behavior of the basic catalyst, each curve also shows effects characteristic of the promoter(3, 6, 12). There is an endothermic crystalline transformation in the case of potassium and water release in the case of calcium and magnesium in the interval ranging up to 190°C, where there is also a considerable endothermic effect from the basic catalyst itself. This shows that in the first stage of heat treatment these promoters are present in the form of distinct phases. Due to the superposition of effects at higher temperatures, it is not possible to separate effects due only to the promoters. The catalyst containing aluminum showed a greater quantity of bound water, which results from the fact that aluminum precipitates as a gel. Catalysts containing aluminum and magnesium showed greater resolution of the two endothermic peaks in the temperature range

170—270°C. Exothermic crystallization effects or the formation of chromates were not noticed in any of the catalysts.

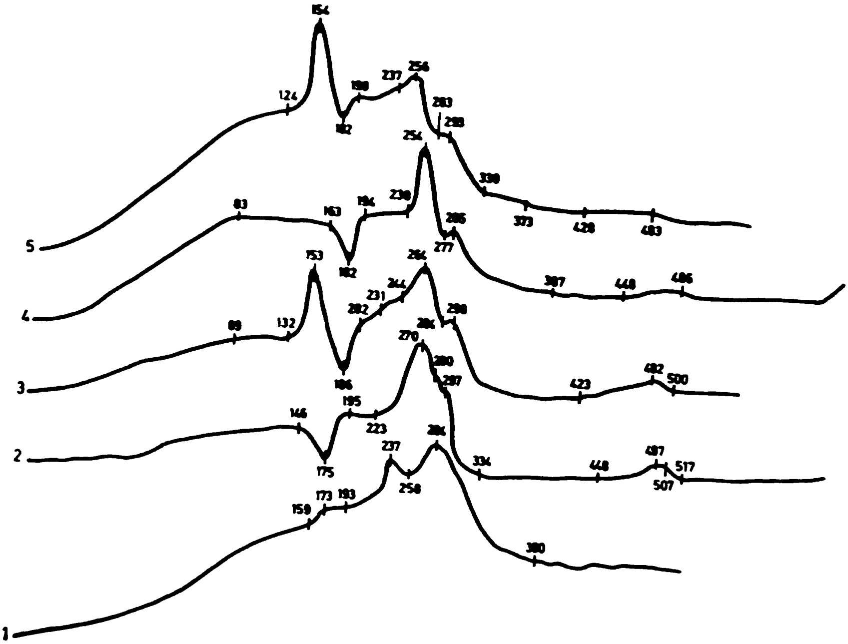

Fig. 2.

DTA of promoted catalyst in air. Catalyst promoted with aluminum (1), manganese (2), potassium (3), magnesium (4), calcium (5).

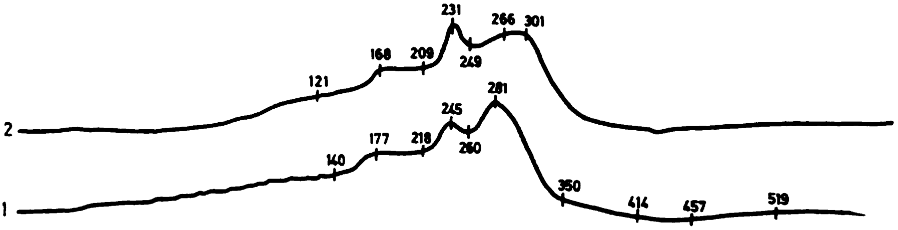

Fig. 3.

DTA in air of catalyst promoted with mixture of promotors, curve 1 with mixture II (aluminum, magnesium and manganese); curve 2 with mixture I (aluminum, magnesium, calcium and potassium).

Samples of catalysts containing two different groups of promoters showed only the endothermic peaks (Fig. 3) already seen in the case of the basic catalyst. Certain differences exist in the region up to 170°C, in which catalysts containing mixed promoters exhibited a more balanced release of water, in a manner very similar to that of the catalyst containing aluminum (Fig. 2, curves 2,3 and 5). This suggests that aluminum makes for precipitation of a more homogeneous gel. There were no significant differences in the behavior of catalysts promoted by manganese (Fig. 3, curve 1) and by potassium and calcium (Fig. 3, curve 2), even if though some thermograms (Fig. 2, curves 2,3 and 5) do exhibit endothermic effects of different magnitude at various temperatures up to 270°C.

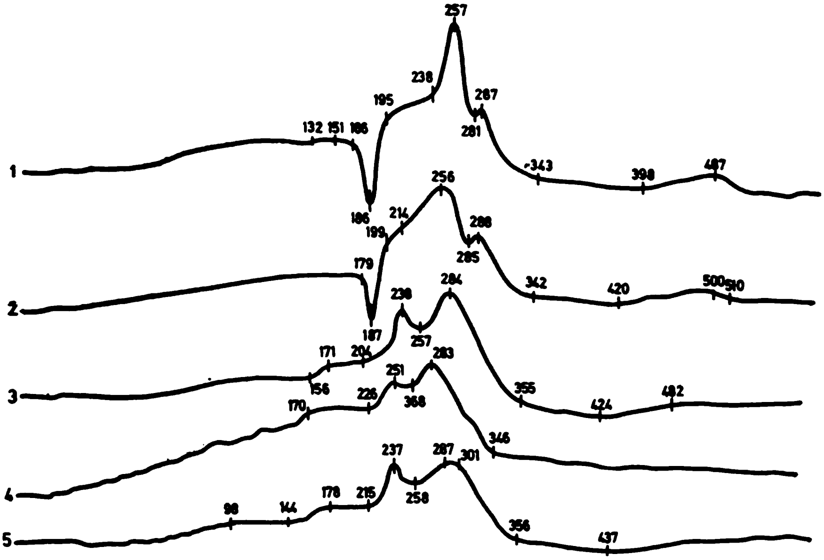

Fig. 4.

DTA of the basic catalyst and promoted samples in a stream of nitrogen. Basic catalyst, (2); catalyst promoted with magnesium (1); with aluminum (3); with mixture II (4); with mixture I (5).

Experiments in nitrogen atmosphere, shown in Fig. 4, do not exhibit substantial differences in thermal effects in any of the samples. Endothermic effects in the region around and above 450°C are somewhat more pronounced, this being due to the release of oxygen from chromium oxide.

Unpromoted catalyst and catalyst promoted by two different mixtures of promoters were examined in vacuum (Fig. 5). As expected, all endothermic peaks were intensified due to stronger dehydration. In the basic catalyst they were less well resolved than in air. There were no substantial characteristic temperature shifts.

The thermic effects in hydrogen, shown in Fig. 6, were considerably more complex. Unpromoted catalyst (curve 1) shows a weak endothermic peak followed by a smaller exothermic peak, starting at 189°C (196°C max.), and a strong exothermic effect which starts at 242°C and ends at 280°C.

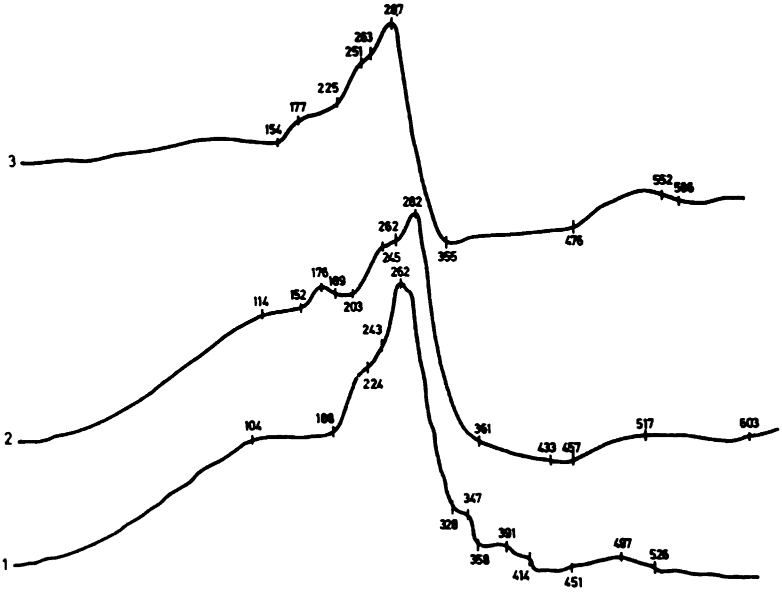

Fig. 5.

DTA in vacuum. Basic catalyst, (1); catalyst promoted with mixture I (2); catalyst promoted with mixture II (3).

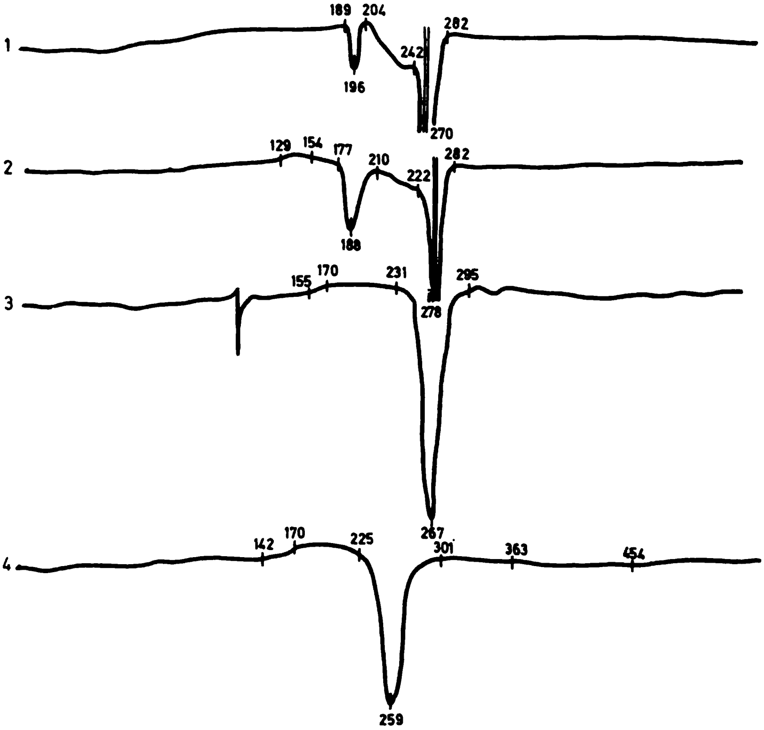

This last can be ascribed to the formation of mixed spinels of zinc, copper and chromium. Catalyst promoted by magnesium (curve 2) shows similar effects. The same holds for catalyst promoted by potassium, by calcium and by magnesium.

Figure 6 (curve 3) shows that aluminum promoter considerably reduced the rate of spinel formation and that in catalyst which contains aluminum together with other promoters its influence is predominant (Fig. 6, curve 4). This is important in defining the role of aluminum as a structural promoter.

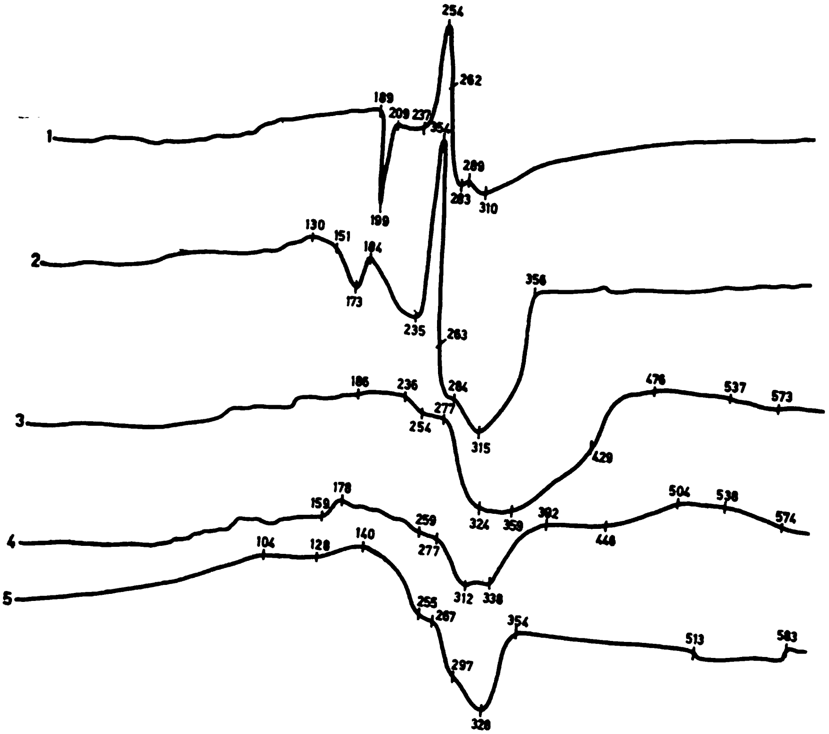

Fig. 7.

DTA in a stream of 70 vol.% nitrogene and 30 vol.% carbon monoxide. Basic catalyst (1); catalyst promoted with manganese (2); with aluminum (3); with mixture I (5); with mixture II (4).

Differential thermal analysis in a stream of a gaseous mixture containing 70 vol. % nitrogen and 30 vol. % carbon monoxide (Fig. 7) showed endothermic processes at temperatures which correspond to those obtained

← ———

Fig. 6.

DTA in a stream of hydrogen. Basic catalyst, curve (1); catalyst promoted with magnesium, curve (2); with aluminum, curve (3); with mixture II, curve (4).

in air or in nitrogen, but with different intensities. A characteristic feature is that two exothermic processes appear, one just before and one after the endothermic effect whose maximum is located around 270°C. In some cases the exothermic character of the first effect is not sufficiently clear and it appears only as a high saddle between two close endothermic effects which manifest themselves as gentle waves in other atmospheres. The second exothermic effect is more peaked in other atmospheres too, but does not take place quite as fast as in hydrogen. We can suppose that the formation of spinels takes place here as well. The effect is particularly prominent with the catalyst which contained manganese. It can also be noticed with the catalyst containing a mixture of promoters including manganese. Catalyst containing a mixture of promoters without manganese did not have clearly exothermic effect here.

The thermic effects recorded in a stream of a gaseous mixture containing 60 vol. % hydrogen, 33 vol. % carbon monoxide and 7 vol. % nitrogen (Fig. 8) correspond to the effects in the individual gaseous components — hydrogen and carbon monoxide, but the effects corresponding to pure hydrogen are predominant. This is not surprising since there is much more hydrogen monoxide in the mixture.

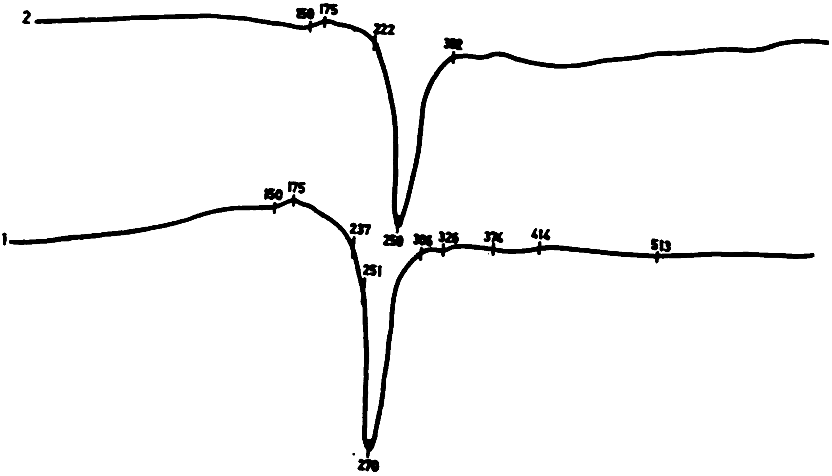

Fig. 8.

DTA in 60 vol.% hydrogen, 33 vol.% carbon monoxide and 7 vol.% nitrogen. Catalyst promoted with mixture I (1); with mixture II (2).

A comparison of the second exothermic peak in various atmospheres (Table 2) shows that in hydrogen this effect takes place at lower temperatures than in the nitrogen-carbon monoxide mixture. The temperatures of its initiation in the hydrogen-carbon monoxide-nitrogen mixture are very close to those in pure hydrogen.

With different promoters and in different atmospheres, differences in transformations which take place in the catalyst were observed by DTA.

TABLE 2

Temperature of Initiation of the Exothermic Effect in Various Atmospheres

Catalyst	Hydrogen	70 vol. % nitrogen 30 vol. % carbon monoxide	60 vol. % hydrogen 33 vol. % carbon monoxide 7 vol. % nitrogen
without promoters	242°C	262°C	237°C
with potassium	245	270	242
with calcium	244	273	237
with magnesium	222	266	220
with aluminum	231	277	253
with manganese	248	263	229
with mixture I	237	280	242
with mixture II	225	267	223

These transformations were particularly pronounced in hydrogen and in hydrogen-carbon monoxide mixture. In both of these cases a spinel structure is formed, which is of the upmost importance for the activity of the catalyst. Aluminum and manganese were the most influential as promoters. DTA showed the temperature region which corresponds to the removal of adsorbed and chemically bound water, and also the region of decomposition of the initial and intermediate compounds of the promoted catalysts.

The activity studies of samples reduced in two ways and structural analysis of theresulting forms and phases in the catalyst should show whether this difference is of importance for catalyst efficiency as well.

SUMMARY

DTA of a low-temperature zinc-copper-chromium CO-shift catalyst without promoters and with promoters coprecipitated with the basic components, was carried out.

The influence of the atmosphere in which the heat treatment takes place, and of the components of the reaction mixture was investigated by DTA in air, nitrogen, hydrogen, vacuum, a mixture of nitrogen and carbon monoxide, and a mixture of hydrogen, carbon monoxide and nitrogen.

The results evidence the influence of the promoters and the atmosphere on the structural formation of the catalyst.

Institute of Chemistry,
Technology and Metalurgy, Belgrade

Received 12 May 1969.

REFERENCES

1. Bhattacharyya, S. K., and V. S. Ramachandran. "Differential Thermal Analysis of Catalyst Powders. Part III. — Differential Thermal Analysis of Zinc Oxide, Chromic Oxide Mixture" — *Journal of Scientific and Industrial Research* (New Delhi) 11B: 550—551, 1952.
2. Chalyĭ, V. P., O. I. Shchor, and S. P. Rozenko. "Termograficheskoe issledovanie gidrookisei nekotorykh metallov. I. Individual'nye gidrookisi" (Thermographic Investigation of Some Metallic Hydroxides. I. Individual Hydroxides) — *Ukrainskiĭ khimicheskiĭ zhurnal (Obshchai͡a, neorganicheskai͡a i fizicheskai͡a khimii͡a)* 27(1): 3—6, 1961.
3. Chalyĭ, V. P., and O. I. Shchor. "Termograficheskoe issledovanie gidrookiseĭ nekotorykh metallov. II. Binarnye sistemy gidrookiseĭ" (Thermographic Investigation of Some Metallic Hydroxides. II. Hydroxide Binary Systems) — *Ukrainskiĭ khimicheskiĭ zhurnal (Obshchai͡a, neorganicheskai͡a i fizikokhimicheskai͡a khimii͡a)* 27(1): 7—11, 1961.
4. Charcosset, H., P. Turlier, and Y. Trambouze. "Etude des reactions a l'etat solide conduisant au chromite cuivrique" — *Comptes rendus hebdomadaires des seances de l'Academie des sciences* (254): 299—302, 1962.
5. Dimitrov, M., and R. Banov. "Izsledovanie vuzmozhnosti za vzaimodeistvie mezhdu zheleznite okisi i promotorite v katalizatorite za sintez na amoniak po metodu na suntai͡avane suobshtenie. I. Izsledovanie izmenenii͡a v sistemata $Fe(OH)_3$-$Al(OH)_3$-NH_4NO_3 (Reaction between Iron Oxide and a Promotor in Catalyst for Ammonia Synthesis. I. Changes in the $Fe(OH)_3$-$Al(OH)_3$-NH_4NO_3 System) — *Khimi͡a i industrii͡a* 1: 17—22, 1967.
6. Gordon, S., and C. Campbell. "Differential Thermal Analysis of Inorganic Compounds. Nitrates and Perchlorates of the Alkali and Alkaline Earth Groups and Their Subgroup" — *Analytical Chemistry* 27(7): 1102—1109, 1955.
7. Kirillov, I. P., N. P. Opolovnikova, and A. M. Alekseev. "Izuchenie prot͡sessa formirovanii͡a t͡sink-khromovykh katalizatorov sinteza spirtov. I." (Formation of Zinc-Chrome Catalyst of Alcohol Synthesis) — *Izvestii͡a vysshikh uchebnykh zavedeniĭ USSR (Khimii͡a i khimicheskai͡a tekhnologii͡a)* (1): 77—83, 1964.
8. Kostrov, V. V., I. P. Kirillov, and A. M. Alekseev. "Izuchenie prot͡sessa formirovanii͡a t͡sinkkhrommednykh katalizatorov konversii okisi ugleroda. II." (Formation of Zinc-Chrome-Copper Catalyst for Carbon Monoxide Conversion II) — *Izvestii͡a vysshikh uchebnykh zavedeniĭ USSR (Khimii͡a i khimicheskai͡a tekhnologii͡a)* (9): 1027—1030, 1967.
9. Kostrov, V. V., I. P. Kirillov, and A. M. Alekseev. "Izuchenie prot͡sessa formirovanii͡a t͡sinkkhrommednykh katalizatorov konversii okisi ugleroda. II." (Formation of Zinc-Chrome-Copper Catalyst for Carbon Monoxide Conversion. II) — *Izvestii͡a vysshikh uchebnykh zavedeniĭ USSR (Khimii͡a i khimicheskai͡a tekhnologii͡a)* (1): 67—70, 1968.
10. Ramachadran, V. S., and S. K. Bhattacharyya. "Differential Analysis of Catalyst Powders. Part II. Differential Thermal Analysis of Zinc Oxide" — *Journal of Scientific and Industrial Research* (New Delhi) 11B: 549—550, 1952.
11. Rode, T. V. *Kislerodnye soedinenia khroma i khromovye katalizatory* (Oxygen Compounds of Chrome and Chrome Catalysts) — Moskva: Izdatel'stvo Akademii nauk *USSR*, 1962.
12. Shargorodskiĭ, S. P., and D. I. Shchor. "Izuchenie termicheskogo rozlozhenii͡a nitratov i karbonatov magnii͡a, t͡sinka i kadmii͡a" (Thermal Decomposition of Magnesium, Zinc and Cadmium Nitrates and Carbonates) — *Ukrainskiĭ khimicheskiĭ zhurnal* 16(4): 426—433, 1950.
13. Zigaĭlo, Ia. V., and L. I. Shpak. "Vlii͡anie termicheskoĭ obrabotki na khimicheskiĭ i fazovyĭ sostav osazhdennnykh t͡sink-khromovykh katalizatorov" (The Effect of Heat Treatment on Chemical and Phase Composition of Precipitated Zinc-Chrome Catalysts) — *Ukrainskiĭ khimicheskiĭ zhurnal* 32(4): 412—418, 1966.

GLASNIK HEMIJSKOG DRUŠTVA, Vol. 35, No. 4-5-6, 1970, pp. 295—312

GHDB-105 539.143.43:547.3/.4

Original Scientific Paper

CONFORMATIONAL ANALYSIS OF ACYCLICS BY NMR. DEPENDENCE OF VICINAL COUPLING CONSTANTS ON NATURE OF SUBSTITUENTS

by

MILORAD M. ROGIĆ

*Contribution from Richard B. Wetherill Laboratory of Purdue University, Lafayette, Indiana 47907.**

Conformational analysis based on the Karplus relationship(1) of vicinal coupling constants and dihedral angles between vicinal hydrogens has been applied in numerous systems(2). Dihedral angle dependence of the vicinal coupling constant J_{vic} is well documented by examples from conformationally homogenous molecules like steroids(3), many cyclohexane derivatives(4), sugars(5), bicyclic systems(6), etc., in which the relationship between two vicinal hydrogens is fixed by the very nature of the molecule. In acyclic systems an analysis of this dependence is complicated by the fact that observed the vicinal coupling constant is an average of several coupling constants present in each of the rapidly equilibrating individual conformational isomers(7–11)

$$J_{\text{vic}} = \sum_i N_i J_i$$

Nevertheless, there are enough experimental data suggesting that in acyclic molecules such a relationship between dihedral angle and vicinal coupling constant also holds(2, 8–15).

In the present paper we wish to report our observations regarding conformational preference in isopropyl alkyl carbinols as deduced from the observed vicinal coupling constants in various solvents and at different temperatures, and to discuss the limitations of certain assumptions which one usually makes in such analyses.

METHODS

Recently Snyder(12) and Whitesides(13) demonstrated how the *nmr* method can be used for conformational elucidation in acyclic three- and four-spin systems, respectively, and a similar approach has been used for analyses of acyclic two-spin systems(8–11, 14, 15) which are often encountered in diastereomers.

---

* Present address: Allied Chemical Corporation, Corporate Research Laboratory, Morristown, New Jersey 07960.

In three- and four-spin systems an analysis of the observed vicinal coupling constants in terms of the vicinal coupling constants of individual conformational isomers is complicated by the fact that the observed value is an average of several vicinal coupling constants which may not necessarily be the same in all the conformational isomers present in equilibrium. From this point of view an analysis of a two-spin system represents a much simpler case because the observed vicinal coupling constants, J_{ab}, are an average of only three constants, J_t, J_g, and J_g'. The vicinal coupling constant in a single conformational isomer is inversely proportional to the electronegativity of the substituents present(1, 16). The stereochemical dependence of this electronegativity effect has been discussed by Bhacca and Williams(17), Booth(18), and more recently by Whitesides(13).

It has been shown that in four-spin systems the vicinal coupling constants of individual conformational isomers are practically constant in a series of similar compounds(13). This suggests that vicinal coupling constants and therefore the appropriate dihedral angles in each individual conformational isomer are practically insensitive to the nature of the substituent.

The assumption about the constancy of J_t, J_g, and J_g' in a two-spin system(14, 15) implies that dihedral angles between vicinal hydrogens in the system are also insensitive to the nature of the substituent. Moreover, in a two-spin system the two *gauche* coupling constants J_g and J_g' are frequently regarded as the same(8, 10, 14, 15), again suggesting that the dihedral angles in two different conformational isomers are the same and therefore insensitive of the substituent. These assumptions have no firm experimental basis and their validity is questionable, especially in cases of heavily substituted ethane molecules.

Therefore it appeared desirable to have an appropriate model on which one would be able to follow whether the change in the average vicinal coupling constant in a two-spin system caused by introduction of substituents of different steric requirements is mainly due to the change in conformational population $N_t/(N_g + N_g')$, or whether it may also be due to a change in the vicinal coupling constants of individual conformational isomers J_t, J_g, and J_g'.

It appeared that the series of isopropyl alkyl carbinols of the following type would constitute a suitable model for these purposes. All H_a protons should be sufficiently shifted

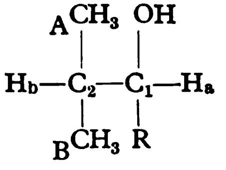

$$H_b{-}\overset{\overset{{}_{A}CH_3}{|}}{\underset{\underset{{}_{B}CH_3}{|}}{C_2}}{-}\overset{\overset{OH}{|}}{\underset{\underset{R}{|}}{C_1}}{-}H_a$$

I, *R* = *D*
II, *R* = *Me*
III, *R* = *i-Pr*
IV, *R* = *Ph*
V, *R* = *t-Bu*

downfield for the vicinal coupling constants J_{ab} to be measured without interference from other protons. Some experimental results suggest that conformations of type *G′* (see Chart I) will become less important as steric requirements of the substituent *R* increase(19). This, hopefully, might eliminate ambiguity about two equal *gauche* vicinal coupling constants, because in these cases the change in the observed vicinal coupling constants J_{ab} affected by the introduction of substituents *R* of different steric requirements should be an average of only one J_t and *one* J_g, which should further simplify the desired analysis. On the other hand, the change in J_{ab} caused by variations in the conformational populations induced either by changing temperature or solvent should substantiate whether the change in average J_{ab} observed on introduction of substituents R of different steric requirements is due only to the change in conformational populations or also to change in the vicinal coupling constants J_t and J_g of individual conformational isomers.

RESULTS AND DISCUSSION

Conformational Preference

Appropriate chemical shifts and vicinal coupling constants J_{ab} for the compounds I—V in different solvents are presented in Table I.

TABLE I

Chemical Shifts and Vicinal Coupling Constants of Compounds I — V in Different Solvents at 60.0 Mc/sec and 35°

Solvent	Compound	$-\nu_A^a$	$-\nu_B^a$	$\nu_A-\nu_B^a$	J_{ab}^b	$-\nu_a^a$
Neat	I	53.0	53.0	0.0	6.30	198
	II	51.5	53.2	1.7	6.35	207
	III	55.0	55.0	0.0	5.53	177.8
	IV	42.0	54.5	12.5	6.65	249.5
	V	54.2	59.1	4.9	2.40	184.5
CCl_4[c]	I	52.5	52.5	0.0	6.00	196
	II	51.8	53.3	1.5	6.10	207.5
	III	53.5	53.5	0.0	5.52	176.5
	IV	43.3	53.6	10.3	6.81	250.4
	V	53.2	57.5	4.3	2.40	181.5
C_6H_6[c]	I	50.5	50.5	0.0	6.15	194
	II	50.6	53.5	2.9	5.90	204.3
	III	50.9	54.1	3.2	5.53	173.5
	IV	49.3	56.8	12.5	6.54	248.2
	V	53.0	55.3	2.3	2.49	176.5
CS_2[c]	I	52.2	52.2	0.0	6.26	196.2
	II	50.0	50.5	0.5	6.07	204.5
	III	51.5	51.5	0.0	5.89	174
	IV	42.4	51.0	8.6	7.21	249.3
	V	51.2	57.0	5.8	2.42	179.5
CH_3COOH[c]	I	53.0	53.0	0.0	6.40	205.0
	II	52.0	53.5	1.5	6.13	215.2
	III	54.0	54.0	0.0	5.91	186
	IV	45.0	58.8	13.8	7.04	261.2
	V	55.2	59.8	4.6	2.48	191.5

---

[a] Chemical shifts are in *cps.* downfield from tetramethylsilane and uncertainty in these values is not larger than ±0.5 *cps.*

[b] The uncertainty in the vicinal coupling constants is estimated to be not greater than ±0.2 *cps.*

[c] Solutions were 10% by volume.

[d] This value was estimated from poorly resolved signal.

Solvent	Compound	$-\nu_A^a$	$-\nu_B^a$	$\nu_A - \nu_B^a$	J_{ab}^b	$-\nu_a^a$
Pyridine[c]	I	58.0	58.0	0.0	6.32	212.2
	II	57.0	60.3	3.3	5.97	223
	III	59.4	64.7	5.3	5.63	189
	IV	55.4	66.0	10.6	6.02	274.5
	V	64.5	64.5	0.0	1.5[d]	194
MeOH[c]	I	54.0	54.0	0.0	— —	—
	II	51.4	53.2	1.8	— —	—
	III	54.0	54.0	0.0	6.22	180
	IV	47.3	59.5	12.2	6.83	257.5
	V	54.2	59.0	4.8	— —	—
$PhNO_2$[c]	I	56.5	56.5	0.0	6.25	208.2
	II	52.9	55.2	2.3	6.02	217.5
	III	53.5	55.8	2.3	5.49	180
	IV	48.2	58.2	10.0	6.52	264
	V	56.1	60.0	3.9	2.50	189
CH_3CN[c]	I	52.0	52.0	0.0	5.80	196
	II	51.7	52.3	0.6	5.85	207
	III	52.3	52.3	0.0	5.78	172
	IV	46.0	54.2	8.2	5.00	186
	V	52.0	57.0	5.0	1.5[d]	182
CF_3COOH[c]	I	60.5	60.5	0.0	6.60	252
	II	61.2	61.2	0.0	6.30	305.5
	III	59.5	59.5	0.0	6.00	203
	IV	49.6	62.3	12.7	7.81	353
	V	61.1	65.5	4.4	2.51	210

Let us assume for the moment that each of the investigated compounds exists in solution as a rapidly equilibrating mixture of perfectly staggered conformations, T, G, and G', in which *anti* hydrogens (like those in conformation T) contribute to the experimentally observed vicinal coupling constant J_{ab} with $J_t = 12$ cps, and *gauche* ones (like those in conformations G and G'), with $J_g = J_{g'} = 2$ cps[(24)]. Then from the experimentally measured J_{ab} it should be possible to calculate the population ratio $N_t/(N_g + N_{g'})$. Furthermore, as a direct consequence of the above assumption, the energy differences between conformations T and G in all cases where R is a symmetrical group should be the same regardless of the steric requirements of the R's, because the nonbonded interactions involving R and one of the methyl groups in T should be essentially the same as the corresponding interactions in G. In the conformations G the hydroxyl group is *gauche* to both methyl groups and is reminiscent of the more crowded environment of an axial hydroxyl on a cyclohexane ring. In conformation T the OH is *gauche* only to one of the methyl groups and is therefore, in a less crowded steric environment, resembling an equatorial OH which is also in a less hindered position. Actually in conformation G, OH faces two *syn*-axial hydrogens and the nonbonded interactions in this conformation should be the same as the

1 : 3 nonbonded interactions of an axial OH and 3,5-*syn*-axial hydrogens in a cyclohexane ring. In passing from G to T only one of these *syn*-axial interactions will be relieved, contrary to the cyclohexanol case where both of these interactions are absent in the equatorial isomer. Therefore, if both conformations T and G are of perfect staggered geometry, the free energy difference for transformation of G to T should be half of the free energy of the transformation of an axial hydroxyl group to the equatorial position(25), and it should be the same for all compounds I — V.

CHART I

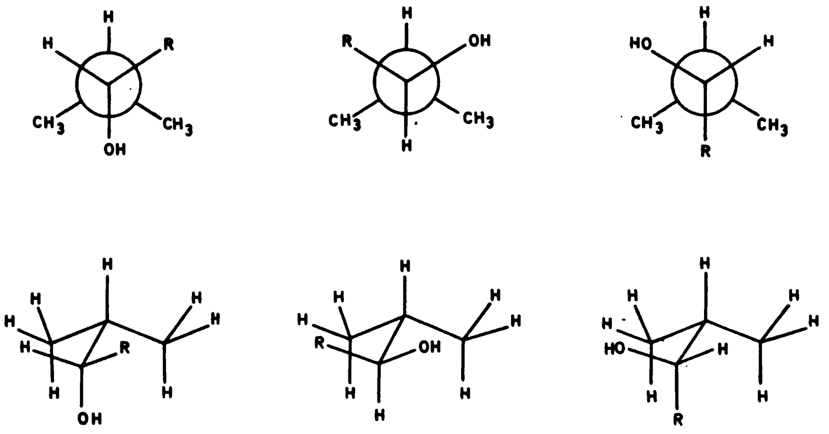

G T G'

Thus, for example, the experimentally observed vicinal coupling constants in I are 6.3 cps in the neat liquid, and 6.0 in dilute carbon tetrachloride solution. Assuming that the steric requirements of the hydrogen and the deuterium on C_1 of I are the same, one can calculate the populations (in mole fractions) of conformations T, G, and G':

$$N_t + N_g + N_{g'} = 1; \quad N_t = 1 - (N_g + N_{g'})$$

then,

$$12N_t + 2(N_g + N_{g'}) = 6.3 \text{ cps}$$

and

$$N_g + N_{g'} = 0.57 \text{ or } N_t = 0.43.$$

However, because $N_t = N_{g'}$, $N_g = 0.14$ and $N_t/N_g = K = 3.07$. Therefore, in the pure liquid I the free energy difference $\Delta G^{\circ}_{35^{\circ}}$ for the equilibrium $G \rightleftarrows T$ is $RT \,.\, \ln K = 0.67$ kcal/mole in favor of the conformational isomer T. A similar calculation for the equilibrium in carbon tetrachloride solution ($J_{ab} = 6.0$ cps) gives $K = 2.0$, and $\Delta G^{\circ}_{35^{\circ}} = -0.42$ kcal/mole, which is

TABLE II

Calculated Populations of Conformational Isomers T, G, and G′ at 35°.[a]

Compound		Neat					CCl_4				
#	*R*	J^b_{ab}	$\frac{N^c_t}{(N_g+N_{g'})}$	N_t	N_g	$N_{g'}{}^d$	J^b_{ab}	$\frac{N^c_t}{(N_g+N_{g'})}$	N_t	N_g	$N^d_{g'}$
I	*D*	6.30	0.755	0.43	0.14	0.43	6.00	0.666	0.40	0.20	0.40
II	*Me*	6.35	0.770	0.435	0.141	0.424	6.10	0.695	0.41	0.205	0.385
III	*i-Pr*	5.53	0.546	0.353	0.115	0.532	5.52	0.543	0.452	0.176	0.472
IV	*Ph*	6.65	0.870	0.465	0.151	0.384	6.81	0.925	0.480	0.240	0.280
V	*t-Bu*	2.40	0.0416	0.040	0.013	0.947	2.40	0.416	0.040	0.020	0.940

[a] It is assumed that N_t/N_g is independent of *R* and that it is the same as the corresponding N_t/N_g in compound I, viz. 3.07 in the neat liquids and 2.0 in solutions of carbon tetrachloride.

[b] Vicinal coupling constants from Table I.

[c] Calculated from the equation J_{ab}—12 $N_t+2(N_g+N_{g'})$.

[d] Populations of conformational isomers *T*, *G*, and *G′* calculated from the ratio $N_t/(N_g+N_{g'})$ and the approriate values for N_t/N_g.

half of the corresponding free energy difference for transformation of an axial hydroxyl group in cyclohexane to the equatorial position, measured by *nmr* in carbon tetrachloride solution under similar experimental conditions(26, 27), in accordance with the prediction arrived at above.

Using the observed coupling constants J_{ab} of compounds I — V in Table I, and assuming that vicinal coupling constants in individual conformational isomers are $J_t = 12$ cps, $J_g = J_{g'} = 2$ cps, and independent of the steric requirements of R, one can calculate population ratios $N_t/(N_g + N_{g'})$ between individual conformational isomers T, G, and G'. The results of these calculations are presented in Table II. As a consequence of the above assumption, values of N_t/N_g in all five compounds should be the same as the appropriate value for compound I, viz. $N_t/N_g = 3.07$ for the neat liquids, or $N_t/N_g = 2.0$ for the solutions in carbon tetrachloride. However, when calculations were carried out on this basis, it was found first that the populations of conformations of type G' increased as the steric requirements of R increase, and second, that in all cases the conformational isomers of type G' were more stable than those of type G.

These results, in the light of all that is known about conformational preference in acyclic (and alicyclic) systems(28), seem highly unreasonable. Therefore, either the assumption that the vicinal coupling constants in individual conformational isomers are $J_t = 12$ cps, $J_g = J_{g'} = 2$ cps and equal in all compounds I — V, or the assumption that the free energy difference between conformational isomers T and G does not depend on steric requirements of R, cannot be correct.

Alternatively, to avoid apparently unreasonable implications from Table II regarding relative stabilities of conformational isomers T, G, and G', we may reasonably assume that conformational isomers of type G' will become of less importance as the steric requirements of R increase(19). Then, instead of considering an equilibrium between three conformations T, G, and G', we may relate observed vicinal coupling constants J_{ab} and conformational preference in compounds III, IV, V, and perhaps even in II, by eq. 1:

$$J_{ab} = N_t \cdot J_t + N_g \cdot J_g \tag{1}$$

However, if we were to hold to the earlier assumption that in all compounds I — V the *anti* hydrogens contribute to the average J_{ab} with $J_t = 12$ cps and the *gauche* ones with $J_g = 2$ cps, then it follows (see Table III) that population ratios N_t/N_g are not independent of the steric requirements of R, and that the conformations of type T are the less stable. The last implication is again unreasonable and is in contrast to what the temperature dependence of the J_{ab} for compounds II, III, and IV suggests (see Fig. 1). On the other hand, values $J_t = 12$ and $J_g = 2$ cps predict that conformation T in compound V is about 1.9 kcal/mole less stable than the corresponding G conformation. Although this value is qualitatively in agreement with experiment, quantitatively it is unlikely. It is therefore apparent that even in discussing conformational preferences in compound V in terms of only two conformational isomers, values of J_t and J_g of 12 and 2 cps respectively are not appropriate.

TABLE III

Populations of Conformational Isomers T and G at 35°, Calculated Assuming that Conformational Isomers G′ Are Not Present in the Equilibrium

Compound		Neat			
#	R	J_{ab}	N_t/N_g^{a}	N_t	N_g
I	D	6.30	0.755	0.43	0.57
II	Me	6.35	0.770	0.435	0.565
III	i-Pr	5.53	0.546	0.353	0.647
IV	Ph	6.65	0.870	0.465	0.535
V	t-Bu	2.40	0.0417	0.040	0.960

[a] Calculated from $J_{ab} = 12\,N_t + 2\,N_g$.

Consequently, to discuss conformational preference in these compounds, even if only two conformations are involved, we need a new set of vicinal coupling constants J_t+ and J_g+ for each of the compounds II — V to account for the experimental facts, namely the magnitude of the coupling constants J_{ab} and their change with temperature.

Generally, in any system, the most stable conformation will be the one in which the energy contributions responsible for bond length distortions, deformations of dihedral and bond angles, and the energies resulting from nonbonded or van der Waals interactions are balanced in such a way as to minimize the total energy of the conformation(29, 30).

On the basis of these principles, it is reasonable to expect that the conformational isomer of type G' in compound V, for example, is populated to a very small extent, if at all, because in this conformation nonbonded interactions between the methyls of the *t-Bu* and *i-Pr* groups will be most severe and inescapable by torsion. On the other hand, the nonbonded interactions in conformations T and G, although significantly reduced compared with conformation G', are still serious. However, in these conformations the energy term resulting from nonbonded interactions, and therefore the total energy of the conformation, can be minimized by deformations of the bond and dihedral angles from their "normal" values 109°28′ and 60°, as is indicated in the following scheme by a and b respectively.

Therefore, disregarding conformations of type G' as energetically very unfavorable, we may consider the observed vicinal coupling constant of 2.4 cps in compound V as resulting from the averaging of the "actual" vicinal coupling constants J_t+ and J_g+ which are present in deformed conformations T^+ and G^+. The same should be true for both compounds III and IV, and perhaps to a smaller extent for compound II too.

Unfortunately, the fact that we realize that some conformations are deformed from their ideal staggered representations does not tell as anything about the extent and type of the deformations. Intuitively, it may be expected that in compounds II — V dihedral and bond angle deformations from their normal values will parallel the "size" of the substituent R. In the cyclohexane system even an axial substituent of average size slightly deforms the

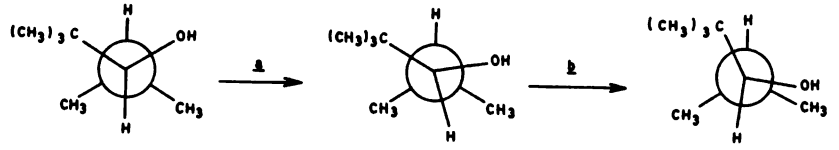

T

T^+

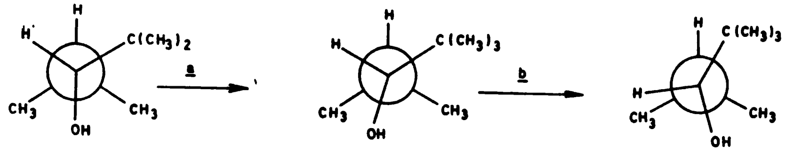

G

G^+

cyclohexane chair conformation(31). When the steric requirements of such a substituent become considerable, as in the case of an axial *t-Bu* group, the cyclohexane ring will rather adopt a skew-boat conformation(33) to evade the severe nonbonded interactions which would be present in the chair form, at the expense of other types of energy now present in the new conformation. Although one does not know how justifiable it may be to compare the cyclohexane system with acyclic systems(34), like those in the present study, it still appears reasonable to conclude that the degree of deformation of the dihedral and bond angles from their ideal values in compounds I — V will follow the order $I \ll II \ll III \leqslant IV \ll V$, i.e., that the deformation, similarly as in the case of the corresponding cyclohexane derivatives, will not be pronounced in compound I and perhaps in II, but that it will be significant in compound V, with compounds III and IV as intermediate cases(35).

If one assume that the Karplus relationship(1) between dihedral angle and vicinal coupling constant holds in two-spin systems, than it may perhaps be possible to estimate the degree of dihedral angle deformation from the temperature dependence of the average vicinal coupling constants J_{ab}, in a manner similar to that used for calculations in related studies(8, 13, 37).

Equation 2, which correlates the observed change in the average vicinal coupling constant J_{ab}, the vicinal coupling constants of individual conformational isomers, the temperature, and the free energy difference between two conformations, is derived from eq. 1 by replacing N_t and N_g by their equivalent expressions:

$$J_{ab} = \frac{J_g^+ + J_t^+ \cdot \exp(-\Delta G^\circ/RT)}{\exp(-\Delta G^\circ/RT) + 1.0} \tag{2}$$

$$N_t = \frac{\exp(-\Delta G^\circ/RT)}{\exp(-\Delta G^\circ/RT) + 1.0} \tag{3}$$

The unknown parameters J_t+, J_g+, and $\Delta G°$ were calculated by an iterative FORTRAN IV program using the method of steepest descent. Starting with an initial set of trial parameters J_t+, J_g+, and $\Delta G°$, the partial derivatives of the average deviation F with respect to each of the parameters are obtained. The values of parameters are changed by an amount proportional to the average deviations, and F is recalculated. This procedure is continued

$$F = \frac{1}{n}\sum_{j}^{n} (|J_{ab}| - |J_{ab}\ \text{calcd}|)/J_{ab}| \tag{4}$$

until no further decrerse in the average deviation (± 0.0001) is possible. After a minimum value of F is reached, the calculated parameters are changed arbitrarily and the calculation repeated. When the recalculated values are the same as those from several previous calculations, it is assumed that the calculated values of the unknown parameters are satisfactory.

Probable errors in the calculated parameters were estimated using the procedure of Gutowsky$^{(8)}$ and Whitesides$^{(13)}$. The sum of squares of deviation from the experimental points, φ, is expanded in a Taylor series in the neighborhood of the minimum value φ_0 calculated using the method of steepest descent. The first derivatives in this equation are zero at φ_0. If third

$$\varphi = \varphi_0 + \left(\frac{\partial \varphi}{\partial \Delta G^0}\right)\Delta\Delta G^0 + \left(\frac{\partial \varphi}{\partial J_t}\right)(\Delta J_t) + \left(\frac{\partial \varphi}{\partial J_g}\right)(\Delta J_g) +$$

$$+ \frac{1}{2}\left(\frac{\partial^2 \varphi}{\partial \Delta G^{0\,2}}\right)(\Delta\Delta G^0)^2 + \ldots + \frac{1}{2}\left(\frac{\partial^2 \varphi}{\partial J_g^2}\right)(\Delta J_g)^2 + \ldots \tag{5}$$

and higher order derivatives are neglected, then by holding all parameters constant but one, an appropriate set of equations for the probable errors in the calculated parameters is obtained. Thus, the probable error in the calculated free energy difference will be given by

$$\Delta\Delta G^0 \cong \left[2(\varphi - \varphi_0) \Big/ \left(\frac{\partial^2 \varphi}{\partial \Delta G^{0\,2}}\right)\right]^{1/2} \tag{6}$$

and the errors in other parameters can be calculated using similar equations.

An upper limit on allowed values of φ is dictated by the accuracy of the experimental measurements of observed vicinal coupling constants

$$\varphi \leqslant \sum_{j}^{n} (\delta J_{ab})^2 \tag{7}$$

In this work we assumed that the experimental errors in the observed coupling constants were not greater than 0.2 cps and that the errors in temperatures were negligible. The second derivatives needed for the estimation of errors by eq. 6 were obtained by differentiating eq. 2, 3, and 7.

The temperature dependence of the average coupling constants J_{ab} of compounds II — V is represented in Fig. 1, and calculated values of J_t^+, J_g^+, and $\Delta G°$, together with the estimated errors, are given in Table IV.

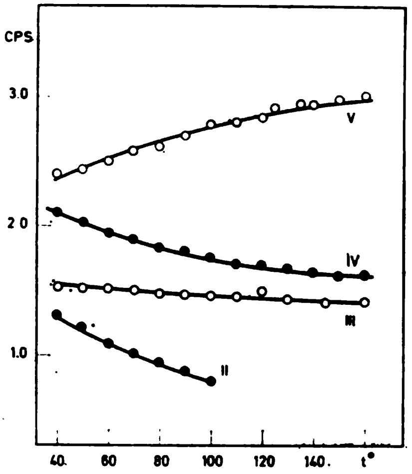

Fig. 1.

Temperature dependence of the vicinal coupling constants J_{ab} of compounds II — V. (For the sake of compactness in representation plotted coupling constants are offset from the actual values given in Table I by 4 *cps* for III, and 4.45 *cps* for IV).

TABLE IV

Calculated Coupling Constants (cps) from Temperature Dependence of Vicinal Coupling Constants of Isopropyl Alkyl Carbinols

Compound		J_t+	J_g+	ΔG^{0a} kcal/mole	n^b
#	*R*				
II	*Me*	9.1 ± 0.3	—3.9 ± 0.8	—0.80 ± 0.02	7
IV	*Ph*	8.1 ± 0.3	0.7 ± 0.8	—0.81 ± 0.04	13
III	*i-Pr*	6.0 ± 0.3	3.7 ± 0.8	—0.81 ± 0.11	12
V	*t-Bu*	10.7 ± 0.8	0.4 ± 0.3	+0.89 ± 0.04	14

[a] Free energy difference between conformational isomers T^+ and G^+.

[b] *n* is the number of different temperature measurements used in the calculation.

If we assume⁽²⁴⁾ that eq. 8 may be used to correlate the thus calculated coupling constants J_t^+, and J_g^+ in individual conformational isomers with the appropriate dihedral angles,

$$J_{vic} = 12 \cos^2 \phi \tag{8}$$

then the dihedral angles between vicinal hydrogens on C_1 and C_2 in the less stable conformations of compounds II, IV, III, V should be approximately 55°, 105°, 123°, and 160°, whereas in the more stable conformations the corresponding dihedral angles should be approximately 150°, 145°, 135° and 100° respectively. It is interesting that, as expected, the degree of deformation of dihedral angles between vicinal hydrogens on C_1 and C_2 from their ideal values of 60° and 180° roughly parallels the size of substituent *R*, the largest deformation being in compound V, where *R* = *t-Bu*. Unfortunately, these approximate indications of deformations of dihedral angles between the hydrogens on C_1 and C_2 do not give us any definitive information about the dihedral angles between other vicinal groups on the same carbon atoms. Nevertheless, it is possible to obtain some idea about these angles from the following considerations. It is quite likely that the bond angle between the isopropyl group and the substituent R will also parallel the steric requirements of R. For $R = Me$, this bond angle, and therefore the other bond angles between the substituents on carbon C_1, probably will not be significantly changed from their normal values. However, when $R = t\text{-}Bu$, this angle is very likely increased, which in turn will result in decrease of the bond angle between the OH and H on the same carbon atom, as indicated earlier. Assuming that the bond angles between the groups on C_1 are the same in both T^+ and G^+ conformations, we may calculate dihedral angles $R—C_1C_2—H$, and bond angles between the groups on C_1 as is shown in Chart II. Thus calculated values are given in Table V. With the exception of compound II, the calculated dihedral angles and bond angles, though very approximate, are in surprisingly good agreement with the qualitative picture which one would intuitively visualize on the basis of energy mini-

CHART II

$\Phi_1 = HC_1C_2H$ $\quad \Phi_3 = RC_1C_2H$ $\quad \Phi_2 = HC_1C_2H$ $\quad \Phi_3 = RC_1C_2H$

$\theta_1 = RC_1H$ $\quad \theta_2 = HC_1OH$

$\theta_1 = \Phi_1 - \Phi_3$ $\quad \theta_1 = \Phi_2 + \Phi_3$

$\Phi_3 = (\Phi_1 - \Phi_2)/2$ $\quad \theta_2 = 360 - 2\,\theta_1$

TABLE V

Calculated Dihedral and Bond Angles in Isopropyl Alkyl Carbinols II—V.[a]

Compound		Dihedral Angles[b]			Bond Angles[c]	
#	R	Φ_1	Φ_2	Φ_3	θ_1	θ_2
II	Me	150°	55°	48°	102°	156°
IV	Ph	145°	105°	20°	125°	110°
III	*i*-Pr	135°	123°	7°	128°	104°
V	*t*-Bu	100°	160°	—30°	130°	100°

[a] Calculated using J_t^+ and J_g^+ from Table IV and assuming that eq. 8 correctly correlates these values and dihedral angles.(24)

[b] ϕ_1 and ϕ_2 are dihedral angles between vicinal hydrogens on C_1 and C_2, and ϕ_3 is dihedral angle between substituent R on C_1 and the hydrogen on C_2.

[c] θ_1 is bond angle between R and the hydrogen or the hydroxyl group on C_1. θ_2 is the bond angle between the hydroxyl group and the hydrogen on C_1. See Chart II.

mization in each conformation. In this light it may not be surprising that the more stable conformation in compound V, (R = *t-Bu*), is that which has the hydroxyl group *gauche* to the two methyl groups. In this conformation OH is almost equidistant from both methyl groups, and the corresponding nonbonded interactions are smaller than in the other conformation, in which the OH is almost eclipsed by one of the methyl groups. Needless to say, in conformations T^+ and G^+ the actual geometry is dictated most probably not by the *Me*-OH nonbonded interaction but by the large *t-Bu* — *Me* interaction.

The calculated free energy differences between conformational isomers T^+ and G^+ of compounds II — V (Table IV) indicate that the interactions between the hydroxyl group and methyl group (s) become more pronounced as the steric requirements of R increase, which is contrary to what the "idealized" model of perfectly staggered geometry would predict.

It is necessary to point out explicitly that the estimated values of the dihedral and bond angles in the various conformational isomers of the compounds investigated should be regarded only as qualitative. Premises making for a qualitative nature of the estimated values are the assumption that the conformational isomer of type G' is not present in the equilibrium(19) (and this especially applies to compound II), and the assumption that coupling constants J_t^+ and J_g^+ in individual conformational isomers are either temperature independent, or if they are affected by temperature, that they are affected in such a manner as to cancel the effect(38). Furthermore, it was assumed that the effect of the electronegativity of substituents R on coupling constants is negligible for the present series of compounds. Finally, the magnitudes of the estimated dihedral angles will depend the equation used to correlate calculated vicinal coupling constants and dihedral angles(24). As Karplus has emphasised(1), the correlation of coupling constants and dihedral angles is only an approximation. Therefore *any approach* in conformational analysis based on this relationship must be considered to be qualitative in nature. Nevertheless in spite of these assumptions and the limitations of the methods employed, the results are qualitatively in good agreement with the picture visualised on the basis of energy minimization in each conformation and it will be of interest to compare these findings with conformations calculated by one of the energy minimization schemas(33b, 39, 40).

In conclusion it may be said that the assumptions sometimes made in *nmr* analyses of acyclic two-spin systems that vicinal coupling constants J_t, J_g, and $J_{g'}$ are insensitive to the nature of the substituents and that the two *gauche* coupling constants J_g and $J_{g'}$ are the same and also insensitive to the nature of R, may not be valid in all cases. Furthermore, an observation of relatively small average vicinal coupling constant in an acyclic two--spin system does not always indicate exclusive existence of a single conformational isomer in which two vicinal hydrogens are *gauche* to each other. Data from the present study suggesting that heavily substituted ethane molecules do not exist in perfectly staggered conformations, and deformations of dihedral and bond angles may be significant in cases where a substituent has large steric requirements(41).

Magnetic nonequivalence

Although the primary purpose of this study was conformational analysis of isopropyl alkyl carbinols I — V, it is of interest to make a few brief comments regarding the magnetic nonequivalence or the chemical shift nonequivalence (42) of the methyl groups of the isopropyl moiety in compounds I — V.

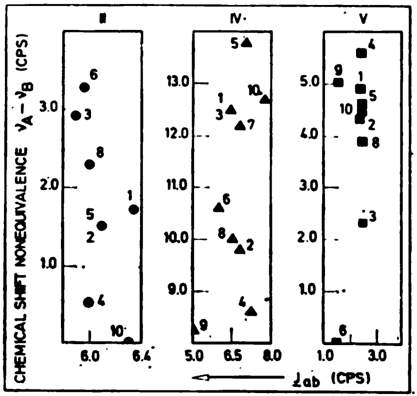

Fig. 2.

Solvent dependence of vicinal coupling constants J_{ab} and chemical shift nonequivalence ν_A—ν_B of compounds II, IV, and V at 35° (see Table I). Key to solvents: 1, neat; 2, carbon tetrachloride; 3, benzene; 4, carbon disulfide; 5, acetic acid; 6, pyridine; 7, methanol; 8, nitrobenzene; 9, acetonitrile; 10, trifluoroacetic acid.

From the data in Table I it can see that the vicinal coupling constants J_{ab} are invariably smaller in carbon tetrachloride solution than in the neat state. On the other hand, the vicinal coupling constants are largest in the acetic and trifluoroacetic acid solutions, as would be expected if hydrogen bonding and protonation favor more stable conformations. Vicinal coupling constants of compound V are practically solvent independent, indicating that in both conformational isomers the hydroxyl group is in a more hindered position than in the compounds I — IV and therefore less accessible for hydrogen bonding and protonation (44). Figure 2 dramatically shows that the change in chemical shift nonequivalence $\nu_A - \nu_B$ does not parallel, with the possible exception of compound IV, the change in the vicinal coupling constants, suggesting again that the conformational population is not primarily responsible for magnetic nonequivalence (45). The temperature dependence of the chemical shift nonequivalence $\nu_A - \nu_B$ is presented in Fig. 3. It is interesting that the magnetically nonequivalent methyl groups of diisopropyl carbinol III in nitrobenzene solution become equivalent in the chemical shift sense at 130°.

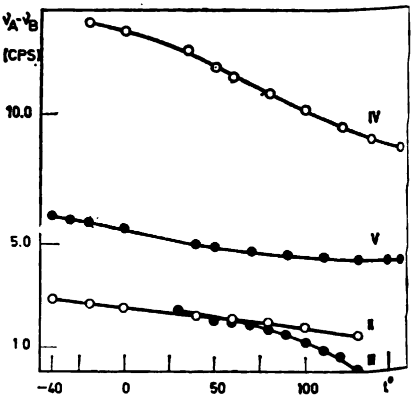

Fig. 3.

Temperature dependence of the chemical shift nonequivalence $\nu_A - \nu_B$ of compounds II—V.

ACKNOWLEDGMENT

The author wishes to express his thanks to Dr. Ernest L. Eliel for helpful discussion and valuable suggestions.

EXPERIMENTAL

All spectra were taken on a Varian A-60 spectrometer equipped with a commercial variable temperature probe. Chemical shifts are reported in cps downfield from tetramethyl silane and the uncertainty in these values is not greater then ±0.5 cps. Vicinal coupling constants were determined from expanded spectra and are average values of 5—10 sweeps. The uncertainties in these determinations were in general better than ±0.2 cps. The low temperature spectra were determined in carbon disulfide solution, and the high temperature spectra were obtained on undiluted alcohols or in nitrobenzene solution (compound III). Spectra at ambient temperature (~35°) were taken on 10% volume/volume solutions in various solvents. The results are listed in Table I.

2-Methyl-1-deuteriopropanol (I) was prepared by lithium aluminum deuteride reduction of freshly distilled isobutyraldehyde and the other compounds used in this work were either prepared following previously described procedures or were commercially available.

ABSTRACT

Average vicinal coupling constants J_{ab} of isopropyl carbinols $(CH_3)_2CHCHOHR$ (pure liquids) were: in I (R = D), 6.30; in II (R = Me), 6.35; in III (R = *i*-Pr), 5.53; in IV (R = Ph), 6.65, and in V (R = *t*-Bu), 2.40 cps respectively. From temperature dependence of the constants it was calculated that the free energy differences between two of the more stable conformational isomers in compounds I — V were 0.67, 0.80, 0.81, 0.81, and —0.89 kcal/mole. It was found that vicinal coupling constants in individual conformational isomers were dependent on the nature of substituent R.

Richard B. Wetherill Laboratory of
Purdue University, Lafayette, Indiana 47907.

Received December 3, 1969

REFERENCES and REMARKS

1. Karplus, M. — *J. Chem. Phys.* 30: 11, 1959, and *J. Amer. Chem. Soc.* 85: 2870, 1963.
2. For a general discussion and an extensive tabular survey of the literature values of vicinal coupling constants see: Bothner-By, A. A. — *Advan. Magnetic Resonance* 1: 195, 1965.
3. Bhacca, N. S., and D. H. Williams. *Application of NMR Spectroscopy in Organic Chemistry* — San Francisco: Holden Day Inc., 1964, Chapter 6 and ref. therein.
4. For conformational analysis of cyclohexane derivatives by NMR spectroscopy see: Franklin, N. C., and H. Feltkamp. — *Angew. Chem. Internat. Edit.* 4: 774, 1965.
5. Lemieux, R. U. — *Can. J. Chem.* 39: 116, 1961.
6. (a) Anet, F. A. L. — *Can. J. Chem.* 39: 789, 1961;
   (b) Wiberg, K. B., B. R. Lowry, and B. J. Nist. — *J. Amer. Chem. Soc.* 84: 1954;
   (c) Cristol, S. J., L. K. Gaston, and D. W. Johnson. — *Tetrahedron Letters* 185: 1963;
   (d) Edwards, O. E., and M. Lesage. — *Can. J. Chem.* 41: 1592, 1963.
7. (a) Pople, J. A. — *J. Mol. Phys.* 1: 3, 1958;
   (b) Pople, J. A., W. G. Schneider, and H. J. Bernstein. *High-resolution Nuclear Magnetic Resonance Spectroscopy* — New York: McGraw-Hill Book Co., Inc., 1959, p. 377.
8. Gutowsky, H. S., G. G. Belford, and P. E. McMahon — *J. Chem. Phys.* 36: 3353, 1962.
9. Sheppard, N., and J. J. Turner — *Proc. Roy. Soc.* (London) A252: 506, 1959.
10. Bothner-By, A. A., and C. Naar-Colin — *J. Amer. Chem. Soc.* 84: 743, 1962.
11. Anet, F. A. L. — *J. Amer. Chem. Soc.* 84: 747, 1962.
12. Snyder, E. I. — *J. Amer. Chem. Soc.* 88: 1165, 1966.
13. Whitesides, G. M., J. P. Sevenair, and R. W. Goetz — *J. Amer. Chem. Soc.* 89: 1135, 1967.
14. Kingsbury, C. A., and D. C. Best — *J. Org. Chem.* 32: 6, 1967.
15. Kingsbury, C. A., and W. B. Thornton — *J. Org. Chem.* 31: 1000, 1966.
16. (a) Sheppard, N., C. N. Banwell, and J. J. Turner — *Spectrochim. Acta* 16: 794, 1960;
   (b) Banwell, C. N., and N. Sheppard — *Mol. Phys.* 3: 350, 1960, and *Disc. Faraday Soc.* 34: 115, 1962;
   (c) Shaefer, T. — *Can. J. Chem.* 40: 1, 1962;
   (d) Williamson, K. L. — *J. Amer. Chem. Soc.* 85: 5162, 1963.
17. Bhacca, N. S., and D. H. Williams — *J. Amer. Chem. Soc.* 86: 2742, 1964.
18. Booth, H. — *Tetrahedron Letters*: 411, 1965.
19. A general discussion and earlier references to "rotational isomerism" are given in the well-known book by Mizushima(20) and in Chapter 4 of Volume 3 of *Progress in Stereochemistry*(21). For example, the free energy difference between conformations *i* and *ii* has been estimated to be about 3.0 kcal/mole in favor

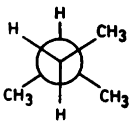

i

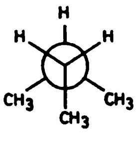

ii

of the conformation *i*(22, 23). However, substitution of one of the geminal hydrogens by a second methyl group reduces this difference to less than 0.1 kcal/mole(22).

20. Mizushima, S. *Structure of Molecules andInternal Rotation* — New York: Academic Press, 1954.
21. Millen, D. J. — *Progr. Stereochem.* 3: 138, 1962.
22. Brown, J. K., and N. Sheppard — *J. Chem. Phys.* 19: 976, 1951.
23. (a) Scott, D. W., J. P. McCullough, K. D. Williamson, and G. Waddington — *J. Amer. Chem. Soc.* 73: 1707, 1951;
    (b) Sheppard, N. *Advances in Spectroscopy. Vol. 1* — New York: Interscience Publishers, Inc., 1959, pp. 303, 307.
24. There are no "fixed values" for these coupling constants in the literature. Different authors used different sets of data. Thus, for example, in Karplus is original treatment(1) these constants were calculated to be 9.22 and 1.85 cps, respectively. Later, Bothner-By(2) suggested a modification of the original Karplus equation which would lead to 13 and 4 cps, and recently Whitesides and coworkers(13) used the set of 14 and 4 cps respectively. Kingsbury in his studies(14, 15) used the set of 12 and 2 cps. However for the present dscussiion it is irrelevant which set of coupling constants is used, because, as will be seen later, the actual coupling constants J_t and J_g do not correspond to so-called "pure" vicinal coupling constants, where "pure" designates coupling constants between vicinal protons with ideal dihedral angles, i.e. 180° and 60° respectively. Similarly, since it will be shown that conformation G′ may, in fact, be disregarded, the assumption that $J_g = J_g'$, is only of transient significance.
25. This assumption disregards the fact that an axial OH group has two equally favored conformations in respect to the cyclohexane ring, while in conformation G the OH is constrained in a single conformation, one in which the O—H bond is *anti* to the C_1—C_2 bond. Therefore, the actual free energy change for transformation of G to T may be still further favored by the resulting entropy difference, which is not found in the cyclohexanol case.
26. Reisse, J., J. C. Celotti, D. Zimmermann, and G. Chiurdouglu — *Tetrahedron Letters:* 2145, 1964.
27. Eliel, E. L., and S. H. Schroeter. — *J. Amer. Chem. Soc.* 87: 5031, 1965.
28. Eliel, E. L., N. L. Allinger, S. J. Angyal, and G. A. Morrison. *Conformational Analysis* — New York: John Wiley and Sons, Inc., 1965, Ch. 1 and 2.
29. Ref. (28), p. 446.
30. Mislow, K. *Introduction to Stereochemistry* — New York: W. A. Benjamin, Inc., p. 33.
31. Eliel, E. L. — *Angew. Chem. Internat. Edit.* 4: 761, 1965. See also references (4) and (32).
32. Feltkamp, H., and N. C. Franklin — *Tetrahedron* 21: 1541, 1965.
33. (a) Allinger, N. L., and L. A. Freiberg — *J. Amer. Chem. Soc.* 82: 2393, 1960;
    (b) Allinger, N. L., M. A. Miller, F. A. VanCatledge, and J. Hirsch — *J. Amer. Chem. Soc.* 89: 4345, 1967.
34. In acyclic systems severe nonbonded interaction may be relieved either by rotation about carbon-carbon bonds or by increasing the bond angles or bond lengths between bulky groups(28, 29), while a corresponding energy minimization in cyclohexane systems will require significant change in molecular geometry(33).
35. Deformation in the dihedral angles in several other cases was also considered(8, 13, 22, 36) as a possible alternative explanation of discrepancies between the experimentally determined and the expected coupling constants.
36. Hine, J. B. — *Can. J. Chem.* 39: 2536, 1961.
37. Emsley, J. W., J. Feeny, and L. H. Sutsliffe. *High Resolution Nuclear Magnetic Resonance Spectroscopy, Vol. 1* — New York: Pergamon Press, 1965, p. 569.
38. The same assumption is usually made in other similar studies(8, 13).
39. (a) Hendrickson, J. B. — *J. Amer. Chem. Soc.* 83: 4537, 1961; 84: 3355, 1962; and 86: 4854, 1964;
    (b) Hendrickson, J. B. — *J. Org. Chem.* 29: 991, 1964.
40. Wiberg, K. B. — *J. Amer. Chem. Soc.* 87: 1070, 1965.

41. For a discussion of the deformations of dihedral and bond angles in a series of 1,2-dialkylethylene glycols see: Eliel, E. L. *Stereochemistry of Carbon Compounds* — New York: McGraw-Hill Book Company, 1962, p. 132 and ref. therein.
42. A summary of the extensive literature on magnetic nonequivalence, or the chemical shift nonequivalence([43]) in the more recent terminology, is given in the review on the subject by Martin, M. L., and G. J. Martin — *Bull. Soc. Chim. Fr.:* 2117, 1966.
43. Mislow, K., and M. Raban, in: Allinger, N. L, and E. L. Eliel. *Topics in Stereochemistry* — New York: John Wiley and Sons, Inc., 1967, Vol. 1.
44. Jackman, L. M., and N. S. Bowman — *J. Amer. Chem. Soc.* 88: 5565, 1966.
45. References for controversial views on the origin of magnetic or chemical shift nonequivalence may be found in Ref. (42), and Ref. (43) contains a comprehensive discussion of the same issue.

GLASNIK HEMIJSKOG DRUŠTVA, Vol. 35, No. 4-5-6, 1970, pp. 313—320

GHDB-106 547.918:633.63

Original Scientific Paper

SOME DATA ON RAW SUGAR BEET SAPONINS*

by

OLGA S. GAŠIĆ and MIROSLAV A. PERGAL

Many synthetic organic products are used in agriculture as pesticides (insecticides, fungicides, bactericides, rodent poisons, etc.). Their synthesis is often uneconomical and therefore a search for pesticides that can easily be isolated from natural products or industrial wastes appears to be worthwhile.

The aim of our study was to isolate saponins from sugar beet cossetes and settled sugar beet mud in order to investigate some of their chemical properties and pesticidal activity.

Sugar beet saponin was first mentioned in 1874 in a paper by Scheibler(1) who isolated it from the sugar beet cell plasma. The substance was then studied by Lippmann, Andrlik and Votoček who found that the isolated compound had a glycosidic character(1). Hydrolysis of sugar beet saponins was performed in 1911 by Smolenski(7), while in 1927 Van der Haar found that cleanolic acid was the sapogenin of sugar beet saponins(2). Oleanolic acid is a pentacyclic triterpenoid-amyrin chain of the oleanolic type(3). Complete synthesis of the isolated saponin was acomplished in 1952 and confirmed the hypothesis that it was the β-D-glucuronide of oleanolic acid(4).

Chromatographic analysis revealed later that sugar beet saponin consisted mainly of β-D-glucuronide of oleanolic acid but that it probably contains some other saponins whose sapogenin is not oleanolic acid(5). The structure of these saponins has not yet been determined because they have not been isolated in the pure state. The saponins are extremely difficult to isolate pure because during isolation they adsorb fats, phosphatides and minerals from the solution(6).

In sugar beet saponins are found mostly in the peel where they prevent microorganisms getting through into the pith.

During industrial processing of sugar beet saponins either remain in the settled sugar beet mud or are discharged in the waste water, while a small fraction remains in the crystal sugar (0.8 *mg* % or less, depending on the purity of the sugar). Sugar saponins and oleanolic acid are partly responsible for the formation of dregs in the production of non-alcoholic sour beverages(7).

Saponin-containing waste water is lethal for fish.

---

* Communicated at the Twelfth Conference of Serbian Chemists, Belgrade, 1967.

EXPERIMENTAL

Material and Method

Crude saponins were isolated from dried sugar beet pulp and settled sugar beet mud by Rother's(8), Johnson's(9) and Bausemann's(10) methods. The isolate showed characteristic qualitative reactions for saponins(8). It was analyzed by thin-layer chromatography on silica gel *G*, following the technique given by Stahl, with a 4 : 7 mixture of *n*-hexane and ethyl acetate solvent system. The chromatograms were developed by sprinkling with:

(1) a solution of $SbCl_5$ in chloroform
(2) a 1 : 1 mixture of 50% H_2SO_4 and 50% H_3PO_4
(3) distilled water

The hemolytic effect of the crude saponins was tested on a thin layer of silica gel *G* with bovine erithrocytes(11).

The effect of the crude saponins on insects was tested on *Kalandra granaria*. 20 *g* wheat was measured into 500 *ml* Erlenmeyer flasks, and twenty live insects put in each flask. The following quantities of crude saponins were measured into flasks:

Test 1 — 0.03 *g*
Test 2 — 0.06 *g*
Test 3 — 0.12 *g*
Test 4 — 0.24 *g*

The flasks were then sealed and left for 1 hour at 30°C. The insecticidal effect was estimated by the number of dead insects.

The fungicidal effect was tested by Van der Kerk's method(13) on *Alternaria tenuis nees*. Crude sugar beet saponins were added in quantities of 0.4, 0.2, 0.1 and 0.05 *g* to the melted sterilized malt-agar and the broth poured into Petri dishes. After cooling the media were inoculated with a strain of *Alternaria tenuis nees*. The size of colonies was estimated after seven days incubation in a thermostat at 27°C and compared with the control (a colony on saponin-free broth). Poorly developed colonies were fixed and examined under the microscope in order to see whether they contained conidia and how many.

RESULTS AND DISCUSSION

The yield of crude saponins obtained from the settled sugar beet mud and dry sugar beet cossetes is shown in Table 1.

The highest yield (1%) was obtained by Rother's method(8) from the settled sugar beet mud, that obtained by Johnson's method was somewhat lower, while Bauserman's(10) appeared to be unsuitable for isolation of saponins from the settled sugar beet mud.

The procedure confirmed the already known fact that saponins are mostly accumulated in the sugar beet peel. The results show that the peel contained ten times more crude saponins than the pith.

The product exhibited positive qualitative reactions characteristic for sugar beet saponins (regardless of the kind of material from which it was isolated)(8).

TABLE 1

Maximum Yield of Crude Saponins (in %)

Material	Methods	Yield (%)
Settled sugar beet mud	Rother[8]	1.00
„	Johnson[9]	0.88
„	Bauserman[10]	0.2
Sugar beet cossetes	Rother[8]	0.32
„ „ peel	Rother	0.40
„ „ pith	Rother	0.038

A chromatogram of the crude saponins is shown in Fig. 1.

Besides the spots of saponaceous components, there are also spots (Rf 0.83—0.94) corresponding to oil firmly bound by the product during precipitation. This phenomenon can be explained by the lipophylic character of the tripentoid part of the saponin molecule which plays an essential role in the mechanism of erithrocyte hemolysis[11].

The tests with bovine erithrocytes impregnated on a thin layer of silica gel *G* (according to Stahl's method) showed that the crude sugar beet saponins induced hemolysis to a somewhat lower extent than *Saponin album* used as a control.

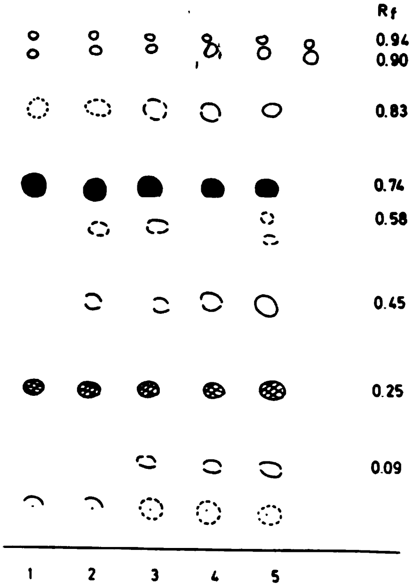

Fig. 1.

Onedimensional chromatogram of crude saponins. Solvent system: *n*-hexane: ethyl acetate = 4 : 7. — (1) and (2) — crude saponins from beet; (3), (4) and (5) — crude saponins from the settled sugar beet mud.

The tests with *Kalandra granaria* showed that the crude saponins had no insecticidal effect; in all tests the insects survived.

The results for the fungicidal effect of the crude saponins *Alternaria tenuis nees* are shown in Table 2 and Figs. 2—5. The results in the fourth column of Table 2 were obtained by examining slides prepared from colonies under the microscope.

TABLE 2

Fungicidal Effect of Crude Sugar Beet Saponins

Figure	Raw saponins (*g*)	Diameter of colony (*cm*)	Number of conidia
2	0.4	1.0	—
3	0.2	1.5	2
4	0.1	4.3	several
—	0.05	6.0	many
5	control	control	many

From Table 2 and the figures it may be concluded that the crude saponins had a strong fungicidal effect at a concentration of 0.4—0.2 *g* per sample. At concentrations below 0.2 *g* the fungicidal effect was less, and at 0.05 *g* zero. This is concluded from the radius of the colonies and the microscopic findings.

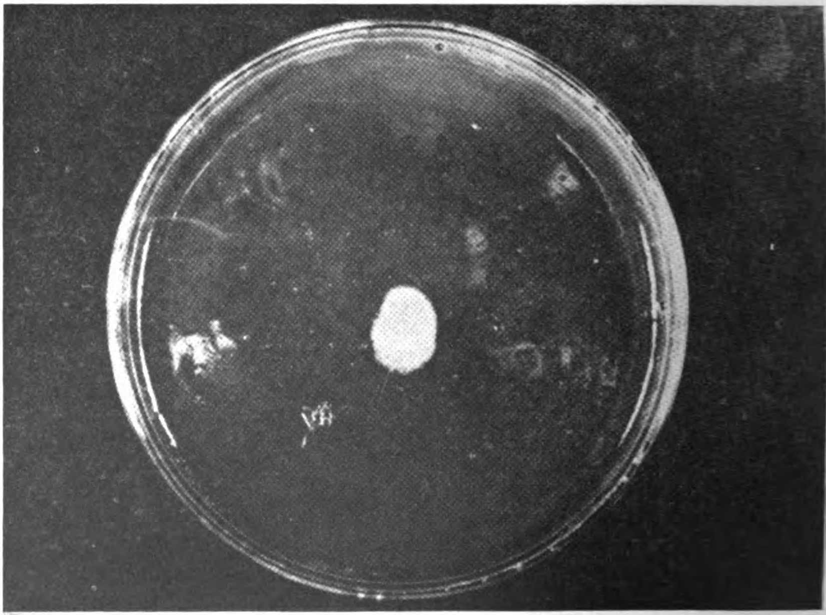

Fig. 2.

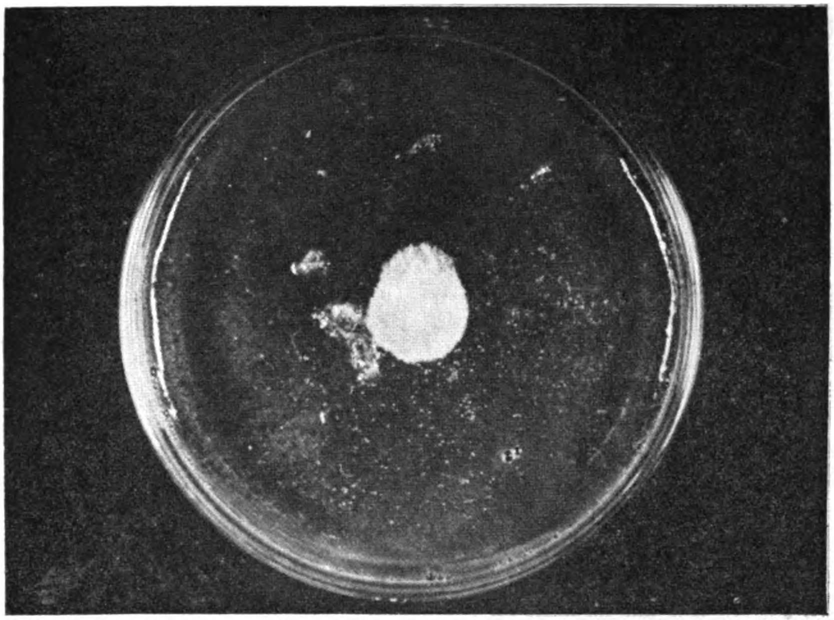

Fig. 3.

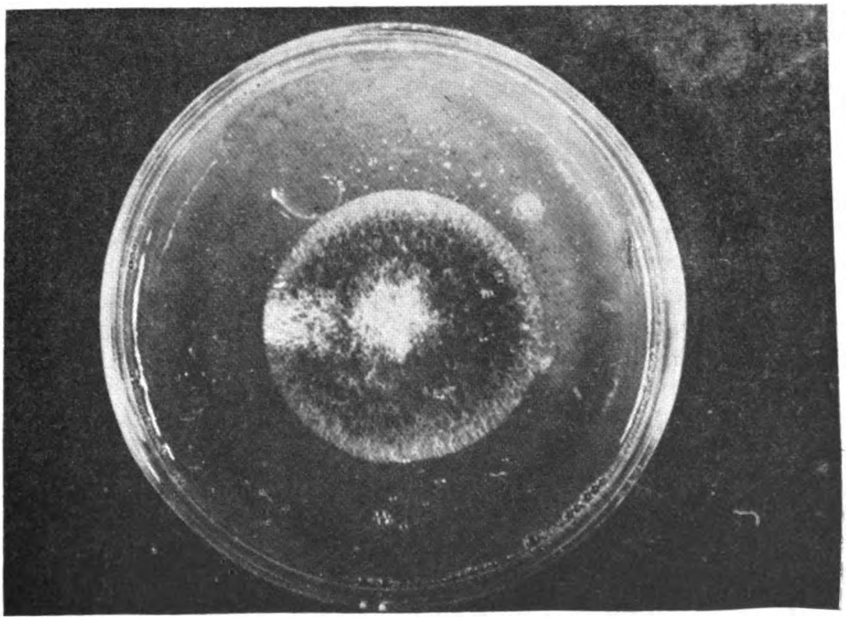

Fig. 4.

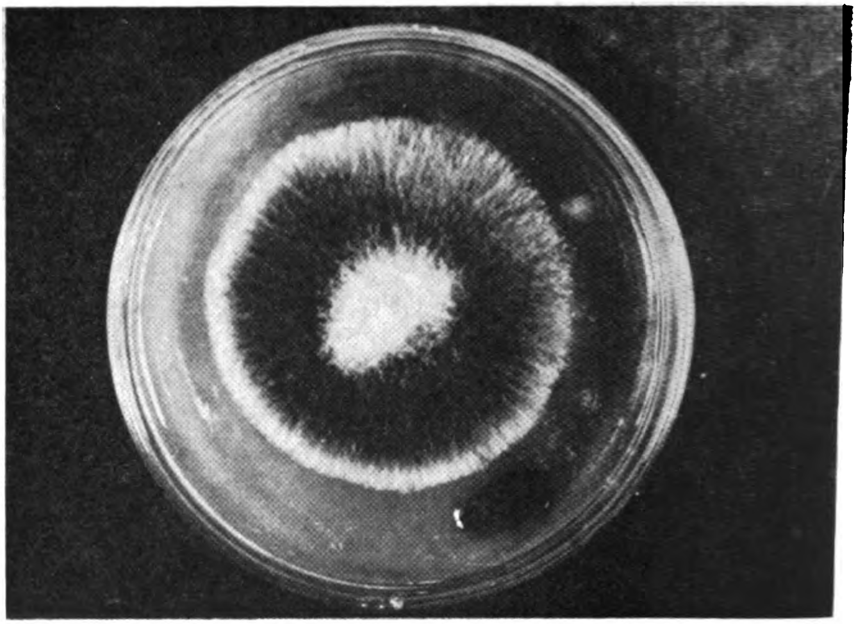

Fig. 5.

SUMMARY

Crude sugar beet saponins were isolated from the settled sugar beet mud and sugar beet by Rother's, Johnson's and Bauserman's methods. The highest yields were obtained with the first method, i.e. 1% raw saponin from the settled sugar beet mud, 0.32% from the beet, 0.40% from the peel, and 0.038% from the pith.

Qualitative and preparative thin layer chromatography methods for determination and isolation of crude saponins have been worked out. The chromatograms were run with a 4 : 7 mixture of *n*-hexane and ethyl acetate as solvent system, and the spots were developed with distilled water. It was found that the crude saponins consisted of six different components.

Biological tests on *Kalandra granaria* showed that the crude saponins were ineffective as insecticide.

On the other hand, they were found to cause hemolysis of erithrocytes.

They deserve attention as fungicides since the laboratory tests on *Alternaria tenuis nees* revealed a strong fungicidal effect.

ACKNOWLEDGEMENTS

The authors wish to thank Dr. Djordje Stefanović of the School of Sciences, Belgrade Univ., for providing the initial idea and valuable advice.

The authors are also much obliged to Dr. Milutin Stefanović of the School of Sciences, Belgrade Univ., for his interest in the work.

Finally, the authors wish to express their sincere thanks to the directors of the Sugar Refinery at Zrenjanin and the Institute at Rimski Šančevi for making available the settled sugar beet mud and sugar beet cossetes.

Department of Chemistry,
School of Agriculture,
and School of Sciences,
University of Novi Sad, Novi Sad

Received 15 September, 1969

REFERENCES

1. Van der Haar, A. W. "Untersuchungen über die Saponine und verwandte Körper. XVIII. Über das Zuckerrüben-sapogenin" — *Rec. Trav. Chim. Pays-Bas* 46: 776, 1927.
2. Van der Haar, A. W. "Untersuchungen über die Saponine und verwandte Körper. XIX. Über die Identität von Zuckerrüber-sapogenin mit Oleanolsäure aus Olivenblatt und Carophyllin" — *Rec. Trav. Chim. Pays-Bas* 46: 793, 1927.
3. Robinson, T. *The Organic Constituents of Higher Plants* — Minneapolis: Burges Publishing Company, 1963, pp. 136—162.
4. Hardegger, E., T. H. Leeman, and G. Robinet. "Steroid und Triterpen glycoside" — *Helvetica Chimica Acta* 35: 824—829, 1952.
5. Duuren, J. A. "Thin Layer Chromatography of Sugar Beet Saponins" — *Journal of the American Society of Sugar Beet Technologists* (Fort Collins) 12: 57—64, 1963.
6. Duuren, J. A. "The Determination of Saponin in Sugar Beet Products" — *Medelingen von Het institut voor rationele snikerproduktie* (Bergen) 1: 3—11, 1963.
7. Schiweck, J. "Der Floc-Pests, seine Durchführung und technologische Bedeutung" — *Zucker* (Hannover) 16: 4, 1963.
8. Rother, H. "Saponintällungen in zuckergesüssten, klaren Erfrischungsgetränken" — *Zucker* (Hannover) 15: 186—191, 1963.
9. Johnson, J. R. "Standard Method for Floc in White Sugar" — (not poblished).
10. Bauserman, M. H., and C. P. Hanzas. "Colorimetric Determination of Saponin as Found in Beet Sugars" — *Journal of Agricultural and Food Chemistry* (Washington) 10: 773—776, 1957.
11. Gašić, O. *Prilog proučavanju saponina šećerne repe* (Magistarski rad) (A Study of Sugar Beet Saponins) — Beograd: 1967.
12. Skender, A. "Fungicidna vrednost nekih do sada nepoznatih polisumpornih jedinjenja aromatičnih ugljovodonika sintetizovanih u SFRJ" (Specijalistički rad) (Fungicidal Value of Some New Polysulphuric Compounds of Aromatic Carbohydrates Synthesized in Yugoslavia) — Novi Sad: 1966.

GLASNIK HEMIJSKOG DRUŠTVA, Vol. 35, No. 4-5-6, 1969, pp. 739—399

GHDB-107

581.192.1

Original Scientific Paper

WEIGHT CORRELATION OF ELEMENTS IN PLANT ASH

by

ZAGORKA J. FILIPOVIĆ

The results of many authors show that the chemical composition of ash in nearly all known plants is the same. The ash consists of the oxides of the following ("basic") elements: K, Na, Ca, Mg, Fe, P, S, Si, and elementary Cl.

However, quantitative differences are so diverse that it is practically impossible to find two plant species with the same percentage composition of their ash[2, 4]. How much a plant takes up of a given element depends both internal (species specific) and external factors (concentration in the soil, availability of its ionic form, soil pH, moisture , aeration, temperature, etc.).

The quantitative composition of plant ash is a resultant of these and many other factors, and as these are extremely diverse under natural conditions, the problem of plant nutrition with mineral ions is (according to Peterburgskiĭ, see Ref. (5)) one of the most complex questions in nature.

Having this in mind, we considered that the results of our present work might be of interest because they show that, regardless of all quantitative differences in ash composition, the total weight of basic elements per 100 *g* ash is approximately the same for all plants.

In order to check this law the results were compared with those of other authors.

DISCUSSION

The quantitative composition of various plant ashes is shown in Table 1. The results for samples 1—9 were obtained in our research, while those from 10—19 were taken from the literature[6, 3, 1] for comparison. The results for samples 10—15 were obtained by Winton[6], 16—18 by Fuhrmann[3], and 19 by Brunel[1]. For the last result the necessary corrections to K, Na, Fe and P weight from the weight of oxides reported in the original paper were made.

As seen from the table, the nine basic elements contributed very different percentages in various plant samples. For an example, let us mention only the following variations: the phosphorus content may vary from 1.3 to 16 *g*, silicon from 0.25 to 11.5 *g*, and calcium from 2.3 to as much as 41 *g*.

TABLE 1

Composition of Plant Ash

No.	Plant	*K* (*g*)	*Na* (*g*)	*Ca* (*g*)	*Mg* (*g*)	*Fe* (*g*)	*P* (*g*)	*S* (*g*)	*Si* (*g*)	*Cl* (*g*)	Total per 100 g oxides	
											Weight	Gram-atom
1.	Lettuce	31.87	5.41	7.46	6.78	2.85	6.93	2.37	0.88	3.39	68.70	2.02
2.	Potato	37.52	0.35	9.96	5.57	1.09	2.96	3.33	2.29	3.25	70.62	1.96
3.	Bean	10.23	0.20	41.25	6.50	0.08	7.67	0.48	0.28	1.25	66.41	1.86
4.	Tomato	24.11	1.20	26.72	1.80	0.03	9.59	1.93	0.25	0.91	66.94	1.83
5.	Sunflower seed	28.68	0.87	22.66	7.51	0.76	1.35	1.37	4.81	0.27	69.46	1.96
6.	Cabbage	21.34	0.53	38.03	4.20	0.15	2.14	1.74	0.83	0.36	70.29	1.88
7.	Maize	36.52	3.93	10.45	4.65	0.41	6.55	2.19	1.77	2.91	69.38	2.00
8.	Rye	31.85	0.46	5.57	1.56	0.26	14.97	1.90	0.93	1.52	63.81	1.79
9.	Soyabean	29.88	0.32	27.24	8.72	0.34	2.25	1.08	0.88	0.80	71.23	2.02
10.	Lettuce	31.43	8.99	8.58	1.06	2.33	1.30	2.08	11.47	traces	67.25	2.01
11.	Potato	48.27	6.01	4.00	2.46	0.37	7.05	1.19	1.00	2.56	72.60	2.08
12.	Potato	49.38	1.63	2.84	3.06	0.89	8.07	1.20	1.82	2.80	71.47	1.98
13.	Pea	35.77	0.70	3.42	4.79	0.57	15.65	1.37	0.42	1.59	64.88	1.86
14.	Bean	36.53	1.10	4.53	4.57	0.22	15.49	1.62	0.27	0.86	64.66	1.86
15.	Lemon	24.94	0.11	17.87	2.40	0.19	4.44	0.99	0.25	0.27	69.09	1.85
16.	Six vegetable samples	30.64	4.13	8.88	2.33	1.30	6.69	3.67	3.90	6.49	68.03	2.00
17.	Seven mush-room samples	40.50	1.28	2.33	0.88	1.47	13.08	3.64	0.54	1.92	65.92	1.83
18.	15 fruit samples	40.56	2.55	6.82	2.86	0.63	5.95	1.73	0.79	1.72	71.47	1.99
19.	10 tropical plant samples	36.16	2.12	14.50	4.54	0.84	5.76	2.47	1.10	2.00	69.90	1.94
										Mean	~68	≈2

On the other hand, not only different species but also plants within the same species (e.g. beans 3 and 14) appear to have ash of different quantitative composition, probably as a result of different ecological conditions.

It seems that the results in Table 1 only confirm that there is no regularity in plant ash composition⁽⁴⁾. However, the following data led us to think that there might be a certain correlation between the elements in plant ash:

— Sample 10 is very high in silicon, but lowest in phosphorus;

— Sample 12 is very rich in potassium but contains an extremely small amount of calcium.

— Sample 3, however, is highest in calcium but lowest in potassium and sodium.

The total weight of ash elements for every plant sample is shown in Table 1.

Note. — In computing the total weight the following was born in mind: It is the convention to express the amount of elements in plant ash oxides per 100 *g* of the latter. Considering that the weight of oxides in the samples (though usually only slightly) deviated from 100, the weight of elements in every sample was computed for 100 *g* of plant ash oxides in order to make the conclusions general.

Theoretically, the total weight of plant ash elements may vary over a wide range (from 40 to 83 *g*), depending on whether there are more light or heavy elements. However, from Table 1 it may be seen that the total weights are found in the relatively narrow interval between 63 and 73 *g*. The average total weight for all samples, with possible ±10% deviation, is 68 *g* (see the table).

Before discussing the above, one more fact must be pointed out. If the quantitative composition of the ash is expressed in fractions of gram-atoms of these elements, the sum of these fractions is 2 gram-atoms in every case (see the average value in Table 1).

These two facts reflect a previously unknown law:

100 *g* plant ash contains approximately 68 *g*, or 2 gram-atom of basic elements.

For an illustration, let examine two samples from Table 1, viz. lettuce 1 (Yugoslavia) and 10 (England).

It may be immediately noted that the first sample contains about 13 times less silicon than the second, but much more magnesium, phosphorus and chlorine. Thanks to adaptability to environmental conditions, these two plants absorbed different amounts of elements from different soils. Nevertheless, their total weights (68.70 and 67.3, respectively) and the sum of gram-atom fractions (2.00 and 2.02) are nearly identical.

All other data in Table 1 (within the limits of an analytical error) confirm the above statement.

Table 1 is lacking another interesting series of data, viz. quantitative changes of plant ash elemental composition during growth. The extent of these changes may be illustrated by the following example⁽⁷⁾:

EXAMPLE 1

Analysis of Lettuce Sample 1 (Yugoslavia)

	K	Na	Ca	Mg	Fe	P	S	Si	Cl	Total per 100 g oxides
grams	31.87	5.41	7.46	6.78	2.85	6.93	2.37	0.88	3.39	68.70
g-atoms	0.82	0.24	0.19	0.28	0.05	0.22	0.07	0.03	0.10	2.00

EXAMPLE 2

Analysis of Lettuce Sample 10 (England)

	K	Na	Ca	Mg	Fe	P	S	Si	Cl	Total per 100 g oxides
grams	31.43	8.99	8.58	1.06	2.33	1.30	2.08	11.47	traces	67.25
g-atoms	0.81	0.39	0.22	0.04	0.04	0.04	0.07	0.41	traces	2.02

EXAMPLE 3

Change in Turnip Ash Composition (in %)

Date of sampling	K	Na	Ca	Mg	Fe	P	S	Si	Cl	Total per 100 g oxides
July 7	18.2	7.3	9.9	5.6	4.2	5.6	4.3	5.0	5.8	65.0
Aug. 11	30.1	11.7	6.8	2.7	1.7	5.9	4.2	1.3	2.5	68.0

Except for P and S which remained almost the same throughout the interval, all other elements underwent appreciable changes. Relative to the first sample (July 7), the second (August 11) had about 40% more potassium and sodium, while Ca, Mg, Fe, Si and Cl decreased (from 30% for Ca to over 70% for Si). But in spite of the great quantitative differences, in both samples the total weight of all elements turned out to be very close (with an appr. 4% error in the first sample), and equal to the above stated value (68).

From the above it may be concluded that the total weight of basic elements per 100 *g* plant ash is always constant. This proves (see page 5) that the amounts of elements in plant ash are mutually dependent variables. Since the sum of the weights of all elements must give a constant number (68), any change in one element must be accompanied by changes in the others.

DISCUSSION OF THE NUMBER 68

As stated in the introductory section, almost all plant ash consists of oxides of the following nine elements: K, Na, Ca, Mg, Fe, P, S, Si, and elementary Cl. We hypothesized that the number 68 might reflect a specific property of these elements, above all their atomic weights.

The following calculation tends to confirm such a hypothesis.

By adding the average weights of the nine basic elements (34.3) to the appropriate average amounts of oxygen in the oxides, the mean (apparent) molecular weight of these oxides is found to be 50.3.

On the basis of all the above said, allowing for a relatively small error, the weight of these oxides may be considered equal to the weight of ash. Hence if there is (approximately) 34 *g* (1 gram-atom) of these elements in 50 *g* of plant ash, then their weight in 100 *g* ash should amount to 68 *g* (2 gram-atom).

According to this simple calculation, the number 68 appears to be double the average atomic weight of all the basic elements in the plant ash.

TABLE 2

Analysis of Basic Elements

K	Na	Ca	Mg	Fe	P	S	Si	Cl	No. of diff. atoms	Total atomic weight	Average atomic weight
39.1	23.0	40.0	24.3	55.8	31.0	32.0	28.0	35.5	9	308.7	34.3
O in corresponding oxides											Average amount of O_2
8	8	16	16	24	40	48	32	—	12	192	16

However, an essential difference between the theoretical and experimental results must be pointed out. From Table 2 it may be seen that in computing the average atomic weight (34), every element contributed an equal part (as there are nine elements, every one participated with 1/9 its atomic weight) to the value 34 (or with 2/9 to 68). However, the results in Table 1 show that such an equality of elements in plant ash is out of question; the whole essence of this article gives evidence of large variations in the quantitative composition of plant ash.

Nevertheless the fact that the total weight of ash elements found experimentally comes out the same as the calculated one suggests the following:

The chemical nature of the basic elements — reflected in their atomic weight — sets a natural limit (68) to their total weight in plant ash. However, it seems that the plants, depending upon their physiological requirements and the influence of environment, are free to take up different amounts of various elements, but always as to keep the total weight within the limit (68).

ACKNOWLEDGEMENTS

The authors are grateful to the Fund for Scientific Research of the Socialist Republic of Serbia for financial support.

Institute of Inorganic Chemistry, School of
Pharmacy, Belgrade University

Received 3 June 1969

REFERENCES

1. Brunel, A. *Traite pratique de Chemie vegetale* — Paris: G. Frere Tourcoing, 1948, pp. 448.
2. *Handbuch der Pflanzenphysiologie. Band IV.* — Berlin: Springer-Verlag, 1958, pp. 859.
3. Fuhrmann, F. *Die Chemie der Nahrungs- und Genusmittel* — Berlin: Urban-Schwarzenberg, 1927.
4. Klein, G. *Handbuch der Pflanzenanalysen. Spezielle Analysen, Teil. I.* — Berlin: J. Springer Verlag, 1932, pp. 99.
5. Peterburgskiĭ, A. V. *Obmënnoe pogloshchenie v pochve i usvoenie rasteni͡ami pitatel'nykh veshchestv* (Exchange Absorption of Nutrients in the Soil and Their Uptake by Plants) — Moskva: Gosudarstvennoe izdatel'stvo "Vyssha͡is shkola", 1959, p. 5.
6. Winton, L. A., and B. K. Winton. *The Structure and Composition of Foods* — New York: John Wiley and Sons, Inc., 1949.
7. Chapek, F. *Biochemie der Pflanzen. Band II.* — Jena: G. Fischer Verlag, 1925, pp. 396.

GLASNIK HEMIJSKOG DRUŠTVA, Vol. 35, No. 4-5-6, 1970, pp. 329—335

GHDB-108 577.164.16:591.436:546.73:621.039.8

Original Scientific Paper

A METHOD OF ISOLATING VITAMIN B_{12} FROM THE LIVER USING RADIOACTIVE COBALT (^{60}Co)

by

BOŽIDAR R. PANIĆ, MARGITA F. ČUPERLOVIĆ and VITOMIR LJ. HRISTIĆ

A convenient and well worked out method for isolating vitamin B_{12} from the content of the digestive tract and the liver could not be found in the available literature. Existing chemical methods for quantitative assay of vitamin B_{12} are based mainly on its isolation and spectrophotometric determination of its concentration in aqueous solution. But all these methods start with a more or less purified product and cannot be applied to samples like the liver and intestinal content.

The aim of our study was to modify some of the existing methods to adapt them for isolation of this vitamin from the liver, and to verify their suitability for this purpose.

METHOD OF ISOLATING VITAMIN B_{12} FROM THE LIVER

Experience shows that it is almost impossible to isolate vitamin B_{12} even from the richest sources without chromatography. However, all chromatographic methods require at least partly purified raw material.

The method employed by Bukin *et al.*(1) was considered the most suitable for obtaining a sufficiently pure raw material for isolation of vitamin B_{12} from the liver. This method is actually a modified and developed version of the method proposed by Cohn *et al.*(2).

The method is based upon the extraction of the vitamin from the liver with water of pH 5—6 and addition of KCN. The extraction is performed by boiling the macerate in an autoclave (at 1 atm. for 10 minutes) in order to release the protein-bound vitamin. After this the extract is filtered, and 2% active charcoal added to the filtrate in order to adsorb the vitamin. Adsorbed vitamin is eluted with 65% ethyl alcohol warmed to 50—60°C. The eluate is then evaporated to 0.1 original volume. Vitamin is several times extracted from the eluate with a mixture of phenol and chloroform, converted to an aqueous solution by the addition of ether and measured on a spectrophotometer at 548 $m\mu$.

The modified version consists in the following:

After mesuring the radioactivity of fresh liver samples, the liver is homogenized in a mixer with the addition of five volumes distilled water.

The pH of the homogeneous pulp is adjusted to 4.5 by adding 10% HCl. Vitamin B_{12} is extracted by boiling the pulp in an autoclave at 1 atm. for 10 minutes. In order to keep vitamin B_{12} from decomposing at the autoclave temperature, 2 *mg* calcium cyanide per milliliter of liver pulp is added.

After boiling the liver extract is filtered *in vacuo* through a Büchner funnel, and the sediment left on the filter washed with hot distilled water. The extract is of satisfactory quality if it is clear after filtering. However, the method cannot be used if the vitamin is present in a very small amount. In order to avoid this, a quantity of 100 *μg* vitamin B_{12} is added to the extract as a carrier. From the extract vitamin is adsorbed on 5 *g* purified active carbon. The adsorption is done by mixing the extract for 15 minutes at room temperature. The suspension is then filtered in vacuo through a Büchner funnel. The procedure is repeated again with 3 *g* active charcoal .Adsorbed vitamin is eluted from the charcoal with fresh double-distilled 65% ethyl alcohol, boiling the suspension in 150 *ml* alcohol for 10 minutes at 50—60°C. Elution is then repeated twice with 100 *ml* alcohol. The charcoal sediment left on the filter is washed once again with 50 *ml* 65% ethyl alcohol, also warmed to 60°C.

The alcoholic eluate is evaporated in vacuo at 40°C to a volume of 2—3 *ml*.

The vitamin B_{12} extract from liver thereby obtained can be used as raw material for various methods of purification. We chose a method based on the selective solubility of vitamin B_{12} in organic solvents. It is described in Ref. (3) and is applicable for relatively pure vitamin B_{12}.

The steamed vitamin extract is transfered quantitatively, by manifold washing with water, into a 100 *ml* centrifuge tube. From this solution vitamin is extracted with a mixture of creasol and carbon tetrachloride (1 : 1). Ten milliters of this mixture is added to the solution, the tube is then sealed with a suitable glass, polythene or aluminum foil-wrapped rubber stopper, and shaken for 5—10 minutes. The emulsion is centrifuged for 10 minutes at 3000 rpm, the lower cresol-carbon tetrachloride layer transferred to another tube, and the upper layer extracted again with 5 *ml* creosol-carbon tetrachloride mixture. The extracts are joined and washed with 1 : 7 sulpuric acid until the decanted acid becomes virtually colorless. If the raw vitamin extract is relatively pure (as in our case), two washings appear to be adequate. After this the extract is washed twice with 10 *ml* phospho-cyanide solution (0.01% KCN dissolved in saturated solution of dibasic sodium phosphate) and finally with 10 *ml* water. All these washings are done by 5—10 min. shaking and then centrifuging the suspension.

After this 30 *ml* of a 1 : 2 mixture (by volume) of carbon tetrachloride and a solution of butanol-benzalkonium chloride (1 volume part of 12.8% benzalkonium chloride and 9 volume parts of *n*- butanol) is added to the washed extract. The vitamin is then extracted twice with 5 *ml* water, with vigorous shaking (for 1 min.) and centrifuging.

The combined aqueous extract is further purified by passing it through an aluminum oxide column. The column is prepared in the usual way. It should be of a height to take 10 milliliter of the extract and may be used only once. The solution of vitamin should pass at a rate of one milliliter per minute, while the layer of fluid above the packing should be about 1 *cm*.

The first eluate fraction (about 5 *ml*) is discarded, and the colored fraction collected in a centrifuge tube containing 0.5 *ml* 2N acetic acid solution. From the eluate, which after eluting the column can be up to 40 *ml*, vitamin is extracted with 5 *ml* creosol-carbon tetrachloride solution. The extract is separated again by shaking for 2—5 min. and centrifuging. Finally, 5 *ml* distilled water, 5 *ml* carbon tetrachloride and 10 *ml* butanol are added and after vigorous shaking the extract is centrifuged. The whole quantity of vitamin goes into the easily separated aqueous layer.

The purity of this vitamin solution was determined by spectrophotometry. Aqueous solutions of vitamin B_{12} have absorption peaks at 278, 361 and 550 $m\mu$. If the solution is pure, the ratio between the extinctions at 361 $m\mu$ and 550 $m\mu$ should be 3.10—3.40. If it lies outside this range, the whole procedure must be repeated starting from running the solution through the column.

Radioactivity of the solution was measured on a well-type scintillation counter for liquids.

CHECKING THE METHOD WITH RADIOACTIVE VITAMIN B_{12}

In order to check whether all vitamin in the liver can be recovered by the method, it was tested using radioactive vitamin B_{12} labelled with ^{60}Co. Hens were perorally administered 0.05 microcurie radioactive vitamin per kg live weight. After a definite time (2—7 days) the hens were killed and radioactivity in their liver determined. Vitamin B_{12} was isolated from the liver in the same way as in the case of hens getting ^{60}Co. The recovery factor was determined by comparing the activity of the isolated vitamin B_{12} with the activity in the liver. The loss of activity in various phases of isolation and purification was measured in the same way. The results are given in Table 1.

TABLE 1

Average Losses in Isolation of Radioactive Vitamin B_{12} from the Liver (in % of the Fresh Liver Activity)

Fresh liver*	100.00
Liver after extraction of vitamin	14.51
Extract after adsorption of vitamin on active charcoal	—
Active charcoal after eluting vitamin with 65% ethanol	18.85
Losses in purification	7.04
Vitamin recovery	59.64

* Four samples.

From Table 1 it may be seen that after extraction of vitamin B_{12} with water there remained on average 14.51% unextracted vitamin in the liver. After adsorption on active charcoal the filtrate did not show any activity, meaning that all extracted vitamin was adsorbed. However, on eluting the vitamin with 65% alcohol, a considerable activity still remained on the active charcoal, 18.85% of the total activity in the liver. The activity of the isolated and purified vitamin was 59.64% of that in the liver.

As anticipated, all the vitamin could not be isolated from the liver. Extraction with water did not remove 12.12—16.04%, or 14.51% vitamin on average. Even so, an average of 85.49% extraction may be considered quite satisfactory. The use of active charcoal for adsorption of vitamin from the liver extract also appears to be efficient because the extracted liver pulp did not contain radioactive vitamin. However, an interesting feature is that vitamin B_{12} adsorbed on the active charcoal cannot be fully eluted with 65% ethyl alcohol, an average of 18.85% vitamin remaining uneluted; this may be considered a relatively large loss. During purification with organic solvents on average 7.04% activity is lost.

TABLE 2

Efficiency of Vitamin B_{12} Purification (Checked with 60 $CoCl_2$)

	Volume (ml)	Activity (cpm/ml)	Percentage of initial activity
Aqueous solution of crystalline vitamin after addition of 60 $CoCl_2$	35	—	100
Residue after extraction with creosol-carbon tetrachloride mixt.	34	88	95.04
Sulphuric acid used for washing	9.8	8	2.47
Phospho-cyanide solution	20	7	1.27
Water after washing	9.8	18	2.54
Solution of purified vitamin*	4.7	—	—

* No radioactivity was shown by the mixture of creosol, carbon tetrachloride, *n*-butanol and benzalkonium chloride after extraction of vitamin with water, the Al_2O_3 after running the vitamin solution, the aqueous solution after extraction of vitamin with creosol-carbon tetrachloride mixture, or the mixture of carbon tetrachloride, creosol and *n*-butanol after extraction of vitamin with water.

Since these large losses of activity during the isolation might have been due to the fact that apart from radioactive vitamin the liver also contains its decay products, primarily inorganic cobalt, special tests were made with radioactive cobalt.

$^{60}CoCl_2$ was added to 200 *ml* distilled water together with 100 *μg* inactive vitamin B_{12}. The activity of the added cobalt was 3000 cpm. After adsorbing vitamin on charcoal the radioactivity of the carbon was measured before and after eluting vitamin with 65% alcohol. The results showed that a considerable amount of the cobalt was adsorbed on the carbon together with vitamin (about 70%), but it was not eluted with alcohol at all. Therefore, in the isolation of vitamin from the liver the alcoholic eluate does not contain inorganic cobalt but only vitamin B_{12} and related compounds.

Even on addition of radioactive cobalt to the eluate, i.e. aqueous extract of inactive vitamin, no activity was found in the vitamin after purification with organic solvents and running it through the alumina column (Table 2).

From Table 2 it may be seen that inorganic radioactive cobalt mostly remained in the aqueous solution (95.04%) from which vitamin was extracted with creosol-carbon tetrachloride solution. Residual cobalt, extracted together with vitamin, is washed out in the subsequent three purification steps, so that the solutions used in the later steps show practically no radioactivity, i.e. they do not contain inorganic cobalt.

Hence the applied method is not a quantitative one, because on average only 59.64% of the vitamin can be isolated from the liver. Most of the losses i.e. about 40%, occur in the isolation steps. These data show that all methods for determination of vitamin B_{12} which employ the same or similar procedure of isolation are not quantitative.

However, in the absence of any better methods, this one may well serve for qualitative investigations. For quantitative work certain corrections should be made for the losses during extraction and purification.

As already pointed out, for the application of chromatography or electrophoresis it is also essential to obtain partly purified and concentrated vitamin extract from the liver or digestive tract content. Because of this, it is almost not possible to extract all vitamin contained in the liver by the known methods, but only to decrease the losses, especially those due to the non--quantitative elution of vitamin from the active charcoal. If all vitamin were eluted by more suitable organic solvents, then after evaporating the eluate and getting vitamin B_{12} into a concentrated enough aqueous solution chromatographic or electrophoretic methods could be very successfully employed not only for the quantitative assay of vitamin B_{12} — cyano-cobalamin, but also of the related compounds cobalamin and the vitamin B_{12} analogs.

SUMMARY

A modified method for isolation and purification of vitamin B_{12} from the liver has been proposed. By perorally administering radioactive vitamin B_{12} subsequently isolating it from hen liver, it was found that an average of 59.64% of the total vitamin was recovered. After extraction with water, 14.51% of vitamin remained in the liver.

By using radioactive cobalt (^{60}CoCl) it was found that inorganic cobalt adsorbed on the active: charcoal together with vitamin B_{12} was not eluted by 65% ethanol, and the eluate contained only vitamin and related compounds.

A considerable amount of vitamin (18.85%) remained adsorbed on the active charcoal even after a threefold elution with 65% alcohol.

An average of 7.04% was lost in the purification with organic solvents.

The results show that the method is only applicable for qualitative investigations, while in quantitative work certain corrections must be made for the losses in extraction and purification.

Institute for the Application of Nuclear Energy in
Agriculture, Veterinary Medicine and Forestry, Zemun, and
School of Agriculture, Belgrade Univ., Zemun

Received 24 April 1967

REFERENCES

1. Bukin, V. N., L. I͡a. Areshkina, and L. S. Kuts͡eva. "Mikro- i makrometodika opredelenii͡a vitamina B_{12}" (Micro and Macromethods for Determination of Vitamin B_{12}) — *Biokhimii͡a* 19: 713—720, 1954.
2. Cohn, E. J., G. R. Minot, G. A. Alles, and W. T. Salter., in: Smith, E. L. *Vitamin B_{12}* — London-New York: John Wiley and Sons, Inc., 1060; — *Biol. Chem.* 77: 325, 1928.
3. Cobalamin Assay Ion-Exchange, Radioisotope Tracer Method, in: *First Supplement to the Pharmacopeia of the United States, Fifteenth Revision* — New York: US Pharmacopeial Convention, Inc., 1956, p. 21.

GLASNIK HEMIJSKOG DRUŠTVA, Vol. 35, No. 4-5-6, 1970, pp. 337—343

GHDB-109

543.257:541.454:547.292
Original Scientific Paper

COULOMETRIC TITRATION OF BASES IN PURE GLACIAL ACETIC ACID

by

VILIM J. VAJGAND, TIBOR J. PASTOR and OLIVERA M. ANTONIĆ

Coulometric determination of bases in a mixture of acetic acid and its anhydride is described in Ref. (1—5). Direct titrations are based on the formation of hydrogen ions by quantitative oxidation of mercury(1, 3, 5) or hydroquinone(3–5) at the anode of the generating circuit. Employing the fact that hydrogen has a low overpotential on platinum, a method of coulometric titration by direct reduction of hydrogen ions from excess perchloric acid added to the bases prior to determination was worked out(2, 3, 5). Quantitative neutralization of hydrogen ions at the cathode of the generator circuit is also achieved in the reduction of quinone(4, 5).

Due to the fact that primary and secondarv amines cannot be determined in the presence of acetic acid anhydride, we have investigated and determined the optimum conditions for their coulometric titration in pure glacial acetic acid.

EXPERIMENTAL

The apparatus is shown diagrammatically in Fig. 1, or is already described in refs. (3) and (5). Hydrogen ions were generated with the aid of a Mihailo Pupin STNS 50260 current and voltage stabilizer A 0.96 cm^2 platinum electrode was connected to the negative and another of 1.20 cm^2 to the positive terminal of the constant current source. The current flowing in the generator circuit was measured with a precision mA-meter (Iskra, Kranj) whose accuracy was checked against a silver coulometer. In determining the titration end-point by photometry we used a Lange differential colorimeter, and photocurrent as a function of the time were recorded on the recorder of a Radelkisz type OH-102 Polarograph. At constant paper speed the length of paper tape between the start and end-point of titration was proportional to the time of electrolysis. The titration cell was made a U-tube and divided into two halves by a G-4 sintered glass plate 1 cm in diameter. The inside diameter of the anode branch was 2.2 cm, and of the cathode 1 cm. The distance between the two branches was 7 cm.

The methods of purification of acetic acid, preparation of sodium perchlorate and perchloric acid, sodium acetate and amine solutions are given in Ref. (5).

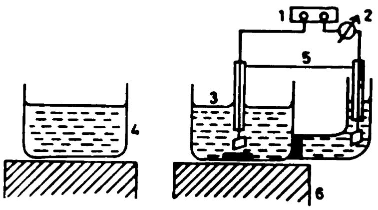

Fig 1.

Apparatus for coulometric titration of bases with colorimetric end-point detection

1. Current and voltage stabilizer
2. Milliammeter
3. Titration cell
4. Reference cell
5. Electrodes

The titration end-point was detected with 0.5% malachite green or gentian violet solution in acetic acid.

Hydroquinone was purified by recrystallization in ethanol. The melting point of the purified product was 170°C.

Potentiometric titration with glass and mercurous acetate electrodes was carried out as a comparison.

PROCEDURE

3 *ml* supporting electrolyte (appr. 0.2 M sodium perchlorate solution) is poured into the cathode (narrower) branch, and a determined volume of base solution measured with a microburette into the anode branch. Then the supporting electrolyte is poured into both branches up to the same level, so that on the anode side there is 10—15 *ml*. About 0.1 *g* hydroquinone and three drops of indicator solution are added to the solution of the base. After this a standard solution is prepared by pouring a neutralized solution of supporting electrolyte and three drops of indicator solution into a vessel having the same shape and dimensions as the titration cell. The cells are placed side by side (in the case of visual detection of the end-point) or in front of the differential colorimeter photocells. The electrodes are immersed in the appropriate places in the vessel for electrolysis and the magnetic stirrer switched on. After dissolving of hydroquinone, a chronometer and constant current source are switched on simultaneously, and in the case of photometric determination also the pen recorder. At the end-point the chronometer is switched off or the titration time is determined from the *i-t* curve. The amount of base in the measured solution is computed by using the formula

$$Q = I \cdot t \cdot \eta,$$

where Q = amount of bases in *mg*, I = current in *A*, t = time of electrolysis in seconds, and η = electrochemical equivalent of bases in *mg*/C.

DISCUSSION

The results of coulometric determination of tertiary amines and organic acid salts in a mixture of acetic acid and its anhydride(1—5) suggested that primary and secondary amines might also be titrated in pure acetic acid. As the resistance of amines dissolved in acetic acid, which has a low dielectric constant ($\varepsilon = 6.13$), is high due to the incomplete dissociation of amines and formation of ionic pairs(6, 7), the reduction of resistance in the system by adding a supporting electrolyte was necessary. For this purpose, the conductivity of the solution was measured on adding sodium or silver perchlorate (which behave as neutral salts in acetic acid). Silver perchlorate turned out to be a better conductor at the same concentration. However, it could not be employed as a supporting electrolyte because of precipitation of silver peroxide at the anode during electrolysis. Due to its low solubility, only 0.1—0.2 M sodium perchlorate solution could be used as a supporting electrolyte.

Hydrogen ions were generated by oxidation of hydroquinone at the generator anode according to the following electrochemical reaction:

$$C_6H_4(OH)_2 \longrightarrow C_6H_4O_2 + 2H^+ + 2e^-$$

The quantitative yield of hydrogen ions in the above reaction was verified by titration with sodium acetate, which does not react at the anode under the conditions for determination of bases. 100% current efficiency was not achieved in the presence of silver perchlorate supporting electrolyte due to formation of silver peroxide at the anode.

The titration end-point was detected by colorimetry or differential potentiometry (as described in Ref. (2) and (5)). On the basis of literature data(8) and personal experience, gentian violet or malachite green were used

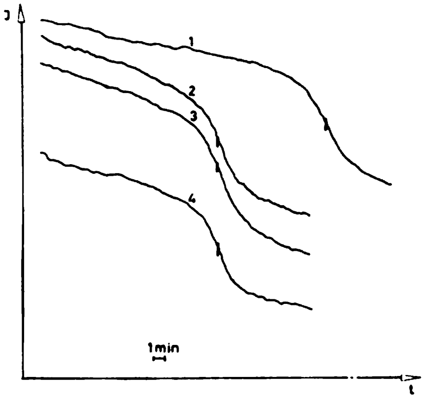

Fig. 2

Coulometric titration of 4.592 *mg* of di-*n*-butylamine. The titration end-point was detected by differential photometry in the presence of malachite green. The current was 2.5 mA curve 1) and 4 mA (2, 3 and 4).

as indicators. The results obtained with malachite green were found to be better. This may be explained by the fact that gentian violet passes through a series of transitional shades in acetic acid during the change of the solution pH from alkaline to acid, while malachite green only changes its color from blue-green (via green) to yellow. The color change of malachite green at the end-point is easily registered. In detecting the end-point by photometry well-developed bilogarithmic *I*-*t* curves were obtained with the use of red filters. The equivalence points are found on the *I*-*t* curve approximately where the change in photocurrent is greatest (see Figs. 1 and 2).

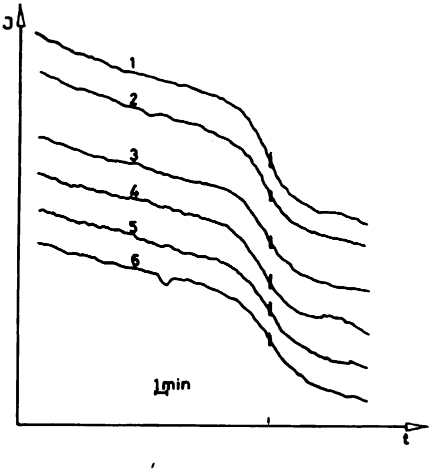

Fig. 3

Curves of six successive titrations of 1.879 *mg* of ethanolamine at 2.5 mA. The end--point was detected by photometry in the presence of malachite green.

As acetic acid is highly hygroscopic, it was of interest to test the effect of water in the solution on the slope at the end-point. By differential photometry it was found that water decreased the gradient of the indicator color transition. As seen in Fig. 4, the change of photocurrent near the end-point was small in the presence of only 1% water, while in the presence of 3% water it completely dissappeared. This may be explained by the weakly basic character of water in acetic acid.

With continuous generation of hydrogen ions the potentiometric method cannot be applied for detecting the end-point due to the strong influence of the constant current source electric field on the function of the glass electrode. Furthermore, the potential jump at the equivalence point is highly decreased in the presence of water.

The results in Table 1, obtained by colorimetric end-point determination, show that primary and secondary amines may successfully be determined by coulometry in pure acetic acid. In the individual determinations errors were not more than ±2.0% relative to potentiometric titration.

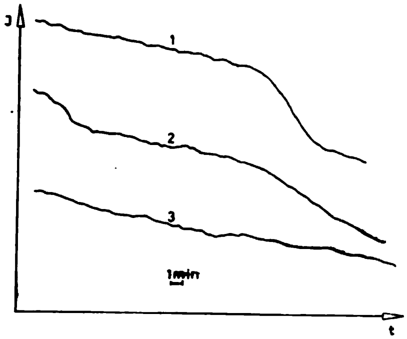

Fig. 4

Coulometric titration of 4.592 *mg* of di-*n*-butylamine with end-point detected by differential photometry in the presence of malachite green

1) In absence of water
2) with 1% water
3) with 3% water

TABLE 1

Coulometric Titration of Primary and Secondary Amines

Substance	Taken (*mg*)	No. of titrations	Found	
			mg	%
Sodium acetate	2.486	11	2.491 ± 0.027	100.2 ± 1.1
Diethylamine	2.774	8	2.772 ± 0.033	99.9 ± 1.2
Diethanolamine	3.217	9	3.243 ± 0.031	100.8 ± 1.0
i-propylamine	1.506	8	1.502 ± 0.012	99.7 ± 0.8
Cyclohexylamine	2.399	6	2.392 ± 0.019	99.9 ± 0.8
Benzylamine	1.143	6	1.136 ± 0.008	99.4 ± 0.7
Ethanolamine	1.879	7	1.888 ± 0.013	100.5 ± 0.7
Aniline	2.288	6	2.301 ± 0.020	100.5 ± 0.9
Di-*n*-butylamine	4.592	8	4.607 ± 0.035	100.3 ± 0.8

Determining a mixture of triethylamine and ethylamine, it was also found that the total bases in a solution can be successfully determined by this method. Since the coulometric titration of tertiary amines in a mixture of acetic acid and its anhydride has already been worked out, the present study suggests the possibility of determining binary mixtures of tertiary and primary or tertiary and secondary amines. The results of these investigations will be given in another paper.

SUMMARY

A method for coulometric titration of primary and secondary amines in pure acetic acid with end-point detection by colorimetry or differential photometry has been worked out. The resistance of titrated solutions is decreased by adding sodium perchlorate as supporting electrolyte. Hydrogen ions are generated with 100% current efficiency by oxidation of hydroquinone at the anode. Errors of individual determination were not more than ±2.0% against potentiometric titrations.

Institute of Chemistry, School of Sciences, Belgrade Univ.,
Institute of Chemistry, Technology and Metallurgy, Belgrade

REFERENCES

1. Mather, W. B., Jr., and F. C. Anson. "Coulometric-Acidimetric Titrations in Anhydrous Acetic Acid" — *Analytica Chemica Acta* (Amsterdam) 21: 468—473, 1959.
2. Vajgand, V., T. Pastor, T. Todorovski, F. Gaál, and M. Todorović. "Determination of Bases in Glacial Acetic Acid by Various Instrumental End-Point Detection Methods", in: *Proceedings of the Analytical Chemical Conference, Budapest, 1966, Vol. 1* — pp. 152—157.
3. Vajgand, V. J., and R. Mihajlović. "Coulometric Titration of Bases in Acetic Acid and Acetonitrile Media" — *Talanta* (Belfast) 16: 1311—1317, 1969.
4. Vajgand, V. J., T. J. Pastor, and L. J. Bjelica. "Kulometrijske titracije baza u smesi sirćetne kiseline i njenog anhidrida određivanjem završne titracione tačke biamperometrijskom metodom pomoću hinhidronovih elektroda" Coulometric Titration of Bases in a Mixture of Acetic Acid and Acetic Anhydride, End-Point Detected by Biamperometric Method in the Presence of Quinhydrone Electrodes) — *Glasnik hemijskog društva* (Beograd): this issue.
5. Pastor, T. J. *Determination of Bases in Acetic Acid by Electrochemical Methods** (Thesis) — Beograd: 1969.
6. Kolthoff, I. M., and S. Bruckenstein. "Acid-Base Equilibria in Glacial Acetic Acid. I. Spectrophotometric Determination of Acid and Base Strengths and of Some Dissociation Constants" — *Journal of the American Chemical Society* (Washington) 78(1): 1—9, 1956.
7. Bruckenstein, S., and I. M. Kolthoff. "Acid-Base Equilibria in Glacial Acetic Acid. II. Spectrophotometric Determination of the Ionization Constants of p,p'-Dimethylaminoasobenzene and Pyridine. The Abnormal Effect of Water on Indicator Bases" — *Journal of the American Chemical Society* (Washington) 78(10): 10—11. 1956.
8. Gyenes, I. *Titration in Non-Aqueous Media** — Budapest: Akadémiai Kiadó, 1967.

GLASNIK HEMIJSKOG DRUŠTVA, Vol. 35, No. 4-5-6, 1970, pp. 345—352

GHDB-110

543.257:541.454:547.292
Original Scientific Paper

COULOMETRIC TITRATION OF BASES IN A MIXTURE OF ACETIC ACID AND ACETIC ANHYDRIDE, END-POINT DETECTED BY BIAMPEROMETRIC METHOD IN THE PRESENCE OF QUINHYDRONE ELECTRODES

by

VILIM J. VAJGAND, TIBOR J. PASTOR and LUKA J. BJELICA

Coulometric determination of bases in a mixture of acetic acid and its anhydride was first successfully performed by Mather and Anson(1) by oxidizing mercury at the anode of the generating circuit. In this process mercurous ions are generated, and in their secondary reaction with acetic acid hydrogen ions are released in an equivalent amount. These authors also observed that in the oxidation of solvent at the platinum anode the yield of hydrogen ions did not exceed 95% of the theoretical value. They explained the phenomenon by formation of base products in the condensatiopn of acetyl cations and acetic anhydride, which bind hydrogen ions(2).

As certain difficulties arise in working with mercury electrode, a method of coulometric back-titration by direct reduction of hydrogen ions originating from excess perchloric acid and employing the fact that the hydrogen overvoltage on platinum appears to be small was developed(3). The conditions of colorimetric and differential photometric detection of the titration end-point with simultaneous recording were also determined in this study (Ref. 3). These methods enable continuous tracking of the neutralization in the coulometric titration and back-titration of bases in a mixture of acetic acid and its anhydride, this being impossible in glass electrode potentiometry due to the strong influence of the constant current source electric field on the potential of the glass electrode.

Although coulometric titration gives good results in determination of a small quantity of bases in a mixture of acetic acid and its anhydride, the method has not been studied thoroughly. The present work investigates optimum conditions of continuous coulometric determination of bases in this solvent, the facilities of the biamperometric method using quinhydrone electrodes (see Ref. 4) for end-point detection. Hydrogen ions were generated in quantitative yield by oxidation of hydroquinone at platinum anode. This was enabled by the fact (as shown in Ref. 5) that in this solvent mixture hydroquinone oxidizes at about a 0.5 V more negative potential than acetate ion.

EXPERIMENTAL

The apparatus is schematically shown in Fig. 1. Hydrogen ions were generated or neutralized by means of a Mihailo Pupin STNS 50260 current and voltage stabilizer and platinum electrodes having about 3 cm^2 surface area. The current flowing in the generating circuit was measured with a precision milliammeter ("Iskra", Kranj) whose accuracy was checked against a silver coulometer. In the indicating circuit current was either measured with a Radiometer GVM 13b multiflex galvanometer or recorded on the recorder of a Radelkisz OH102 or Radiometer PO3 polarograph. The solution was mixed with a magnetic stirrer. Platinum electrodes having 0.5 cm^2 surface area and spaced at a distance of 1 *mm* were used in the indicating circuit. A potential of about 100 *mV* was applied across the indicating electrodes from an accumulator via a 100 Ω potentiometer ("Elektroveze", Ljubljana). The titration cell was H-shaped and divided into two halves by G-4 sintered glass.

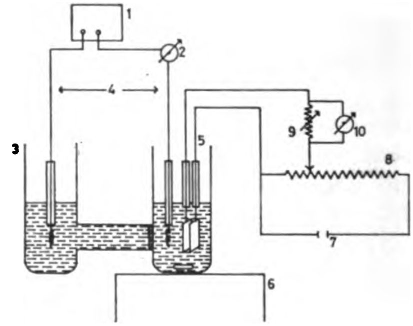

Fig. 1.

Apparatus for coulometric titration of bases, end-point detected biamperometrically in the presence of quinhydrone electrodes

1 — Current stabilizer
2 — Milliammeter
3 — Titration cell
4 — Generator electrodes
5 — Indicator electrodes
6 — Magnetic stirrer
7 — Accumulator
8 — 100 Ω potentiometer
9 — 1 kΩ potentiometer
10 — Multiflex galvanometer or pen recorder

The titrated bases were prepared as 10^{-2} N solutions, and their exact concentration was determined by potentiometric titration with glass and mercurous acetate electrodes.

In order to decrease the resistance in the electrolysis cell in coulometric determinations the solution was made 0.1 M relative to sodium perchlorate.

PROCEDURE

A volume of base solution was measured out and made up to 10—20 *ml* with the solution of sodium perchlorate whose correction term was already determined. In the back-titration a known volume of the standard solution perchloric acid was added in excess to the measured solution of base prior to its dilution. Sodium perchlorate solution was poured into the other half of electrolysis cell in an amount such that the solutions in both halves were at the same level. The electrodes of the generating circuit were placed in the cell in such a way that in the case of direct coulometric titration the positive, and in back-titration the negative electrode was in the tested solution. Indicating electrodes were immersed into the titrating solution and the magnetic stirrer switched on after adding 100 *mg* quinhydrone. A chronometer was started simultaneously with the constant current source. At the end-point the chronometer was stopped and the time of electrolysis read.

The quantity of bases in the titrated solution was calculated with the help of following formulas:

$$Q = It\,\eta \text{ (direct titration)}$$
$$Q = (q - It)\eta \text{ (back-titration)}$$

where Q = quantity of base in *mg*, I = current in A, t = time of electrolysis in seconds, η = electrochemical equivalence of base in mg/C, and q = number of coulombs required to neutralize all added perchloric acid in back titration.

DISCUSSION

The titration curve of direct coulometric titration with quinhydrone indicating electrodes has a minimum at the titration end-point, while in the back-titration there i sa prominent maximum (Fig. 2). The current rise in the indicating circuit at the end-point in the case of direct coulometric titration may be explained by reversible processes at the anode in the presence of water (acting as a weak base) in the titrated solution. The effect of water on

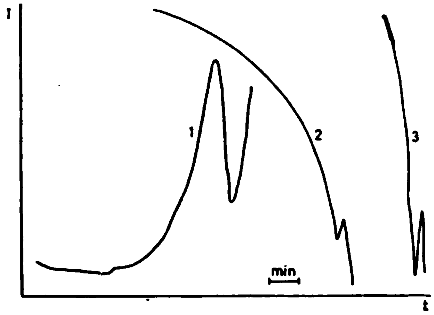

Fig. 2.

Coulometric titration of triethylamine with apparatus in Fig. 1.

1) Coulometric back-titration,
2) Direct coulometric titration,
3) Direct coulometric titration at higher sensitivity of indicator circuit galvanometer.

the shape of the titration curve for the supporting electrolyte is illustrated in Fig. 3. It may be seen that the minimum on the titration curve decreases and eventually completely disappears with increasing water concentration, while the maximum increases. It may also be seen that in direct coulometric titration of supporting electrolyte neutralization of water also occurs, because its increase in the solution causes an increase of the time of electrolysis between the minimum and maximum points. By coulometric titration of supporting electrolyte it was found that in determination of bases a correction term for the supporting electrolyte should be introduced in identifying the end-point by biamperometric method. The magnitude of this term, i.e. the time required for neutralizing the supporting electrolyte, depends upon the purity of the acetic acid and acetic anhydride; it was found to be 0.07—0.10 coulomb. This was concluded after using acetic acid and its anhydride made by various manufacturers, having a p.a. quality but without purification prior to use. As a definite number of ions must be consumed in the neutralization of supporting electrolyte, the time required for it must, in the case of direct coulometric titration, be substracted from the total time of electrolysis, while in the case of back-titration it should be added to the time required for neutralization of hydrogen ions originating from free perchloric acid, before calculating the number of coulombs consumed in constant current coulometric titration. In all our determinations the current in the generating circuit was kept constant at 5—10 mA.

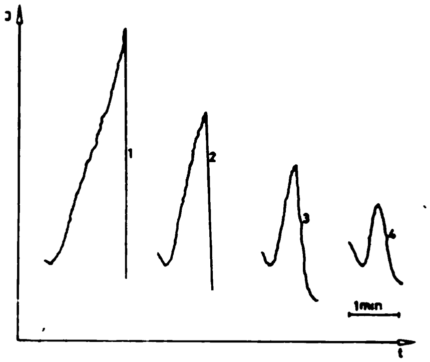

Fig. 3.

Direct coulometric titration of supporting electrolyte. Electrolysis followed by biamperometric method in the presence of quinhydrone electrodes:

1) In the presence of 1% water
2) 0.5% water
3) 0.25% water
4) Absence of water

In order to define the electrochemical processes occurring at the generator electrodes in the presence of quinhydrone in one half of the cell, the potential difference between them and relative to mercurous acetate electrode were measured. With quinhydrone-saturated anolite the potential difference between the electrodes of the generating circuit was 8 V, while without quinhydrone it was 9.5 V. As identical electrochemical processes occur at the cathode in both cases, this difference is due to different reactions at the anode and difference of resistance in the titrated system. According to our measurements, in the presence of quinhydrone the generator anode had a potential of 775 mV, and the cathode 420 mV. It must be noted that in determining the potential of the mercurous acetate electrode with saturated calomel electrode the phase end diffusion potentials and the potential drop in the solution were not taken into account.

In order to define the process at the electrodes of generating circuit, the *I* — *V* curve of a platinum electrode in 0.1 *M* sodium perchlorate solution in a mixture of acetic acid and its anhydride (in a supporting electrolyte) in the presence of quinhydrone was plotted at various polarization rates with a Tacussel PRT 500L potentiostat. Mercurous acetate was the reference electrode. The results show that under the given experimental conditions the hydroquinone oxidation potential is 250—300 mV more negative than the oxidation potential of acetate ion. From this and the results obtained by Mather and Anson at negative-polarized platinum electrode in the same electrolyte(²), we deduce that in the presence of quinhydrone hydrogen ions are generated or neutralized at the cathode of the generating circuit as a result of the following electrochemical processes:

$$C_6H_4(OH)_2 \underset{K}{\overset{A}{\rightleftarrows}} C_6H_4O_2 + 2\,H^+ + 2e^-$$

In coulometric analysis with biamperometric end-point detection extreme attention must be paid to the position of electrodes in the electrolysis cell. In order to neutralize the influence of the generating circuit on the functioning of the indicating electrodes, the latter should not be placed between the former. The generating circuit can be prevented from interfering with the indicator circuit may be avoided by appropriate adjustment of their position in the cell. However, it must be pointed out that in working with quinhydrone electrodes the size and position of the platinum electrodes essentially affect the sharpness of the end-point. With small-area electrodes the maximum and minimum at the end-point are not sharp; this may be explained by slow equilibration at them.

Accuracy and reproducibility of the results obtained by coulometry in the presence of quinhydrone with end-point detected by biamperometric method may be seen from Table 1. The results confirm that the reactions at the generating circuit electrodes take place with 100% current efficiency and also the assumption that the method is applicable both for direct and back-titration of strong and weak bases. All titrated bases neutralized one hydrogen ion equivalent. In all uniacid bases the titration curves had the same shape (Fig. 2). In biacid bases, e.g. aminopyrine, the shape of titration curve changed after reaching the first equivalence point due to neutralization of the second base group in the molecule. However, in titrating aminopyrine the second equivalence point could not be determined because the change of slope of the two branches of the titration curve at the point where two hydrogen ion equivalents are consumed was not sharp.

TABLE 1.

Coulometric Titration of Bases, End-Point Detected by Biamperometric Method

Substance	Potentiometric titrations	Coulometric titration							
		Direct titration				Back titration			
	Found (*mg*)	No. of titrations	Taken (*mg*)	Found		No. of titrations	Taken (*mg*)	Found	
				mg	%			*mg*	%
Antipyrine	99.43	6	5.92	5.88 ± 0.02	99.4 ± 0.3	6	4.00	3.96 ± 0.01	99.1 ± 0.3
Triethylamine	99.54	6	5.00	5.02 ± 0.02	100.4 ± 0.4	6	2.00	2.02 ± 0.01	100.7 ± 0.4
Sodium acetate	100.00	7	2.88	2.90 ± 0.01	100.6 ± 0.3	6	1.153	1.145 ± 0.005	99.6 ± 0.4
N,N-Diethylaniline	98.59	6	8.93	8.61 ± 0.03	98.9 ± 0.4	6	3.49	3.43 ± 0.01	98.2 ± 0.3
Triethanolamine	99.49	7	5.78	5.72 ± 0.02	99.0 ± 0.3	7	3.85	3.78 ± 0.01	98.2 ± 0.3
Tributylamine	99.30	6	9.07	9.15 ± 0.01	100.9 ± 0.1	6	2.72	2.76 ± 0.01	101.5 ± 0.3
Isoniazide	99.69	6	4.24	4.24 ± 0.01	100.0 ± 0.2	6	2.82	2.80 ± 0.00	99.3 ± 0.1
Aminopyrine	99.72	6	7.01	6.99 ± 0.02	99.8 ± 0.3	6	3.50	3.54 ± 0.02	101.1 ± 0.6

SUMMARY

Based on the electrochemical equation

$$C_6H_4(OH)_2 \underset{C}{\overset{A}{\rightleftarrows}} C_6H_4O_2 + 2\,H^+ + 2\,e^-$$

a method of coulometric direct and back-titration of bases in 0.1 *M* sodium perchlorate solution in a 1 : 6 mixture of acetic acid and its anhydride, with biamperometric end-point detection has been worked out. In direct titration the end-point is observed as a minimum, in back-titration as a maximum on the *I*-*t* curve.

The shape of titration curves and the accuracy of the results were affected by previous treatment, area and spacing of platinum indicator electrodes, their position relative to the electrodes of the generating circuit, and composition of the solutions investigated.

The errors in direct titration were not more than ±1%, and in back-titration not more than ±2%. Reproducibility is good. The method is applicable both to strong and weak bases.

Institute of Chemistry, School of Sciences,
Belgrade University,
and Institute of Chemistry, Technology
and Metallurgy, Belgrade

Received 12 January 1970

REFERENCES

1. Mather, W. B., Jr., and F. C. Anson. "Coulometric-Acidimetric Titrations in Anhydrous Acetic Acid" — *Analytica Chimica Acta* (Amsterdam) 21: 468—473, 1959.
2. Mather, W. B., Jr., and F. C. Anson. "Chronopotentiometry in Acetic Anhydride, Oxidation and Reduction of the Solvent" — *Analytical Chemistry* (Washington) 33(12): 1634—1637, 1961.
3. Vajgand, V., T. Pastor, T. Todorovski, F. Gaàl, and M. Todorović. "Determination of Bases in Glacial Acetic Acid by Various Instrumental End-Point Detection Methods" in: *Proceedings of the Analytical Chemical Conference, Budapest, 1966, Vol. 1* — pp 152—157.
4. Vajgand, V., and T. Pastor. "Determination of Tertiary Amines and Salts of Organic Acids in Glacial Acetic Acid by Dead-Stop Method" — *Journal of Electroanalytical Chemistry* (Amsterdam) 8(1): 49—54, 1964.
5. Vajgand, V. J., and R. Mihajlović. "Coulometric Titration of Bases in Acetic Acid and Acetonitrile Media" — *Talanta* (Belfast) 16: 1311—1317, 1969.

GLASNIK HEMIJSKOG DRUŠTVA, Vol. 35, No. 4-5-6, 1970, pp. 353—358

GHDB-111

543.253:546.811:546.815
Original Scientific Paper

POLAROGRAPHIC DETERMINATION OF TIN IN PRESENCE OF LEAD*

by

SRETEN N. MLADENOVIĆ and ILONA LUC

Reduction of lead and tin ions at the dropping mercury electrode usually take place at nearly identical electrochemical potentials(1). Hence lead and tin are difficult to determine in each other's presence.

In a solution of hydrochloric acid and Na-salt of EDTA lead may be determined in the presence of tin by polarography(2), but not the converse (tin in the presence of lead).

In a fluoride supporting electrolyte tin may be determined in the presence of limited amounts of lead(1) because its half-wave potential in this electrolyte is more positive than that of lead.

Polarographic determination of tin after its precipitation with strontium sulphate collector(3) is laborious and time-consuming.

In order to find a more reliable and quicker method of polarographic determination of tin in the presence of lead, its determination in an ammonium acetate + Na-salt of EDTA supporting electrolyte has been studied.

EXPERIMENTAL

Determinations were made on Radiometer PO3 and Radiometer PO4 polarographs (Copenhagen, Denmark). All chemicals were of the highest purity (p.a.).

In 0.8 *M* ammonium acetate supporting electrolyte (see Fig. 1) tin gave two waves: the anodic with a half-wave potential of ~ –0.22 V, and the cathodic with a half-wave potential of ~ –0.57 V. It may be seen that the two waves of tin are satisfactorily resolved, but the anodic one is not sharp.

In the same supporting electrolyte lead produced a cathodic wave with a half-wave potential of ~ 0.46 V (Fig. 2). In this electrolyte the lead wave occurs between the two tin waves. The anodic wave of tin in the presence of lead is not well defined, and this makes its determination very difficult. The difference between the half-wave potential of lead and of the cathodic wave of tin is small and there is always a possibility of their coalescence and superposition, preventing determination of tin by the height of its cathodic wave.

---

* Communicated at the 14th Conference of Serbian Chemists, Belgrade.

In the ammonium acetate + Na-EDTA supporting electrolyte lead did not produce a polarographic wave at a more positive potential than -1.0 V relative to saturated calomel electrode (Fig. 3), while tin gave only the anodic wave (Fig. 4). The tin wave well defined and regular in shape No lead wave appeared either before or after the tin wave and so did not interfere in the determination of tin. The effect of lead on the polarographic determination of tin was thus completely obviated. This means that in this electrolyte the polarographic determination of tin is posible in the presence of considerable amounts of lead.

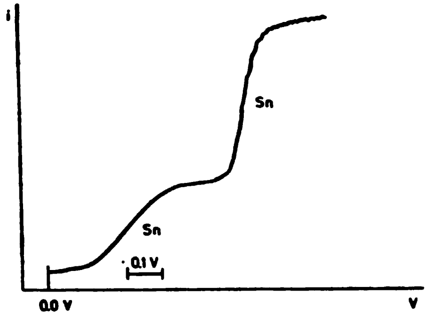

Fig. 1

Polarography of tin in 0.8 M ammonium acetate supporting electrolyte

The height of the tin wave in the presence of various amounts of lead is given in Table 1. It may be seen that there is a linear relationship between the wave height and the amount of tin, even in an electrolyte containing a hundred times more lead than tin. The anodic wave of tin was well defined and its height could be easily measured. In this supporting electrolyte the half-wave potential was about —0.18 V.

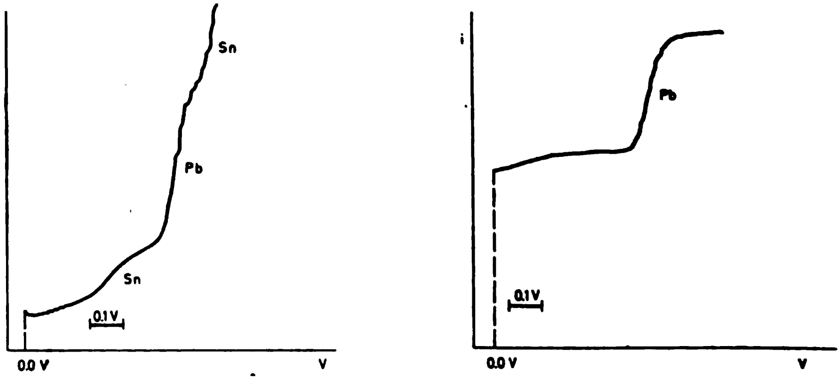

Fig. 2a

Polarography of lead in 0.8 M ammonium acetate supporting electrolyte

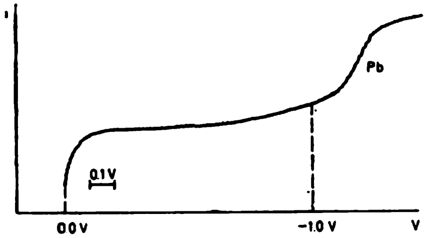

Fig. 3

Polarography of tin in ammonium acetate + EDTA Na-salt supporting electrolyte

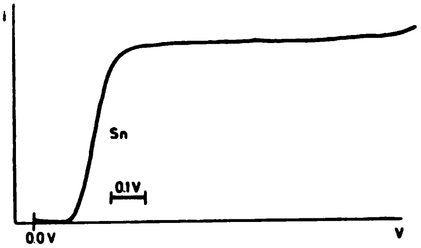

Fig. 4

Polarography of lead in ammonium acetate + EDTA Na-salt supporting electrolyte

TABLE 1

Height of Tin Wave in the Presence of 5—100 mg Pb
Supporting electrolyte: 15.0 ml/62 g ammonium acetate + 19 g Na-EDTA + 0.1 g gelatin + water ad 1 lit).

Tin (II) (*mg*)	Lead (*mg*)	Height of Sn wave (*mm*)
1.00	5.0	13.0
2.00	5.0	25.0
3.00	5.0	39.0
4.00	5.0	53.0
5.00	5.0	67.0
1.00	10.0	8.0
2.00	10.0	16.0
3.00	10.0	23.0
4.00	10.0	33.0
5.00	10.0	41.0
1.00	25.0	6.0
2.00	25.0	11.0
3.00	25.0	17.0
4.00	25.0	23.0
5.00	25.0	29.0
1.00	50.0	6.0
2.00	50.0	12.0
3.00	50.0	17.0
4.00	50.0	23.0
5.00	50.0	29.0
1.00	75.0	14.0
2.00	75.0	27.0
3.00	75.0	41.0
4.00	75.0	56.0
5.00	75.0	71.0
1.00	100	13.0
2.00	100	27.0
3.00	100	39.0
4.00	100	53.0
5.00	100	66.0

In the solution of ammonium acetate alone tin could not be determined from its cathodic wave if cadmium was also present as well as lead. In this case the tin wave was superimposed on the cadmium wave. However, in the solution of ammonium acetate and Na-salt of EDTA cadmium and lead did not produce waves at more positive potentials than —1.0 V, and this allowed easy determination of tin in their presence (Table 2). In this electrolyte the half-wave potential of tin was about —0.20 V. As there is a direct correlation

TABLE 2

Height of Tin Wave in the Presence of 1—2 mg Pb and 5—10 mg Cd
Supporting electrolyte: 15.0 ml (62 g ammonium acetate + 0.1 g gelatin + water ad 1 lit + Na-EDTA to saturation)

Tin (II) (*mg*)	Lead (*mg*)	Cadmium (*mg*)	Height of Sn wave (*mm*)
1.00	1.00	10.0	12.0
2.00	1.00	10.0	23.0
3.00	1.00	10.0	35.0
4.00	1.00	10.0	48.0
5.00	1.00	10.0	61.0
1.00	2.00	5.00	15.0
2.00	2.00	5.00	31.0
3.00	2.00	5.00	45.0
4.00	2.00	5.00	61.0
5.00	2.00	5.00	76.0

TABLE 3

Height of Tin Wave in the Presence of 25—100 mg Zn
Supporting electrolyte: 15.0 ml (62 g ammonium acetate + 0.1 g gelatin + water ad 1 lit + EDTA to saturation)

Tin (II) (*mg*)	Zinc (*mg*)	Height of Sn wave (*mm*)
1.00	25.0	9.0
2.00	25.0	17.0
3.00	25.0	26.0
4.00	25.0	36.0
5.00	25.0	45.0
1.00	50.0	10.0
2.00	50.0	19.0
3.00	50.0	31.0
4.00	50.0	41.0
5.00	50.0	51.0
1.00	100	6.0
2.00	100	12.0
3.00	100	17.0
4.00	100	24.0
5.00	100	31.0

between the wave height and the amount of tin, it may be determined in the presence of cadmium and lead. Tin compounds often contain lead, cadmium and zinc as well. Therefore the effect of zinc on the determination of tin was also investigated.

From Table 3 it may be seen that zinc did not affect the linear correlation between wave height and amount of tin, even if present in quite large amounts.

The errors of polarographic determination of tin were ±5.0%, well within the usual limits of this method.

In the ammonium acetate + Na-salt of EDTA the waves of lead, cadmium and zinc did not appear immediately after the anodic wave of tin, which had a very regular shape, allowing polarographic determination of tin in the presence of these metals.

SUMMARY

In the reduction of lead and tin ions at dropping mercury electrode in all common supporting electrolytes their half-wave potentials are usually very close. Therefore direct polarographic determination of tin in the presence of lead is impossible in these electrolytes. But in an ammonium acetate + Na-salt of EDTA supporting electrolyte tin can be determined in the presence of lead due to the fact that the latter forms a complex with EDTA. Large amounts of zinc in the electrolyte did not interfere in the polarographic determination of tin in the presence of lead.

Polarographic determination of tin in this electrolyte was also possible in the presence of lead, cadmium and zinc.

School of Technology and Metallurgy,
Department of Physical Chemistry
and Electrochemistry, Belgrade University

Received 11 December 1969

REFERENCES

1. Kri͡ukova, T. A., S. I. Sini͡akova, and T. V. Aref'eva. *Poli͡arograficheskiĭ analiz* (Polarographic Analysis) — Moskva: Goskhimizdat, 1959.
2. Mladenović, S. N., and M. Gemović. "Polarografsko određivanje olova pored kalaja" (Polarographic Determination of Lead in the Presence of Tin) — *Glasnik hemijskog društva* (Beograd) (to be published).
3. Mladenović, S. N. "Polarografsko određivanje kalaja u cinku" (Polarographic Determination of Tin in Zinc) — *Glasnik hemijskog društva* (Beograd) 29*: 203, 1964.

---

* Available in English translation from National Technical Information Service, Springfield, Virginia, 22151.

GLASNIK HEMIJSKOG DRUŠTVA, Vol. 35, No. 4-5-6, 1970, pp. 359—362

GHDB-112

543.253:546.47:546.48
Original Scientific Paper

POLAROGRAPHIC DETERMINATION OF ZINC IN CADMIUM*

by

SRETEN N. MLADENOVIĆ and MILIVOJE ISAKOVIĆ

The polarographic determination of small amounts of zinc in the presence of large amounts of cadmium in a supporting electrolyte consisting of ammonium hydroxide and ammonium chloride is either impossible or very tedious(1, 2). The wave of cadmium, which precedes that of zinc and is much higher, cannot usually be shifted and eliminated by a counter current on most available polarographs.

Polarographic determination of zinc in the presence of large amounts of cadmium is possible in ammonium carbonate supporting electrolyte(2). In this electrolyte cadmium precipitates in the form of hardly soluble cadmium carbonate, and is thereby eliminated from the solution and does not interfere with the polarographic determination of zinc. However, ammonium carbonate solution is very unstable and easily decomposes even at room temperature. If decomposition occurs, cadmium cannot be completely precipitated, and again zinc often cannot be determined.

Zinc and cadmium may also be determined by volumetric titration in a solution of ammonium hydroxide and ammonium chloride(3). Both metals are first titrated with a solution of EDTA in the presence of eriochrome black indicator until the color change. After this a small amount of sodium diethyl dithiocarbamate (Cupral) is added to the solution, this leading to the precipitation of cadmium and liberation of the equivalent amount of EDTA which is then titrated with a solution of magnesium chloride in order to determine cadmium. This procedure was used as a basis for developing of a method for polarographic determination of zinc in the presence of cadmium.

EXPERIMENTAL

Polarographic determinations were carried out on a Radiometer PO4 polarograph (Copenhagen, Denmark). All chemicals were of the highest purity (p.a.).

In polarographic determination of zinc in the presence of cadmium in the ammonium supporting electrolyte in the presence of Cupral the cadmium wave was almost or completely undetectable, while the height of zinc wave was proportional to the quantity of zinc (Table 1).

---

* Communicated in the 14th Conference of Serbian Chemists, Belgrade.

TABLE 1

Polarographic Step of Zinc in the Presence of 1 mg Cd
Supporting electrolyte: 20.0 ml (1 N NH_4OH + 1N NH_4Cl + 0.005% gelatin) + 1.0 ml saturated Na_2SO_3 + 2.0 ml 0.5% sodium diethyl dithiocarbamate (Cupral).

Cadmium (*mg*)	Zinc (*mg*)	Height of Zn wave (*mm*)
1.0	0.10	12.0
1.0	0.20	24.0
1.0	0.30	37.0
1.0	0.40	48.0
1.0	0.50	59.0

In determination of small amounts of zinc (0.03—0.15 *mg*) in the presence of large amounts of cadmium (3 *mg*) in the above supporting electrolyte the polarographic wave of zinc was also proportional to its amount (Table 2).

TABLE 2

Polarographic Step of Zinc in the Presence of 3 mg Cd
Supporting electrolyte: 20.0 ml (1 N NH_4OH + 1 N NH_4Cl + 0.005% gelatin) + 2.0 ml saturated Na_2SO_3 + 3.0 ml 0.5% sodium diethyl dithiocarbamate (Cupral)

Cadmium (*mg*)	Zinc (*mg*)	Height of Zn wave (*mm*)
3.0	0.03	10.0
3.0	0.06	20.0
3.0	0.09	31.0
3.0	0.12	40.0
3.0	0.15	51.0

From Table 3 it may be seen that polarography in the supporting electrolyte of ammonium hydroxide, ammonium chloride and Cupral enabled determination of zinc (0.15—0.75 *mg*) in the presence of as much as 15 *mg* of cadmium.

From the results in Table 3 it may be seen that the height of the zinc step was proportional to the amount of zinc in the electrolyte even in the presence of much larger amounts of cadmium. However, in polarographic determination of zinc (0.15—0.75 *mg*) in 20—25 milliliter of ammoniacal supporting electrolyte with the addition of Cupral, in the presence of over 25 *mg* cadmium zinc may be coprecipitated with the precipitate originating from the reaction between Cupral and cadmium. In this case there is no longer a strictly linear relation between the amount of zinc and the height of its polarographic wave.

TABLE 3

Polarographic Step of Zinc in the Presence of 15 mg Cd
Supporting electrolyte: 25.0 ml (1 N NH_4OH + 1 N NH_4Cl + 0.005% gelatin) + 2.0 ml saturated Na_2SO_3 + 0.065 g sodium diethyl dithiocarbamate (Cupral)

Cadmium (*mg*)	Zinc (*mg*)	Height of Zn wave (*mm*)
15.0	0.15	23.0
15.0	0.30	47.0
15.0	0.45	68.0
15.0	0.60	93.0
15.0	0.75	115.0

In all these determinations the zinc waves had regular shape, and the cadmium present in the solution did not interfere at all. The precipitate formed in the supporting electrolyte (NH_4OH + NH_4Cl + Cupral) need not be removed prior to the polarographic determination.

The method was employed for polarographic determination of zinc in electrolytic cadmium. After extracting zinc with ethyl ether(1) and subsequent evaporation of the solvent, zinc was determined by polarography in NH_4OH + NH_4Cl + Cupral supporting electrolyte. Cupral must always be present in excess of the amount needed to bind all the cadmium. The results are reproducible and reliable, and the errors were not more than ±3.0%.

SUMMARY

In a supporting electrolyte consisting of ammonium hydroxide and ammonium chloride the wave of cadmium precedes that of zinc and may interfere in the polarographic determination of zinc.

Due to the instability of ammonium carbonate, polarographic determination of zinc in this electrolyte is not reliable.

Complexing cadmium with sodium diethyl dithiocarbamate (Cupral) allows determination of zinc in the presence of cadmium in a supporting electrolyte consisting of ammonium hydroxide and ammonium chloride.

Department of Physical Chemistry and
Electrochemistry, School of Technology
and Metallurgy, Belgrade University

Received 11 December 1969

REFERENCES

1. Makari͡ant͡s, A. I., T. V. Zaglodina, E. D. Shuvalova, A. N. Minenko, and R. G. Pat͡s "Novyĭ metod opredelenii͡a t͡sinka v aliuminii i silumine", (New Method of Determination of Zinc in Aluminum and Silumin) in: *Analiz rud t͡svetnykh metallov i produktov ikh pererabotky, Analysis of Non*-Ferrous Ores and Metals) — Moskva: Gossudarstvennoe nauchno-tekhnicheskoe izdatel'stvo literatury po chernoĭ i t͡svetnoĭ metallurgii, 1956, p. 138—144.
2. Mladenović, S. N. "Polarografsko određivanje cinka u kadmijumu" (Polarographic Determination of Zinc in Cadmium) — *Glasnik hemijskog društva* (Beograd) 23—24: 529, 1958—1959.
3. Prshibil, R. *Kompleksony v khimicheskom analize* (Complexons in Chemical Analysis) — Moskva: Izdatel'stvo inostrannoĭ literatury, 1960, pp. 497.

GLASNIK HEMIJSKOG DRUŠTVA, Vol. 35, No. 4-5-6, 1970, pp. 363—368

GHDB-113

628.165:546.41 + 546.46

Original Scientific Paper

REMOVAL OF Ca^{2+} AND Mg^{2+} FROM NaCl SOLUTION. I.

INDUCTION PERIOD OF $CaCO_3 + Mg(OH)_2$ SLURRY

by

SVETOZAR M PRIBIĆEVIĆ and BOGDAN M. STANČIĆ

Natural brine contains considerable amounts of dissolved salts, such as $CaCO_3$, $Ca(HCO_3)_2$, $CaSO_4$, $CaCl_2$, $MgSO_4$, $MgCl_2$, etc. In using the brine they cause a lot of trouble due to the incrustation on evaporation, contamination of NaCl, etc.

In order to avoid these effects, modern technology requires purification of brine prior to its processing. This is achieved by eliminating Ca^{2+}, Mg^{2+} and HCO_3^- in the form of $CaCO_3$ and $Mg(OH)_2$.

The $CaCO_3 + Mg(OH)_2$ suspension is very sensitive to the concentration of Ca^{2+} and Mg^{2+} in the brine, and also to the conditions of precipitation.

Qualitative characteristics of this suspension and their dependence on various factors are known, but published data on the matter are scarce due to the low reproducibility of results because of the effect of various, often accidental, factors on the precipitation(1, 2, 3).

In this paper we tried to take a new approach to the problem of designing brine purification plants for industrial purposes (salt mines at Tuzla).

On adding a reagent (usually Na_2CO_3 and NaOH) to brine containing Ca^{2+}, Mg^{2+} and HCO_3^-, the following reactions take place:

$$\begin{array}{lll} HCO_3^- + OH^- & \longrightarrow & H_2O + CO_3^{2-} \\ CO_3^{2-} + Ca^{2+} & \longrightarrow & CaCO_3 \\ Mg^{2+} + 2OH^- & \longrightarrow & Mg(OH)_2 \end{array}$$

In the first phase of this reaction microscopic particles of amorphous $CaCO_3$ coated with a layer of $Mg(OH)_2$ are formed. Their diameter is 10^{-6} *mm* and therefore they exhibit Brownian motion. The mixture is a homogeneous milky fluid. With time the particles grow to 10^{-4} *mm* diameter forming a colloidal suspension. In the next phase amorphous nuclei crystallize out and form the elementary particles of the slurry.

The size of these particles depends on the conditions of precipitation. This is especially the case with $CaCO_3$, whose particle diameter reaches a maximum of 1 μ, but depending on the amount of Mg^{2+} in the slurry may vary by a factor of 300 to 400. Microscopic particles are bound into more or less stable floccules which settle to the bottom.

On mixing the brine and reagent the process in the suspension is manifested by the formation of solid particles which stay dispersed for a while, and then a rapid separation of solid and liquid phases takes place with precipitation of floccules.

EXPERIMENTAL

The method consisted in plotting the precipitation curve of the slurry, thickness of slurry on the ordinate and time on the abscissa. The following four parameters of the curve were used as criteria of the behavior of the slurry:

$\tau_2 - \tau_1$ = induction period

$(H_2 - H_3) / (\tau_3 - \tau_2)$ = floccule precipitation rate.

The tangent to any point between III and IV = rate of compressed precipitation of slurry

H_5 = thickness of precipitate after τ_5.

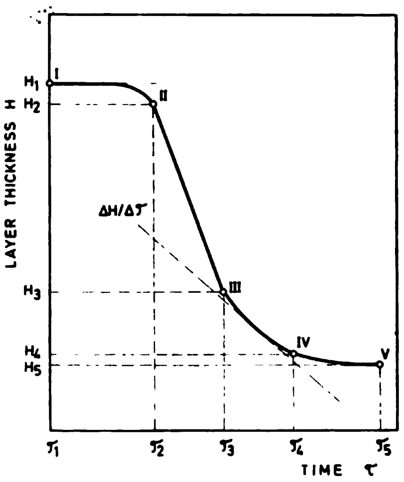

Fig. 1.

Curve for use in investigating suspension behavior.

The induction period of brines having various concentrations of Ca^{2+} and Mg^{2+} was systematically investigated. The brine was prepared from NaCl, $CaCl_2$ and $MgCl_2$ of p.a. quality. The solution contained 300 *mg* of NaCl per liter, while the amount of Ca^{2+} and Mg^{2+} varied: 0.2, 0.4, 0.6, 0.8 or 1.0 *g* per liter of brine, while Ca^{2+} contributing 0%, 20%, 60%, 80% or 100% to the mixture.

Tests were made at 20 and 40°C under identical conditions, either with or without a flocculating agent (NALKO-2-1782). Precipitation was carried out with a mixture of 20% NaOH and 10% Na_2CO_3 in the required quantities. The quantity of Na_2CO_3 ensured a 0.3 *g* per liter excess of Na_2CO_3, while NaOH brought the brine up to pH 11. After adding the reagents the brine was vigorously stirred for 0.5 min., and the time τ_1 recorded from the cessation of stirring.

RESULTS AND DISCUSSION

The change of induction period with the concentration of $Ca^{2+} + Mg^{2+}$ in the brine and the proportion of Ca^{2+} in the Ca^{2+} and Mg^{2+} mixture may be seen from Figs. 1 and 2. It may be seen that:

(a) the induction period decreased with temperature,

(b) the induction period was longest in the suspension containing the most Mg^{2+}, minimum when Ca^{2+} contributed 50—80%, and increased slowly with increasing Ca^{2+}

(c) the induction period increased with increasing total $Ca^{2+} + Mg^{2+}$ in the solution

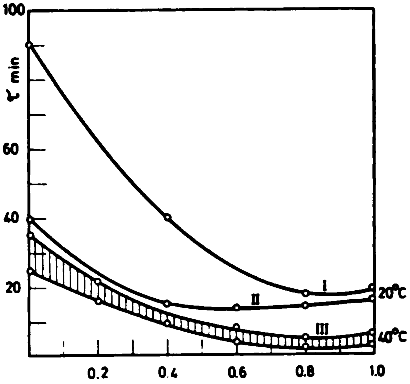

Fig. 2.

Dependence of the induction period of a $CaCO_3 + Mg(OH)_2$ suspension on the amount of $Ca^{2+} + Mg^{2+}$ in the solution and the proportion of Ca^{2+} in the $Ca^{2+} + Mg^{2+}$ mixture.

I t=20°C $Ca^{2+}+Mg^{2+}=1.0$ g/l.
II t=20°C $Ca^{2+}+Mg^{2+}=0.8$ g/l.
III t=40°C field covered by the points for $Ca^{2+}+Mg^{2+}=0.2, 0.4, 0.6, 0.8$ and 1.0 g/l.

The relation between induction period and temperature may be seen from Fig. 3. The figure shows the relative duration of the induction period all other conditions for a given slurry being identical. A rapid decrease with rising temperature may be seen.

The relation between the induction period and Mg^{2+} concentration in the solution may be seen from Fig. 4. The induction period was very short at appr. 0.16 *g* Mg^{2+} per liter of brine, with 60% Ca^{2+} in the $Ca^{2+} + Mg^{2+}$ mixture. At a concentration of 0.12—0.16 *g* Mg^{2+} per liter the induction

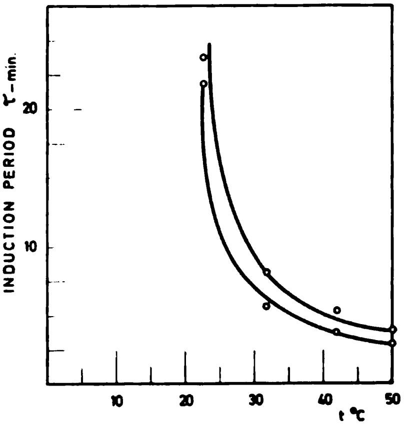

Fig. 3.

Temperature dependence of the induction period.

period was still shorter, but the amount of solids was small and the precipitate did not consolidate properly. At a concentration below 0.12 *g* Mg^{2+} per liter there was no consolidated precipitation and the slurry remained stable for hours. At above 0.16 *g* Mg^{2+} per liter of brine the precipitation was regular, but the induction period prolonged.

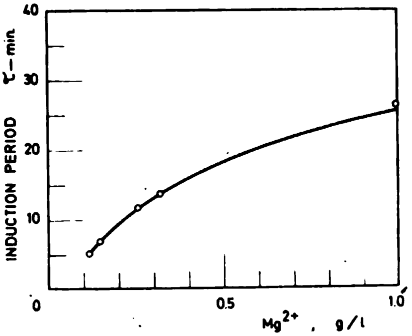

Fig. 4.

Dependence of the induction period of a slurry with 60% Ca^{2+} on the total quantity of Mg^{2+} at 40°C.

The effect of the flocculating agent NALKO-2-1782 on the induction period was also studied. A series of experiments was carried out with 2 *mg* flocculant per liter of brine, added prior to the addition of the reagents. The tests were made at 20 and 40°C, in the same way as those whose results are shown in Fig. 2. For both cases the following conclusions may be drawn:

(a) the induction period was decreased by addition of the flocculating agent.

(b) the general shape of the curves in Fig. 2 is preserved, but the values are lower

(c) the relation between induction period and temperature is similar to that in the case of precipitation without the flocculating agent.

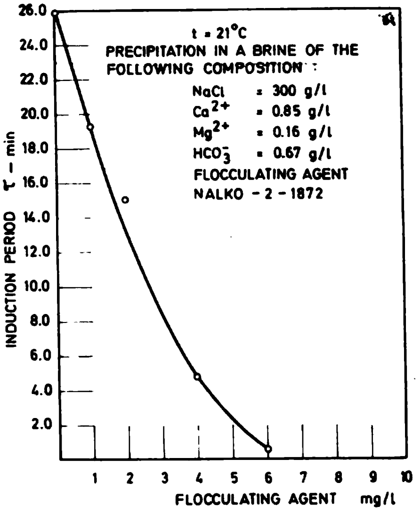

Fig. 5.

Dependence of the induction period on the amount of flocculating agent added.

The change of induction period with concentration of flocculant, other conditions identical, may be seen from Fig. 5.

The flocculating agent (trade name NALKO-2-1782) was highly effective. From Fig. 5 it may be seen that every milligram added to the brine shortened the induction period by 20%. Over 6 *mg* flocculant resulted in instant formation of large clusters of floccules.

SUMMARY

The induction period of $CaCO_3 + Mg(OH)_2$ slurry in the purification of brine by means of Na_2CO_3 and NaOH has been studied.

The induction period was shortest with 50—80% Ca^{2+} in the $Ca^{2+} + Mg^{2+}$ mixture. With increasing Mg^{2+} % in the slurry its duration rose rapidly, while with increasing Ca^{2+} % it rose slowly . It decreased rapidly with increasing temperature of the slurry.

The induction period was found to depend on the amount of Ca^{2+} and Mg^{2+} in the solution, i.e. the total amount of Mg^{2+}, increasing with their increasing concentration.

Department of General Chemistry,
School of Technology, Sarajevo University,
Tuzla, and Laboratories of Salt
Mine and Salt Works, Tuzla

Received 21 November 1969

REFERENCES

1. Furman, A. A., and S. S. Shreĭbman. *Prigotovlenie i ochistka rassola* (Preparation and Purification of Brine) — Moskva: Khimii͡a, 1966.
2. Chernov, V. F. *Proizvodstvo kal'tsinirovannoĭ sody* (Production of Calcinated Soda) — Moskva: Goskhimizdat, 1956.
3. Bori͡achek, A. F., and E. K. Ovechkin. "K teorii i praktike rassolochistki" (Theory and Practice of Brine Purification), in: *I͡ubilarnyi zbornik posvi͡ashchēnnyĭ 15*-leti͡iu *VISP.*

GLASNIK HEMIJSKOG DRUŠTVA, Vol. 35, No. 4-5-6, 1970, pp. 369—376

GHDB-114

528.165:546.41 + 546.46
Original Scientific Paper

REMOVAL OF Ca^{2+} AND Mg^{2+} FROM NaCl SOLUTION. II.

PRECIPITATION RATE OF SLURRY

by

SVETOZAR M. PRIBIĆEVIĆ and BOGDAN M. STANČIĆ

The precipitation rate of $CaCO_3 + Mg(OH)_2$ slurry was measured under various conditions by the method described in Part I (in this issue). The precipitation rate is taken to mean the rate of downward movement of the boundary layer between the slurry and clear solution.

The dependence of the rate of free precipitation of slurry on the Ca^{2+} : : Mg^{2+} ratio in it (other conditions being equal) may be seen from Fig. 1.

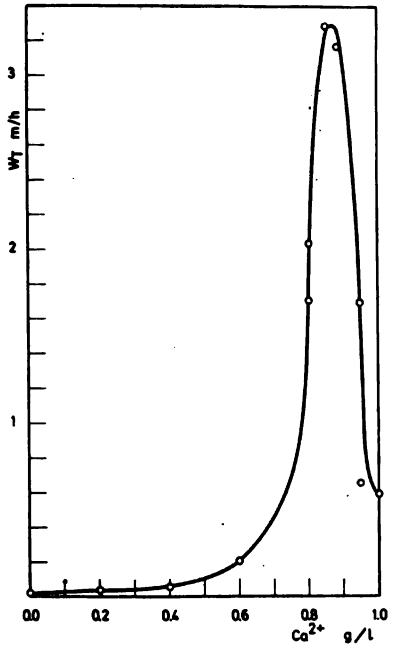

Fig. 1.

Dependence of the precipitation rate of the suspension on the Ca^{2+}/Mg^{2+} ratio.

The results were obtained at 21°C, according to the technique described in the Part I. Total $Ca^{2+} + Mg^{2+}$ in the brine was 1 *g* per liter, but their proportions within the mixture varied.

As seen from Fig. 1, the $Ca^{2+} : Mg^{2+}$ ratio had much influence on the compactness and weight of floccules(1, 2, 3), and therefore also on the precipitation rate. Maximum precipitation rate was achieved at 80—90% Ca^{2+} in the $Ca^{2+} + Mg^{2+}$ mixture. An increase of Mg^{2+} caused the formation of loose fluffy floccules which precipitated much slower. At Mg^{2+} below 10—15% the precipitation rate decreased sharply; this may be explained by a deficiency of "binding" material, i.e. $Mg(OH)_2$, whose role consists in uniting $CaCO_3$ crystals into floccules. At 100% Ca^{2+} the floccule precipitation rate was much lower, corresponding to the rate of pure $CaCO_3$. The precipitation rate of pure $Mg(OH)_2$ slurry was very low (a few *mm* per hour), while that of pure $CaCO_3$ was relatively high (about 8—10 times higher than that of $Mg(OH)_2$). At the optimum $Ca^{2+} : Mg^{2+}$ ratio approximately five times higher rates were achieved than that of $CaCO_3$, 200—300 times higher than the precipitation rate of pure $Mg(OH)_2$.

The dependence of precipitation rate on the $Ca^{2+} : Mg^{2+}$ ratio was maintained throughout a wide range of $Ca^{2+} + Mg^{2+}$ concentration in the brine. The rate of free precipitation of the slurry at temperatures of 20 and 40°C, at various $Ca^{2+} + Mg^{2+}$ concentrations and various proportions of Ca^{2+} in the mixture may be seen from Fig. 2. The conditions of precipitation were the same as described in Part I. It may be seen that the precipitation rate of floccules depends on the temperature and the total $Ca^{2+} + Mg^{2+}$ in the solution. It is clear that precipitation is faster in a solution containing less $Ca^{2+} + Mg^{2+}$. The effect of $Ca^{2+} + Mg^{2+}$ content of the brine at a $Ca^{2+} : Mg^{2+}$ ratio of 0.6 : 0.4 and a temperature of 20°C may be seen from Fig. 3. At concentrations lower than 0.35 *g* per liter a stable suspension was obtained, because the quantity of material was obviously inadequate to form large floccules. Flocculation started at a concentration of 0.35—0.4 *g* per liter, but the precipite was unconsolidated. Well-developed floccules were obtained at a $Ca^{2+} + Mg^{2+}$ concentration of 0.4 g per liter, with fast and consolidated precipitation.

With increase of the $Ca^{2+} + Mg^{2+}$ content of the solution the precipitation rate decreased, and at a certain level the transition compressed precipitation occurred. Figure 2 also shows a considerable decrease in the precipitation rate with rising temperature. The rate change in the interval 20—50°C may be seen from Fig. 4. The precipitation rate increased rapidly with temperature, up to 40—50°C. At higher temperature thermal migration within the solution is pronounced: the solution slides down the walls of the vat and ascends in the middle. The current breaks up floccules and carries them up into the clear solution. The tests showed that the upper temperature limit depends on floccule mobility. Those with a higher content of Mg^{2+} broke up at lower temperatures, while at the optimum $Ca^{2+} : Mg^{2+}$ ratio they give a consolidated precipitate at much higher temperature.

The addition of a flocculating agent produced very good results. The effect of NALKO-2-1782 flocculant on precipitation rate may be seen from Fig. 5. The brine contained 300 *g* NaCl, 0.8 *g* Ca^{2+} and 0.2 *g* Mg^{2+} per liter. Purification was carried out at 20°C. From Fig. 5 (curve 1) it may be seen that the flocculating agent accelerated flocculation, and therefore the preci-

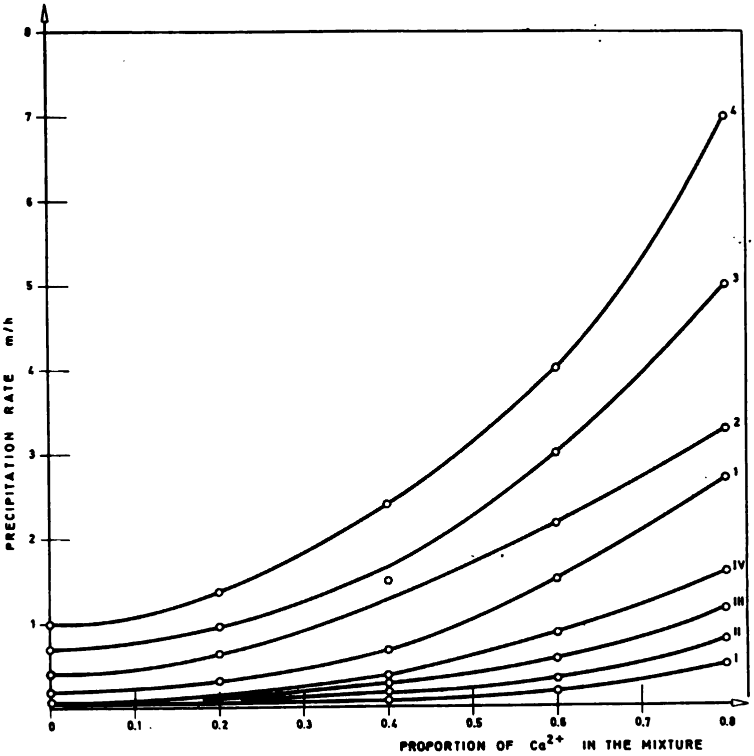

Fig. 2.

Dependence of the precipitation rate of the suspension on the Ca^{2+}/Mg^{2+} ratio and the temperature.

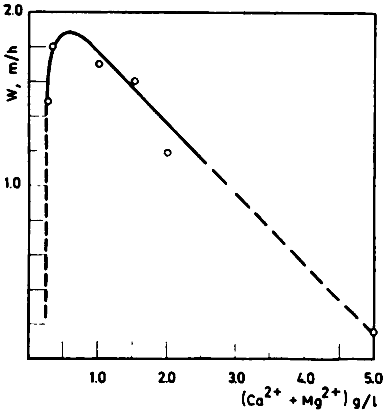

Fig. 3.

Dependence of the precipitation rate on suspension concentration.

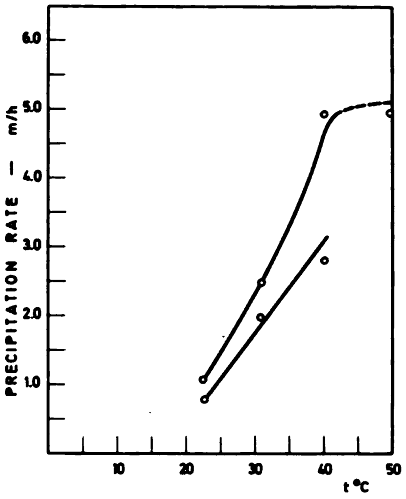

Fig. 4.

Temperature dependence of the precipitation rate of the suspension.

pitation rate rapidly rose. However, with increasing quantity of flocculant the floccules became too large and the rate decreased. This was especially the case if air was brought in with the brine, because air bubbles stuck to floccules and flotation occurred. However, if the solution was stirred during induction (curve 2) the large floccules were broken up and the flocculating agent had only a compacting influence.

The flocculating agent did not change the influence of Ca^{2+} : Mg^{2+} ratio on the precipitation rate (Fig. 2), only the rate was higher.

Compressed precipitation of floccules shows considerable differences between floccule precipitation and the precipitation of material which reacts

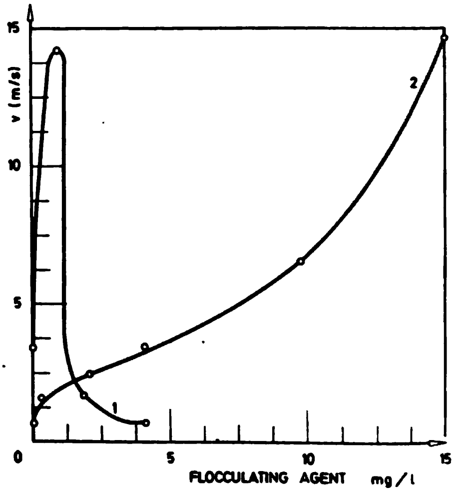

Fig. 5.

(1) Suspension not stirred during the induction period;
(2) Suspension stirred durring the induction period.

less with the liquid phase. The rate of compressed precipitation (W) relative to the rate of free precipitation (W_0) may be seen from Fig. 6. Curve 1 represents the calculated W : W_0 ratio, while curve 2 represents the experimental results.

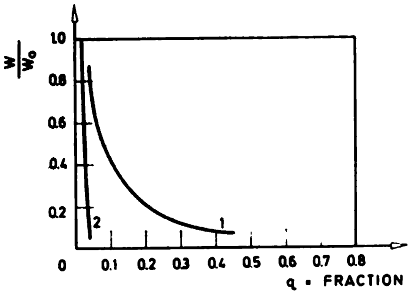

Fig. 6.

Ratio of the rates of compressed precipitation (W) and free precipitation (W_0) at different concentrations of solids in the suspension (q = fraction)

1. Inert spheres
2. $CaCO_3 + Mg(OH)_2$ suspension in brine

The change of precipitation rate with the concentration of solids in the slurry may be seen from Fig. 7, for the case of a slurry having a 0.8 : 0.2 ratio between Ca^{2+} and Mg^{2+}. Curve 1 is for precipitation at a temperature of 20°C, curve 2 for 40°C, and curve 3 also for 40°C but with the addition of 2 *mg* of NALKO-2-1782 flocculating agent.

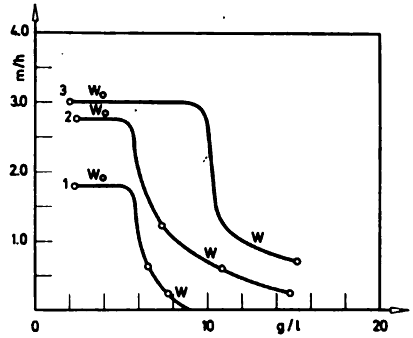

Fig. 7.

Variation of precipitation rate with suspension concentration

All these results suggest an intensive influence of processes at the solid-liquid boundary on the behavior of the slurry, which is the only explanation for the considerable differences between the precipitation rate of $CaCO_3 +$ $+ Mg(OH)_2$ and the slurry of other materials. From Figs. 1 and 2 the reason for this effect may be seen to be the presence of $Mg(OH)_2$, because it has a large specific surface, ability to adsorb ions, etc. The extent of interaction between the liquid phase and the precipitate at various Mg^{2+} concentrations was examined by filtering the brine through a layer of precipitate under identical conditions in two experiments. In one the brine with a Ca^{2+} : Mg^{2+} ratio 0.8 : 0.2 was passed through a determined quantity of $CaCO_3$ + + $Mg(OH)_2$ precipitate. In the second the quantity of sediment was the same but the Ca^{2+} : Mg^{2+} ratio was reversed (0.2: 0.8). The volume of brine that passed through was 8 : 3 in favor of the slurry with a higher proportion of Ca^{2+}.

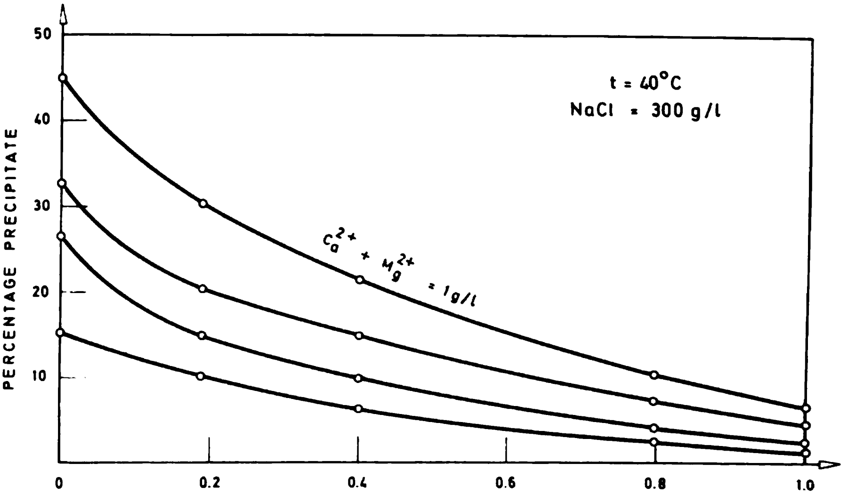

Fig. 8.

Volume of the $CaCO_3 + Mg(OH)_2$ layer precipitated after 90 min expressed as the percentage of the volume of the initial solution.

The same effect was observed in the volume of precipitate after precipitation. After compressed precipitation packing of the precipitate began, accompanied by squeezing of brine out of the lower layers. The volume of precipitate 90 minutes after the beginning of precipitation is given in Fig. 8. Precipitation was carried out at 40°C. It is clearly seen that the volume rose rapidly with increasing Mg^{2+} %. It also increased with decreasing temperature, but decreased in the presence of flocculating agent.

SUMMARY

Factors affecting the rate of free and compressed precipitation of $CaCO_3$ + $Mg(OH)_2$ slurry in brine were studied. The proportions cf Ca^{2+} and Mg^{2+} in the slurry, temperature and flocculating agent were found to have an essential influence.

The factors were studied in the process of purification of brine with a mixture of NaOH and Na_2CO_3.

The optimum Ca^{2+} : Mg^{2+} ratio was found to be 0.8 : 0.2 (by weight). The fastest precipitation was obtained if the brine contained about 1.0 *g/lit* of $Ca^{2+} + Mg^{2+}$ prior to purification. The precipitation rate increased with rising temperature, and precipitation was accelerated by the addition of a flocculating agent.

Department of General Chemistry,
School of Technology, Sarajevo University,
Tuzla, and Laboratories of the Salt Mine
and Saltworks, Tuzla

Received 21 November 1969

REFERENCES

1. Furman, A. A., and S. S. Shreĭbman. *Prigotovlenie i ochistka rassola* (Preparation and Purification of Brine) — Moskva: Khimii͡a, 1966.
2. Chernov, V. F. *Proizvodstvo kalʼt͡sinirovannoĭ sody* (Production of Calcinated Soda) — Moskva: Goskhimizdat, 1956.
3. Bori͡achek, A. F., and E. K. Ovechkin. "K teorii i praktike rassolochistki" (Theory and Practice of Brine Purification), in: *I͡ubilarnyĭ zbornik posvi͡ashennyĭ 15-letii͡u VISP.*

GLASNIK HEMIJSKOG DRUŠTVA, Vol. 35, No. 4-5-6, 1970, pp. 377—385

GHDB-115 546.26:669.822
Original Scientific Paper

CARBON CONTENT OF VACUUM MELTED METALIC URANIUM

by

ĐORĐE B. CVETANOVIĆ, IVKO D. STOJŠIĆ,
and NENAD D. OBRADOVIĆ

Crude metalic uranium obtained by metallothermic reduction with calcium or magnesium contains metalic and non-metalic inclusions as a result of contamination during production. For purification it is vacuum melted in a furnace heated either by a resistive element or by an induction coil.

Although magnesium, zirconium, beryllium and thorium oxides, considering the physics and chemistry of melted uranium, may seem the most suitable material for making the crucibles and moulds, they are not used due to their low thermal stability; graphite is usually employed for this purpose. As graphite reacts with uranium forming carbides, the behavior of carbon and the change of its concentration in uranium vacuum -melted in a graphite crucible was studied.

Although graphite does not make uranium unusable as a nuclear fuel because it has no effect on the effective neutron cross-section, it is still considered a harmful impurity due to the fact that carbides impair the structural, physical, mechanical and chemical properties of uranium.

EXPERIMENTAL

The experiments with vacuum melting uranium in batches of 150 *g* were carried out in a 15 kW 9400 cps laboratory induction furnace at a vacuum of 10^{-4} torr. The vacuum was maintained by an oil diffusion pump of 600 *lit/sec* capacity backed by a 28 m^3/h rotary pump. It was measured with thermoelectric and ionization vacuum meters.

Uranium was melted in a graphite crucible placed inside the receptacle of the furnace together with thermal insulation and a susceptor. At the bottom the crucible had a pouring hole normally closed by a graphite spike 10 *mm* in diameter with a Pt-Pt Rh 5% ceramic insulated thermocouple inside it, by means of which the temperature in the crucible center was registered. A graphite mould was placed below the crucible inside the furnace receptacle. A sketch of the melting and pouring system is given in Fig. 1.

With a view to preventing the molten metal getting contaminated by carbon from the crucible, the effect of coating it with aluminum oxide, magnesium oxide or magnesium zirconate, acting at the same time as thermal insulation, was also investigated. Protective coatings 0.1—0.15 *mm* thick were

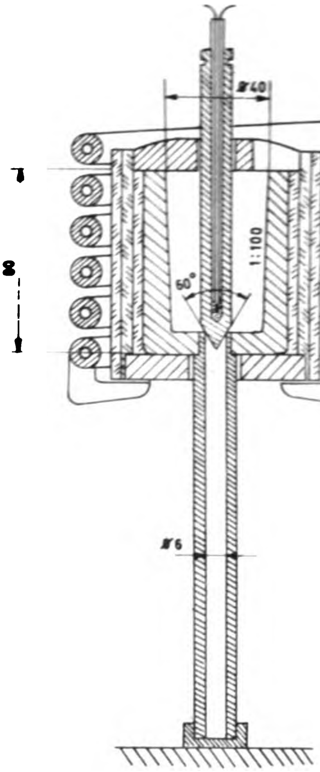

Fig. 1.

Melting and pouring system

applied to the inner surface of the crucible (previously heated in vacuum for one hour at 1200°C) in two ways:

(a) Wet method: brushing on a suspension of magnesium oxide in 20% solution of magnesium sulphate, or magnesium zirconate in 3% solution of polyvinil alcohol (PVA) to the required thickness and subsequent drying;

(b) Dry method: spraying on powdered aluminum oxide or magnesium zirconate with a "Metco Thermospray" spray-gun pistol. The gun fluidizes the powders as they pass through an acetylene burner, and they stick uniformly to the surface of the crucible.

The time for which the uranium remains molten in the mould is very, short, especially because of the small diameter of the casting, so all carbon in it may be considered to originate from the crucible. Therefore the inner surface of accurately machined graphite mould was not coated with a protective layer.

The influence of various factors on the carbon content of the cast uranium was investigated in two series of experiments. In the first series the influence of the time (10—30 min.) spent by the molten uranium at a vacuum of 10^{-4} torr and a temperature of 1350°C in a graphite crucible with various kinds of protective lining was studied. In the second series the influence of temperature was studied, at a constant vacuum of 10^{-4} torr and a constant retention time (10 min) in crucibles lined in the same way as in the first series.

For each test a new crucible and mould were used in order to assure identical experimental conditions.

After melting the metal, it was poured into the mould by pulling up the spike closing the hole in the crucible bottom. After cooling, the furnace was opened and the 6 *mm* diameter uranium rod extracted. Both ends ot the rod were cut off on a grinding wheel. In order to eliminate any errors due to adhering and mechanically removed graphite, the outer layer of metal at the lower end of rod was removed in a length of 20 *mm* and a sample taken for chemical analysis and metallographic examination.

Carbon was determined by conductometry. Metallographic samples were prepared by electrolytic polishing at 18 V and a current density of 63 mA/*cm*^{2} in a solution of 5 parts ethylene glycol, 5 parts orthophosphoric acid and 8 parts alcchol (all by volume).

RESULTS AND THEIR INTERPRETATION

In the first experimental series crude uranium obtained by metallothermic reduction with magnesium was used, while for the second the uranium was first refined by remelting.

Carbon, nitrogen, oxygen and hydrogen and some nuclear impurities in the starting material are given in Table 1.

TABLE 1

Impurities in the Uranium

Element	Carbon in uranium (*ppm*)	
	First experimental series	Second experimental series
C	145	111
N_2	130	—
O_2	15	12
H_2	1.5	3
Fe	230	1600
Si	25	130
Cu	15	39
Al	10	15

The chemical analysis for carbon of cast samples from the first experimental series is given in Table 2. The molten uranium was kept at 1350°C

TABLE 2

Carbon in Uranium for Various Retention Times

Protective coating	Carbon in uranium (*ppm*)			
	Before melting	After melting for		
		10 *min*	20 *min*	30 *min*
$MgO + 20\% MgSO_4$	145	688	1112	1225
$MgO \cdot ZrO_2 + 3\%$ PVA	145	313	390	907
Al_2O_3 (Metco)	145	322	374	382
$MgO \cdot ZrO_2$ (Metco)	145	217	258	362

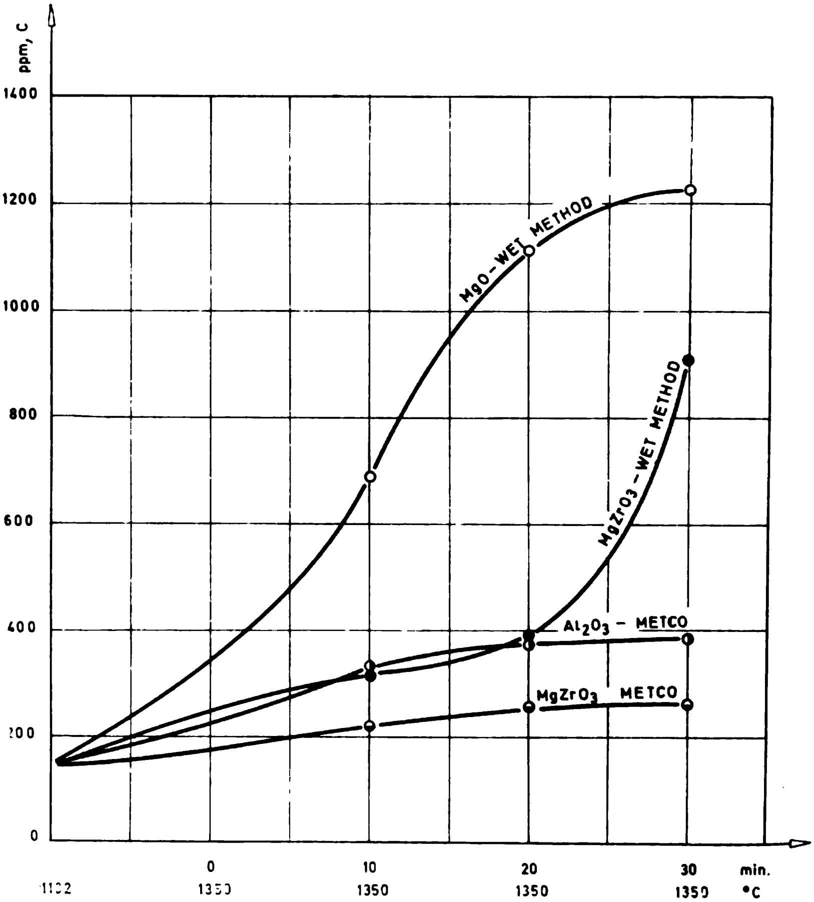

Fig. 2.

Carbon content against retention time at 1350°C for 10, 20 and 30 minutes in the crucible. The results are also presented as a graph of carbon content against retention time in Fig. 2.

In the second series the molten uranium was kept in the crucible for 10 minutes at temperatures of 1250, 1300, 1350 and 1400°C. The results are given in Table 3, and a graph of carbon content against temperature is plotted in Fig. 3.

TABLE 3

Carbon in Uranium for Various Melting Temperatures

Protective coating	Carbon in uranium *ppm*				
	Before melting	After melting at			
		1250°C	1300°C	1350°C	1400°C
$MgO + 20\% MgSO_4$	111	480	502	526	530
$MgO \cdot ZrO_2 + 3\%$ PVA	111	243	310	312	440
Al_2O_3 (Metco)	111	208	215	268	464
$MgO \cdot ZrO_2$ (Metco)	111	180	168	225	332

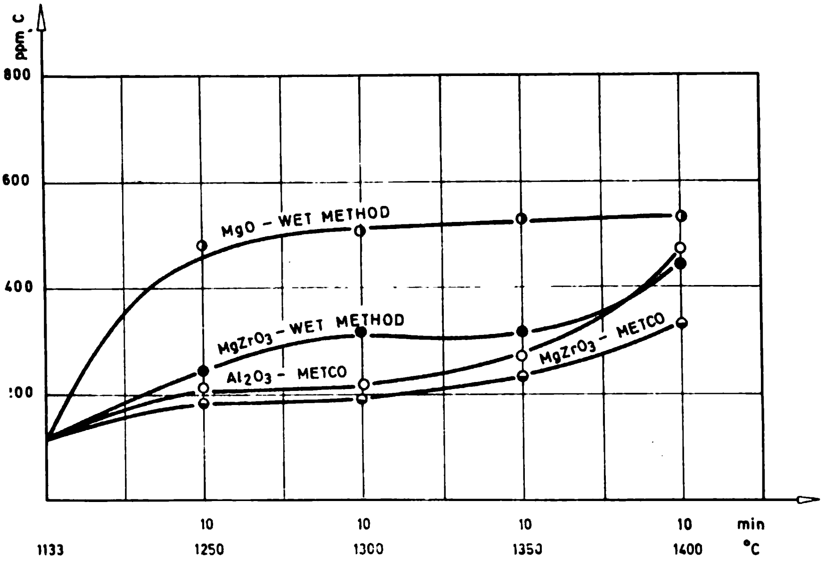

Fig. 3.

Carbon content against temperature of molten uranium

The results show that the vacuum melting resulted in an increase of carbon content. The time the molten metal was in contact with the crucible had a greater influence than the temperature.

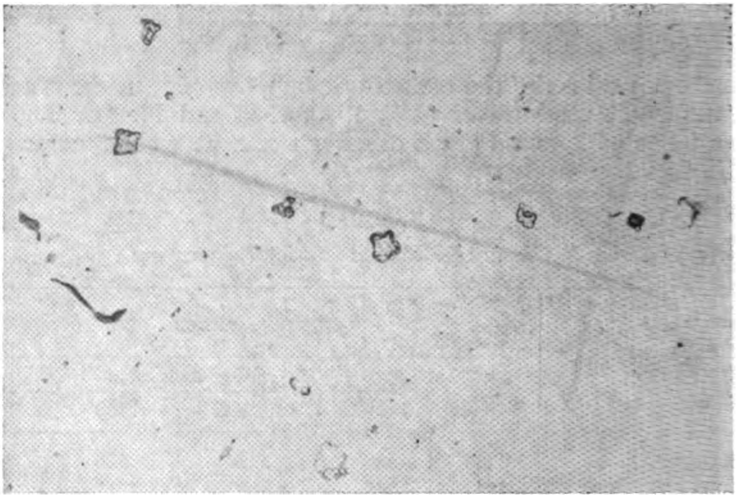

Fig. 4.

Metallography showed that the content of regularly distributed non--metalic inclusions was higher in the remelted uranium, and it was higher the higher the carbon content. The size of non-metalic particles varied with the rate of cooling the casting. A photomicrograph of a metallographic sample of the starting uranium in the first experimental series is shown in Fig. 4. Figure 5 is a photomicrograph of a sample obtained with the crucible coated

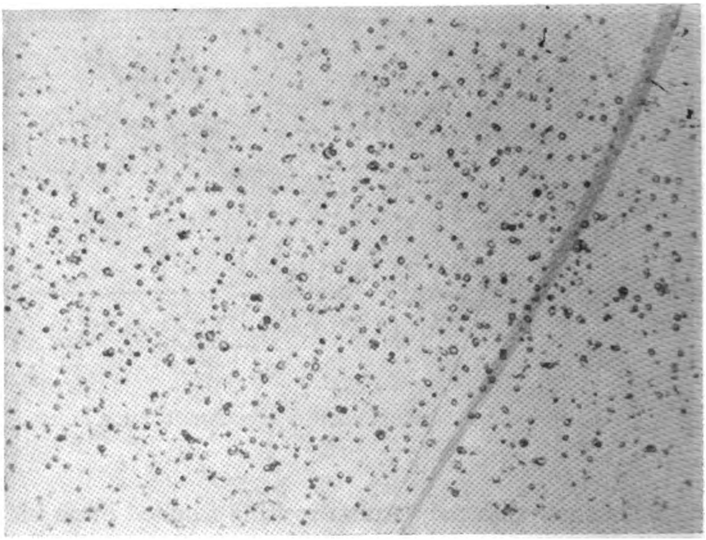

Fig. 5.

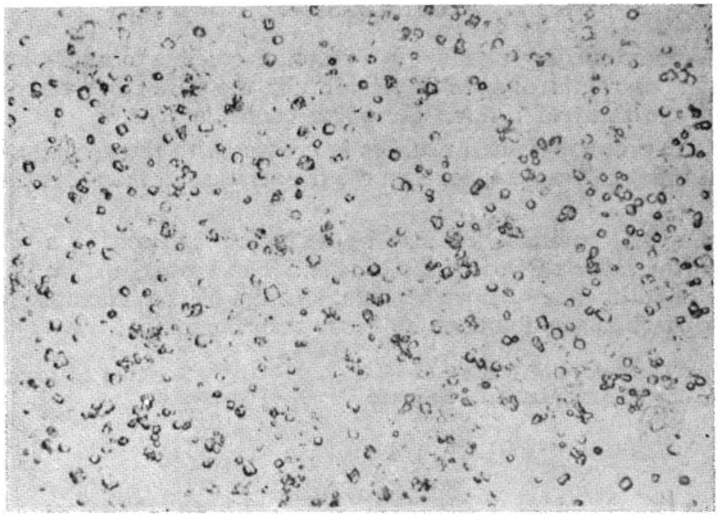

Fig. 6.

with a suspension of magnesium oxide in 20% $MgSO_4$ solution, at a retention time of 20 min at 1350°C. That in Fig. 6 was obtained under identical conditions except that the retention time was 30 min.

Precipitation of carbon in the form of carbide, i.e. oxycarbonitride, due to exceeding the limit of its solubility in uranium, may in this case be explained by a brief reference of the U-C phase diagram. Carbon forms three compounds with uranium, i.e. UC, U_2C_3 and UC_3. In metalic uranium UC, having a melting point 2350—2400°C(1), occurs most frequently. The solubility of carbon in gamma phase uranium decreases from 106 ppm at the eutectic temperature to 45 ppm at the eutectoid temperature of the gamma transformation. On the other hand, its solubility in beta uranium is less than 10 ppm, and in alpha uranium less than 3 ppm. Above the liquidus the solubility is complete, and in molten uranium carbides (at usual casting tempeperatures) do not occur at below 0.15% carbon(2).

From these results it may be seen that the carbon content of the uranium depends on the character of the protective coating on the crucible, but also its mode of application, because carbon can diffuse through a porous or damaged layer. The best coating was magnesium zirconate, and the poorest magnesium oxide. As the coating is destroyed not only by the chemical action of the molten metal but also by mechanical erosion due to convection currents and vortices, better results were obtained by using the Metco Thermospray than by brushing on an oxide emulsion.

The increase of carbon content with the time the molten metal is kept at a certain temperature, with the same protective coating, was due to the longer time for diffusion and chemical and mechanical damage. As increasing temperature led to an intensification of these effects, the carbon content also rose with rising temperature.

CONCLUSION

1. Vacuum melting uranium is a graphite crucible increases its carbon content, and above the limit of its solubility in the solid metal carbon precipitates in the form of carbide i.e. oxycarbonitride.

2. The time the molten metal is in contact with the graphite crucible (retention time) had more effect than the temperature in the range of 1250—1400 °C.

3. Carbon contamination may be decreased by applying a protective coating to the inner surface of the crucible. The best protective properties were exhibited by magnesium zirconate, and the Metco Thermospray process of application was found to be better than brushing.

Institute for Technology of Nuclear
and Other Mineral Raw Materials, Belgrade

Received 13 January, 1970

REFERENCES

1. Sterling, I͡a. M. *Metallurgii͡a urana* (Metallurgy of Uranium) — Moskva: Gostatomizdat, 1962.
2. Blumenthal, B. "Constitution of Low Carbon U—C Alloys" — *Journal of Nuclear Materials* (Amsterdam), 2(3): 197—208, 1960.

Izdavač
IZDAVAČKO PREDUZEĆE "NOLIT", BEOGRAD, TERAZIJE 27/II

◆

Štampa
GRAFIČKO PREDUZEĆE "PROSVETA"
BEOGRAD — ĐURE ĐAKOVIĆA 21.

SRPSKO HEMIJSKO DRUŠTVO (BEOGRAD)

BULLETIN OF THE CHEMICAL SOCIETY

Belgrade

(Glasnik Hemijskog društva — Beograd)

Vol. 35, No. 7-8, 1970

Published by
SRPSKO HEMIJSKO DRUŠTVO (BEOGRAD)
1970

Translated and published for U.S. Department of Commerce and
the National Science Foundation, Washington, D.C., by
the NOLIT Publishing House, Terazije 27/II, Belgrade, Yugoslavia
1972

Translated by
PAVEL ČMELIK

Edited by
PAUL PIGNON

Printed by Prosveta, Beograd

CONTENTS

GLASNIK HEMIJSKOG DRUŠTVA, Vol. 35, No. 7—8, 1970, pp. 387—396

GHDB-116

53.082.7:531.756:541.123.2:54—14

Original Scientific Paper

DETERMINATION OF THE DENSITY OF VOLATILE LIQUID MIXTURES BY MAGNETIC FLOAT METHOD

by

ALEKSANDAR TASIĆ, PAVLE PAVLOVIĆ and BOJAN ĐORĐEVIĆ

INTRODUCTION

From the extensive literature on measurement of the density of liquids it may by concluded that there are three essentially different approaches to the problem, viz. pyknometric(1), displacement(2), and mass oscillation methods(3). The aim of the present study was to work out a method for the quick determination of density of volatile liquid mixtures. In addition, the method had to give satisfactory accuracy over a wide range of densities.

An analysis of available techniques revealed their advantages and shortcomings, and served as a guide in the choice of method. The displacement method appeared to be most suited to our purpose.

The principle of the magnetic float method is the equilibration of forces acting on a float immersed in the liquid: the buoyancy force is balanced by gravity and an additional, in this case magnetic, force. The principle was first imployed by Lamb and Lee(2). Characteristic features of their apparatus was the large sample needed (50—300 *ml*) and the high precision attained ($\pm 1 \cdot 10^{-6}$ *p*/*cm*^{3}). Other authors(4) modified the method. More recent papers report improvements in reducing sample size and increasing precision(5—8). A simple and practical apparatus for this method was designed by Richards(9), of which a modified version was used in the present study.

THEORETICAL

From the laws of electro-magnetism, Richards(9) derived the fundamental equation for the electromagnetic force (F_m) acting on a float in the field of a solenoid passing a current (I):

$$F_m = CI^2. \tag{1}$$

The constant (C) is given by

$$C = V k^2 \frac{N^2}{2 L^2} f(s), \tag{2}$$

where V = volume of iron (m^3)

k = magnetic susceptibility of the iron (H/m)

μ = magnetic permeability of the system (H/m) μ depends on the liquid, but for most organic liquids, which are non-ferromagnetic, it differs very little.

N = number of turns

L = length of the solenoid (m)

$f(s)$ = a function of the position of the float relative to the solenoid, which is a constant if the float does not change its position.

The magnitude of the magnetic force may be changed by changing the current (square law) and also by altering the parameters determining C, above all the float position and the number of turns on the solenoid.

The forces acting on the float are in equilibrium if

$$F_p = F_m + G \tag{3}$$

where: $F_p = \gamma V_p$, the buoyancy force (upthrust) (p),

γ = density of the liquid (p/cm^3)

V_p = volume of the float (cm^3)

F_m = magnetic force (p)

G = weight of the float.

As the density is determined under isothermal conditions the volume of the float and density of the liquid are constants, and equation (3) becomes

$$\gamma = \frac{F_m}{V_p} + \gamma_p, \tag{4}$$

where: $\gamma_p = G/Vp$, i.e. bulk density of the float.

Substituting for F_m from (2), equation (4) becomes

$$\gamma = \frac{C\,I^2}{V_p} + \gamma_p. \tag{5}$$

Under certain conditions $C/Vp = a$, a constant, expressed in units of g/(cm^3 . A^2). This constant is determined experimentally. Equation (5) may be written in the final form:

$$\gamma = AI^2 + \gamma_p. \tag{5a}$$

EXPERIMENTAL

Apparatus

The apparatus (Fig. 1), made of Pyrex glass, consists of a ten cm^3 container for the liquid (1), a magnetic float with a soft iron core (2), a solenoid (3), and a piston for adjusting the position of the float relative to the solenoid (5) and whose upper end (5) keeps the apparatus gas tight. The solenoid (3) has 1000 turns of 0.55 *mm* diameter copper wire. The container has an insulating lining, and the temperature within it is kept constant at 25 ± 0.005°C.

By opening the stopcock(7) the liquid stored in reservoir(6) is introduced into the apparatus via the capillary(8). The liquid must flood the whole piston. The float ascends to the position determined by the piston. The forces acting on the float are balanced out by gradually increasing the current flowing through the solenoid until the float comes away from the piston. At this moment the current flowing through the solenoid is recorded, and by using equation (5a) the density of the sample may be calculated.

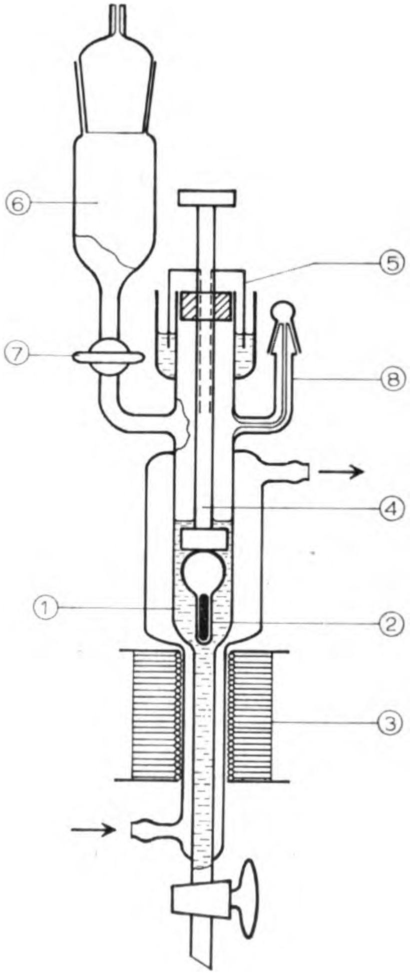

Fig. 1.
Apparatus for density determination

Current regulating and reading circuit

The circuit diagram of the current regulator and meter is shown in Fig. 2. The current range chosen (100—500 *mA*) enables determination

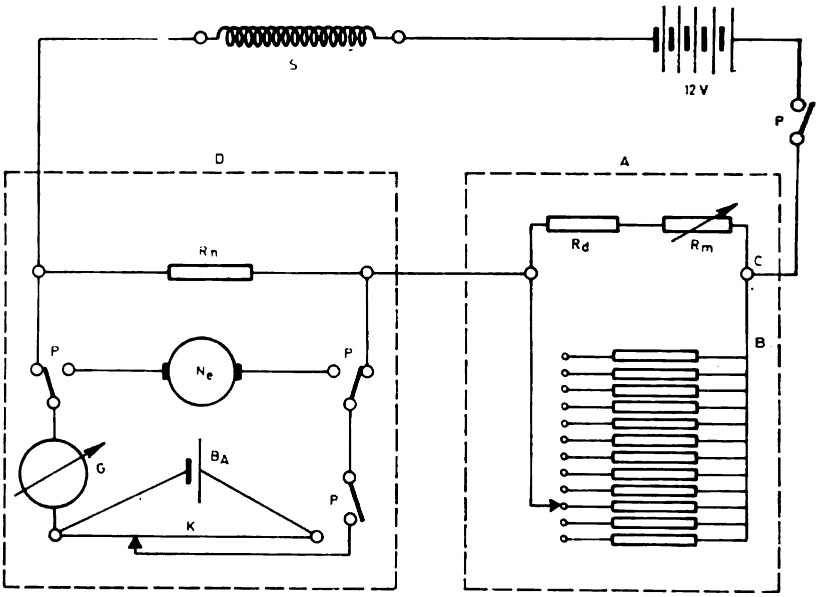

Fig. 2.

Current regulating and reading circuit

of densities from 0.7 to 1.6 *p/cm*^{3} (by using one of two floats). The regulator (A) consists of branch (B) with 13 fixed resistors which can be switched in parallel with the branch (C) consisting of a fixed resistor R_d in series with potentiometer R_n. The resistors in branch (B) are specified in the second column of Table 1. The range within which the current may be varied with a given resistor in branch B is specified in the fourth and fifth column. This circuit allows current adjustment in steps of 0.5 mA over the entire range of 100—500 mA. The fixed resistors in branch B may be replaced by two decade boxes in parallel. So as not to exceed the maximum current ratings of the decade resistors it is recommendable to load them equally (column 3 in Table 1).

The current in the solenoid circuit is measured indirectly by backing off the potential drop across a standard resistor. The measuring circuit (*D*) in Fig. 2 consists of the compensator (K), galvanometer (G), standard 1000 Ω resistor (R_n), Weston standard cell (Ne), and 4.5 battery (B).

Calibration

As shown in the theoretical section (equation 5a), the equilibrium current is proportional to the square of the density and depends on the constant *a* and the bulk density of the float.

The bulk density of the float was determined with specially constructed bicapillary pyknometers.

TABLE 1

Branch B of Current Regulating Circuit

Range	R (Ω)	Two resistors in parallel (Ω)	I_{min}	I_{max}
1	0	0	58.4	117
2	270	540	100	150
3	133	266	145	198
4	90	180	180	230
5	66	132	220	266
6	54.7	110	250	300
7	44.4	88+89	290	335
8	37.3	74+75	330	375
9	32.5	65	365	416
10	29.6	59	390	432
11	26.8	53+54	420	458
12	24.2	48+49	450	490
13	12.2	44+45	480	520

The constant a for each float was determined at a defined position of the piston using pure liquids of known density. The position of the float relative to the solenoid was determined with a cathethometer. The densities of the liquids were first measured with bicapillary pyknometers⁽¹⁾ to $\pm 1 \cdot 10^{-4}$ p/cm³. Characteristics of these pyknometers are given in Table 2.

The apparatus was calibrated with analytical grade pure acetone (Reanal), benzene (Veb Berlin Chemie), and carbon tetrachloride (Veb Laborchemie Apoloa).

RESULTS

With the described apparatus the density of acetone-benzene, benzene--carbon tetrachloride, and acetone-carbon tetrachloride mixtures was determined. The results obtained for the last mixture (Table 3) illustrate the applicability of the apparatus for determination of highly volatile mixtures with a wide range of densities. Experimental data were interpreted graphically using the logarithmic form of (5a):

$$\log(\gamma - \gamma_p) = 2 \log I + \log a \qquad (5b)$$

Plotting $\log(\gamma - \gamma_p)$ against $\log I$ (Fig. 3) should give a straight line. The scattering about the straight line provides a measure of the correctness of calibration. The form of the basic equation (5a) shows that the total error of determination depends on the errors of calibration, current measurement, and determination of bulk density of the float.

TABLE 2

Some Characteristics of the Bicapillary Pyknometers

Pyknometer No. 1			Pyknometer No. 2		
Weight (p)		Volume of Hg in both arms (ml)	Weight (p)		Volume of Hg in both arms (ml)
Filled with Hg	Empty	0.005	Filled with Hg	Empty	0.012
317.2718	28.3728	0.006	313.5942	29.0094	0.012
$G_{Hg} = 288.8990$		Total 0.011	$G_{Hg} = 284.5848$		Total 0.024
	$V_{0_1} = 21.3678$ ml			$V_{0_2} = 21.0333$ ml	

TABLE 3

Experimental Results for Acetone-Carbon Tetrachloride Mixture

Test	Acetone		Carbon tetrachloride		γ	$\gamma-\gamma_p$	[log ($\gamma-\gamma_p$)—2]	I^2	I	[log *I*—3]
	vol.%	*ml*	vol. %	*ml*	(p/cm^3)	(p/cm^3)		(A^2)	(A)	
1	100	50.0	0	0	0.7849	0.0482	0.68305	0.04731	0.2175	2.3375
2	90	43.6	10	6.4	0.8870	0.1503	1.17696	0.15547	0.3943	2.5958
3	80	36.6	20	12.6	0.9843	0.2476	1.39375	0.25752	0.5075	2.7054
4	70	31.9	30	18.1	1.0764	0.0410	0.61278	0.01272	0.1128	2.0523
5	60	26.6	40	23.4	1.1609	0.1255	1.09830	0.04170	0.2042	2.3101
6	50	21.5	50	28.5	1.2421	0.2067	1.31534	0.06788	0.2605	2.4258
7	40	16.1	60	31.9	1.3441	0.3087	1.48954	0.10120	0.3177	2.5020
8	30	12.2	70	37.8	1.4026	0.3672	1.56490	0.11806	0.3436	2.5360
9	20	7.9	80	42.1	1.4543	0.4189	1.62211	0.14060	0.3750	2.5740
10	10	3.9	90	46.1	1.5222	0.4868	1.68735	0.16009	0.4026	2.6027
11	0	0	100	50.0	1.5845	0.5491	1.73965	0.18318	0.4280	2.6314

Test 1—3, float No. 5, position 2.60 cm, $\gamma_p=0.736$ p/cm³, $a=0.976$

Test 4—11, float No. 2, position 2.20 cm, $\gamma_p=1.035$ p/cm³, $a=2.960$

In calibration with a bicapillary pyknometer the density of a liquid can be determined to $\pm 1 \cdot 10^{-4}$ p/cm^3.

The current was measured to an accuracy of $\pm 1 \cdot 10^{-5}$ A, the results being reproducible to within $\pm 2 \cdot 10^{-4}$ A.

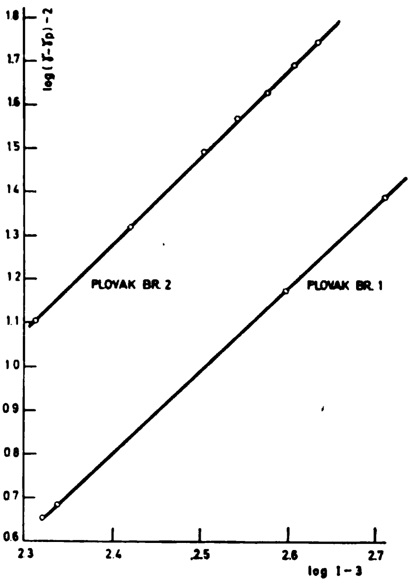

Fig. 3.
Relative density against current

The bulk density of the float was determined with the accuracy of $\pm 0.5 \cdot 10^{-3}$ p/cm^3.

Therefore the resultant total error in density determination with this apparatus is $\pm 1.1 \cdot 10^{-3}$ p/cm^3.

DISCUSSION

The method proved to be simple and suitable for series measurements. Its simplicity is enhanced by the fact that the weight and volume need not be measured. Replacement of the sample is easy and quick. Thermal insulation is very good thanks to the small volume of the sample (10 cm^3). With suitable floats densities can be measured over a wide range, this being not the case in earlier studies.

However, certain drawbacks of the method must also be mentioned. If a wide range of densities is to be measured, more than one float has to be used. The apparatus has to be recalibrated on changing the float or changing its position relative to the solenoid. Finally, the method is less accurate than a pyknometer.

ACKNOWLEDGEMENTS

The authors are grateful to Professor B. Pavlović and Professor D. Bajić, whose guidance and suggestions in the design and testing of the apparatus proved very valuable. The authors are also grateful to the staff of the Reactor Materials Laboratory of the Boris Kidrič Institute, the Institute of Chemistry, Technology and Metallurgy, and the Nikola Tesla Institute, for the loan of equipment.

School of Technology and Metallurgy, Belgrade
University, Belgrade
Boris Kidrič Institute of Nuclear Sciences, Vinča,
Institute of Chemistry, Technology
and Metallurgy, Belgrade

REFERENCES

1. Weissberger, A. (Ed.). *Physical Methods of Organic Chemistry. Vol. 1* — New York: Interscience Publishers, Inc., 1960.
2. Lamb, A. and F. Lee — *Journal of the American Chemical Society* 35: 1966, 1913.
3. Kratky, O., H. Leopold, and H. Stabinger — *Zeitschrift für Angewandte Physik* (Berlin) 27: 273—277, 1969.
4. Hall, N. F. and T. O. Jones — *Journal of the American Chemical Society* 58: 1915—1919, 1936.
5. Hargens, C. W. — *Review of Scientific Instruments* 28: 921—923, 1957.
6. Beams, J. W. and A. M. Clarke — *Review of Scientific Instruments* 33: 750—753, 1962.
7. Millero, F. J., Jr. — *Review of Scientific Instruments* 38: 1441—1444, 1967.
8. Vukanović, V. and B. Pavlović — *Institut de Recherches sur la structure de la matiere* (Beograd) (04): 103—106, 1952.
9. Richards, A. R. — *Industrial and Engineering Chemistry* (*Analytical Ed.*) 14: 595—596, 1942.

GLASNIK HEMIJSKOG DRUŠTVA, Vol. 35, No. 7—8, 1970, pp. 397—403

GHDB-117

66.095.27:546.222:546.33'22

Original Scientific Paper

POLYSULFIDE POLYMERS. I.

DEPOLYMERIZATION OF POLYSULFIDE POLYMERS BY SODIUM HYDROSULFIDE AND SODIUM SULFITE

by

SLOBODAN S. RADOSAVLJEVIĆ, MIRJANA E. TENC-POPOVIĆ
and VLADIMIR J. REKALIĆ

Polysulfide polymers can be prepared by condensing alkyl dihalides with alkali polysulfides:

$$n\ \mathrm{Hal — R — Hal} + n\ \mathrm{Na_2S_x} = (\mathrm{—RS_x—})_n + 2n\ \mathrm{Na\text{-}Hal}$$

This is in fact a nucleophilic displacement of the reactive terminal by the polysulfide anion.

Depending on the polysulfide being used, polymers with from 2 to 4 sulfur atoms per segment of polymer are created$^{(1)}$. Although bromides are more reactive than chlorides, alkyl dichlorides are used in practice for condensation.

Of the polysulfide polymers the best tried so far are the polymers obtained from 1,2-dichloroethane$^{(2)}$, 1,2-dichloropropane, bis-2-chloroethyl ether and bis-2-chloroethyl formal. These polymers are used as rubber, sealants, cements, coatings and impregnation substances. Polymers obtained from bis-2-chloroethyl formal with an additional 2 mole percent 1,2,3-trichloropropane and with an average of two atoms of sulfur per segment of polymer can be depolymerized, and with the action of oxidizing agents can be retransferred into high molecular weight polymers. But in order to obtain a polymer with an average of two sulfur atoms per segment an alkaline polysulfide must be used that has a sulfur content of more than two atoms per molecule. For this purpose sodium tetrasulfide is most often used. Condensation of bis-2-chloroethyl formal and sodium tetrasulfide

$$n\ \mathrm{H_2C(OCH_2CH_2Cl)_2} + n\ \mathrm{Na_2S_4} = n\ \mathrm{H_2C(OCH_2CH_2S_4^-)_2} + 2n\mathrm{NaCl}$$

yields a polymer with an average four atoms of sulfur per segment of polymer. To obtain a polymer with an average of two atoms of sulfur per segment of polymer, the tetrasulfide polymer is submitted to desulfurization by boiling it with a 50% solution of sodium hydroxide according to the equation

$$5\ \mathrm{—RS_4R—} + 6\,\mathrm{NaOH} = 5\ \mathrm{—RSSR—} + 2\,\mathrm{Na_2S_4} + \mathrm{Na_2S_2O_3} + 3\mathrm{H_2O}$$

when the so-called "labile sulfur" is removed. However, the application of these polymers is limited because of their relatively high molecular weight.

Therefore disulfide polymer is subjected to depolymerization in order to reduce the average molecular weight. This can be achieved by controlled cleavage of disulfide bonds leading to the formation of polymers of lower molecular weight. According to J. C. Patrick and H. R. Ferguson(4), depolymerization of desulfurated tetrasulfide polymers with sodium hydrosulfide in the presence of sodium sulfite takes place according to the equations

$$\text{—RSSR— + NaHS} \rightleftarrows \text{—RSH + —RSSNa}$$

$$\text{—RSSNa} + Na_2SO_3 \rightarrow \text{—RSNa} + Na_2S_2O_3$$

There is not much data on the influence of individual reagent on the average molecular weight of the resulting polymers. The present work deals with the influence of sodium hydrosulfide and sodium sulfite on the average molecular weight of the polymers after depolymerization. During the study, however, it was found that the reproducibility of results and accordingly the effectivenes of depolymerization depend on a further parameter. The presence of sodium sulfide during the reaction was also found to be of great importance; sodium sulfide is always present in the reaction system because it is introduced as an ingredient in the sodium hydrosulfide. The influence of sodium sulfide on the depolymerization was therefore also studied.

EXPERIMENTAL

The depolymerization reaction was studied on a polymer obtained by condensation reaction of bis-2-chloroethyl formal and sodium tetrasulfide with 0.02 moles of 1,2,3-trichloro propane, 1.2 moles of sodium tetrasulfide, 0.08 moles of sodium hydroxide and 0.04 moles of magnesium chloride, per mole of bis-2-chloroethyl formal. We used 1.2 moles of sodium hydroxide per mole of bis-2-chloroethyl formal for desulfurization.

Eight drops of sulfonated ricinoleic acid and a solution of 4.8 grams of sodium hydroxide in 15 ml water are added to 900 ml of 2M sodium tetrasulfide solution in a round-bottomed flask. Then a solution of 12.18 g $MgCl_2 \cdot 6H_2O$ in 30 ml water is slowly mixed in. When this solution is heated to 75°C, the dropwise addition through a separating funnel of 254.4 g of bis-2-chloroethyl formal to which 4.41 g of 1,2,3-trichloropropane has been added is begun. After this has been completed, the reaction system is worked up for another hour at 98—100°C till all the bis-2-chloroethyl formal has reacted. During the reaction the polymer forms as a dispersion, which is easily washed. After washing the product is subjected to the desulfurization reaction. The "labile" sulfur is removed by boiling the mixture at 90 to 95°C with 150 grams of 50% sodium hydroxide solution with intensive mixing for one hour. Afterwards the polymer dispersion is washed again and then depolymerized. The dispersion is first heated to 75°C and then the appropriate amount of sodium hydrosulfide is added, previously dissolved in water and filtered. After that the appropriate amount of solid sodium sulfite is added, the dispersion is heated to 85°C and the mixture kept at this temperature for an hour. After the reaction is complete and the flask has cooled, 20% sulfuric acid is added dropwise until the pH reaches 4, to make the dispersion coagulate. The polymer thus obtained is first washed free of soluble salts and then vacuum dried at 20 to 30 mm Hg at a temperature of around 80°C.

The molecular weights of the polymers were determined by iodimetric titration for terminal thiol groups (5).

RESULTS AND DISCUSSION

Effect of sodium hydrosulfide

The influence of sodium hydrosulfide was examined in a series of experiments with a constant amount of sodium sulfite and varying amounts of sodium hydrosulfide which contained a constant amount of sodium sulfide. From the results shown in Table 1 it can be concluded that with increasing amount of sodium hydrosulfide, where 0.475—0.500 moles of sodium sulfite is used per segment of polymer, the molecular weight of the polysulfide polymers falls. These result are in accordance with those obtained by E. M. Fettes and H. Mark.(4)

TABLE 1

Dependence of Molecular Weight of Depolymerization Product on the Amount of Sodium Hydrosulfide Used

Synthesis no.	Na_2SO_3 moles/segm.	NaHS moles/segm.	Na_2SO_3:NaHS	M
1	0.475	0.237	1: 0.50	3052
2	„	0.356	1: 0.75	3000
3	„	0.475	1: 1.00	2380
4	„	0.712	1: 1.50	2290
5	„	0.800	1: 1.68	1400
6	„	0.900	1: 1.90	950
7	„	1.00	1: 2.10	873
8	0.500	0.250	1: 0.50	2500
9	„	0.375	1: 0.75	1900
10	„	0.500	1: 1.00	1304
11	„	0.750	1: 1.50	1176
12	„	1.000	1: 2.00	1033

Accordingly, the effectiveness of the depolymerization reaction on polysulfide polymers increases with increasing amount of sodium hydrosulfide, but this conclusion should not be generalized. For example, Table 2 shows the results of polymer reduction with 0.700 and 1.000 moles of sodium sulfite per segment of polymer, with different numbers of moles of sodium hydrosulfide.

From these results it follows that the optimum effect is obtained by using the molar ratio Na_2SO_3 : NaHS = 1 : 0.5. With a higher sodium hydrosulfide molar ratio the polymer average molecular weight does not fall but rather unexpectedly increases and this growth is somewhat greater the greatter the quantity of sodium sulfite used. It may therefore be concluded that the same depolymerization result may be obtained by use of a correspondingly smaller quantity of sodium hydrosulfide when a larger amount of sulfite is used.

TABLE 2

Depolymerization Efficiency for Different Quantities of Sodium Hydrosulfide Using a High Molar Ratio of Sodium Sulfite

Synthesis no.	Na_2SO_3 moles/segm.	NaHS moles/segm.	Na_2SO_3 : NaHS	M
1	0.700	0.175	1: 0.25	1717
2	»	0.350	1: 0.50	908
3	»	0.525	1: 0.75	1219
4	»	0.700	1: 1.00	3185
5	1.000	0.250	1: 0.25	1900
6	»	0.375	1: 0.375	925
7	»	0.500	1: 0.50	927
8	»	0.750	1: 0.75	1233
9	»	1.000	1: 1.00	4600

Effect of sodium sulfite

In a series of experiments we used a constant quantity of sodium hydrosulfide with a determined content of sodium sulfide and altered the amount of sodium sulfite. From results given in Table 3 it follows that given a constant quantity of sodium hydrosulfide (0.500 moles per segment of polymer), the average molecular weight decreases as the amount of sodium sulfite increases. But at a greater molar ratio of sodium hydrosulfide (0.700—1.000 moles per segment) we were unable to obtain reproducible results, which indicates some degree of agreement with the results of depolymerization as shown in Table 4. In our opinion these results may be ascribed to the fact that the depolymerization involves formation of water-soluble polymers, mainly of low molecular weight. During washing after coagulation these polymers get rinsed leaving only the larger polymers and the average mole-

TABLE 3

Molecular Weight of the Depolymerization Product as a Function of the Amount of Sodium Sulfite Used

Synthesis no.	Na_2SO_3 moles/segm.	NaHS moles/segm.	Na_2SO_3 : NaHS	M
1	0.250	0.500	1: 2.00	7720
2	0.334	»	1: 1.50	2944
3	0.500	»	1: 1.00	1304
4	0.666	»	1: 0.75	1284
5	1.000	»	1: 0.50	927

TABLE 4

Depolymerization Efficiency for Different Quantities of Sodium Sulfite Using a High Mole Ratio of Sodium Hydrosulfide

Synthesis no.	Na_2SO_3 moles/segm.	NaHS moles/segm.	Na_2SO_3: NaHS	M
1	0.500	1.000	1: 2.00	1033
2	0.666	»	1: 1.50	1785
3	»	»	»	6754
4	1.330	»	1: 0.75	1659
5	»	»	»	996
6	0.466	0.700	1: 1.50	4124
7	0.700	»	1: 1.00	3197
8	0.933	»	1: 0:75	7498

cular weight is therefore considerably higher then expected. Further evidence for this hypothesis is the fact that the yield is always somewhat lower. Also, it should not be forgotten that larger amounts of sodium hydrosulfide and sodium sulfite lead to a great increase in the system alkalinity, which can influence the success of the depolymerization reaction. This is the subject of our further investigation.

Effect of sodium sulfide

Results given in Table 5 show the change in average molecular weight of the polymer brought about by a change in the amount of sodium sulfide in the system during depolymerization with constant quantities of sodium hydrosulfide and sodium sulfite. From them the conclusion may be drawn that the average molecular weights of depolymerized polysulfide polymers can only be reproduced if sodium hydrosulfide with an approximatively equal percentage of sodium sulfide is used. If the amounts of sulfide are not approximatively equal, some deviation will be obtained, depending on the amount of sodium sulfide present. Taken as a whole, the efficiency of depolymerization decreases as the sulfide content of the sodium hydrosulfide increases.

TABLE 5

The Influence on Depolymerization Efficiency of Sodium Sulfide as a By-Product of Sodium Hydrosulfide

Synthesis no.	Na_2SO_3 moles/segm.	NaHS moles/segm.	% Na_2S in the NaHS	M
1	0.600	0.475	0.20	900
2	»	»	3.24	1330
3	»	»	3.96	2390
4	»	»	4.10	2400

It is interesting that good depolymerization can be achieved with relatively small amounts of sodium hydrosulfide. We were able to get polymers with an average molecular weight of 4000 to 5000 as shown in Table 6.

TABLE 6

Average Molecular Weights of Polymers Obtained by Depolymerization with Low Molar Ratio of Sodium Hydrosulfide (less than 0.06 *moles/segment)*

Synthesis no.	Na_2SO_3 moles/segm.	NaHS moles/segm.	Na_2S content of the NaHS (%)	M
1	0.475	—	—	rubber
2	„	0.01	3.2	rubber
3	„	0.03	„	5420
4	„	0.05	„	4033
5	„	0.06	„	4075

With 0.475 moles of sodium sulfite per segment of polymer the degree of depolymerization changes much less with reduced molar ratio of sodium hydrosulfide than with 0.350 moles per segment of polymer.

SUMMARY

The influence of sodium hydrosulfide, sodium sulfite and sodium sulfide on the average molecular weight of liquid polymers obtained by depolymerization of desulfurated tetrasulfide polymers using a mixture of sodium hydrosulfide and sodium sulfite for depolymerization has been studied.

The experimental results show that the degree of depolymerization is greater if more sodium hydrosulfide is used with a constant quantity of sodium sulfite (up to 0.500 moles per segment of polymer), or if more sodium sulfite is used with a constant amount of sodium hydrosulfide (up to 0.500 moles per segment of polymer). Moreover from these investigations it follows that reproducibility of depolymerization results, i.e. of the average molecular weight of the polymers, can only be obtained if sodium hydrosulfide containing approximatively the same amount of sodium sulfide is used.

School of Technology and Metallurgy,
University of Belgrade
Institute of Chemistry, Technology
and Metallurgy, Belgrade

Received March 10, 1970.

REFERENCES

1. Berenbaum, M. B. “Polysulfide Polymers. I. Chemistry”, in: N. G. Gaylord. *Polyethers. Part* 3. *Ch. 13* — New York: Interscience Publishers, 1962, p. 43—114.
2. Patrick, J. C. “Plastic Products” — *US Patent No. 1,890,191*, Dec. 6, 1932.
3. Patrick, J. C. and H. R. Ferguson. “Polysulfide Polymer” — *US Patent No.* 2,*466,963*, Apr. 12, 1949.
4. Fettes, E. M. and H. Mark “Cleavage of Disulfide Polymers. I. By Inorganic Sulfides” — *Journal of Applied Polymer Science* 5: 7—15, 1961.
5. Sampley, J. R. and E. E. Reid. “Some Analytical Reactions of Alkyl Mercaptans in Benzene Solution” — *Journal of the American Chemical Society* 54: 3404, 1932.

GLASNIK HEMIJSKOG DRUŠTVA, Vol. 35, No. 7—8, 1970, pp. 405—414

GHDB-118

539.24:669.35'296
Original Scientific Paper

MICROSTRUCTURAL CHARACTERISTICS OF CAST COPPER-ZIRCONIUM ALLOYS

by

B. BOŽIĆ, D. MIHAJLOVIĆ, and M. KOSTIĆ

By alloying copper with zirconium its mechanical properties at room temperature are moderately improved without any substantial change in electrical or thermal conductivity. The best balance of mechanical and physical properties is obtained by the following treatment: annealing — cold deformation — ageing.

However, the specific effect of alloying with zirconium is particularly pronounced at high temperatures. The addition of only 0.15—0.20% Zr appreciably increases the temperature of recrystallisation of copper, so that its mechanical properties remain stable to about 500°C. This may be explained by slow diffusion of zirconium due to the great difference between the diameter of copper and zirconium atoms. In addition, slow diffusion decreases grain growth at high temperatures and improves static strength. A particularly valuable feature is that zirconium copper loses its plasticity much less readily at high temperature than the pure metal or its thermal-precipitating alloys, e.g. chromium-copper, which means an increase in durability.

Today copper-zirconium alloys are being improved to get better mechanical properties at normal and high temperatures and better oxidation stability, retaining at the same time the advantages of a two-component system. Additional components are, therefore, selected from among those elements which, when added in small quantities, contribute to the strength through thermal precipitation, or which increase stability and compactness of the oxide layer.

Earlier studies were mainly concerned with the plastic deformable alloys. However, according to some results(1), there are reasons to expect a very good combination of mechanical and electric properties in a cast four-component alloy based on copper-zirconium with small quantities of beryllium and nickel, given suitable heat-treatment. From experimental results it appears that zirconium has a decisive influence on the microstructural characteristics of the four-component alloy. However, the correct interpretation of these phenomena is only possible through a study of the effect of each alloying component separately. As the literature data on metallographic characteristics of copper-zirconium alloys, particularly cast ones, are meagre, we studied, as a first step the microstructure of alloys containing 0.064—

—1.2% Zr, inter-crystalline segregation occurring in them, and the effect of subsequent heat-treatment. The results of these studies are given in the present paper.

MATERIAL AND METHOD

The alloys were made by melting in an electric vacuum furnace. The copper was OFHC, and zirconium was added as an alloy composed of 30% Zr and 70% Cu. The alloys were cast in 20 × 150 mm rods by pouring the melt in argon atmosphere into the metal moulds preheated to 200 °C. The studies were carried out with alloys setting as a solid solution(1), containing zirconium slightly above solubility(2), and with a considerable amount of eutectic, i.e. a content of zirconium which used to be considered the upper limit for technical alloys(3, 4). The chemical compositions may be seen in Table 1.

TABLE 1

Zirconium Content of Alloys

Alloy	Zirconium content (wt. pct.)
1	0.064
2	0.14
3	0.64
4	1.20

Microstructure of cast and heat-treated alloys was examined under an optical microscope. The heat-treatments were:

- — annealing at 800 or 900 °C for one hour in argon atmosphere and quenching in water
- — annealing as above, quenching in water, and ageing at 300, 400 and 500 °C for 1, 2 and 5 hours.

Crystalline segregation and all changes in the alpha-solid solution were investigated by concurrent determination of microhardness.

RESULTS AND DISCUSSION

The examination of microstructure revealed that, under the given conditions of cooling, the eutectic (alpha + Cu_3Zr) appeared in the alloy with as little as 0.064% Zr (Fig. 1). It segregated, Cu_3Zr occurring as a distinct phase. In all the alloys the eutectic was found on grain boundaries and within the grains between the dendritic branches, and could clearly be detected even on unetched specimens by the pale-blue color of Cu_3Zr. In the low-zirconium alloys the eutectic in the grains occurs as drops and its distribution reveals the orientation of dendrites, while at the grain boundaries it is in platelet or rod form (Fig. 2). In the high-zirconium alloys the eutectic in the grain appears as platelets almost continuously joined in hexagonal cells around the alpha-phase, and often linked with the eutectic micro-component on the grain boundary (Fig. 3). The alpha-phase of the eutectic precipitates as very fine fragments which, due to the shadow cast by the surrounding convex Cu_3Zr phase, appear as dark spots (Fig. 4).

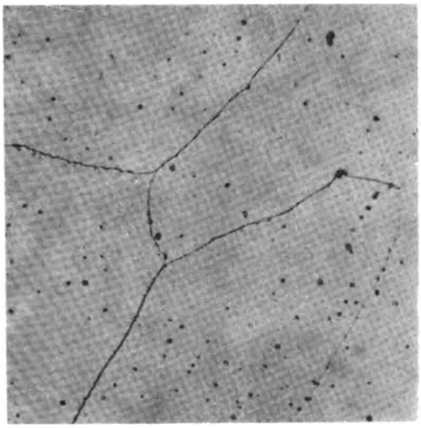

Fig. 1.

Cu—0.064% Zr, as cast; etched

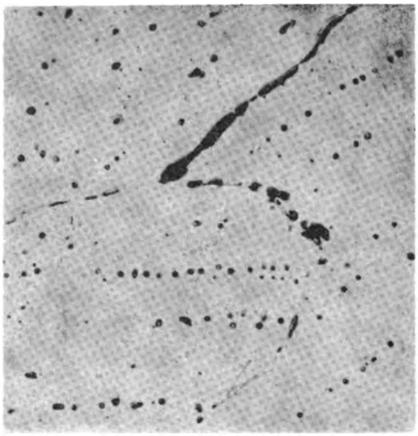

Fig. 2.

Cu—0.14% Zr, as cast; etched

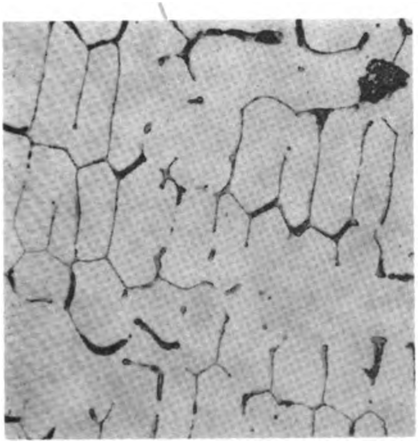

Fig. 3.

Cu—0.64% Zr, as cast; etched

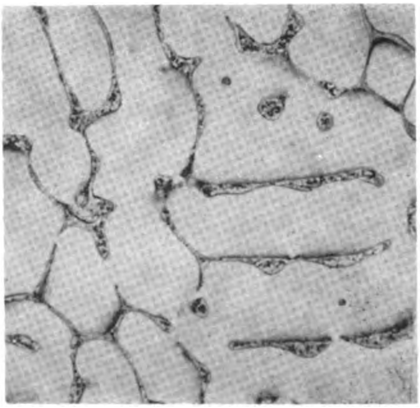

Figure 4.

Cu—1.24% Zr, as cast; unetched

Microhardness of the alpha-phase is given in Table 2. The results show the scattering range. It may be seen that the microhardness is highly inhomogeneous: the minimum was measured in the central part of the alpha-phase, and the maximum near the eutectic. This difference increases with zirconium content, and is particularly pronounced in the cell structure. Bulk grain alloying in the alpha solid solution contributes little to the microhardness relative to pure copper ($H_m = 45—50$ *kp/mm^2*), while its dependence on zirconium content in the alloy is irregular.

Macrohardness tests of the same specimens are also given in Table 2(1). It may be seen that macrohardness is improved relative to pure copper (about 35 kp/mm^2), even at 0.064% Zr. Its further increase is appreciable and proportional to zirconium content.

According to the literature data on the equilibrium phase diagram of zirconium copper, the occurrence of an intermediate Cu_3Zr phase and eutectic (alpha + Cu_3Zr) in copper-rich alloys is not controversial, but there are still different views on the position of the solvus and eutectic point(2-6).

For interpreting the microstructure we took maximum solubility of zirconium in the alpha-solid solution to be 0.11% Zr. This value was determined by Zwicker(6), and it is accepted as most probable by many other authors. We also accepted that the eutectic Zr concentration is about 13.7%(7). Hence at equilibrium the microstructure of an alloy with 0.064% Zr should consist almost entirely of alpha-phase, with a very small amount (about 0.19%) of the secondary Cu_3Zr phase precipitated according to the solvus. An alloy with 0.14% Zr should contain about 0.22% eutectic as well as alpha-phase, while those with 0.64% and 1.2% Zr should contain 3.1% and 8% eutectic, respectively. If the microstructure is compared with these data, it may be concluded that strong inter-crystalline segregation took place in these alloys due to irregular cooling, and was probably intensified by the slow diffusion of zirconium. The segregation was so pronounced that eutectic appeared even in the alloy with 0.064% Zr. In other alloys there is much more eutectic than would be expected from the phase diagram.

The effects of dendritic segregation are increased macrohardness due to higher content of Cu_3Zr phase and inhomogeneous microhardness of the alpha-solid solution, which evidences an irregular distribution of the alloying element.

TABLE 2.

Microhardness of Alpha-Phase (H_m, kp/mm^2) and Vickers Pyramid Hardness (HV, kp/mm^2) of Copper-Zirconium Alloys

Alloy	As cast		Annealed at 800°C, quenched in water	
	H_m	HV	H_m	HV
1	45.0—57.0	57	58.5—63.5	53
2	48.0—57.0	60	57.0—69.0 68.0—69.0**	51 53**
3	52.5—58.5 (79.0)*	72	56.0—58.5 (78.0—109.0)*	57
4	55.0—63.0 (84,0—96,0)*	80	57.0—66.0 (85.0—120.0)*	66

* Near Cu_3Zr phase

** Annealed at 900°C

The effect of homogenization temperature on microstructure and hardness was studied by annealing the alloys at 800 or 900°C for one hour. By annealing at 800°C for one hour a certain amount of Cu_3Zr phase was dissolved, both in the grain and on grain boundaries. In alloys with higher zirconium content these microstructural changes were less conspicuous due to the presence of equilibrium eutectic. The micro- and macrohardness tests after annealing are given in Table 2. Microhardness of the alpha-phase is somewhat increased in alloys 1 and 2, but it is still not homogeneous throughout the grain. Alloys 3 and 4 exhibit practically no change in the core of the grain, but microhardness in the zone near the eutectic is increased considerably. In all alloys macrohardness is much lower after annealing at 800°C and quenching in water than without heat treatment.

After annealing at 900°C for one hour the non-equilibrium component of the Cu_3Zr phase was found to have dissolve much more than at 800°C. This may particularly be seen at the grain boundaries in the alloys whose zirconium content is below or near the solubility limit (Figs. 5 and 6). Microhardness of the alpha-phase measured on the same specimen was very uniform and corresponds to the maximum attained by homogenization at 800°C.

Thus annealing at 800°C for one hour does not produce satisfactory results. The segregating non-equilibrium phase dissolves partly but no homogenization of the alpha-phase composition is achieved. On the other hand, annealing at 900°C for the same time is efficient, but the optimum annealing time depends on alloy composition. All the alloys studied have large grains when cast. The homogenization temperature was not observed to have any effect on grain size.

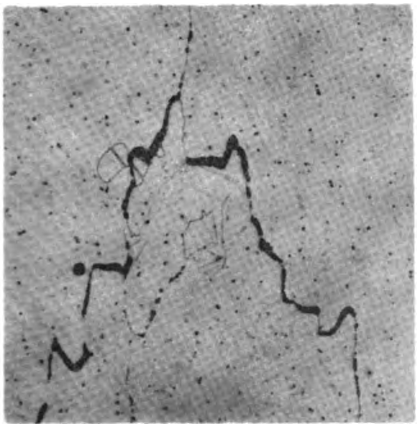

Fig. 5.

Cu—0.14 % Zr, cast, annealed at 800° — 1 h, quenched in water; etched

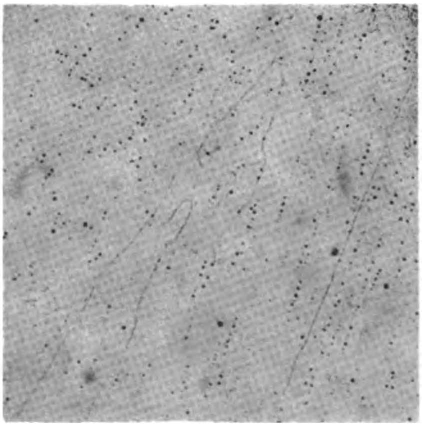

Fig. 6.

Cu—0.14 % Zr, cast, annealed at 900° — 1 h, quenched in water; etched

Due to decreased solubility of zirconium in copper, these alloys could theoretically be hardened by precipitation. However, experiments have shown(2, 8) that thermal precipitation has little effect on hardness, and good results can only be achieved by a combination of cold treatment and preci-

TABLE 3.

Influence of Aging on Microhardness of the Alpha-phase. (kp/mm²) and Vickers Pyramid Hardness (HV kp/mm²) of Copper —0.14% Zr Alloy

		Solution-annealed at 800°							Solution-annealed at 900°				
H_m	HV	Aged at:							H_m	HV	Aged at:		
		Time h	300°		400°		500°				Time h	400°	
			H_m	HV	H_m	HV	H_m	HV				H_m	HV
		1	*47.0—56.0	47	57.0—60.0	—	63.5—67.0	53			1	71.5—77.0	55
57.0—69.0	51	2	49.0—57.0*	47	60.0—67.0	53	61.5—65.0	52	67.0—69.0	53	2	61.5—65.0	54
		5	54.0—57.0	52	54.0—58.5	52	60.0—61.5	51			5	62.0—65.0	56

* After 3 hours

pitation. Hence the same could be expected for our alloys, considering that they were cast. However, with a view to determining the effect of auxiliary components in subsequent studies on many-component alloys, the effect of thermal precipitation in the basic two-component copper-zirconium alloy had to be studied. Tests were made by thermal dissolution at 800 and 900°C with the aim of determining the effect of chemical homogeneity on thermal precipitation, although according to the literature data(8) 800°C is low for thermal dissolution, i.e. the precipitation effect is small.

The effect of the temperature and time of thermal precipitation on microhardness of the alpha-solid solution and macrohardness of alloy 2, for which the effect should be greatest, is illustrated in Table 3. From the table it may be seen that in all specimens treated at 800°C for one hour, quenched in water, and then aged at 300, 400 or 500°C for one to five hours, microhardness of the alpha-phase is lower than obtained after tempering. Although the differences between the specimens are relatively small, certain regularities may nevertheless be seen. Microhardness was lowest after one and two hours of ageing at 300°C, while after five hours it is higher again. Ageing at 400°C gave a higher microhardness than at 300°C. The maximum was achieved after two hours, and then it decreased again. At 500°C the same effect was achieved after only one hour. Similar effects were observed for macrohardness, but the changes were negligible.

There was no change in the microstructure of specimens aged at 300°C for one or two hours. After five hours some precipitation was found at the sub-grain boundaries and within the body of the grain. In all specimens aged at 400°C precipitation was pronounced (Fig. 7). Within the grain body it was uniform, except for a narrow zone near the grain boundary. In suitably oriented grains precipitation in two mutually perpendicular planes, i.e. priviledged crystallographic planes, may clearly be seen (Fig. 8). Similar changes may be seen after ageing at 500°C, but of somewhat different intensity.

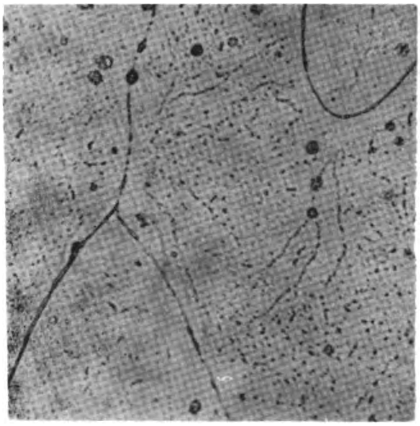

Figure 7.

Cu—0.14% Zr, cast, annealed at 900° — 1 h, quenched in water, aged at 400° — 5 h; etched

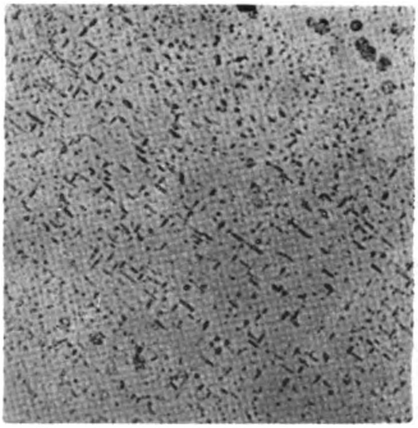

Figure 8.

Cu—0.064% Zr, cast, annealed at 800° — 1 h, quenched in water, aged at 400° — 5 h; etched

In the alloy 2 specimens thermally dissolved at 900°C for one hour and then quenched in water, microhardness was higher than for the tempered state, even after one-hour ageing at 400°C. This microhardness is at the same time the highest for the alpha-phase achieved by the treatments described. The changes in microstructure correspond to those already described for aging at 400°C after thermal dissolution at 800°C.

A preliminary study of the effect of ageing on the properties of alloys 1, 3 and 4, showed that 1 behaves similarly to 2, while a fine precipitate in the alpha-phase grains after aging at 500°C is characteristic for 3 and 4. Microhardness was observed to change with aging, beginning from 400°C, in the zone near the eutectic, while practically no change was found in the center of alpha-phase grains.

Considering all these phenomena it may be concluded that the microhardness of the alpha-phase in tempered specimens increased after thermal dissolution because of increased zirconium content in the solid solution due to dissolution of the Cu_3Zr phase and homogenization, but probably also to the stresses induced by tempering. By further ageing the stresses were removed and this effect was superimposed on the opposite effect of thermal precipitation, so that the resulting change depends on aging temperature and time. This conclusion is borne out by the results of aging at 400°C after thermal dissolution at 900°C: the effect of aging was probably higher due to more complete dissolution. Whether the slight decrease of hardness with longer aging is due to over-aging it is difficult to say from the present results. Aging phenomena in copper-zirconium alloys have been studied very little and for their exact interpretation more sensitive techniques would be required.

To sum up it may be said that: (a) The changes in microhardness of cast copper-zirconium alloys caused by aging at 300, 400 or 500°C after thermal dissolution at 800 or 900°C are small and of no practical significance, and (b) chemical inhomogeneity of the solid solution arising from the cast structure also affects the properties achieved by aging.

CONCLUSION

A characteristic feature of cast copper-zirconium alloys is pronounced dendritic segregation. This leads to an inhomogeneous distribution of the alloying element in the grains of alpha-solid solution and higher eutectic in the microstructure than the equilibrium.

By heating at 900°C for one hour a nearly homogeneous structure may be attained. The optimum heating time is determined by the composition of the alloy and the degree of inhomogeneity. Aging has little effect on cast (undeformed) alloy, and hardness is principally affected by the amount of eutectic. Therefore aging is of no use for increasing hardness while homogenizing has advantages from the aspect of other properties. However, in a multi-component alloy, where zirconium takes part in precipitation together with other elements, an appropriate homogenization treatment assuring regular distribution of the alloying element appears indispensable.

School of Technology and Metallurgy,
Iron and Steel Institute,
Belgrade University, Belgrade

REFERENCES

1. Mihajlović, A., S. Malčić, and B. Đurić. *Melting and Heat-Treatment of Some Copper-Base Alloys* (Boris Kidrič Institute of Nuclear Sciences Report No. 911) — Beograd: 1969.
2. Saarivirta, J. M. "High Conductivity Copper-Rich Cu-Zr Alloys" — *Transactions of the Metallurgical Society of AIME* (New York) 218 (3): 431—437, 1960.
3. Pogodin, A., T. S. Shumova, and F. A. Kugucheva. "Constitution and Properties of Copper-Zirconium Alloys" † — *Compte Rendu de l'Academie des Sciences USSR* † (Moskva) 27: 670—674, 1940.
4. Showak, W. "The Solid Solubility of Zirconium in Copper" — *Transactions of the Metallurgical Society of AIME* (New York) 224 (6): 1297—1298, 1962.
5. Raub, E. and M. Engel. "Alloys of Zirconium with Copper, Silver and Gold" — *Zeitschrift fur Metallkunde* (Stuttgart) 39 (2): 172—175, 1948.
6. Zwicker, U. "Untersuchungen an Cu-Zr Legierungen. I. Bestimmung der Löslichkeit von Zr in hochreinem Cu" — *Metall* (Berlin) 16 (5): 409—412, 1962.
7. Dies, K. *Kupfer und Kupferlegierungen in der Technik* — Berlin: Springer Verlag, 1967, pp. 639.
8. Saarivirta, J. M. and P. P. Taubenblat. "Some High-Temperature Properties of Copper-Zirconium and Copper-Chromium High Conductivity Alloys" — *Transactions of the Metallurgical Society of AIME* (New York) 218 (5): 935—939, 1960.

---

† Original title not given.

GLASNIK HEMIJSKOG DRUŠTVA, Vol. 35, No. 7—8, 1970, pp. 415—418

GHDB-119

66.095.26:547.538.141
Original Scientific Paper

CALCULATION OF THE INITIATION RATE CONSTANT OF THERMAL POLYMERIZATION OF STYRENE*

by

DRAGAN JOVANOVIĆ

In the free-radical or any other synthesis of macromolecular compounds the product obtained is a mixture of components having different molecular weights, as seen from its polymolecular character, i.e. distribution of molecular weights. The form of the distribution and polymerization kinetics of macromolecular polydispersed compounds may be investigated by statistical methods of analysis.

The present paper describes a method for calculating the initiation rate constant of thermal polymerization of styrene from the molecular weight distribution moments and the polymerization rate.

It is known from the literature that the distribution moment (μ) for a given polymerization system can be related to the rate constants k_i, k_p, and k_t, i.e., rate constants of initiation, propagation, and termination of chain growth. Hence, if the initiation rate is assumed to correspond to a second order reaction in terms of monomer concentration,

$$I = k_i[M]^2, \tag{1}$$

then

$$\mu_r = \frac{1}{2}(r+1)!(M_o)^r[k_p/(k_i k_t)^{\frac{1}{2}}]^{r-1}(1-[M]/[M]_o), \tag{2}$$

where: μ_r is the rth moment of the molecular weight distribution function ($r = 0, 1, 2, 3$, etc.), M_o is the molecular weight of the monomer, and $[M]_o$ and $[M]$ are the concentrations of the monomer at the beginning and at termination of polymerization. Equation (2) is a general expression for the relationship between the rate constants of various polymerization stages and the kinetic length of the chain. Dividing equation (2) for $r = 0$ by that for $r = 1$ yields

$$\mu_1/\mu_0 = \overline{M_n} = 2(M_0)k_p/(k_i k_t)^{\frac{1}{2}},$$

or

$$\overline{DP_n} = 2\, k_p/\,(k_i k_t)^{\frac{1}{2}} = 2 + 2\, k_p/(k_i k_t)^{\frac{1}{2}}, \tag{3}$$

---

* Communicated at 14th Conference of Chemists of the SR of Serbia.

In studying the distribution of molecular weights in a styrene sample thermally polymerized at 60 °C, applying the Gauss-Laguere integration the results of fractionation, Goodrich and Cantow[(2)] calculated the distribution moments and verified equation (2). The function log $\mu_r/(r+1)!$ plotted against r was a straight line. From the slope of this line to the r axis they calculated the bulk polymerization constant. By using k_p^2/k_t from literature data, which was obtained by measuring the polymerization rate of styrene in the presence of a catalyst, they calculated the rate constant of initiation at 60 °C, but the result was not satisfactory.

In our work it was noticed that by using the expression for the rate of thermal polymerization

$$-d[M]/d_t = (k_i/k_t)^{\frac{1}{2}}\, k_p[M]^2, \tag{4}$$

the rate constant of initiation may be obtained directly by differentiation and division of equations (4) and (2):

$$\frac{\left(\frac{d}{d[M]}\right)(-d[M]/dt)^{\frac{1}{2}}}{1/(M_0)\{\exp\left(\frac{d}{d_r}\right)[\log \mu_r/(r+1)!]\}} = k_i \tag{5}$$

According to this method, in initiation rate constant of thermal polymerization is determined by carrying out the polymerization at constant temperature and various concentrations of the monomer and determining the resulting polymerization rates. Then the polymer is fractionated and distribution moments determined. The constant is then calculated by using equation (5).

The polymerization rate is given as[(3)]

$$-d[M]/dt = 10^{5.07}\exp(-19\,200/RT)[M]^2, \tag{6}$$

and from it the calculated values of the bulk polymerization constant at 100° and 60° are:

100°C	$k_p(k_ik_t)^{\frac{1}{2}}$	$6.54 \cdot 10^{-7}$[*lit/mol. sec*]
60°C	„	$2.94 \cdot 10^{-8}$ [*lit/mol. sec*]

The denominator in equation (5) was calculated from the results of fractionation of thermally polymerized styrene at 60 °C[(2)]:

$$1/(M_0)\,\{\exp\left(\frac{d}{d_r}\right)[\log \mu_r/(r+1)!]\} = 4.3 \cdot 10^{-3},$$

Hence the rate constant of initiation

$$k_i = 2.94 \cdot 10^{-8}/4.3 \cdot 10^{-3} = 6.8 \cdot 10^{-12}\ [lit/mol.\ sec].$$

From the dependence of the initiation rate on temperature in the thermal polymerization of styrene (valid for the range from 100° to 132 °C⁽⁴⁾ we have

$$I = 1.5 \,.\, 10^4 \exp\,(-23300/RT)\ [M]^2, \tag{7}$$

so that the rate constant of initiation at 100 °C is

$$k_t = 3.3 \cdot 10^{-10}\ [lit/mol.\ sec].$$

From this value and that obtained for 60 °C, the dependence of the rate of thermal initiation of styrene on temperature is

$$I = 3.9 \,.\, 10^4 \exp\,(-24000/RT)\ [M]^2, \tag{8}$$

which agrees with equation (7).

DISCUSSION AND CONCLUSION

The method described for calculating the initiation rate constant is direct because it uses exclusively results obtained by thermal polymerization of styrene. The results obtained for k_t at 60 °C and the energy of 24000 [cal/mol] show that the calculation is consistent with the value obtained for the temperature range 100—135°C. The fact that satisfactory results cannot be obtained with values above k_p^2/k_t indicates that Flory's values here are probably inaccurate⁽⁵⁾.

School of Technology and Metallurgy,
Institute of Organic Technology,
Belgrade University, Belgrade

REFERENCES

1. Goodrich, F. C. *Polymer Fractionation* — New York: Academic Press, 1967, pp. 415—438
2. Goodrich, F. C. and M. J. R. Cantow — *Journal of Polymer Science* C8: 269, 1965.
3. Boundy, R. H. and R. F. Boyer *Styrene* — New York: Reinhold Publishing Co., 1952.
4. Bagdasar'i͡an, Kh. S. *Teorii͡a radikal'noi polimerizat͡sii* (The Theory of Radical Polymerization) — Moskva: Nauka, 1966.
5. Goodrich, F. C. — Personal communication.

GLASNIK HEMIJSKOG DRUŠTVA, Vol. 35, No. 7—8, 1970, pp. 419—427

GHDB-120

66.095.26:678.744

Original Scientific Paper

BULK POLYMERIZATION OF CETYLMETHACRYLATE

by

RUŽA P. BORISAVLJEVIĆ, SLOBODAN M. JOVANOVIĆ,
and ĐURA R. KOSANOVIĆ

Because of its practical importance and the fact that very interesting data about the effect of size and structure of monomer molecules on their polymerization ability may be obtained by studying polymerization kinetics, there is ample literature on the polymerization kinetics of methacrylic acid and its esters(1, 2). But, although the polymerization kinetics of methacrylic acid and its esters has been studied fairly thoroughly, there is little data on the polymerization of cetylmethacrylate; only five studies have been published(3—7). The first two(3, 4) deal with polymerization kinetics, one for X-ray initiated bulk polymerization(3), and the other for bulk polymerization and polymerization in a solution of carbon tetrachloride and isopropylbenzene initiated by benzoil peroxide(4). The remaining three studies are concerned with determination of the $[\eta]$-M relationship and the effect of the side-chain on conformation and optical properties of the polycetylmethacrylate molecule in solution. The scarcity of available data and the growing demand for this plastic prompted us to study the kinetics of bulk polymerization of cetylmethacrylate with α, α'-azoisobutyronitrile (AIBN) as initiator.

EXPERIMENTAL

Cetylmethacrylate was obtained by re-esterification of methylmethacrylate with cetyl alcohol(8). Prior to use the monomer was purified in three successive steps by vacuum distillation at 2 mm Hg. At this pressure the boiling point of the purified monomer is 178°C.

The initiator was AIBN of *p.a.* quality (Fluka) recrystallized from pure alcohol prior to use.

Other reagents were chloroform, methanol, acetone, heptane, and petroleum ether, all *p.a.* and purified by distillation before use.

The polymerization rate for 10% conversion was measured by dilatometry, and for higher conversions by gravimetry. The dilatometer volume was 10 cm^3, and its capillary was 1.5 mm in diameter. Prior to polymerization it was filled with nitrogen. Polymerization was allowed to proceed to 10% conversion and then the reaction was interrupted by immersing the dilatometer in a mixture of dry ice and acetone. The product was then dissolved in chloroform and the polymer precipitated with methanol, separated on a

Gooch filter and dried in vacuum at 25°C to constant weight. In gravimetric determination the monomer was put into vials together with the initiator, the air was replaced by nitrogen, and then the vials were stored in a thermostat. After the required polymerization period the vials were taken out and immersed in a mixture of dry ice and acetone in order to stop the reaction. The polymer was isolated from the mixture in the same way as in the previous case.

The molecular weight of the polymer was determined by viscosimetry. Determinations were made with Ostwald's viscosimeter at 25°C, using heptane as the solvent. For calculating the molecular weight from the viscosity index the [η]-M relationship given by Chien Jen-yuan and Chin-Liang-ho(5) was used:

$$[\eta] = 7.25 \cdot 10^{-5} \cdot M^{0.65}.$$

RESULTS AND DISCUSSION

Bulk polymerization of cetylmethacrylate with AIBN as initiator was carried out at 50, 60, 70 and 80°C. The concentration of initiator varied from 4.06 to 306 . 10^{-4} mol l^{-1}. The experimental conditions and results are shown in Table 1. The values of U_{br} and K (equation 1) in Table 1 were calculated from the yield-time curves obtained by dilatometry.

TABLE 1.

Bulk Polymerization of Cetyl Methacrylate Initiated by α α' Azobisisobutyronitrile

Test	Temp. °C	Concentration		$V_{br} \cdot 10^5$ *mol* l^{-1} *sec*$^{-1}$	$K \cdot 10^{-3}$	[η] dl g^{-1}
		[M] *mol* l^{-1}	[I] · 10^4 *mol* l^{-1}			
1	70	2.699	4.06	8.4	1.556	4.91
2	70	2.699	9.12	11.8	1.457	3.44
3	70	2.699	30.24	23.1	1.556	3.10
4	70	2.699	100.8	42.4	1.570	2.09
5	70	2.699	203.0	59.1	1.542	1.73
6	70	2.699	306.6	72.5	1.534	1.582
7	50	2.739	100.8	7.6	0.275	—
8	60	2.718	100.8	18.7	0.684	—
9	80	2.678	100.8	80.6	2.980	—

The dependence of conversion degree on polymerization time for the three different concentrations of initiator and at 70°C is shown in Fig. 1. These results were obtained by gravimetry.

From the figure it may be seen that at 15—20% conversion there was no acceleration of polymerization such as is characteristic for the lower esters of methacrylic acid(4, 9). The bulk polymerization rate is practically constant

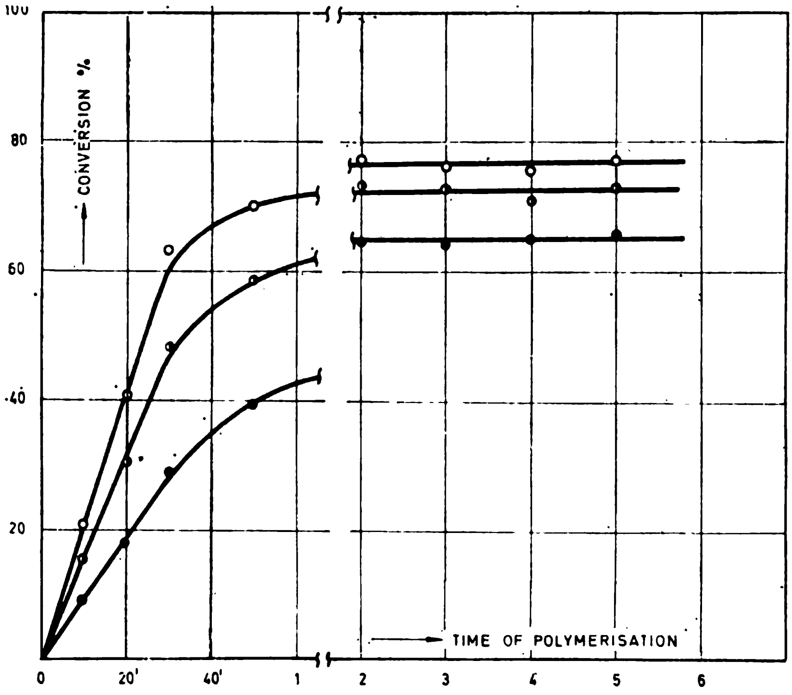

Fig. 1.

Kinetics of bulk polymerization of cetylmethacrylate initiated with α, α′-azoisobutyronitrile

until it begins to fall asymptotically to zero when the viscosity rises to such an extent that the diffusion rate of the monomer begins to control the rate of polymerization. Unlike methylmethacrylate, in which polymerization slows up at 90% polymerization, in cetylmethacrylate this takes place far earlier. The maximum degree of conversion depends on the concentration of the initiator, and for 4.87 . 10^{-2} mol l^{-1} it is only 70%.

If U_{br} from Table 1 is plotted against $[I]^{\frac{1}{2}}$ for polymerization at 70°C a straight line (Fig. 2) passing through the origin is obtained. This means that there is practically no inhibition period, that termination is a second order reaction, and that for this particular case the following expression for the initial static rate of polymerization holds:

$$U_{br} = \frac{k_i^{1/2} k_p}{k_t^{1/2}} \cdot [M] \cdot [I]^{\frac{1}{2}} = K \cdot [M] \cdot [I]^{\frac{1}{2}} \tag{1}$$

where u_{br} = rate of bulk polymerization

k_i = rate constant of initiation

k_p = rate constant of propagation

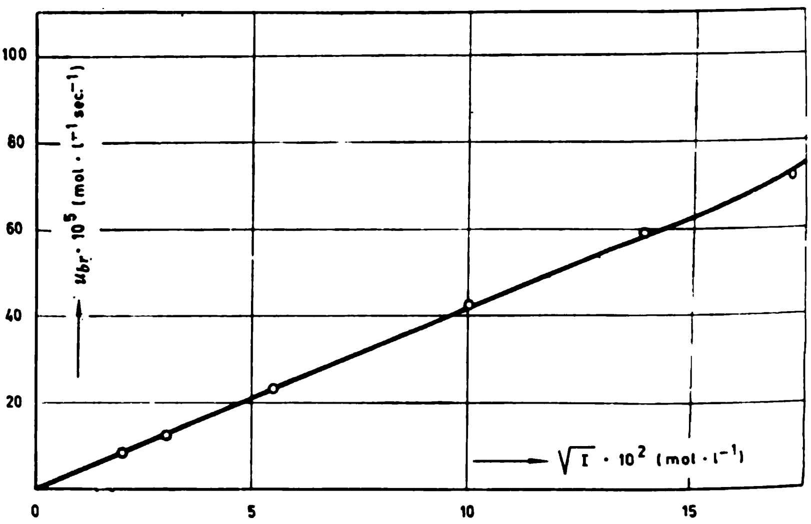

Fig. 2.

Bulk polymerization rate u_{br} as a function of initiator concentration

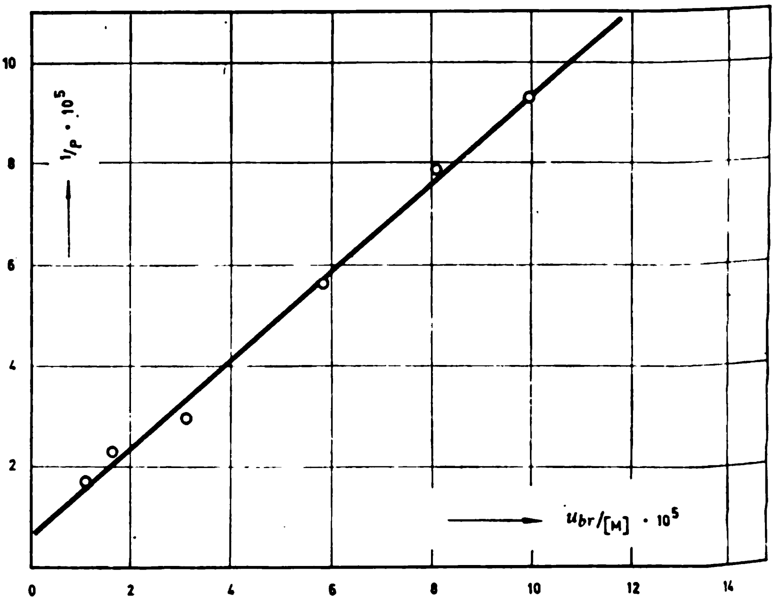

Fig. 3.

$\frac{1}{P}$ as a function of $\frac{u_{br}}{[M]^2}$.

k_t = rate constant of termination of the growing polymer chain
$[M]$ = concentration of monomer
$[I]$ = concentration of initiator

In bulk polymerization of methacrylic acid the growing polymer chain is terminated mainly by the disproportionation reaction. For small degrees of conversion the chain propagation transfer reaction involves only monomer molecules, and the following expression holds:

$$\frac{1}{P} = \frac{k_t}{k_p^2}, \frac{u_{br}}{[M]^2} + \frac{k_m}{k_p}. \tag{2}$$

where P = polymerization degree, $C_M = \frac{k_m}{k_p}$ = ratio between the reaction constant of propagation transfer and k_p, while k_t, k_p, u_{br}, and $[M]$ have the same meaning as in equation (1).

The dependence of $\frac{1}{P}$ on $\frac{u_{br}}{[M]^2}$ is shown in Fig. 3. $\frac{k_t}{k_p^2}$ was determined from the gradient of the straight line in Fig. 3. Using this and $\frac{k_i^{\frac{1}{2}} \cdot k_p}{k_t^{\frac{1}{2}}}$ from Fig. 2, a rate constant of initiation $k_i = 2.08 \,.\, 10^{-6}$ was calculated. The rate constant of initiation is

$$k_i = 2k_d f \tag{3}$$

where k_d = rate constant of initiator decomposition, and f = utilization coefficient of initiator. Substituting the calculated k_i and the value of k_d for decomposition of AIBN in methylmethacrylate at 70°C(10) into equation (3) gives the initiator utilization coefficient $f = 0.03$.

The dependence of the logarithm of the bulk rate constant of polymerization K on the reciprocal of temperature is shown in Fig. 4. From the gradient of the straight line the bulk activation energy of polymerization was determined as $E_{br} = 18.2$ *kcal mol*$^{-1}$. The bulk activation energy is

$$E_{br} = \frac{1}{2} E_i + E_p - \frac{1}{2} E_t, \tag{4}$$

where E_i, E_p, and E_t are the activation energies of initiation, propagation, and termination of the polymer chain. The activation energy for initiation with AIBN at 70°C was found from the literature(10) to be $E_i = 32.0$ *kcal mol*$^{-1}$. Introducing E_{br} and E_i into (4) gives

$$E_p - \frac{E_t}{2} = 2.2 \text{ kcal mol}^{-1}.$$

This result is about 2 kcal mol^{-1} less than for the lower esters of methacrylic acid. As at low conversion the activation energy of chain growth does

TABLE 2

k_i, $\frac{k_p}{k_t^{\frac{1}{2}}}$ and f for Polymerization of Some Esters of Methacrylic Acid

Monomer	Temp. °C	$k_i \cdot 10^6$	$k_p/k_t^{1/2}$	f	[M] of monomer	Reference
Methylmethacrylate	60	13.4	0.086	0.80	100.1	11
Ethylmethacrylate	60	9.97	0.136	0.66	115.1	11
Isobutylmethacrylate	60	8.54	0.206	0.48	143.1	11
Nonylmethacrylate	60	4.36	0.48	0.24	211	11
Cetylmethacrylate	70	2.08	1.07	0.03	310	this paper

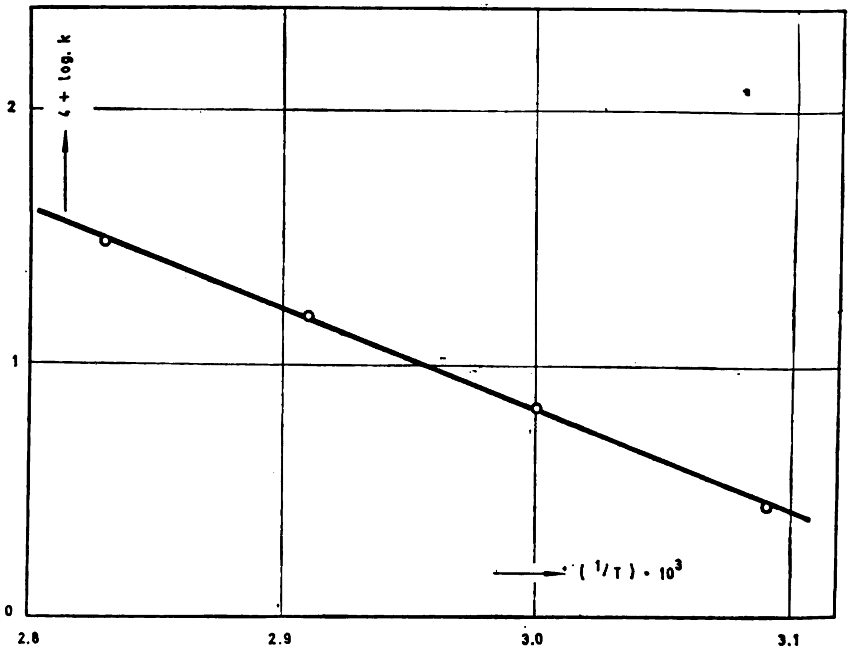

Fig. 4.

Rate constant K as a function of temperature (at initiator concentration of 0.01 mol l^{-1})

not change essentially with increasing molecular weight of the monomer, it may be said that the lower value of $E_p - \frac{E_t}{2}$ in the case of cetylmethacrylate is due to a higher activation energy of termination.

Along with k_i, $\frac{k_p}{k_t^{\frac{1}{2}}}$ and f for the bulk polymerization of cetylmethacrylate with AIBN initiator as found in this study, Table 2 also gives these constants for methyl-, ethyl-, isobutyl- and nonylmethacrylate from the literature(11).

From Table 2 it may be seen that for cetylmethacrylate the initiation constant ($k_i = 2.08 . 10^{-6}$) is far smaller than for the lower esters of methacrylic acid, and also smaller than that obtained by Hardy(4) for polymerization of cetylmethacrylate initiated with benzoil peroxide ($k_i = 3.09 \cdot 10^{-6}$). It is quite clear that the lower k_i is due to increased viscosity of the monomer, but whether this is caused only by a decreased initiator utilization coefficient f, or also by a change k_d with increased viscosity, as maintained by Gladyshev *et al.*(12, 13), is still controversial.

The initiator utilization coefficient $f = 0.03$ obtained in this study is a good deal smaller than that found for bulk polymerization of cetylmethacrylate initiated with benzoil peroxide ($f = 0.14$)(4). It has already been noticed that in polymerization with AIBN f decreases with increasing viscosity more rapidly than with benzoil peroxide(12), but such a great difference between these two initiators has not previously been recorded.

For cetylmethacrylate $\frac{k_p}{k_t^{\frac{1}{2}}}$ is an order of magnitude higher than for methyl- and ethylmethacrylate. In studying the polymerization kinetics of methylmethacrylate polymerization from solutions of different viscosity, Benson(14), and more recently Schulz(15), showed that the rate constant of termination is inversely proportional to the starting viscosity of the solution (monomer + solvent) and that for low conversion it is independent of the polymer molecular weight. As the viscosity of cetylmethacrylate is about ten times higher than that of methylmethacrylate, the higher $\frac{k_p}{k_t^{\frac{1}{2}}}$ is due to a reduced rate constant of termination. Individual values of k_t and k_p were not determined in this study, but, considering the linear dependence of conversion on polymerization time (Fig. 1) and equation (1), it may be said that $k_p k_t^{\frac{1}{2}}$ $[M]$ $[I]^{\frac{1}{2}}$ changes in the same way as $k_t^{\frac{1}{2}}$. The fact that in this case there was no acceleration of polymerization, characteristic for the lower esters of methacrylic acid, shows that the lower k_t due to a bigger reaction mixture viscosity increase with polymerization, and leading to a "gelling effect", was compensated by decreased k_t, k_p and concentration of the monomer.

Galenika Pharmaceuticals and Chemicals, Belgrade
School of Technology and Metallurgy,
Belgrade University

Received April 21, 1970

REFERENCES

1. Rauch-Puntigam, H. and T. Völker. *Acryl und Methacrylverbindungen* — Berlin-Heidelberg-New York: Springer Verlag, 1967.
2. Bagdasari͡an, H. S. *Teorii͡a radikal'noĭ polimerizat͡sii* (Theory of Radical Polymerization) — Moskva: Izdatel'stvo Akademii nauk SSSR, 1966, pp. 116—121.
3. Dobo, J. and K. Friese — *Plaste und Kautschuk* 9: 188—189, 1962.
4. Hardy, D., K. Nitrai, N. Federova, and G. Kovacs — *Vysokomolekuli͡arnye soedineniia* 4: 1872—1878, 1962.
5. Chien Jen-yuan and Shin Liang-ho — *Zeitschrift für Physikalische Chemie* 207: 60—69, 1957.
6. Rafikov, S. R., E. A. Bekturov, S. V. Vereza, and L. A. Bimendina — *Izvestii͡a Akademii nauk Kazakhskoĭ SSR:* 67—72, 1967.
7. T͡svetkov, V. N., D. Hardy, I. N. Shtennikova, E. V. Korneeva, G. F. Pirogova, and K. Nitrai — *Vysokomolekuli͡arnye soedinenii͡a* 11: 349—358, 1969.
8. Borisavljević, R., Đ. Kosanović, and O. Stojanović — *Hemijska industrija* 22: 281—285, 1968.
9. Trommsdorf, E., H. Kohle, and P. Lagally — *Die Makromolekulare Chemie* 1: 169—175, 1947.
10. Moroni, A. F. — *Die Makromolekulare Chemie* 105: 43—49, 1967.
11. Khana, S. N., S. R. Shatterje, V. S. Nandi, and S. R. Palit — *Transactions of the Faraday Society* 58: 1827—1831, 1962.
12. Messerle, P. E. and G. P. Gladyshev — *Vysokomolekuli͡arnye soedinenii͡a* 8: 1818—1822, 1966.
13. Messerle, P. El., S. R. Rafikov, and G. P. Gladyshev — *Doklady Akademii nauk SSS* 166: 158—159, 1966.
14. Benson, S. W. and A. M. North — *Journal of the American Chemical Society* 81: 1339—1345, 1959.
15. Fisher, J. P., G. Mücke, and G. V. Schulz — *Berichte der Bunsengesellschaft für physikalische Chemie* 73: 154—161, 1969.

GLASNIK HEMIJSKOG DRUŠTVA, Vol. 35, No. 7—8, 1970, pp. 429—436

GHDB-121

543.544.6:(546.226—325 + 547.476.3)

Original Scientific Paper

DETERMINATION OF SULPHURIC AND TARTARIC ACIDS IN THEIR MIXTURES AS A TOOL FOR ION EXCHANGER SEPARATION EFFICIENCY STUDIES

by

DARINKA J. STOJKOVIĆ and JANJA ĐUKIĆ

Ion-exchange chromatography has been found very efficient for separation or elimination of various ions. Our particular interest was the separation of sulphate from the tartarate ion on a cation exchanger. Experiments showed that there was no ion-exchange in the system of these two ions, only sulphuric acid appeared to be eliminated due to a Donan's potential. On eluting the column with water, sulphuric acid appeared in the eluate first, followed by tartaric acid. The efficiency of separation of the two ions was found to depend on the elution rate, and the nature and amount of the ion-exchanger.

An quick and efficient method is needed for monitoring the separation of these two acids on ion-exchange columns. Potentiometric titration was out of the question for selective determination, because the second order dissociation constant of sulphuric acid(1, 2) and the first order dissociation constant of tartaric acid differ by only 10^2 (instead of at least 10^4). Hence titration of a 1 : 1 mixture produced only a potential jump corresponding to an amount of base equivalent to the total amount of the two acids (Fig. 1).

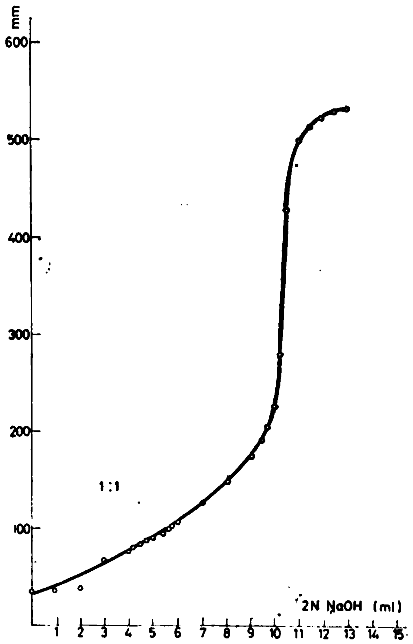

Fig. 1.

Potentiometric titration of the mixture of sulfuric acid and tartaric acid (Sb/s.c.e.)

However, it was found that the two acids can be determined by conductometric titration. Two equivalence points corresponding to the typical conductometric curve of a strong and weak acid are obtained. These determinations were made using 2 N solutions of sulphuric and tartaric acid and sodium hydroxide as the titrant. Titration was carried out with various ratios between the two acids. The results are shown in Table 1 and Fig. 2.

TABLE 1.

Conductometric Titration of Sulphuric and Tartaric Acids in a Mixture

Total acid $V_1:V_2$*	1.9150 N NaOH Consumed (ml)	1.9150 N NaOH Calculated (ml)	Difference (ml)	Error (%)
2:8	14.5	14.4	0.1	+0.7
4:6	14.4	14.4	—	—
1:1	14.5	14.4	0.3	+0.5
H_2SO_4				
2:8	3.0	2.9	0.1	+3.0
4:6	5.7	5.7	—	—
1:1	7.2	7.2	—	—
$H_2C_4H_4O_6$				
2:8	11.5	11.5	—	—
4:6	8.7	8.7	—	—
1:1	7.3	7.2	0.1	+1.2

* V_1 = ml H_2SO_4
V_2 = ml $H_2C_4H_4O_6$

Conductometric titration was found to give satisfactory results for total concentrations of the acid mixture of 0.133 *meq-/ml*. However, due to the fact that the concentrations are much lower in ion-exchange chromatography columns, the method turned out to be unsuited to the purpose.

Experiments showed that a combination of pH-metry and complexometry could be used; total acid can be determined by the former in one sample and sulphate ion$^{(3)}$, corresponding to the content of sulphuric acid, by the latter in another sample.

The combined method was first checked on acid mixtures which were not run on an ion-exchange column.

Reagents (*p.a.*):

M/100 solution of Na_2EDTA;

Solution of $CaCl_2$ for determination of the EDTA factor — made by dissolving 1.042 *g* $CaCO_3$ in HCl, and then diluting to 1 *l*;

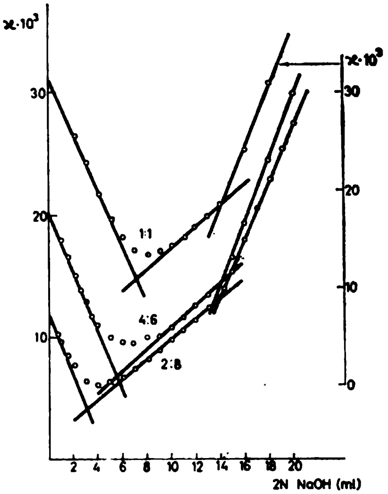

Fig. 2.

Conductometric titration of a mixture of sulfuric acid and tartaric acid

Buffer solution — 10 g $K_2MgEDTA$ (Complexal Mg) dissolved in 200 ml distilled water, then 70 g of NH_4Cl in 1800 ml 25% ammonia added to the solution;

Indikator — 0.5 *g* eriochrome black *T* and 4.5 g hydroxylamino-chlorhydrate dissolved in 100 ml 96% alcohol;

M/200 solution of $BaCl_2$;

2 N solution of HCl.

Determination of So_4^{2-} *ion*

To an aliquot of the acid mixture or, if tractionated, to the whole fraction or its aliquot (depending on the concentration of sulphate ion), 2 ml 2 N HCl and 50 ml $BaCl_2$ are added and the mixture heated up for five minutes. The solution is then kept in a sand bath for at least four hours. After it has cooled down, 4 ml buffer solution and two to three drops of indicator are added and the solution titrated immediately with the standard EDTA until it turns blue.

The concentration of SO_4^{2-} ion is determined as meq SO_4^{2-} = ml EDTA × × M_{EDTA} × F_{EDTA} × dilution ratio × 2.

The results obtained for 9 : 1 to 2 : 8 mixtures of sulphuric and tartaric acids are given in Table 2.

TABLE 2

Complexometric Determination of Sulphuric and Tartaric Acids in Artificial Mixtures

$H_2SO_4 : H_2C_4H_4O_6$ mixture	0.01 M EDTA consumed to neutralize excess of $BaCl_2$	0.01 M EDTA equivalent to the SO_4^{2-}	SO_4^{2-}		Error
			Found	Taken	
(ml:ml)	*(ml)*	*(ml)*	*(meq.)*	*(meq.)*	%
10:0	11.6	11.9	4.95	4.96	—0.1
9:1	12.8	10.7	4.42	4.46	—0.5
8:2	13.8	9.1	3.93	3.96	—1.0
7:3	14.6	8.1	3.49	3.47	+0.7
6:4	16.5	17.1	2.96	2.97	—0.2
5:5	18.0	5.6	2.43	2.33	+1.3
4:6	18.7	4.8	2.00	1.98	+0.8
3:7	19.9	3.6	1.50	1.49	+0.5
2:8	18.3	4.6	0.99	0.99	—

Considering the fact that complexometric determination of SO_4^{2-} ion in mixtures of sulphuric and tartaric acids did not produce satisfactory results, attempts were made to analyze the fractions appearing in the eluate after running the mixture on an H^+ ion-exchange column.

The Amberlite 200 resin column packing (Rohn Hass Company, Philadelphia, USA) is a sulphonated styrene copolymer with divinylbenzene. It was converted to the H^+ form by running 3 N HCl through the column. After regeneration, the resin was washed with water until neutral reaction.

A 1 : 1 mixture, i.e. 9.96 meq tartaric to 9.84 meq sulphuric acid, was then put through the column. The total acidity introduced was 19.8 meq, at a rate of 1.5 ml/min. The analysis of the fractions is shown in Table 3.

The total concentration of sulphate and tartarate ions was determined in each eluate fraction and the results compared with the total amount of the acid mixture put into the column (Table 4).

From the table it may be seen that there is a negligible difference between the amount introduced and the quantities of the acids found in the eluate fractions, with an average error of —0.20% for each, and —0.05% for the total.

A combined method of potentiometric complexometric determination of two acids in the eluate was tried. However, the optimum conditions for separation of the two acids on suitable ion-eliminating, exchange resins have yet to be found.

TABLE 3.

Determination of Sulphuric and Tartaric Acid in Eluate Fractions

Fraction	Volume	N/2 NaOH ($F = 0.9950$) to neutralize the fraction	Total acid	0.01 M EDTA to neutralize excess $BaCl_2$	0.01 *M* EDTA ($F = 0.039$) equivalent to the SO_4^{2-}	Total SO_4^{2-}	Total $C_4H_4O_6^{2-}$	SO_4^{2-} Concentration	$C_4H_4O_6^{2-}$ Concentration
No.	(ml)	(ml)	(meq)	(ml)	(ml)	(meq)	(meq)	(meq/ml 10^{-3})	
1	10	—	—	—	—	—	—	—	—
2	10	—	—	—	—	—	—	—	—
3	10	0.05	0.03	23.00	0.45	0.01	0.02	1	1
4	10	2.65	1.32	16.90	6.55 · 5*	0.68	0.64	60	64
5**	10	7.35	3.66	29.25	17.65 · 5	1.84	1.82	183	182
6	10	6.35	3.23	30.85	16.05 · 5	1.67	1.56	167	156
7	10	7.05	3.51	15.30	8.15 · 10	1.70	1.81	170	181
8	10	5.21	2.59	17.05	6.70 · 10	1.37	1.22	137	122
9	10	4.20	2.09	18.25	5.50 · 10	1.14	0.95	114	95
10	10	3.12	1.55	18.85	4.90 · 5	1.03	0.52	103	52
11	10	2.12	1.06	21.45	2.30 · 5	0.24	0.82	24	82
12	10	1.42	0.71	21.90	1.42 · 5	0.19	0.52	19	52
13	10	0.05	0.03	23.75	0.00	0.00	0.03	0	2
14	10	0.05	0.03	23.75	0.00	0.00	0.03	0	2

* Dilution.

** 100 ml $BaCl_2$ added. 23.75 ml EDTA consumed to bind Ba^{2+} in 50.0 ml 0.02 M $BaCl_2$.

TABLE 4.

	H_2SO_4	$H_2C_4H_4O_6$	Total acid
Taken (meq)	9.84	9.96	19.80
Found (meq)	9.87	9.91	19.78
Difference (meq)	+0.03	—0.05	—0.02
Error (%)	+0.30	—0.50	+0.05

The results in Tables 1—4 show that the combined method is applicable not only for the analysis of artificial mixtures of these acids, but also for their eluate fractions, and may be applied to other acid systems that behaving in a similar way.

Institute of Technology and Metallurgy,
Department of Electrochemistry, Belgrade
Institute of Physical Chemistry and
Electrochemistry, School of Technology,
Belgrade University, Belgrade

REFERENCES

1. Lîalikov, S. I͡u. *Fiziko-khimicheckie metody analiza* (Methods of Analysis in Physical Chemistry — Moskva: Khimii͡a, 1964.
2. Vorob′ëv, N. K., V. A. Golt͡sshmidt, M. Kh. Karapet′i͡ant͡s, V. L. Kiseleva, and K. S. Krasnov. *Praktikum po fizicheskoĭ khimii* (Manual of Physical Chemistry) — Moskva: Khimii͡a, 1964.
3. Sijderius, R. "Titrimetric Determination of Sulfate by Means of the Disodium Salt of Ethylenediaminetetraacetic Acid" — *Analytica Chimica Acta* (11): 28—32, 1954.

GLASNIK HEMIJSKOG DRUŠTVA, Vol. 35, No. 7-8, 1970, pp. 437—441

GHDB-122

543.244.6:543.257.1:(546.815 + 546.46)
Original Scientific Paper

COULOMETRIC-COMPLEXOMETRIC-POTENTIOMETRIC-DETERMINATION OF LEAD AND MAGNESIUM IN THEIR MIXTURES

by

DARINKA J. STOJKOVIĆ and SVETLANA R. DRAVIĆ

In the light of results obtained in determination of some cations by the coulometric complexometric potentiometric method(1, 2, 3), it appeared interesting to expand the scope of its application to binary and many-component systems, determining suitable titrating conditions and using electrolytically generated ethylenediaminetetraacetate (EDTA) ion as the coulometric reagent.

Although the selective properties of the EDTA are rather limited, by using the pH two or three cations (but not more) may nevertheless be determined, provided they form complexes with EDTA whose stability constants differ by at least 10^6.

However, it was found that the difference in stability constants was not a sufficient condition for selective determination with EDTA, but a certain masking effect must be achieved by adjusting the pH of the medium. At low solution pH the complexing of the metal with the lower stability constant is suppressed, so that the other, forming a more stable complex with the EDTA, may be easily titrated. In this case the H^+ ions behave as a masking agent. After separate determination of Co^{2+} and Mg^{2+} ions(2), their determination in a mixture was tried.

From the graph showing the dependence of the stability constants of EDTA complexes with various cations on pH(2) it may be seen that a difference of 10^6 between the Co^{2+} and Mg^{2+} ions can be achieved if cobalt is titrated at pH = 4 and magnesium at pH = 10. However, from the effect that pH has on the coulometric complexometric potentiometric titration of cobalt(2), it was concluded that at pH = 5 the potentiometric curve would not show a well-defined turning point, meaning that the cobalt chelate dissociates considerably at this pH, and hence even more at pH = 4, so that quantitative determination of the two cations in a mixture appeared impossible. For this reason, the system Pb^{2+} and Mg^{2+} was chosen as more suitable, because Pb^{2+} forms a more stable complex with EDTA than Co^{2+}, and since this ion can be very accurately determined in the presence of Ca^{2+}, which has properties similar to those of magnesium, determination of Pb^{2+} and Mg^{2+} ions in a mixture seemed feasible.

For the determinations solutions were prepared containing 1.09 mg/ml magnesium and 3.76 mg/ml lead. The titer of these solutions was determined with Complexon III. The apparatus was identical to that employed for separate determinations of cobalt and magnesium(2).

A solution of mercury ethylenediaminetetraacetate was used as the catolyte, and saturated solution of K_2SO_4 as the anolyte. The excess of mercury ions in the catolyte was neutralized by pre-titration at pH = 7(1, 2, 3). After this a mixture of Pb^{2+} and Mg^{2+} ions was added and the pH of the solution adjusted to 5.5 with concentrated ammonia solution. This pH was then stabilized by the addition of 5 *ml* 0.5 N sodium acetate. Gaseous nitrogen was bubbled through for 5 minutes to remove dissolved oxygen, though its reduction at the cathode was unlikely since the potentials were much more positive than the half-wave potential of oxygen reduction. Then the coulometric circuit was closed and Pb^{2+} titrated with the EDTA ions released by electrolysis, monitoring the change of potential with time until the highest potential jump i.e. the end-point, was reached, this indicating that all lead had complexed with EDTA. After this the pH was increased 10.5, nitrogen again bubbled through for 5 minutes, and then the coulometric titration was continued until the next potential jump, indicating that all the magnesium had complexed with the EDTA.

RESULTS AND DISCUSSION

The complexometric potentiometric determinations of Pb^{2+} and Mg^{2+} in their mixtures are given in Table 1; the corresponding potentiometric curves $E = f(t)$ are given in Fig. 1.

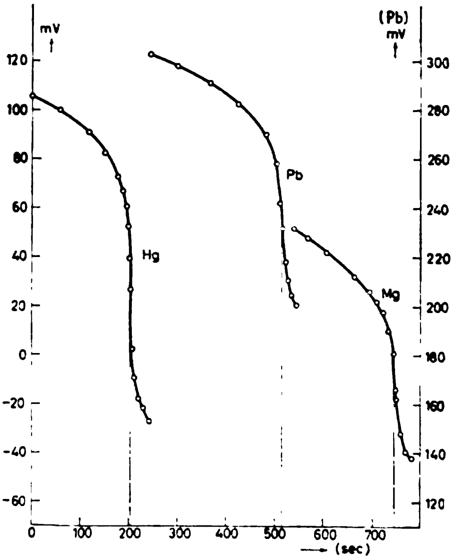

Fig. 1.
The potentiometric curves of coulometric-complexometric determinations of lead and magnesium in their mixtures

TABLE 1

Coulometric-complexometric Determination of Lead and Magnesium in Their Mixtures

Test	Taken		Found		Error				Theoretical time (*sec*)	
	Pb	Mg	Pb	Mg	Pb		Mg		Pb	Mg
	mg	*mg*	*mg*	*mg*	*mg*	%	*mg*	%		
1	11.280	1.500	11.196	1.506	—0.084	—0.7	+0.006	0.4	267	228
2	13.160	2.250	13.018	2.268	—0.042	—0.3	+0.018	0.8	311	242
3	9.400	3.150	9.442	3.162	+0.042	0.4	0.012	0.4	223	467
4	7.520	3.150	7.604	3.162	+0.084	1.1	+0.012	0.4	178	467
5	12.210	1.870	12.252	1.864	+0.042	0.3	—0.006	—0.3	289	284
6	11.280	2.250	11.196	2.244	—0.084	—0.7	—0.006	—0.2	267	342

The graph in Fig. 1 clearly illustrates the possibilities of the method for determining the time needed for titration of each cation separately. Thus from the time corresponding to the equivalence point and the constant titration current the concentration of each cation can be determined by Faraday's law.

From the results in Table 1 it may be seen that lead in quantities from 7.5 to 11.28 mg was determined with a maximum error of 0.7%, while magnesium was determined in quantities from 1.5 to 3.15 mg with a maximum 0.8% error.

From the table and graph it may also be seen that coulometric complexometric determination of Pb^{2+} and Mg^{2+} in mixtures produced good results, but the method has to be elaborate because of maneuvers to increase the selectivity of the EDTA, and its scope of application for the analysis of many-component mixtures is rather restricted.

Institute of Chemistry, Technology and Metallurgy,
Department of Electrochemistry, Belgrade

REFERENCES

1. Reilley, C. N. and W. W. Porterfield. "Coulometric Titrations with Electrically Released Ethylenediaminetetraacetic Acid" — *Analytical Chemistry* 28: 443—447, 1956.
2. Stojković, D. J. and S. R. Dravić. "Kulometrijsko-kompleksometrijsko određivanje jednog ili više katjona" (Coulometric Complexometric Determination of One or More Cations), in: II Jugoslovenski kongres za čistu i primenjenu hemiju, Beograd, Juni 1966 (2nd Yugoslav Congress on Pure and Applied Chemistry Belgrade, June 1966) (Abstract 165) — *Glasnik hemijskog društva* (Beograd) (to be published)*.
3. Stojković, D. J. and S. R. Dravić. "Kulometrijsko-kompleksometrijsko određivanje katjona" (Coulometric Complexometric Determination of Cations) — *Glasnik hemijskog društva* (Beograd) (to be published).*
4. Reilley, C. N. and R. W. Schmid. "Chelatometric Titrations with Potentiometric End-Point Detection" — *Analytical Chemistry* 30: 947—953, 1958.
5. Přibil, R. *Komplexometrie* — Praha: Chemapol, 1955.
6. Schwarzenbach, G. *Die Komplexometrische Titration. 2nd Ed.* — Stuttgart: F. Encke Verlag, 1956.

---

* Available in English translation from National Technical Information Service, Springfield, Virginia, 22151.

GLASNIK HEMIJSKOG DRUŠTVA, Vol. 35, No. 7-8, 1970, pp. 443—448

GHDB-123 543.24:543.257.5:(546.722'32'267 + 546.723'32'267)

Original Scientific Paper

COULOMETRIC ARGENTOMETRIC AMPEROMETRIC DETERMINATION OF POTASSIUM FERRICYANIDE AND POTASSIUM FERROCYANIDE

by

DARINKA J. STOJKOVIĆ

The Ag^+ ion generated by anodic oxidation was the first coulometric metallometric reagent(1—5). Most published studies deal with the coulometric determination of halides with the use of Ag (1—5), but oxidation/ /reduction with use of the Ag^{2+} ion has also been described (4, 5).

Excellent results obtained in micro and semi-micro determinations of halides and the exceptionally good properties of the silver anode prompted us to try to expand the scope of coulometric argentometry to other anions forming hardly soluble compounds with silver. Ferricyanide and ferrocyanide ions were judged suitable because of their low solubility ratios, 10^{-26} for silver ferricyanide and 10^{-41} for silver ferrocyanide, at 25°C.

EXPERIMENTAL

Reagents. — All chemicals of *p.a.* quality (Merck), were dried at 110°C prior to use. Molar solutions were prepared and aliquots measured out with a graduated burette. A solution of KNO_3, which in the anolyte was 10^{-3} to 10^{-4} M relative to HNO_3, was used as the supporting electrolyte for both arms of the electrolytic cell. To avoid migration of the OH ions enriching the catolyte and their passage into the anodic space, which would greatly interfere with the quantitative determination of the anion, 1—2 ml 1 N H_2SO_4 was added to the catolyte.

Apparatus. — The apparatus employed in these determinations was essentially the same as used for coulometric plumbometry(7), mercurometry(8), and bismuthometry(9). It consisted of two current circuits: a) a coulometric electrolysis circuit with a silver (*p.a.*) anode and platinum cathode; b) an amperometric indicator circuit with dropping mercury electrode and SCE. The circuit components were as usual(7—9), except that a syphon (Fig. 1) was added to the cathode or anode, arm in argentometric determinations. This syphon was employed by Khadeev(6) in amperometric titration of silver nitrate with potassium ferricyanide. The reason for introducing the syphon was the fact that mercury collecting at the bottom of the cathode arm reduces either the substance being determined or the coulometric reagent (in this case ferricyanide) up to, and silver ions after the end-point.

A simple solution to this problem is to collect and automatically remove the drops of mercury during the titration. For this purpose the stopper closing the anode (cathode) arm is provided with a hole through which a

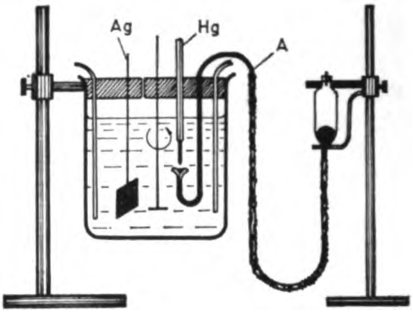

Fig. 1.

Anodic (cathodic) compartment with siphon A

capillary is insert into the arm. The drops of mercury collect in its slightly widened end, so that the area of direct contact between the solution and mercury is quite small. The upper end of the capillary is connected with the levelling vessel via a capillary bridge and vacuum tubing. The vessel is raised causing mercury to enter the vacuum tubing and fill the capillary as far as its widened end, and then rapidly lowered to equalize the level in it with at the capillary mouth. This procedure assures a good syphonic action and continuous removal of mercury drops throughout the determination.

Amperometric end-point detection was chosen because of less probable subjective error and due to the natural coloring of the solutions being determined, which excludes the use of chemical indicators.

The amperometric curves obtained had the usual shapes, i.e. *V* or inverted *L*. As oxygen was not removed from the solution, non-zero residual currents corresponding to the reduction of oxygen may be noticed on these graphs.

Stirring of the electrolyte, as required in coulometry for accelerating the reaction and decreasing the adsorption of ions on the precipitate, was interrupted from time to time to connect the amperometric indicator circuit. This was done 3—5 times before and as many times after the end-point in order to measure the parameters required for plotting the $Id = f(t)$ curve.

For coulometric generation of Ag^+ ion proper conditions must be obtained in the medium in which the anodic oxidation is carried out. It was found best for the reaction of the medium to be neutral or slightly acid; in an alkaline medium silver oxide, and in a highly acid one Ag^{2+} ions would be formed. The latter are sometimes also employed as a coulometric reagent(4, 5).

Argentometric Determination of Ferricyanide Ion

Potassium ferri- and ferrocyanide proved to be very interesting reagents for titrimetry of metallic ions, e.g. Ag, Zn, Cu, Pb, Co, Ni, and Cd, not only for analytical purposes but also for analysis of the compounds obtained. A comprehensive theoretical study of amperometric titration has been given by Khadeev(6), who not only derived a mathematical model of the titration curves and estimated their shape, but also examined their geometrical properties. He checked his theoretical work on a number of examples, one of these being the amperometric determination of silver nitrate with potassium ferricyanide. He carried out this titration in an electrolyte composed of 0.2 M $NaNO_3$ and 0.01 M HNO_3, and found that the reaction was strictly stoichiometric, with formation of $Ag_3[Fe(CN)_6]$. He also found that with higher concentrations the curves obtained had branches coinciding with their asymptotes.

Khadeev's work justified our attempts to use coulometric titration for determination of ferricyanide ion with silver ion generated at the anode.

The determination was performed in a solution of 0.2 M KNO_3 which was 10^{-3} to 10^{-4} M relative to HNO_3. An external voltage of 0.75 V was applied to the amperometric circuit. The slopes of the *V* curve obtained were found to depend on concentration, potential difference in the external circuit, and galvanometer sensitivity.

The indicator reactions were the following:

before the end-point

$$Fe(CN)_6^{3-} + e = Fe(CN)_6^{4-};$$

after the end point

$$Ag^+ + e = Ag(Hg) \text{ amalgam.}$$

The titration reaction was

$$3\,Ag^+ + Fe(CN)_6^{3-} = Ag_3Fe(CN)_6.$$

The results are shown in Table 1.

TABLE 1.

Coulometric Determination of $Fe(CN)_6^{3-}$.

Supporting electrolyte 0.2 M KNO_3 and 0.001 M HNO_3. Volume of catolyte and anolyte: 50 ml each. Amperometric indicator circuit: dropping mercury electrode and SCE; external voltage: 0.75 V.

Approximate concentration $K_3Fe(CN)_6 \cdot 3H_2O$	Taken $Fe(CN)_6^{3-}$	Found $Fe(CN)_6^{3-}$	Error		Current	Time
mol/l	mg	mg	mg	%	mg	sec
$36.2 \cdot 10^{-4}$	3.511	3.495	0.016	−0.50	40.0	120.6
$36.2 \cdot 10^{-4}$	3.511	3.493	0.018	−0.52	20.0	241.2
$18.1 \cdot 10^{-4}$	1.755	1.744	0.011	−0.60	10.0	241.2
$9.05 \cdot 10^{-4}$	0.877	0.892	0.015	+ 1.7	10.0	120.6

As seen from the table, ferricyanide ion was determined in quantities of 0.855 mg, 1.755 mg, and 3.511 mg, with a relative eror of 0.5%. The titration of 0.855 mg ferricyanide ions required 1.2 coulombs, this corresponding to a rate of silver ion generation of 1.02 . 10^{-7} gram equivalent per second.

Argentometric Determination of Ferrocyanide Ion

Coulometric determination of ferrocyanide ion was performed in the same way as for ferricyanide. The anolyte in the coulometric circuit was a solution of 0.15 M KNO_3, which was 0.001 M and 0.0001 M relative to HNO_3. The catolyte also contained 0.15 M KNO_3, with an addition of 1 ml 1 N H_2SO_4. The amperometric circuit fed at 650 mV. At this voltage Ag^+ ions are reduced after reaching the equivalence point, and since ferrocyanide ion is not reduced the potentiometric curve is an inverted L.

There was no indicator reaction before the end-point. After it,

$$Ag^+ + e = Ag\,(Hg)\ \text{amalgam}$$

The titration reaction was

$$4\,Ag^+ + 4\,Fe(CN)_6^{4-} = Ag_4Fe(CN)_6.$$

The results of these determinations are given in Table 2.

TABLE 2.

Coulometric Determination of $Fe(CN)_6^{4-}$

Supporting electrolyte: 0.15 M KNO_3 *and 0.0001 M* HNO_3.
Volume of catolyte and anolyte: 50 ml each. Generator current: 10.0 and 40.0 mA.
Amperometric indicator circuit: dropping mercury electrode and SCE; external voltage: 0.65 V.

Approximate concentration $K_4Fe(CN)_6$	Taken $Fe(CN)_6^{4-}$	Found $Fe(CN)_6^{3-}$	Error		Current	Time
mol/l	mg	mg	mg	%	mA	sec
$33.7 \cdot 10^{-4}$	5.297	5.220	0.077	—1.20	40.0	241.2
$23.8 \cdot 10^{-4}$	3.750	3.715	0.035	—0.95	40.0	136.8
$16.8 \cdot 10^{-4}$	2.648	2.075	0.027	+ 1.02	40.0	121.6
$8.42 \cdot 10^{-4}$	1.324	1.304	0.020	—1.52	10.0	241.2
$4.22 \cdot 10^{-4}$	0.664	0.657	0.007	—1.05	10.0	120.6

As may be seen from the table, ferrocyanide ion was determined in quantities of 0.664, 1.328, 2.645, 3.750, and 5.290 *mg*, with a mean relative error of —0.70%. 1.21 coulomb was consumed to titrate 0.664 *mg* ferrocyanide ions, corresponding to a rate of silver ion generation of $1.02 \cdot 10^{-7}$ gram equivalent per second.

The mean relative error in the determinations of ferrocyanide ion was less than in the individual determinations. The errors were larger than in determination of ferricyanide ion, which may partly be ascribed to the adsorption of ferrocyanide ion on the precipitate or perhaps to the formation of an intermediate, also hardly soluble compound which is subsequently converted into the final form $Ag_4Fe(CN)_6$.

The method of coulometric metallometry in general, in these two examples employed in coulometric argentometry of ferro- and ferricyanide ions, again showed its advantage, particularly for microdeterminations, over the classical methods. The titrant agent is generated at the site of use and at the desired rate, the determination is rapid and sensitive, the method of generating the titrant and end-point detection is not subjective, and the procedure is suitable for automation of serial determinations.

School of Technology and Metallurgy,
Department of Physical Chemistry
and Electrochemistry, Belgrade
University, Belgrade

Received September 13, 1970

REFERENCES

1. Kowalkowski, R. L., J. H. Kennedy, and P. S. Farrington. "Titration of Iodide with Electrolytically Generated Silver Ion" — *Analytical Chemistry* 26: 626—628, 1954.
2. Lingane, J. J. "Automatic Coulometric Titration with Electrolytically Generated Silver Ion. Determination of Chloride, Bromide, and Iodide Ions" — *Analytical Chemistry* 26: 622—626, 1954.
3. Tutundžić, P. S., I. Doroslovački, and O. Tatić. "Coulometrische Argentometrie Bestimmung von Chlor-, Brom-, und Jodidionen" — *Analytica Chimica Acta* (Amsterdam, 12: 481—488, 1955.
4. Abresch, K. and I. Claassen. *Die coulometrische Analyse* — Weinheim: Verlag Chemie, GmbH., 1961.
5. Zozula, A. P. *Kulonometricheskiĭ analiz* (Coulometric Analysis) — Moskva: Khimii͡a, 1965.
6. Khadeev, V. A. *Nekotorye voprosy teorii amperometricheskogo metoda titrovanii͡a* (Some Problems of the Theory of Amperometric Titration) — Erevan: Izdatel'stvo Erevanskogo universiteta, 1957.
7. Tutundžić, P. S. and D. J. Stojković. "Coulometrische Wismutometrie. Quantitative Bestimmung von Posphationen" — *Microchimica Acta* (4—5): 666—675, 1966.
8. Tutundzhich, P. S. and D. Ĭ. Stoĭkovich. "Kulonometricheskai͡a metallometrii͡a. Kulonometricheskoe opredelenie anionov" (Coulometric Metallometry. Coulometric Determination of Anions) — *Zhurnal analiticheskoĭ khimii* 21: 436—442, 1966.
9. Tutundžić, P. S. and D. J. Stojković. "Kulometrijska metalometrija. Kulometrijsko-merkurometrijsko određivanje anjona" (Coulometric Metallometry. Coulometric Mercurometric Determination of Anions) — *Glasnik hemijskog društva* (Beograd) (to be published).*

*** Available in English translation from National Technical Information Service, Springfield, Virginia, 22151.**

Izdavač
IZDAVAČKO PREDUZEĆE "NOLIT", BEOGRAD, TERAZIJE 27/II

*

Štampa
GRAFIČKO PREDUZEĆE "PROSVETA"
BEOGRAD — ĐURE ĐAKOVIĆA 21.

SRPSKO HEMIJSKO DRUŠTVO (BEOGRAD)

BULLETIN OF THE CHEMICAL SOCIETY Belgrade

(Glasnik Hemijskog društva — Beograd)
Vol. 35, No. 9-10, 1970

Editor:
ALEKSANDAR DESPIĆ

Published by
SRPSKO HEMIJSKO DRUŠTVO (BEOGRAD)
1970

Translated and published for U. S. Department of Commerce and the National Science Foundation, Washington, D. C., by the Nolit Publishing House, Terazije 27/II, Belgrade, Yugoslavia
1972

Translated by
PAVEL ČMELIK

Edited by
PAUL PIGNON

Printed by Birografika — Subotica

CONTENTS

GLASNIK HEMIJSKOG DRUŠTVA, Vol. 35, No. 9–10, 1970, pp. 449–457

GHDB-124 541.124:546.73:547.466:54.07:541.62:541.49
Original Scientific Paper

ON THE REACTIONS OF HEXANITROCOBALTATES (III) WITH AMINO ACIDS. VI. SYNTHESIS AND GEOMETRICAL ISOMERISM OF DINITROBIS (AMINOACIDATO) COBALTATE (III) COMPLEXES WITH HIGHER MONOCARBOXYLIC AMINO ACIDS

by

MILENKO B. ĆELAP, MIHAJLO B. DIMITRIJEVIĆ,
DUŠAN J. RADANOVIĆ, FRANJO A. ČOHA, TOMISLAV I. NIKOLIĆ, and
TOMISLAV J. JANJIĆ

Substitution reactions of the alkali hexanitrocobaltates (III) with the alkali salts of glycine(1), or alanine or β-alanine(2) led to the creation of a new class of coordination compounds of the type: dinitrobis (aminoacidato) cobaltate (III), $M^I[Co\,Am_2(NO_2)_2]$. The glycine complex was also obtained by direct synthesis, i. e. atmospheric oxidation of the divalent into trivalent cobalt in the presence of alkali nitrite and alkali glycinate(3)*. The geometrical and absolute configuration of these compounds were determined by chemical and physical means(2, 5, 6).

Continuing with these investigations, we have now studied analogous substitutions with higher monocarbonic amino acids (DL-α-aminobutyric acid, α-aminoisobutyric acid, β-aminobutyric acid, β-aminoisobutyric acid, DL-valine, DL-norvaline, DL-norleucine, and DL-isoleucine) in order to investigate the effect of the ligand voluminousness on the configuration of the complexes obtained. In these experiments the higher members of the above mentioned class of dinitrobis (aminoacidato) cobaltate (III) compounds were obtained. In addition, a method of preparation of dinitrobis (aminoacidato) cobaltate (III) complexes with the above mentioned amino acids and with DL-alanine and β-alanine by direct synthesis, similarly as for that with glycine(3), is described. With these methods sodium and potassium salts were obtained. The silver salts were prepared by the double decomposition of silver nitrate with the alkali salt, and the free acids were obtained by ion-exchange.

The dinitrobis (aminoacidato) cobaltate (III) ion could appear in five geometrical isomers, of which two would contain the nitro group in the *trans* position and the other three in the *cis* position(4). In order to determine which the new compounds were, we analyzed their absorption spectra in the visible and UV. It was found that the spectra of all the complexes with α-amino acids were almost identical, and identical to those of the earlier synthetized dinitrobis (α-aminoacidato) cobaltate (III) ions, in which the *cis* position was proved by their decomposition into the optical antipodes(2, 4, 5). From this it can be concluded that the new compounds also have the nitro

---

* Other preparative techniques may be found in ref. (4).

groups in the *cis* position. This agrees with Shimura's rule on the position of the nitro-specific bands(7), which are superimposed on the second absorption band of the d-d electron transitions $(1A_{1g} \rightarrow 1T_{1g})$.

In the case of the complex with β-aminobutyric acid, the product had an absorption spectrum identical with that of the analogous complex with β-alanine, in which the *cis*-dinitrobis configuration was earlier proved by its decomposition into the optical antipodes(2). Hence we consider that in this complex ion the nitro group is also in the *cis* position.

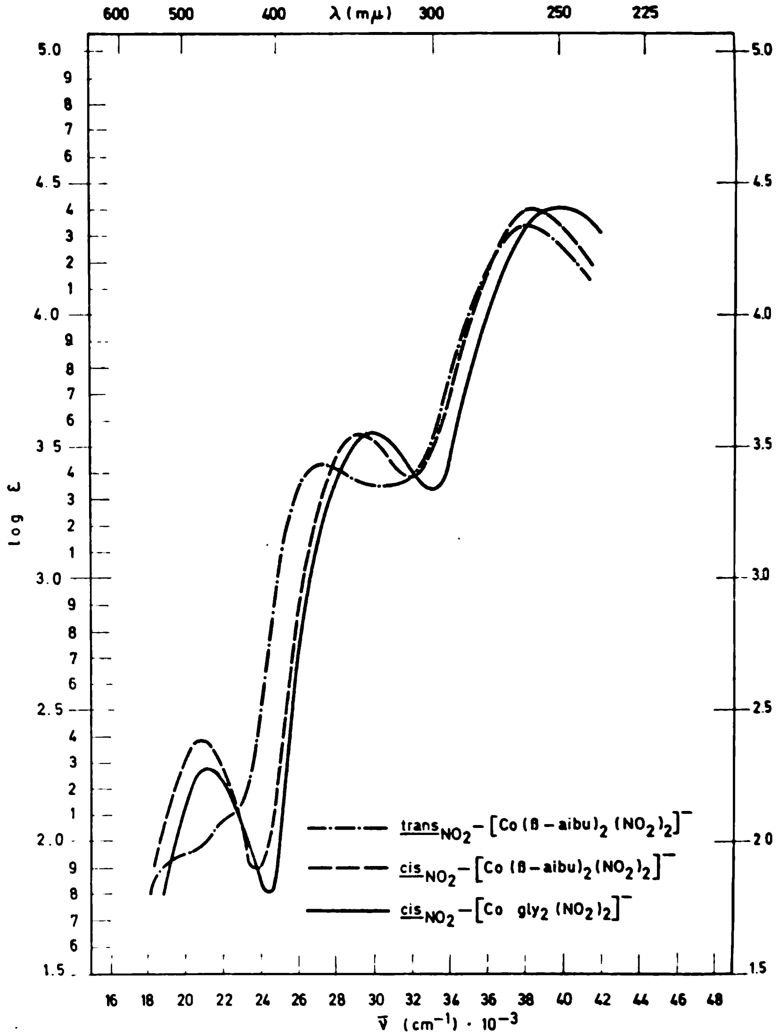

Fig. 1.

Electronic absortion spectra of cis_{NO_2}—dinitroglycinatocobaltate (III) ion and cis_{NO_2}— —and $trans_{NO_2}$—dinitrobis (β—aminoisobutyrato) cobaltate (III) ions

Finally, by the reaction between β-aminoisobutyric acid and sodium hexanitrocobaltate (III) two isomers were obtained. In the first, obtained in much the higher yield (51%), the *cis* position was proved in the same way as for the complex with β-aminobutyric acid. In the second (7% yield) the configuration was also analyzed by absorption spectrum (Fig. 1 and Table 1). From the figure it may be seen that its spectrum differs from that of *cis*$_{\mathrm{NO_2}}$ -dinitrobis (β-aminoacidato) cobaltate (III) ions.* The first absorption band of the d-d electron transitions $(1A_{1g} \rightarrow 1T_{1g})$ is here split into two components, this not being the case with other complexes with β-amino acids. From this it can be assumed that either two nitro groups$^{(8)}$ or two carboxy groups$^{(9)}$, or both, are here in the *trans* position. However, the downward shift of the nitro-specific band (at 24 mμ) of this isomer relative to the corresponding bands of *cis*-dinitrobis (β-aminoacidato) cobaltate (III) ions suggests the *trans* position of the nitro groups$^{(7)}$. The orientation of the amino acid ligands in the *trans*-$_{\mathrm{NO_2}}$ -ion cannot be determined from the present experimental data; our future studies will be aimed at the solution

TABLE 1.

Position of Absorption Maxima λ (mμ) and log ε *Values of Dinitrobis (aminoacidato) cobaltate (III) Ions*

Complex ion*	Absorption maxima**					
	λ_1	$\log \varepsilon_1$	λ_2	$\log \varepsilon_2$	λ_3	$\log \varepsilon_3$
cis- $[\mathrm{Co\ gly_2(NO_2)_2}]^-$	468	2.29	334	3.56	250	4.42
cis- $[\mathrm{Co\ abu_2(NO_2)_2}]^-$	468	2.28	334	3.49	250	4.39
cis- $[\mathrm{Co\ aibu_2(NO_2)_2}]^-$	468	2.32	334	3.51	252	4.41
cis- $[\mathrm{Co\ val_2(NO_2)_2}]^-$	468	2.33	334	3.52	250	4.42
cis- $[\mathrm{Co\ nva_2(NO_2)_2}]^-$	468	2.30	334	3.52	252	4.42
cis- $[\mathrm{Co\ nle_2(NO_2)_2}]^-$	468	2.34	334	3.53	252	4.42
cis- $[\mathrm{Co\ ile_2(NO_2)_2}]^-$	468	2.29	334	3.50	252	4.39
cis- $[\mathrm{Co\,(\beta\text{-}ala)_2(NO_2)_2}]^-$	478	2.39	343	3.56	258	4.40
cis- $[\mathrm{Co\,(\beta\text{-}abu)_2(NO_2)_2}]^-$	478	2.39	343	3.54	258	4.39
cis- $[\mathrm{Co\,(\beta\text{-}aibu)_2(NO_2)_2}]^-$	478	2.42	343	3.54	258	4.39
trans- $[\mathrm{Co\,(\beta\text{-}aibu)_2(NO_2)_2}]^-$	522(p) ~460(p)	1.93 2.07	367	3.43	262	4.33

* gly$_2$ = glycine; abu$_2$ = α-aminobutyric acid; aibu$_2$ = α-aminoisobutyric acid; val$_2$ = valine; nva$_2$ = norvaline; nle$_2$ = norleucine; ile$_2$ = isoleucine; β-ala$_2$ = β-alanine; β-abu$_2$ = β-aminobutyric acid; β-aibu$_2$ = β-aminoisobutyric acid; p = shoulder.

** Electronic absorption spectra were recorded on a Perkin-Elmer 137-UV spectrometer in aqueous solutions with a concentration of $3 \cdot 10^{-3}$ to $3.5 \cdot 10^{-5}$ M.

---

* *Cis*$_{\mathrm{NO_2}}$ — and *trans*$_{\mathrm{NO_2}}$ — will henceforth be referred to as *cis*- and *trans*-.

of this problem. However, from the absorption spectra, which correspond to those of the similar compounds studied earlier(2), it can be assumed that the *cis*-dinitrobis (aminoacidato) cobaltate (III) ions obtained are in fact cis_{NO_2}-$trans_N$-isomers. In future studies this will be checked by analysis of the circular-dichroic, NMR and infrared spectra of the isolated optical isomers.

EXPERIMENTAL

Preparation of dinitrobis (aminoacidato) cobaltate (III) complexes containing DL-α-aminobutyric acid, α-aminoisobutyric acid, β-aminobutyric acid, β-aminoisobutyric acid, DL-valine, DL-norvaline, DL-norleucine, or DL-isoleucine as ligands.

1. *Preparation of alkali salts*

(a) *Indirect synthesis.* — A solution of 0.02 mole of the amino acid and 0.72 g (0.018 mole) NaOH in 15 ml water is added to a solution of 4.04 g (0.01 mole) sodium hexanitrocobaltate (III) in 5 ml water. The mixture is heated on a water bath with stirring for one hour. The brown solution is then filtered, the filtrate is reduced to half its original volume with a vacuum evaporator (at this stage the salt formed partly crystallizes) and left for a few hours in the refrigerator. The brown crystalline sediment of the *cis*-dinitrobis (aminoacidato) cobaltate (III) is separated by filtering, washed with a little water, ethanol and ether, and air-dried. The crude compound is then recrystallized several times from aqueous solution or from a water-ethanol mixture.

Due to the high solubility of sodium dinitrobis (β-aminoisobutyrato) cobaltate (III), the complex was isolated as the potassium salt. The brown solution obtained by the above procedure was then run on an ion-exchange column (Merck I cation-exchanger) previously converted to the potassium form, and the eluate reduced to 10 ml with a vacuum evaporator. The solution was then left overnight in the refrigerator. The sediment (0.3 g) of potassium *trans*-dinitrobis(β-aminoisobutyrato) cobaltate (III) monohydrate was isolated by filtering and recrystallized several times from aqueous solution at 60°C. From the filtrate 2 g of highly soluble potassium *cis*-dinitrobis (β-aminoisobutyrato) cobaltate (III) monohydrate was obtained by further evaporation and refrigeration. It was then recrystallized several times from water-ethanol mixture at 60°C. The yield and analysis are given in Table 2.*

---

* In the analysis of all compounds obtained in this study water was determined from the difference in weight before and after drying at 105°C; alkali metals and silver were determined by gravimetry (as sulphates, or chloride); cobalt was determined by electrogravimetry.

TABLE 2.

Yield and Analysis of the Alkali Dinitrobis (aminoacidato) cobaltate (III) Salts Obtained by Indirect Synthesis

Compound	Yield %	Analysis*			
		Calculated		Found	
cis-Na [Co abu$_2$(NO$_2$)$_2$]	76	Co	15.58	Co	15.50
		Na	6.08	Na	5.84
cis-Na [Co aibu$_2$(NO$_2$)$_2$] · 2H_2O	76	Co	14.88	Co	14.68
		Na	5.80	Na	6.08
		H_2O	4.55	H_2O	5.30
cis-Na [Co (β-abu)$_2$(NO$_2$)$_2$] · 3H_2O	81	Co	15.58	Co	15.47
		Na	6.08	Na	5.96
		3H_2O	12.50	3H_2O	12.60
cis-K [Co (β-aibu)$_2$(NO$_2$)$_2$] · H_2O	51	Co	14.95	Co	14.82
		K	9.91	K	10.02
		H_2O	4.37	H_2O	4.40
trans-K [Co (β-aibu)$_2$(NO$_2$)$_2$] · H_2O	7	Co	14.95	Co	14.75
		K	9.91	K	9.83
		H_2O	4.37	H_2O	4.30
cis-Na [Co val$_2$ (NO$_2$)$_2$]	76	Co	14.51	Co	14.65
		Na	5.66	Na	5.29
cis-Na [Co nva$_2$(NO$_2$)$_2$] · H_2O	78	Co	14.51	Co	14.39
		Na	5.66	Na	5.50
		H_2O	4.23	H_2O	4.42
cis-Na [Co nle$_2$(NO$_2$)$_2$] · H_2O	76	Co	13.57	Co	13.43
		Na	5.29	Na	5.05
		H_2O	3.98	H_2O	4.36
cis-Na [Co ile$_2$(NO$_2$)$_2$] · 2H_2O	80	Co	13.57	Co	13.64
		Na	5.29	Na	5.17
		2H_2O	7.66	2H_2O	7.95

* For analysis the substances were dried at 105°C for two hours. The values for potassium, sodium, and cobalt were calculated as for anhydrous salts, except for the sodium salt with α-aminoisobutirate-complex, which remains monohydrate even at 140°C.

(b) *Direct synthesis.* — A solution of 3.40 g (0.04 mole) potassium nitrite in 10 ml water was added to a solution of 0.04 mole of the amino acid and 1.12 g (0.02 mole) KOH in 20 ml water.** Finally, a solution of 4.98 g (0.02 mole) cobalto-acetate-tetrahydrate in 10 ml water was added to the above mixture. Air was bubbled through vigorously for three hours (at this stage some of the salt sometimes crystallized out). The sediment was then isolated by filtration, and from the filtrate brown crystals of the *cis*-dinitrobis (aminoacidato) cobaltate (III) salts is obtained by evaporation and refrigeration. The salt is recrystallized from aqueous or water-ethanol solutions. The yield and analysis are given in Table 3.

** In the preparation of complexes with β-aminoisobutyric acid sodium hydroxide and sodium nitrite were used instead of the corresponding potassium compounds.

TABLE 3.

Yield and Analysis of the Cis-dinitrobis (aminoacidato) cobaltate (III) Salts Obtained by Direct Synthesis

Compound	Yield %	Analysis*			
		Calculated		Found	
cis-K $[Co\ ala_2(NO_2)_2]$	72	Co	16.09	Co	16.13
		K	10.66	K	10.52
cis-K $[Co\ (\beta\text{-ala})_2\ (NO_2)_2]$	63	Co	16.09	Co	16.20
		K	10.66	K	10.75
cis-K $[Co\ abu_2(NO_2)_2]$	67	Co	14.95	Co	14.94
		K	9.91	K	9.79
cis-K $[Co\ aibu_2(NO_2)_2] \cdot 2H_2O$	65	Co.	14.29	Co	14.50
		K	9.48	K	9.36
		H_2O	4.37	H_2O	4.89
cis-Na $[Co\ (\beta\text{-abu})_2(NO_2)_2] \cdot 3H_2O$	56	Co	15.58	Co	15.62
		Na	6.08	Na	6.00
		$3H_2O$	12.50	H_2O	12.74
cis-K $[Co\ (\beta\text{-aibu})_2(NO_2)_2] \cdot H_2O$	57	Co	14.95	Co	14.94
		K	9.91	K	9.93
		H_2O	4.37	H_2O	4.50
cis-K $[Co\ val_2(NO_2)_2]$	64	Co	13.95	Co	14.04
		K	9.25	K	9.21
cis-K $[Co\ nva_2(NO_2)_2] \cdot H_2O$	67	Co	13.95	Co	13.95
		K	9.25	K	9.18
		H_2O	4.09	H_2O	4.55
cis-K $[Co\ nle_2(NO_2)_2] \cdot H_2O$	51	Co	13.08	Co	12.97
		K	8.68	K	8.55
		H_2O	3.84	H_2O	4.16
cis-K $[Co\ ile_2(NO_2)_2] \cdot H_2O$	66	Co	13.08	Co	12.97
		K	8.68	K	8.60
		H_2O	3.84	H_2O	4.70

* Calculated values are for anhydrous salts, except for the potassium salt of the α-amino-isobutyrate-complex, which remained monohydrate at 140°C.

2. *Preparation of Ag salts*

0.005 mole of the alkali *cis*-dinitrobis (aminoacidato) cobaltate (III) salt was dissolved in 10 ml water and 1.2 ml 5M silver nitrate (0.006 mole) slowly added to this with stirring. The sediment was filtered, washed with a little water, ethanol and ether and air-dried. The compound was then recrystallized several times from warm aqueous solution. The yield and analysis are given in Table 4.

TABLE 4.

Yield and Analysis of the Silver and Hydrogen Cis-*dinitrobis (aminoacidato) cobaltate (III) Complexes*

Compound	Yield* %	Analysis**			
		Calculated		Found	
cis-Ag [Co $\mathrm{abu_2(NO_2)_2}$]	90	Ag	23.29	Ag	23.23
cis-Ag [Co $\mathrm{aibu_2(NO_2)_2}$] · $3H_2O$	81	Ag $3H_2O$	23.29 10.45	Ag $3H_2O$	23.30 10.58
cis-Ag [Co $\mathrm{(\beta\text{-}abu)_2(NO_2)_2}$]	86	Ag	23.29	Ag	23.10
cis-Ag [Co $\mathrm{(\beta\text{-}aibu)_2(NO_2)_2}$]	86	Ag	23.29	Ag	23.20
cis-Ag [Co $\mathrm{val_2(NO_2)_2}$] · H_2O	76	Ag H_2O	21.96 3.52	Ag H_2O	22.06 3.70
cis-Ag [Co $\mathrm{nva_2(NO_2)_2}$]	85	Ag	21.96	Ag	21.99
cis-Ag [Co $\mathrm{nle_2(NO_2)_2}$]	72	Ag	20.78	Ag	20.95
cis-Ag [Co $\mathrm{ile_2(NO_2)_2}$]	77	Ag	20.78	Ag	20.80
cis-H [Co $\mathrm{abu_2(NO_2)_2}$]		Co	16.55	Co	16.56
cis-H [Co $\mathrm{aibu_2(NO_2)_2}$] · H_2O		Co H_2O	16.55 4.82	Co H_2O	16.45 6.00
cis-H [Co $\mathrm{(\beta\text{-}abu)_2(NO_2)_2}$]		Co	16.55	Co	16.63
cis-H [Co $\mathrm{(\beta\text{-}aibu)_2(NO_2)_2}$] · H_2O		Co H_2O	16.55 4.82	Co H_2O	16.48 4.90
cis-H [Co $\mathrm{val_2(NO_2)_2}$]		Co	15.34	Co	15.23
cis-H [Co $\mathrm{nva_2(NO_2)_2}$]		Co	15.34	Co	15.22
cis-H [Co $\mathrm{nle_2(NO_2)_2}$]		Co	14.29	Co	14.22
cis-H [Co $\mathrm{ile_2(NO_2)_2}$]		Co	14.29	Co	14.22

* Complex acids were obtained in almost quantitative yield.

** For analysis the substances were dried at 105°C for one hour, or at 80°C in vacuum. Calculated values for silver and cobalt are for anhydrous substance.

3. *Preparation of free acids*

The hydrogen *cis*-dinitrobis (aminoacidato) cobaltates (III) were obtained by running a 10% aqueous solution of the corresponding alkali salt on a column of a very acid cation-exchanger (Merck I) previously converted to the hydrogen form. The eluate was evaporated to dryness and the complex acids obtained in almost 100% yield. The results are given in Table 4.

School of Sciences, Institute of Chemistry,
Belgrade University
Institute of Chemistry, Technology and Metallurgy,
Belgrade

REFERENCES

1. Janjić, T., M. Ćelap, and P. Spevak. "Proučavanje reakcija heksanitro-kobaltata (III) s amino-kiselinama. I. Dobivanje dinitro-diglicinato-kobaltata(III)" (On the Reactions of Hexanitrocobaltates (III) with Amino Acids. I. Preparation of Dinitrodiglycinatocobaltates (III)) — *Glasnik hemijskog društva* (Beograd) 27 (2—3)*: 111—115, 1962.
2. Ćelap, M., T. Janjić, and D. Radanović. "Study of the Reactions of Hexanitrocobaltates (III) with Amino Acids. IV. The Reactions with DL-Alanine, D-Alanine, L-Alanine and β-Alanine" — *Inorganica Chimica Acta* 2: 52—57, 1968.
3. Ćelap, M., T. Janjić, and D. Radanović. "Salts of Dinitrobis (glycinato) cobalte(III)" — *Inorganic Syntheses* 9: 173—175, 1967.
4. Ćelap, M., D. Radanović, T. Janjić, and M. Malinar. "Proučavanje reakcija heksanitro-kobalta (III) s amino-kiselinama. III. Dobivanje dinitro-diglicinato-kobaltata (III) iz kompleksnih jedinjenja trovalentnog kobalta diaminskog, triaminskog, tetraaminskog, pentaminskog i heksaminskog tipa" (On the Reactions of Hexanitrocobaltates (III) with Amino Acids. III. Preparation of Potassium Dinitrodiglycinato-cobaltate (III) from Complex Cobaltic Compounds of the Diamine, Triamine, Tetramine, Pentamine and Hexamine Type) — *Glasnik hemijskog društva* (Beograd) 32 (8—9—10)*: 417——428, 1967.
5. Ćelap, M., D. Radanović, and T. Janjić. "Study of the Reactions of Hexanitrocobaltates (III) with Amino Acids. II. Determination of the Configuration of Dinitrobis (glycinato) cobaltate (III) Ions" — *Inorganic Chemistry* 4: 1494—1495, 1965.
6. Denning, R., M. Ćelap, and D. Radanović. "Study of the Reactions of Hexanitrocobaltates (III) with Amino Acids. V. Absolute Configuration and Geometrical Isomerism of Dinitrobis (aminoacidato) cobaltate (III) Ions" — *Inorganica Chimica Acta* 2: 58——61, 1968.
7. Shimura, Y. "The Relation Between the Geometrical Configurations of Inorganic Complexes and Their Absorption Bands. I. The Third Absorption Band of Trans--Dirhodanato-bis-Ethylenediamine-Cobalt (III) Chloride" — *Journal of the American Chemical Society* 73: 5079—5082, 1951.
8. Wentworth, R. A. D. and T. S. Piper. "Optical Activity of Pseudotetragonal Coordination Compounds. The Dissymmetric Ligand Field in Diacidobis (1-Propylenediamine) Cobalt Complexes" — *Inorganic Chemistry* 4: 202—205, 1965.
9. Matsuoka, N., J. Hidaka, and Y. Shimura. "Studies of the Mixed Amino-Acid Complexes of Cobalt (III). II. A Complete Series of [Co (ox)$_x$ (gly)$_y$ (en)$_z$] Complexes" — *Bulletin of the Chemical Society of Japan* 40: 1868—1874, 1967.

---

[*] Available in English translation from National Technical Information Service, Springfield, Virginia, 22151.

GLASNIK HEMIJSKOG DRUŠTVA, Vol. 35, No. 9–10, 1970, pp. 459–471

GHDB-125

563.36:539.219.1:547.538.141
Original Scientific Paper

LIGHT SCATTERING AND CHEMICAL INHOMOGENEITY OF POLY (STYRENE-CO-DIBUTHYLITACONATE)

by

JOVAN S. VELIČKOVIĆ AND JOVANKA M. FILIPOVIĆ

It has been found that the mean molecular weight of a copolymer cannot generally be determined by the light scattering technique usually used for homopolymers(1, 2). In 1952 Trembley, Rinfert and Rivest(3) showed that the intensity of scattering by dilute solutions of poly (styrene-co-butadiene) does not depend only on molecular weight but also on the distribution of monomer blocks within the copolymer chain. Shortly after this, Stockmayer and co-workers(4) derived an expression for the dependence of zero angle of scattering on chemical inhomogeneity when extrapolated to infinite dilution and zero scattering. In deriving this equation, a linear dependence of the increment of the refractive index of the copolymer solution on its molecular weight was assumed. Applying the relationship for calculating the mean molecular wieght of a homopolymer from the scattering of a dilute solutions to a copolymer, an equation for the apparent molecular weight (M_{ap}) is obtained:

$$\left(\frac{C}{R_\theta}\right)_{\substack{c\to o\\ \theta\to o}}=\frac{1}{K'\,\nu_o^2\,M_{ap}} \qquad (1)$$

where R=Rayleigh scattering ratio, c=concentration of the polymer in the solvent, ν_o=increment of the polymer refractive index in the solvent, and $K'=(2\pi^2\,n_o^2/\lambda_o^4\,N)\,.\,(1+\cos^2\theta)$, where n_o is the refractive index of the solvent in vacuum at wavelength λ_o, and N = Avogadro's constant.

Stockmayer's equation was soon verified by Buschuk and Benoit(5, 6), who found that the molecular weight of two different poly (styrene-co-methylmethacrylate) samples dissolved in different solvents obeyed it. They expanded Stockmayer's equation, which in a somewhat modified form not only proved to be suitable for calculating the true molecular weight, but also enabled quantitative determination of the inhomogeneity of the copolymer (by M_{ap}/M_w).

The basic relationship between the apparent molecular weight and the true molecular weights of the fractions is given by the equation

$$M_{ap}=\frac{1}{\nu_o^2}\sum\nu_i^2\,\gamma_i\,M_i, \qquad (2)$$

where ν_0 = increment of the copolymer refractive index in the solvent, and ν_i, γ_i and M_i the increment of the refractive index, weight proportion and molecular weight of the ith-fraction. If $\bar{x}$ denotes the weight that component a contributes to the copolymer, then ν_0 is given by

$$\nu_0 = \bar{x}\nu_a + (1-\bar{x})\,\nu_b, \tag{3}$$

where ν_a and ν_b are the increments of the refractive index of the primary homopolymers. Further, if δx_i is the deviation of the chemical composition x_i of the ith-fraction from the average composition of the copolymer, i. e.

$$\delta x_i = \bar{x} - x_i, \tag{4}$$

then by introducing

$$P = \sum \gamma_i M_i\,\delta x_i \tag{5}$$

and

$$Q = \sum \gamma_i M_i\,(\delta x_i)^2 \tag{6}$$

and combining equations (2—6), the relation between the apparent and true molecular weight may be written

$$M_{ap} = M_w + 2P\left(\frac{\nu_a - \nu_b}{\nu_0}\right) + Q\left(\frac{\nu_a - \nu_b}{\nu_0}\right)^2. \tag{7}$$

From equation (7) it may be seen that the apparent molecular weight is always larger than the true one, and that the difference between them is a sum of the products of the parameters of chemical inhomogeneity P and Q and terms involving only ν_0, ν_a and ν_b. In the physical sense P describes the change of chemical composition with the change of molecular weight, while Q is a measure of chemical heterogeneity. It may be seen that $M_{ap} = M_w$ only for chemically uniform copolymers, with $\delta x_i = 0$ (because then $P = Q = 0$), or for chemically heterogeneous polymers with $\nu_a = \nu_b$ (because then the second and third terms in the equation are zero).

According to Stockmayer⁽⁷⁾, in copolymers with azeotropic composition, or those with only a small degree of monomer conversion, and in random copolymers, in general, the change of composition with molecular weight is infinitesimal. Putting for these $P = 0$, equation (7) can be rewritten as a parabolic function symmetrical about the ordinate:

$$\frac{M_{ap}}{M_w} = 1 + \frac{Q}{M_w}\left(\frac{\nu_a - \nu_b}{\nu_0}\right)^2. \tag{8}$$

In this form it is independent of the molecular weight and much more convenient for graphical analysis. Possible Q values are defined by the inequality $0 < Q < M_w\,\bar{x}\,(1-\bar{x})$, so that Q/M_w, an even more convenient measure of chemical inhomogeneity, cannot (at least for a copolymer with equal parts by weight of the two monomers) exceed the maximum of $\bar{x}.\,(1-\bar{x}) = 0.25$

True molecular weight and P and Q can therefore be determined by the light scattered in three different solvents, and solving equation (7) for M_w, P and Q. However, experimental determination of the three variables involves great difficulties because in measuring light scattering the error may approach ±5%, and statistical "best fit" appears necessary even for a simplified parabolic function ($P=0$) in most solvents. In addition, determination of the coefficients of the parabola is difficult for its left half, because of the limited range of suitable solvents, and values approaching $M_{ap}/M_w=1$ are completely inaccessible.

Alternatively, the apparent and true molecular weight can, on the same principles⁽⁵⁾, be expressed as a function of M_w^A and M_w^B, i. e. of the molecular weights of the copolymer components A and B. While for a homopolymer mixture M_w can be determined by an equation equivalent to (2), for copolymers the equation is analogous to (8):

$$M_{ap}=\frac{\nu_a \cdot \nu_b}{\nu_0^2} M_w+\frac{\nu_a(\nu_a-\nu_b)}{\nu_0^2} \bar{x} M_w^A+\frac{\nu_b(\nu_b-\nu_a)}{\nu_0^2}(1-\bar{x}) M_w^B \tag{9}$$

For light scattering in solvents where either $\nu_a=0$ or $\nu_b=0$

$$M_{ap}=(1-\bar{x}) M_w^B \tag{10}$$

and

$$M_{ap}=\bar{x} M_w^A. \tag{11}$$

From these equations, the molecular weights of the components can easily be determined. In this method the extent of chemical inhomogeneity is expressed by

$$\bar{x} M_w^A+(1-\bar{x}) M_w^B \leqslant M_w \leqslant \frac{\bar{x} M_w^A+(1-\bar{x}) M_w^B}{1-2 \bar{x}(1-\bar{x})}, \tag{12}$$

where the left-hand side gives M_w for a homopolymer mixture, and the right for a chemically homogeneous copolymer.

The above theory of light scattering in copolymers has only been applied to a limited number of copolymer systems. For random copolymers, besides poly (styrene-co-methylmethacrylate) ⁽⁴⁻⁸, ¹⁰⁾, on which the theory was based, there are also some data in the literature on poly (styrene-co-acrylonitrile) by Japanese authors⁽¹¹⁻¹³⁾, and a recently published paper on poly (styrene-co-methylacrylate)⁽¹⁴⁾. These principles were successfully applied to anionically prepared poly (styrene-co-methylmethacrylate)⁽¹⁵⁾, in spite of the fact that with such block copolymers in solution segregation may take place in the polymer coil⁽¹⁶, ¹⁷⁾. On the other hand, there are papers in which the apparent molecular weight is, quite justifiably, taken as the true one in the case of solvents with a large increment of refractive index⁽¹⁸, ¹⁹⁾.

Determination of chemical inhomogeneity is particularly difficult if the refractive index increments of the primary homopolymers are close together. For such copolymers Kratochvil and Tuzar propose a method in which the copolymer solution is subjected to equilibrium dialysis before measuring the scattering⁽²⁰⁾; this method has been employed for poly (ethylene-glycolmethacrylate-methylmethacrylate)⁽²¹⁾.

Our aim was to apply the theory of light scattering to poly (styrene-co--di-n-buthylitaconate) with various average compositions critically examining the various limits of the technique and the accuracy attainable in calculating the molecular weights and inhomogeneity parameters. For comparison purposes, some experiments were also made with polystyrene.

EXPERIMENTAL

Copolymers were prepared by bulk polymerization of a mixture of monomers and α, α′-azobisisobuthyronitrile. Details of the synthesis and characterization may be found in ref. (22). Data on conversion, average content of styrene (calculated from carbon content, increment of refractive index and UV-absorption), viscosity in toluene at 25.0 °C, and the increment of refractive index in methylketone, are given in Table 1. All measurements were made in *p. a.* solvents of various manufacturers (BDH, Fluka, Merck), which were distilled, but without any further purification.

TABLE 1.
PS/DBI Copolymer, Synthesis and Characterization

Copolymer	Monomer conversion (%)	Average styrene content (%)	Viscosity (dl/g)	Increment of refractive index in MEK (cm^3/g)
PS/DBI-11	18.6	16.9±0.3	0.197	0.118
PS/DBI-21	22.7	33.7±0.2	0.404	0.141
PS/DBI-31	20.4	56.8±0.2	0.550	0.174
PS/DBI-41	26.2	73.8±0.2	0.575	0.193
PS/DBI-42	33.2	74.4±0.2	0.668	—
PS*	—	100	0.752	0.228

* Monsanto “Lustrex” (IUPAC INDUSTRIAL POLYSTYRENE)

The refractive index increments were measured at $20.0 \pm 0.^{02}$ °C at 436 m μ on a Brice-Phoenix Model 2000 differential refractometer, or were calculated according to equation (3). The solvents, their refractive indexes and the increment of refractive index of the primary homopolymers polystyrene (PS) and poly (di-n-buthylitaconate) (PDBI) are given in Table 2(23).

TABLE 2.
Refractive Index Increments of Primary Polymers in Various Solvents at λ =436 m μ *and* 20°*C*

Solvent	Abbr.	n_{20}	Increment of refractive index		
			PS	(cm^3/g)	PDBI
Ethylacetate	EAC	1.370	0.234		0.104
Methylethylketone	MEK	1.377	0.228		0.046
Amylacetate	AAC	1.400	0.205		0.074
Chloroform	CLF	1.444	0.165		0.036
Carbon tetrachloride	TCK	1.459	0.156		0.020
Toluene	TOL	1.494	0.112		—0.023
Benzyl alcohol	BOH	1.540	0.079		—0.056
Chlorbenzol	CLB	1.523	0.082		—0.050
Styrene monomer	MST	1.587	0.054		—0.077

Light scattering was measured at 20°C in the angle range from 30 to 135° using the same apparatus and a (C-105) cell of 50 cc volume. Molecular weight was determined by Zimm's extrapolation(24). The results for PS/DBI-21 copolymer in MEK and CHL are shown in Figs. 1 and 2. True molecular weights and inhomogeneity parameter Q were calculated statistically, using equation (7), and M_w^A and M_w^B by using equation (9).

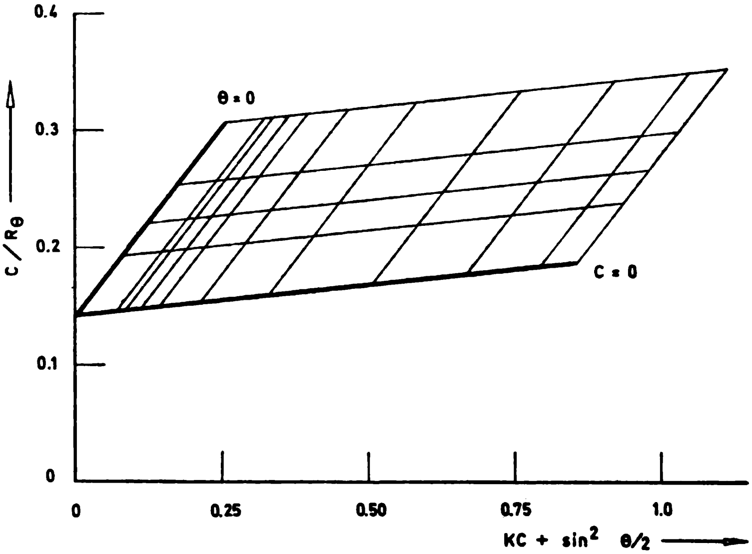

Fig. 1.
Extrapolation for PS/DBI-21 methylketone, at k=25

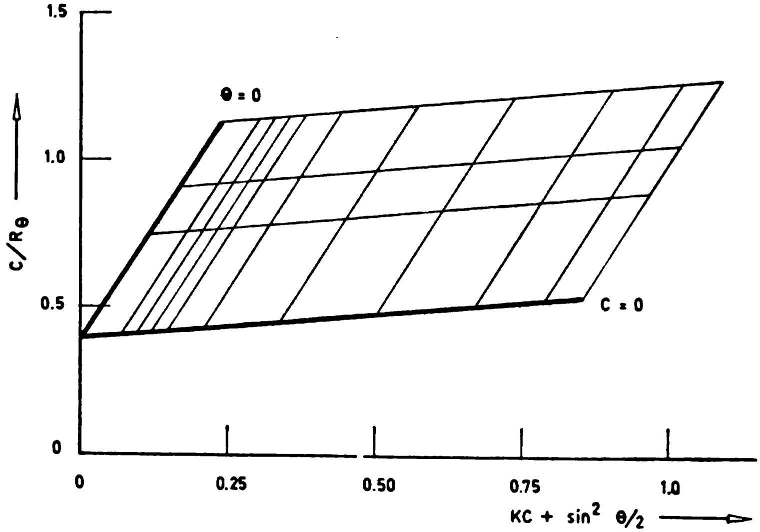

Fig. 2.
Extrapolation for PS/DBI-21 in chloroform, at k=25

RESULTS AND DISCUSSION

The results for apparent molecular weight of PS/DBI-11 copolymer with an average of 16.9% styrene (by weight) will first be discussed. Suitable solvents for light scattering measurements were chosen by reference to Fig. 3, which shows the refractive index increment in all potential solvents both for the primary homopolymers and all copolymers tested. Solvents in which the refractive index increment of a polymer is small are unsuitable due to the small scattering effect, since ν_0 appears in eqation (1) to the second power, and with the usual error of 0.001 in determination of the increments and dn/dc from —0.040 to +0.040, calculated molecular weights may differ by more than 5%. The shaded area in Fig. 3 shows the region of prohibitively small increments. Care must be taken that the solvent chosen is not too polar or volatile, but that it dissolves the polymer. Except for PS (and corresponding copolymers with small content of DBI) in acetone, the copolymer system studied is soluble in all the solvents considered here. Similar tests with poly (styrene-co-dimethylitaconate) were temporarily abandoned because it proved to be soluble at room temperature in only a few of the solvents used: only EAC, MEK, CLF and MST proved to be suitable for this copolymer.

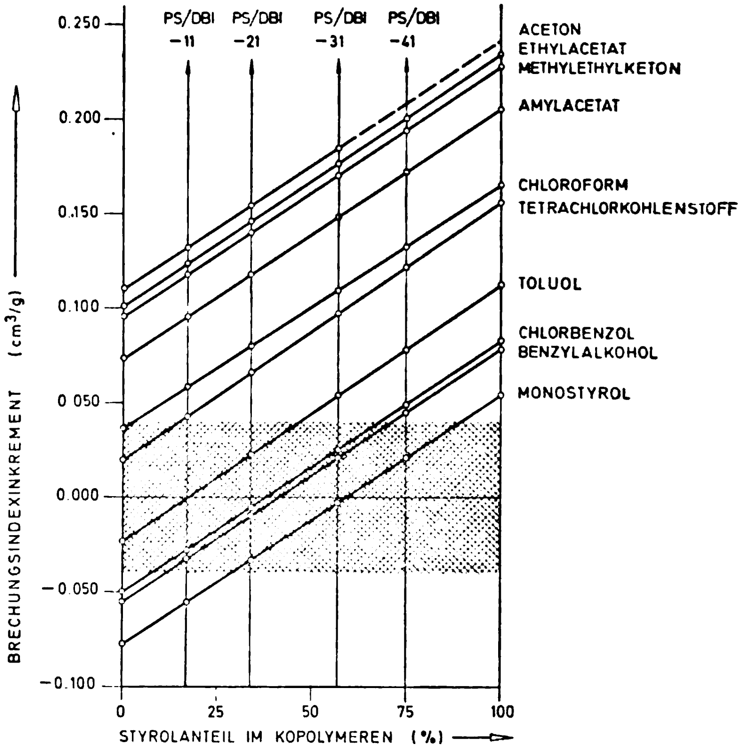

Fig. 3.

Refractive index increments in various solvents

For presentation of the results in the form of equation (8), numerical values of the ratio $(\nu_a - \nu_b) : \nu_o$ are most important. For polymers with very similar densities ($d_{PS} = 1.05$, $d_{PDBI} = 1.06 - 1.08$), as can be seen from the Gladstone-Dale equation for the dependence of the refractive index increment on polymer density(23), the difference $(\nu_a - \nu_b)$ does not depend on the solvent, and for such a copolymer system only the numerical value of ν_o need be examined.

The smallest positive value of this ratio is that in EAC, or even more acetone, and here the measured apparent molecular weight will be closest to the true one, but this point on the parabolic function is still too distant from the origin. However, for PS/DBI-41 the position of the minimum is clearly much more favorable.

In order to obtain the values on the left-hand part of the curve, ν_o must be negative. From Fig. 3 it may be seen that negative values of ν are practicable only for PS/DBI-11. Owing to the few solvents with a refractive index greater than 1.575, measurements were made in a carefully purified styrene monomer, stabilized with 0.01% hydroquinone.

The experimental results for molecular weight*, the corresponding ratios of the refractive index increment required for construction of the parabolic curve according to equation (8), and statistical values of M_w and Q for PS/DBI-11 copolymer are given in Table 3. The parabolic curve is shown in Fig. 4. The shaded areas A, B and E are inaccessible to the experimental technique. The boundaries B/C and C/D were calculated for bromoform and acetone.

TABLE 3.

Apparent Molecular Weight and Inhomogeneity Parameters of PS/DBI-11

Solvent	ν_o (cm³/g)	$\frac{\nu_a - \nu_b}{\nu_o}$	M_{ap}	$\frac{M_{ap}}{M_w}$
EAC	0.1235	1.077	80.800	1.171
MEK	0.1185	1.114	76.700	1.112
AAC	0.096	1.365	82.300	1.193
TCK	0.043	3.163	144.800	2.098
MST	—0.055	—2.382	109.300	1.584

$M_w = 69.000$
$Q = 7464$

$Q/M_w = 0.108$
$Q/Q_{max} = 0.77$

---

* The virial coefficient A_2, determined from Zimm's diagrams, ranged from 2.5 to $8.0 \cdot 10^{-4}$. The lower values were obtained for EAC, AAC and MEK, somewhat higher for TCK and TOL, and the highest for CLF. The results were not analyzed quantitatively because the copolymers tested had different molecular weights and the solvents used have different functional groups and solubility parameters, so that any analysis based on A_2 could only be qualitative.

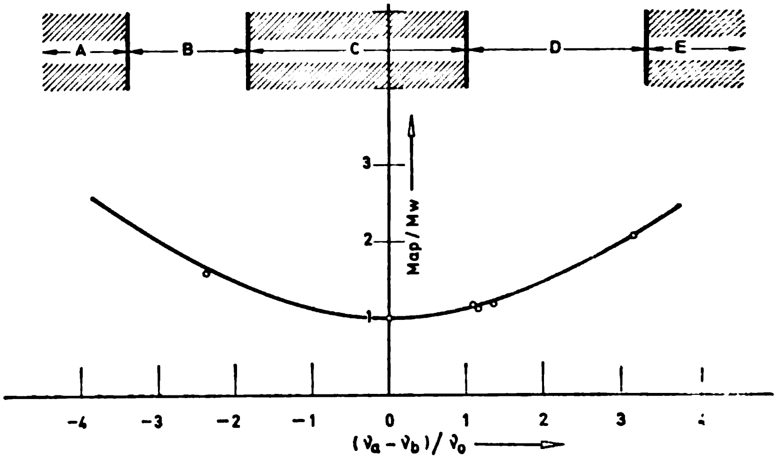

Fig. 4.
Results for PS/DBI-11 treated according to equation (8)

Experimental values of the apparent molecular weight of other copolymers tested in various solvents, and the true molecular weight of PS, are given in Table 4. The solvent independence of the molecular weight is evident for PS, while for all other copolymers there is a clear increase of M_{ap} with decreasing refractive index increment.

TABLE 4.
Apparent and True Molecular Weight of PS and Its Copolymers ($M_{ap} \cdot 10^{-}$)

Solvent	PS/DBI-21	PS/DBI-31	PS/DBI-41	PS/DBI-42	PS
EAC	—	223.6	191.4	262.2	257.9
MEK	172.2	228.0	195.4	259.5	260.0
AAC	173.4	248.8	198.5	262.4	255.0
CLF	203.5	275.4	—	277.2	—
TCK	210.3	301.4	212.4	277.0	259.4
TOL	—	363.2	208.8	294.0	—
M_w	156.0	229.6	194.6	257.6	258.2

In order to check whether the apparent molecular weights found fit with the theory of light scattering applied to the given copolymers, let us analyze Fig. 5 showing graphically the results from Table 4 (according to equation (7)). All the relationships for the various copolymers, and the PS/DBI-11 ratio from Fig. 4, show that the theory is uniquely satisfied for the whole copolymer system tested. This conclusion holds true in spite of the relatively short sections of the parabolic curve covered in Fig. 5, because especially for copolymers with PS/DBI-21 up to 42 any further determinations of the apparent molecular weight outside the range shown in Fig. 5 are inaccurate due to high experimental error.

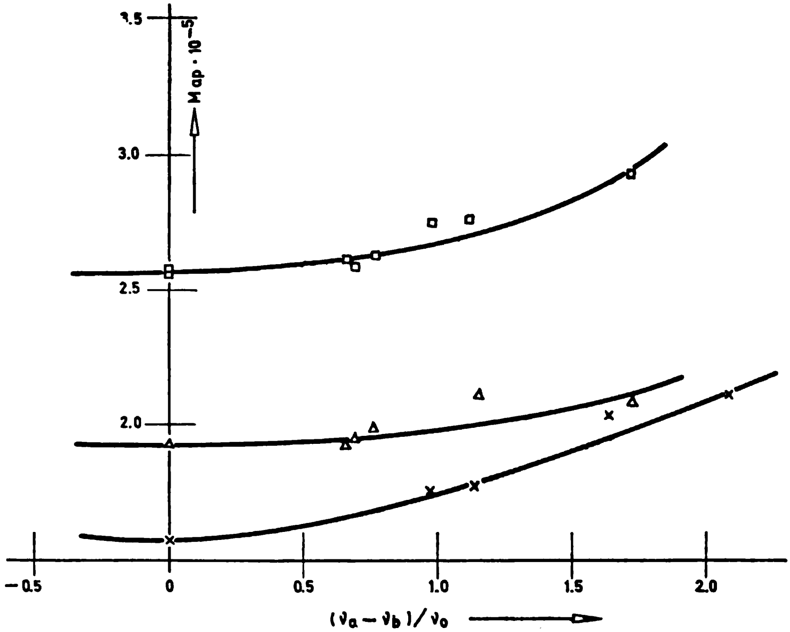

Fig. 5.
Results for PS (o), PS/DBI-21 (x), PS/DBI-41 (△), and PS/DBI-42 (□), treated according to equation (7)

The degree of chemical inhomogeneity is expressed by the parameters listed in Table 5. Of all the parameters, that in the last column is the most significant because it enables direct comparison of inhomogeneity, independently

TABLE 5.
Inhomogeneity Parameters of PS/DBI Copolymers

Copolymer	Q/M_w	$(Q/M_w)_{max}$	Q/Q_{max}
PS/DBI-11	0.108	0.140	0.77
PS/DBI-21	0.120	0.220	0.54
PS/DBI-31	0.099	0.245	0.40
PS/DBI-41	0.030	0.190	0.16
PS/DBI-42	0.050	0.190	0.26

of molecular weight and overall composition. According to the values shown, PS/DBI-41 can be considered chemically very homogeneous, while PS/DBI-42, which was polymerized with somewhat higher conversion (this leading to a gell-effect), can be considered highly heterogeneous. The relatively small value of 0.40 for PS/DBI-31 is probably due to its nearly azeotropic composition.

The apparent molecular weights found were analyzed statistically according to equation (9). The numerical values for the various copolymers are shown in Table 6.

TABLE 6.

Molecular Weights of the Copolymer Components

Copolymer	M_w^A	M_w^B	$\bar{x}M_w^A+(1-\bar{x})M_w^B$	$\frac{\bar{x}M_w^A+(1-\bar{x})M_w^B}{M_w}$	$1-2\bar{x}(1-\bar{x}$
PS/DBI-11	54.800	65.500	63.690	0.925	0.719
PS/DBI-21	91.200	120.300	110.550	0.709	0.553
PS/DBI-31	168.700	175.100	171.460	0.746	0.510
PS/DBI-41	153.000	87.200	135.890	0.700	0.613
PS/DBI-42	211.100	138.500	192.600	0.748	0.619

From this interpretation of the results, and as indicated by equation (12), $[\bar{x}\,M_w^A+(1-\bar{x})\,M_w^B] : M_w$ lies between unity (homopolymer mixture) and $1-2\bar{x}\,(1-\bar{x})$ (perfect homogeneity). From the values in the last two columns, using

$$\frac{Q}{Q_{\max}}=\frac{\dfrac{\bar{x}M_w^A+(1-\bar{x})M_w^B}{M_w}+2\bar{x}(1-\bar{x})-1}{2\bar{x}(1-\bar{x})},$$

the parameter of chemical heterogeneity $Q/Q_{\max}$ may be obtained.

Certain small deviations of these results from, e. g., 0.75 for PS/DBI-11, and 0.20 for PS/DBI-41, are probably due partly to the fact that equation (9) has not been reduced to only two unknowns.

ACKNOWLEDGEMENTS

The authors wish to express their thanks to the Fund for Scientific Work of the Socialist Republic of Serbia for financial support. Institute of Chemistry, Technology and Metallurgy, Belgrade School of Technology and Metallurgy, Belgrade University.

REFERENCES

1. Benoit, H. "Etude des solutions de copolymers par diffusion de la lumiere et viscosite" — *Berichte der Bunsengesellschaft für physikalische Chemie* (70): 286—296, 1966.
2. Rempp, P. and H. Benoit. "Determination of Copolymer Molecular Weight" — *Rubber Chemistry and Technology* (41): 245—253, 1968.
3. Tremblay, R., M. Rinfort, and R. Rivest. "Light Scattering by GR-S Solutions" — *Journal of Chemical Physics* (20): 523—532, 1952.
4. Stockmayer, W. H., L. D. Moore, Jr., M. Fixman, and B. N. Epstein. "Copolymers in Dilute Solutions. I. Preliminary Report for Styrene-Methylmethacrylate" — *Journal of Polymer Science* 14: 517—530, 1955.
5. Bushuk, W. and H. Benoit. "Light Scattering Studies of Copolymers. Effect of Chain Composition on the Molecular Weight" — *Canadian Journal of Chemistry* (36): 1616——1626, 1958.
6. Bushuk, W. and H. Benoit. "Etude de l'effet des heterogeneites de composition sur la determination du poids moleculaires des copolymers par diffusion de la lumiere" — *Comptes rendues* 246: 3167—3170, 1958.
7. Stockmayer, W. H. "Distribution of Chain Lengths and Compositions in Copolymers" — *Journal of Chemical Physics* (13): 199—207, 1945.
8. Baranovskai͡a, I. A., A. D. Litmanovich, M. S. Protasova, and V. E. Eskin. "Kompozit͡sionnai͡a neodnorodnost' statisticheskikh sopolimerov stirola s metilmetakrilatom" (Compositional Heterogeneity of Random Copolymers of Styrene with Methylmethacrylate) — *Vysokomolekul͡iarnye soedinenii͡a* 7: 509—512, 1965.
9. Eskin, V. E., I. A. Baranovskai͡a, A. D. Litmanovich, and A. V. Topchiev. "Kompozit͡sionnai͡a neodnorodnost' i frakt͡sionirovannie sopolimeravstirola s metilmetakrilatom" (Compositional Heterogeneity and Fractionation of Styrene -Methylmethacrylate) *Vysokomolekul͡iarnye soedinenii͡a* 6: 896—900, 1964.
10. Kotaka, T., Y. Murakami, and H. Inagaki. "Dilute Solution Properties of Styrene--Methylmethacrylate Random Copolymers" — *Journal of Physical Chemistry* (72): 829—841, 1968.
11. Shimura, Y., I. Mita, and H. Kambe. "Viscosity-Molecular Weight Relationship and Molecular Expansion of Styrene-Acrylonitrile Copolymers in Solution" — *Polymer Letters* 2: 403—407, 1964.
12. Kambe, H., I. Mita, and Y. Shimura. "The Influence of the Distribution of the Composition on the Light Scattering of the Styrene-Acrylonitrile Copolymer" — *Aeronautical Research Institute, University of Tokyo, Report No. 381* 29 (3): 31—37, 1964.
13. Shimura, Y. "Effects of Composition on the Solution Properties of Styrene-Acrylonitrile Copolymers" — *Journal of Polymer Science* A-2: 423—435, 1966.
14. Matsuda, H., K. Yamano, and H. Inagaki. "Styrene-Methacrylate Copolymers and Acrylate Homopolymers in Solution" — *Journal of Polymer Science* A-2: (7): 609—633 1969.
15. Krause, S. "Light Scattering of Copolymers. I. The Composition Distribution of a Styrene-Methylmethacrylate Block Copolymer" — *Journal of Physical Chemistry* (65): 1618—1622, 1969.
16. Freyss, D., P. Rempp, and H. Benoit. "Polydispersity of Anionically Prepared Block Polymers" — *Polymer Letters* 2: 403—404, 1964.
17. Dondos, A., P. Rempp, and H. Benoit. "Investigation on Conformation of Block and of Random Copolymers in Dilute Solutions" — *Macromoleculare Chemie* 130: 233—242, 1969.
18. Fischer, A. H. and W. Mächtle. "Untersuchungen an hochverdünnten Lössungen von statistischen Styrol-Acrylsäuremethylester Copolymeren" — *Kolloid Zeitschrift und Zeitschrift für Polymere* 230: 221—229, 1969.
19. Mächtle, W. "Untersuchungen an hochverdünnten Lösungen von einigen statistischen Copolymeren" — *Die angewandte macromolekulare Chemie* (10): 1—20, 1970.
20. Kratochvil, P. and Z. Tuzar. "Notes on the Determination of Heterogeneity in Chemical Composition of Copolymers by the Light Scattering Method", in: *6th IUPAC*

Microsymposium "Light Scattering in Polymer Science", *Communication F-4* — Praha: 1969.

21. Tuzar, Z., D. Strakova, and P. Kratochvil. "A Light Scattering Study of Ethylene Glycol Methacrylate-Methyl Methacrylate Copolymers", in: *6th IUPAC Microsymposium "Light Scattering in Polymer Science"*, *Communication F-4* — Praha: 1969.
22. Veličković, J., D. Jovanović, and J. Vukajlović. "The Unperturbed Dimensions of Poly (Styrene-Co-Dimethylitaconate)" — *Macromolekulare Chemie* 129: 203—214. 1969.
23. Veličković, J. and J. Vukajlović-Filipović. "Refractive Index of Di-n-Alkylitaconate Polymers and Copolymers" — *Angewandte Macromolekulare Chemie* (13): 79—88, 1970.
24. Zimm, B. H. "The Dependence of the Scattering of Light on Angle and Concentration in Linear Polymer Solutions" — *Journal of Physical and Colloid Chemistry* 52: 260—267, 1940.

GLASNIK HEMIJSKOG DRUŠTVA, Vol. 35, No. 9—10, 1970, pp. 473—479

GHDB-126 591.147:612.015.3:447.915:599.325;591.111.1

THE EFFECT OF INSULIN ON THE METABOLISM OF PROTEINS, LIPIDS AND GLUCIDES. XII. INFLUENCE OF SUCCESSIVE HYPERINSULINEMIA ON THE LIPOPROTEINS OF RABBIT BLOOD SERUM*

by

ANKA D. JEVTOVIĆ, PREDRAG P. MILOŠEVIĆ, and
JELENA J. BOJANOVIĆ

Earlier studies on blood serum lipoprotein levels in schizophrenic patients in insulin shock(1) revealed complex changes which depended on the state established several hours after administration of insulin. We judged that these results should be supplemented with a more detailed study of both the direct and delayed effects of insulin on blood serum lipoproteins in animals. More reliable data on the changes would thus be obtained, and the influence of various specific factors, such as disease, nutrition, behavior and earlier treatment, would be excluded(2, 3). Here we present the results obtained in studying the effect of successive hyperinsulinemia on the blood serum lipoproteins in rabbit. In one experimental group the changes taking place shortly after the injection of insulin (after 90 min.), and in the other the state established after some time (24 hours) were studied. From the results we tried to find if there was any correlation between the changes in the lipoproteins and other components of the blood serum and to trace the cause for the different distribution of electrophoretic lipoprotein fractions found in successive hyperinsulinemia.

MATERIAL AND METHOD

For these studies we used male rabbits of 2000 to 2500 g live weight. In one group the direct effect of insulin was studied, 90 minutes after administration, in the first, fifth, tenth and twentieth successive hyperglucemic shock. In the other group the delayed effect, i. e. the state established 24 hours after administration, after the first, fifth, tenth and twentieth successive dose, was studied. The effect was studied in two separate groups because successive taking of large quantities of blood would affect the state and changes caused by insulin. In both groups hyperinsulinemia was indu-

---

* A part of this paper was communicated at the 2nd Yugoslav Congress on Medical Biochemistry, Vrnjačka Banja, 1967.

ced with the same insulin dose, i. e. 15 units of crystalline insulin per kg live weight. Hypoglucemic coma was interrupted by injecting 3 ml 50% glucose into a marginal vein and 5 ml intramuscularly. When blood was not taken for analysis, hypoglucemic coma was interrupted by intramuscular injection of 16 ml 25% glucose. Blood samples were taken by cardiac puncture. Serum was obtained in the usual way. Lipoproteins were analyzed by paper electrophoresis after Swahn(5).

RESULTS AND DISCUSSION

The results for the lipoproteins evidence similar changes as those found in schizophrenic patients treated by insulin shock(1). After the first insulin injection, the changes of the relative content of lipoprotein fractions are small, manifested in a very slight decrease of large-molecule lipoproteins and an increase of small-molecule ones (Table 1). With repeated injections these changes are the same, but much more pronounced. The high level of large-molecule lipoproteins established 24 hours after administration of insulin (Table 2) is certainly caused by their increased production in the liver, which is highly stimulated by successive administration of insulin. This also explains the phenomenon that shortly after the injection of insulin (in shock) β-lipoproteins are very high, in spite of the fact that insulin removes them from the circulation. From the β:α ratio it is clear that the maximum changes in the lipoprotein fractions take place with the fifth insulin shock. The same applies to the delayed effect, i. e. 24 hours after the administration of insulin. Under the same experimental conditions, the changes in total proteins are greatest with the tenth shock(4), but the changes in the fractions with the lipid prosthetic groups reach their maximum much earlier, which agrees with the results obtained for lipoproteins.

In successive hyperinsulinemia the serum chylomicron content changed little, except with the fifth shock, when it decreased. However, 24 hours after administration of insulin it had dropped below normal, especially after the tenth and twentieth shock.

Institute of Chemistry, School of Medicine,
Belgrade University
Institute of Biochemistry, School of Medicine,
Belgrade University

TABLE 1. *Serum Liporotein Fractions in Successive Hyperinsulinemia (A) in first, (B) fifth, (C) tenth, and (D) twentieth insulin shock*

	α – lipoproteins					β – lipoproteins				
	N	A	B	C	D	N	A	B	C	D
No	12	8	9	7	8	12	8	9	7	8
R	28.6–37.2	27.9–37.6	26.8–35.7	18.9–34.2	24.8–31.6	40.1–52.4	43.4–52.7	48.9–59.4	45.6–59.5	49.6–62.2
M	32.9	33.3	29.8	28.5	27.4	48.3	47.7	54.0	52.9	53.2
SD	2.54	3.18	2.97	6.28	2.37	3.33	3.73	3.72	4.94	4.10
SE	0.73	1.12	0.99	2.37	0.84	0.96	1.32	1.24	1.87	1.45
CV%	7.72	9.55	9.97	22.03	8.65	6.89	7.82	6.89	9.34	7.71
a		+1.21	–9.42	–13.37	–16.72		–1.24	+11.80	+9.52	+10.14
b			–10.51	–14.41	–16.52			+13.21	+10.90	+11.53
c				–4.36	–8.05				–2.04	–1.48
d					–3.86					+0.57
a		$p>0.05$	$p<0.05$	$p\approx0.05$	$p<0.001$		$p>0.05$	$p<0.01$	$p<0.05$	$p<0.05$
b			$p=0.05$	$p>0.05$	$p<0.001$			$p<0.01$	$p=0.05$	$p<0.05$
c				$p>0.05$	$p>0.05$				$p>0.05$	$p>0.05$
d					$p>0.05$					$p>0.05$

	Chylomicrons					β/α				
	N	A	B	C	D	N	A	B	C	D
No	12	8	9	7	8	12	8	9	7	8
R	13.3–23.3	13.8–23.4	13.8–21.1	13.5–26.3	11.4–24.0	1.08–1.74	1.19–1.74	1.45–2.28	1.47–2.91	1.69–2.60
M	18.8	19.0	16.2	18.6	19.3	1.48	1.47	1.90	1.99	2.02
SD	3.39	3.73	2.37	4.71	4.16	0.17	0.20	0.27	0.62	0.29
CV%	18.03	19.63	14.63	25.32	21.55	11.48	13.61	14.21	31.16	14.36
a		+1.06	–13.83	–1.06	+2.66		–0.68	+28.38	+34.46	+36.49
b			–14.74	–2.11	+1.58			+29.25	+35.37	+37.41
c				+14.81	+19.14				+4.74	+6.32
d					+3.76					+1.51
a		$p>0.05$	$p\approx0.05$	$p>0.05$	$p>0.05$		$p>0.05$	$p<0.001$	$p<0.05$	$p<0.001$
b			$p>0.05$	$p>0.05$	$p>0.05$			$p<0.01$	$p\approx0.05$	$p<0.001$
c			$p>0.05$	$p>0.05$	$p>0.05$				$p>0.05$	$p>0.05$
d					$p>0.05$					$p>0.05$

No – number of cases
N – normal values
R – range of values
M – mean values

SD – standard deviation
SE – standard error
CV% – coefficient of variation

Percentage of decrease or increase and significance are given as regards the level before (a) and first (b), fifth (c) and tenth (d) insulin shock.

TABLE 2. *Serum Lipoprotein Fractions Before and 24 Hours After First (A), Fifth (B), Tenth (C), and Twentieth (D) Insulin Shock*

	α — lipoproteins					β — lipoproteins				
	N	A	B	C	D	N	A	B	C	D
No	12	8	8	9	9	12	8	8	9	9
R	28.6−37.2	31.2−42.9	22.5−30.9	22.1−36.4	24.8−39.8	40.1−52.4	41.2−54.6	48.7−62.6	49.5−60.8	45.7−62.3
M	32.9	36.4	26.2	26.5	31.5	48.3	47.9	55.8	56.6	55.0
SD	2.54	4.25	3.42	4.85	4.75	3.33	4.67	4.43	3.84	5.34
SE	0.73	1.50	1.21	1.62	1.50	0.06	1.65	1.57	1.28	1.78
CV%	7.72	11.68	13.05	18.30	15.08	6.89	9.75	7.94	6.78	9.71
a		+10.64	−20.36	−19.45	−4.25		+0.83	+15.53	+17.18	+13.87
b			−28.02	−27.20	−13.46			+16.49	+18.16	+14.82
c				+1.14	+20.23				+1.43	−1.43
d					+18.87					−2.83
a		$p=0.05$	$p<0.001$	$p\approx0.001$	$p>0.05$		$p>0.05$	$p<0.001$	$p<0.001$	$p<0.01$
b			$p<0.001$	$p<0.001$	$p\approx0.05$			$p<0.01$	$p=0.001$	$p<0.05$
c				$p>0.05$	$p<0.05$				$p>0.05$	$p>0.05$
d					$p=0.05$					$p>0.05$

	Chylomicrons					β/α				
	N	A	B	C	D	N	A	B	C	D
No	12	8	8	9	9	12	8	8	9	9
R	13.3−23.3	9.8−21.3	12.7−22.5	14.1−22.1	10.8−17.4	1.08−1.74	1.03−1.75	1.58−2.73	1.36−2.66	1.15−2.42
M	18.8	15.6	18.0	16.9	13.5	1.48	1.34	2.17	2.21	1.80
SD	3.39	3.57	3.35	2.49	2.51	0.17	0.26	0.40	0.47	0.42
SE	0.98	1.26	1.19	0.83	0.84	0.05	0.09	0.14	0.16	0.14
CV%	18.03	22.88	18.61	14.73	18.59	11.48	19.40	18.43	21.27	23.33
a		−17.02	−4.26	−10.11	−28.19		−9.46	+46.62	+49.32	+21.62
b			+15.38	+8.33	−13.46			+61.94	+64.93	+34.33
c				−6.11	−25.00				−1.84	−17.05
d					−20.12					−18.55
a		$p\approx0.05$	$p>0.05$	$p>0.05$	$p\approx0.001$		$p>0.05$	$p<0.001$	$p<0.001$	$p<0.05$
b			$p>0.05$	$p>0.05$	$p>0.05$			$p<0.001$	$p<0.001$	$p<0.05$
c				$p>0.05$	$p=0.01$				$p>0.05$	$p>0.05$
d					$p=0.01$					$p\approx0.05$

No — number of cases
R — range of values
M — mean values

SD — standard deviation
SE — standard error
CV% — coefficient of variation

Percentage of decrease or increase and significance are given as regards the level before (a) and 24 hours after first (b), fifth (c) and tenth (d) insulin shock.

REFERENCES

1. Bojanović, J., A. Jevtović, and M. Čorbić. "Uticaj insulina na metabolizam belančevina, lipida i glicida. VIII. Dejstvo uzastopnih hiperinsulinemija na lipoproteine krvnog seruma" (The Effect of Insulin on the Metabolism of Proteins, Lipids and Glucides. VIII. Influence of Successive Hyperinsulinemia on Blood Serum Lipoproteins) — *Glasnik hemijskog društva* (Beograd) 29*: 157—163, 1964.
2. Bojanović, J., M. Levental-Karakušević, and K. Nikolić. "Uticaj insulina na metabolizam belančevina, lipida i glicida. II. Sadržaj lipidnih sastojaka seruma osoba obolelih od šizofrenije, i njihove promene u dubokoj insulinskoj komi" (The Effect of Insulin on the Metabolism of Proteins, Lipids and Glucides. II. The Content of Serum Lipids in Schizophrenic Patients in Deep Insulin Coma) — *Acta Medica Iugoslavica* 16*: 151—165, 1962.
3. Bojanović, J., A. Jevtović, M. Čorbić, and K. Nikolić. "Uticaj insulina na metabolizam belančevina, lipida i glicida. V. Dejstvo uzastopnih hiperinsulinemija na belančevine krvnog seruma" (The Effect of Insulin on the Metabolism of Proteins, Lipids and Glucides. V. Influence of Successive Hyperinsulinemia on Blood Serum Lipoproteins) — *Glasnik hemijskog društva* (Beograd) 28*: 465—477, 1963.
4. Jevtović, A. *Uticaj neposrednog i produženog efekta insulina na metabolizam belančevina* (The Direct and Delayed Effects of Insulin on the Metabolism of Proteins) (Thesis) — Beograd: 1965.
5. Swahn, B. "Determination of Total Lipids in Serum" — *Scandinavian Journal of Clinical Laboratory Investigation* 4: 98, 1952; *Blood Lipids Suppl.* 5: 9, 1953.

---

* Available in English translation from National Technical Information Service, Springfield, Virginia, 22151

GLASNIK HEMIJSKOG DRUŠTVA, Vol. 35, No. 9—10, 1970, pp. 481—485

GHDB-127 591.147:612.015.3:547.96:547.915:599.325

THE EFFECT OF INSULIN ON THE METABOLISM OF PROTEINS, LIPIDS AND GLUCIDES. XIII. INFLUENCE OF SUCCESSIVE HYPERINSULINEMIA ON BLOOD SUGAR LEVEL IN RABBIT

by

JELENA J. BOJANOVIĆ, ANKA D. JEVTOVIĆ, and
PREDRAG P. MILOŠEVIĆ

Its remarkable effect on glucemia was the earliest noticed and for long the most studied effect of insulin. The decrease in blood sugar was explained by an increased incorporation of glucose into the liver glycogen and suppression of its release into the circulation(1). The works of Cori and co-workers(6–8) contributed considerably to the explanation of the role of endogenous insulin in the metabolism of carbohydrates and constituted a breakthrough in the study of its physiological role. More recent studies, especially those employing labelled compounds and isolated tissues, have yielded much new which may help explain not only the various effects of insulin but also the mechanism of the processes involved(2, 12, 14–16). Our earlier studies of the effect of insulin on the metabolism of proteins, amino acids, lipoproteins and nucleic acids(3–5, 11, 13) showed that both the direct and delayed effect observed for a single injection of insulin are changed in successive hyperinsulinemia. Therefore we considered it interesting to study glucemia and liver glycogen in animals given large doses of insulin every day. We considered that the results might help elucidate the processes induced by insulin and the relationship between the altered metabolisms of proteins, lipids and carbohydrates, and contribute to our knowledge of the state established by long-term insulin treatment of human patients. The direct and delayed, effects of successive hyperinsulinemia on glucemia are described in the present paper.

MATERIAL AND METHOD

Male rabbits of 2000—2500 g live weight were given 15 units of crystalline insulin per kg weight (*i. m.*) per day for 20 days. Glucemia was determined by the method given by Hagedorn and Jensen(9, 10), on blood samples taken by cardial puncture before the first, and then in the first, fifth, tenth and twentieth insulin shock, 90 minutes after the administration of insulin. Immediately after taking the blood sample, the hypoglucemic coma was interrupted by injecting 3 ml 50% glucose into a marginal vein. In order to maintain the glucemic state until the animal recovered from the hypoglucemic coma, 5 ml 50% glucose was injected intramuscularly. On the days when blood was not sampled the hypoglucemic coma was interrupted by intramuscular injection of glucose. In the second experimental group, for the study of the delayed effect of insulin, blood was taken 24 hours after the first, fifth, tenth and twentieth insulin injection. The results are given in Tables 1 and 2.

RESULTS AND DISCUSSION

Earlier studies of the effect of hyperinsulinemia on proteins, lipoproteins, polypeptides and amino acids(3–5, 11) showed that daily administration of large doses of insulin altered the intensity of changes. Similarly, the effect on glucemia was not only pronounced but also much intensified. In successive hyperinsulinemia the level of blood sugar is appreciably lower than is the case with a single injection of insulin (Table 1). Blood sugar was

TABLE 1.

Direct Effect of Insulin on Blood Sugar Level in Rabbit

	N	1	5	10	20
R	112—144	55—78	37—67	37—64	39—55
M	125	67	54	54	46
SD	8.54	8.28	10.22	9.50	5.38
SE	2.13	2.94	3.61	3.59	2.03
CV%	6.83	12.37	18.92	17.59	11.69
a		—46.40	—56.80	—56.80	—63.20
b			—19.40	—19.40	—31.34
c				—	—14.81
d					—14.81
a		$p<0.001$	$p<0.001$	$p<0.001$	$p<0.001$
b			$p<0.05$	$p<0.05$	$p<0.001$
c				—	$p>0.05$
d					$p>0.05$

Glucemia was determined in blood of 16 rabbits (N). The same were given insulin every day for total twenty days. Blood was taken for analysis 90 minutes after first (1; 8 animals), fifth (5; 8 animals), tenth (10; 7 animals), and twentieth (20; 7 animals) insulin shock.

R — range of values
M — mean values
SD — standard deviation
SE — standard error
CV% — coefficient of variation

Percentage of decrease or increase and significance are given as regards the level in normal animals (a) and in first (b), fifth (c) and tenth (d) insulin shock.

lowest at the twentieth insulin shock — 30% lower than in the first and 15% lower than in the fifth and tenth shock. Several hours after the injection of insulin (delayed effect) it returned to almost normal (Table 2). The glucemia found 24 hours after the injection of insulin suggests that blood sugar increased more the lower it fell during the shock. However, in spite of the great increase, 24 hours after the insulin injection blood sugar did not reach its normal level (64% increase above the level in the first shock). After the fifth and tenth shock, when it was 19% less than in the first, blood sugar increased much more than after the first insulin injection (increases of 146% and 152%, respectively, relative to the level during the shock). After the twentieth shock, when it was lowest, blood sugar did not reach its normal level at all, in spite of a 152% increase (two and a half times as great as after the first shock). Assuming that the level of liver glycogen changes with successive administration of insulin and that it is high (as found in rats(17)), it may be concluded that the steady release of glucose into the circulation does not depend on the amount of bound glucose but tends to establish normal glucemia. However, the direct and delayed effect of successive insulin shots on the metabolism of glucose (e. g. catabolism, lipogenesis, absorption into the cells of other organs) and its connection with the changes of glucemia require study.

TABLE 2.

Delayed Effect of Insulin on Blood Sugar Level in Rabbit

	N	1	5	10	20
R	111—144	94—130	123—146	117—143	104—134
M	125	110	133	136	116
SD	8.54	12.5	7.9	9.4	10.9
SE	2.13	4.4	3.2	3.5	4.4
CV%	6.83	11.4	5.9	6.9	9.4
a		—12.00	+6.40	+8.80	—7.20
b			+20.91	+23.64	+5.45
c				+2.26	—12.78
d					—14.71
a		$p<0.01$	$p\approx0.05$	$p<0.05$	$p\approx0.05$
b			$p<0.01$	$p=0.01$	$p>0.05$
c				$p>0.05$	$p=0.01$
d					$p<0.01$

Glucemia was determined in blood of 16 rabbits (N). The same were given insulin every day for 20 days. Blood was taken for analysis 24 hours after first (1; 8 animals), fifth (5; 6 animals), tenth (10; 7 animals), and twentieth (20; 6 animals) insulin shock.

R — range of values
M — mean values
SD — standard deviation
SE — standard error
CV% — coefficient of variation

Percentage of decrease or increase and significance are given as regards the level in normal animals (a) and in first (b), fifth (c) and tenth (d) insulin shock.

From the results it is evident that the direct effect on the metabolism of carbohydrates (i.e. their release into the circulation), unlike effect on the metabolism of proteins$^{(3-5, 11)}$, is more pronounced in successive hyperinsulinemia. The changes induced by the direct effect are corrected during the delayed effect (i. e. the effects are opposite), which is not the case for the protein fractions of blood serum.

Institute of Chemistry, School of Medicine,
Belgrade University

Institute of Biochemistry, School of Medicine,
Belgrade University

REFERENCES

1. Banting, F. G. and C. H. Best. "The Internal Secretion of the Pancreas" — *The Journal of Laboratory and Clinical Medicine* 7: 251—266, 1922.
2. Berthet, J., P. Jacques, H. G. Hers, and C. De Duve. "Influence de l'insuline et du glucagon sur la synthèse de glycogène hépatique" — *Biochimica et Biophysica Acta* 20: 190—200, 1956.
3. Bojanović, J., A. Jevtović, and M. Čorbić. "Uticaj insulina na metabolizam belančevina, lipida i glicida. VIII. Dejstvo uzastopnih hiperinsulinemija na lipoproteine krvnog seruma" (The Effect of Insulin on the Metabolism of Proteins, Lipids and Glucides. VIII. The Influence of Successive Hyperinsulinemia on Blood Serum Lipoproteins) — *Glasnik hemijskog društva* (Beograd) 29*: 157—163, 1964.
4. Bojanović. J., A. Jevtović, M. Čorbić, and K. Nikolić. "Uticaj insulina na metabolizam belančevina, lipida i glicida. V. Dejstvo uzastopnih hiperinsulinemija na belančevine krvnog seruma" (The Effect of Insulin on the Metabolism of Proteins, Lipids and Glucides. V. The Influence of Successive Hyperinsulinemia on Blood Serum Proteins) — *Glasnik hemijskog društva* (Beograd) 28*: 465—477, 1963.
5. Bojanović, J., A. Jevtović, M. Čorbić, and O. Bugarski. "Uticaj insulina na metabolizam belančevina, lipida i glicida. X. Dejstvo uzastopnih hiperinsulinemija na raspodelu elektroforetskih frakcija belančevina krvnog seruma osoba obolelih od šizofrenije" (The Effect of Insulin on the Metabolism of Proteins, Lipids and Glucides. X. The Influence of Successive Hyperinsulinemia on the Distribution of Electrophoretic Fractions of Blood Serum Proteins in Schizophrenic Patients) — *Glasnik hemijskog društva* (Beograd) 32*: 343—356, 1967.
6. Cori, C. F. "Insulin and Liver Glycogen" — *The Journal of Pharmacology and Experimental Therapeutics* 25: 1—33, 1925.
7. Cori, C. F. and G. T. Cori. "The Fate of Sugar in the Animal Body. VIII. The Influence of Insulin on the Utilization of Glucose, Fructose and Dihydroxy-Acetone" — *The Journal of Biological Chemistry* 76: 755—795, 1928.
8. Cori, C. F. "Enzymic Reactions in Carbohydrate Metabolism" — *Harvey Lecture Series* 41: 253—272, 1945—1946.
9. Hagedorn, H. C. and B. N. Jensen. "The Microdetermination of Blood Sugar by Means of Ferricyanide" — *Biochemische Zeitschrift* 135: 46—58, 1923.
10. Hagedorn, H. C. and B. N. Jensen. "The Ferricyanide Method for Blood Sugar. II. "— *Biochemische Zeitschrift* 137: 92—95, 1923.
11. Jevtović, A., P. Milošević, and J. Bojanović. "Uticaj insulina na metabolizam belančevina, lipida i glicida. XII. Dejstvo uzastopnih hiperinsulinemija na lipoproteine krvnog seruma zeca" (The Effect of Insulin on the Metabolism of Proteins, Lipids and Glucides. XII. The Influence of Successive Hyperinsulinemia on the Lipoproteins of Rabbit Blood Serum) — *Glasnik hemijskog društva* (Beograd) 36 (*9—10*): 1970 (this issue).

12. Madison, L. L., B. Combes, R. Adams, and W. Strickland. "The Physiological Significance of the Secretion of Endogenous Insulin Into the Portal Circulation. III. Evidence for a Direct Immediate Effect of Insulin on the Balance of Glucose Across the Liver" — *The Journal of Clinical Investigation* 39: 507—522, 1960.
13. Milošević, P. Habilitation thesis, Belgrade, 1966.
14. Mortimore, G. E. "Effect of Insulin on Release of Glucose and urea by Isolated Rat Liver" — *The American Journal of Physiology* 204: 699—704, 1963.
15. Steiner, D. F. and J. King. "Induced Synthesis of Hepatic Uridine Diphosphate Glucose-Glycogen Glucosyltransferase after Administration of Insulin to Alloxan--Diabetic Rats" — *The Journal of Biochemical Chemistry* 239: 1392—1398, 1964.
16. Vinuela, E., M. Salas, and A. Sols. "Glucokinase and Hexokinase in Liver in Relation to Glycogen Synthesis" — *The Journal of Biological Chemistry* 238: PC 1175-7, 1963.
17. Bojanović, J., P. Milošević, R. Kovačević, and O. Djordjević-Čomba. "Uticaj insulina na metabolizam belančevina, lipida i glicida. XI. Dejstvo uzastopnih hiperinsulinemija na nivo glikogena u jetri pacova" (The Effect of Insulin on the Metabolism of Proteins, Lipids and Glucides. XI. The Influence of Successive Hyperinsulinemia on Rat Liver Glycogen) — *Glasnik hemijskog društva* (Beograd) 33*: 387—391, 1968.

---

* Available in English translation from National Technical Information Service, Springfield, Virginia, 22151.

GLASNIK HEMIJSKOG DRUŠTVA, Vol. 35, No. 9–10, 1970, pp. 487–495

GHDB-128

543.257:543.244.6:546.73:546.46
Original Scientific Paper

COULOMETRIC-COMPLEXOMETRIC DETERMINATION OF CATIONS

by

DARINKA J. STOJKOVIĆ AND SVETLANA R. DRAVIĆ

There are two principal ways of using EDTA in coulometry, i. e. either the chelate is determined coulometrically or the ethylenediaminetetraacetate (EDTA) ion is first generated by electrolysis and then used for coulometric determination of the cations forming stable complexes with it.

In these determinations we employed a method given by Reilley and Porterfield⁽¹⁾. EDTA ion Y^{4-} generated by constant current electrolytic reduction of freshly prepared mercuric chelate is used for coulometric titration of the metalic ion concerned:

$$HgY^{2-} + 2e \xrightarrow{\qquad} Hg + Y^{4-}$$

$$Ca^{2+} + Y^{4-} \xrightarrow{\qquad} CaY^{2-}$$

We used Y^{4-} for determination of cobalt and magnesium.

EXPERIMENTAL

The apparatus for coulometric-complexometric-potentiometric determinations (Fig. 1) consists of a coulometric (or generator) and a potentiometric (or indicator) circuit. The coulometric cell has three compartments: anodic, cathodic, and a middle one separated from the first two by sintered-glass discs. Because of the coarse grains of these discs they were coated with a layer of agar-agar: K_2SO_4 mixture. The cathode was a layer of mercury at the bottom of the cathodic compartment. This compartment was closed with a four-hole stopper. The catholyte was agitated with magnetic stirrer. The anode was a platinum spiral. The cell was connected to an SCE through the middle compartment.

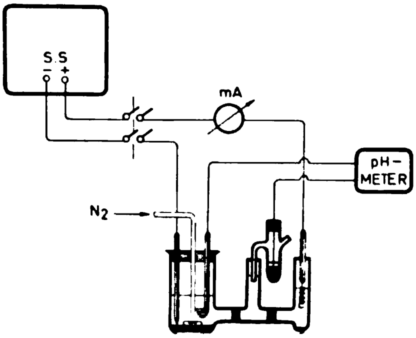

Fig. 1.
Apparatus used for coulometric-complexometric-potentiometric determination of cations

Potentiometric circuit consisted of a dropping mercury indicator electrode and a reference SCE. The potential changes were monitored by pH-meter.

All chemicals were *p. a.*, and their solutions were prepared with double distilled water.

The solution of mercuric chelate (HgH_2Y; or Hg-EDTA solution) was made by dissolving 9.3 g of disodium ethylene-diaminetetraacetate ($Na_2H_2Y \cdot 2H_2O$) and 8.65 g $Hg(NO_3)_2 \cdot 1/2H_2O$ in 250 ml water. The solution (0.1 N HgH_2Y) had an excess of mercuric ions, because in order to ensure thorough chelating of H_2Y^{2-} with mercury $Hg(NO_3)_2 \cdot 1/2H_2O$ was taken in somewhat more than the stoichiometric ratio. This excess was eliminated by electrolysis before use. The solution was acid (pH=1) and unstable; after standing for a while white flakes precipitated, but it can be stabilized by adding NH_4OH to pH7 and 0.1 N NH_4NO_3 buffer. The actual electrolyte thus consisted of 250 ml 0.1 N HgH_2Y and 670 ml 0.1 N NH_4NO_3⁽¹⁾.

For successful titration EDTA ion should be generated with 100% current utilization. This was achieved by electrolyzing the ammoniacal solution of mercuric chelate (HgH_2Y) at a constant current of 40 mA. This current was chosen because with HgH_2Y at its lowest critical concentration ($7 \cdot 10^{-3}$ M,) according to Reilley and Porterfield⁽¹⁾, EDTA ion is generated with 100% current utilization at a maximum of 43±0.04 mA. As, in our example, the concentration was much higher than critical and the current smaller than maximum, the conditions for 100% current efficiency were favorable.

DETERMINATION OF COBALT

All complexometric techniques require a certain pH at which the reaction will be quantitative. The pH corresponding to various cations can be found from curves of the potential difference against pH (pK—pH)⁽¹⁾, or logarithm of K against pH⁽³⁾. These curves show that cobalt forms a stable complex

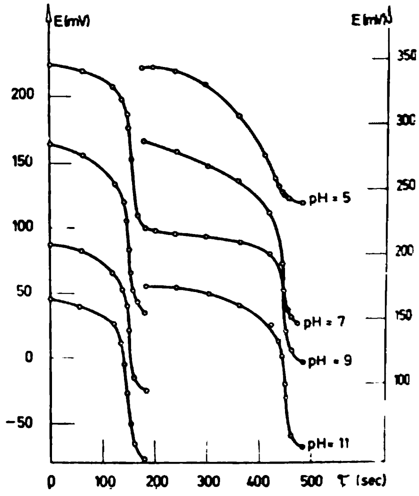

Fig. 2.
Effect of pH on the coulometric-potentiometric curves in titration of Co^{2+} ions

with EDTA ($K=10^{16}$) and can be determined in solutions at pH=4. But, as the concentration of Co-chelate increases with pH, the conditions for its accurate determination are also improved.

In order to find out the best pH for coulometric-complexometric titration of cobalt, we plotted several potentiometric curves for various pHs. From these we concluded that the best results were obtained at pH 8.5, i. e. the same as used in volumetric and potentiometric complexometry(4, 8).

Procedure

Standard solution of cobalt, made by dissolving 1.50 g $Co(NO_3)_2$ in 250 ml water, was titrated with 0.1 M Complexon III at pH 9 using catechol as indicator(4). One ml of the solution was found to contain 1.23 mg cobalt.

The cathodic compartment of the generator circuit was filled with 40 ml mercuric chelate and its pH adjusted to 8.5 by adding concentrated ammo-

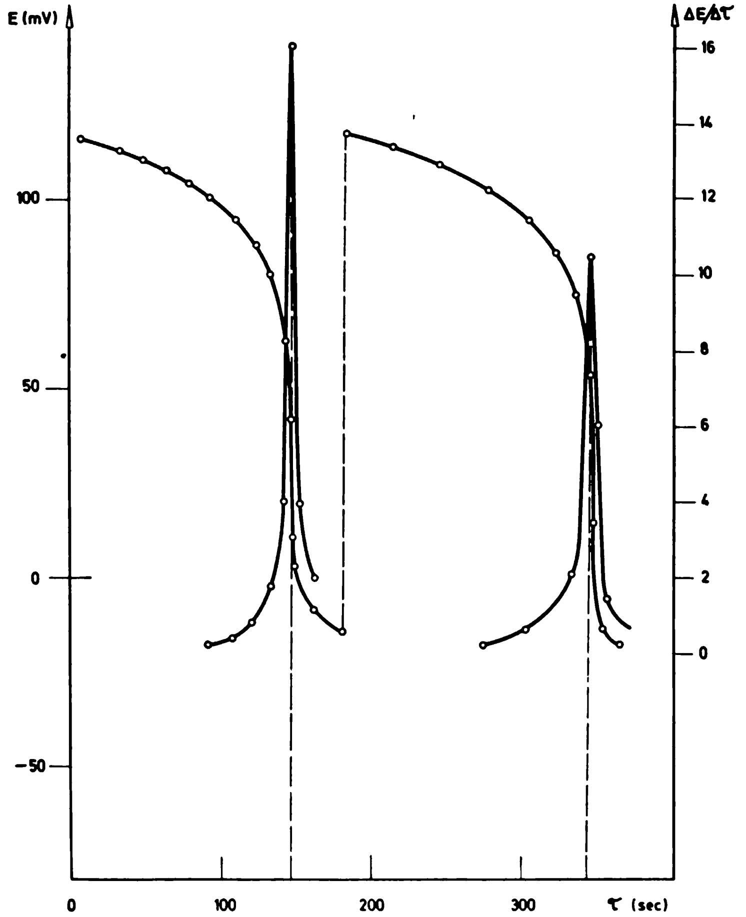

Fig. 3.
Coulometric-potentiometric titration of Co^{2+} ion

nia. Ammonia was, in fact, added until the potential difference between the indicator electrode and SCE reached 0.1—0.12 V. We made use of the linear relation between the potential of mercury and pH. In order to remove oxygen, nitrogen was bubbled through the catholyte for 10 minutes. The anolyte and the middle compartment were filled with saturated solution of K_2SO_4.

The excess of mercuric ions was first neutralized by electrolytic reduction, recording the change of potential with time. An abrupt potential jump indicated that all the excess had been neutralized. There upon electrolysis was stopped, some cobalt solution added from a microburette, and the pH again adjusted to 8.5, at which the indicator electrode regained its former potential of 100—120 mV. After this nitrogen was bubbled through for 5 minutes and the coulometric (electrolytic) circuit switched on again, monitoring the titration with the pH-meter.

For illustration, the potentiometric curves E=f(t) and E/t=f(t) are shown in Fig. 3.

The titration time of cobalt is taken to be the interval between the singular points on the pre-titration and titration curves (Fig. 3).

The amount of cobalt is calculated from the time and the titration current, using Faraday's laws.

The results of coulometric titration of cobalt with EDTA are given in Table 1.

TABLE 1.
Coulometric Titration of Co^{2+} with EDTA
at pH=8.5 and I=40.0 mA

No.	Taken mg	Found mg	Error		Current mA	Time (theoretical) sec.
			mg	%		
1	1.230	1.218	—0.012	—0.9	40.0	99.0
2		1.206	—0.024	—1.1		
3		1.218	—0.012	—0.9		
4	2.460	2.472	+0.012	0.4		198.0
5		2.466	+0.006	0.2		
6		2.448	—0.012	—0.4		
7	3.690	3.684	+0.006	0.1		297.0
8		3.690	—	—		
9		3.702	+0.012	0.3		
10	4.920	4.920	—	—		396.0
11		4.932	+0.012	0.2		
12		4.918	—0.012	—0.2		
13	6.150	6.150	—	—		495.0
14		6.162	+0.012	0.2		
15		6.150	—	—		

DETERMINATION OF MAGNESIUM

The apparatus and procedure were the same as for Co. Potentiometric-coulometric curves E=f(t) were recorded for various pH. From Fig. 4 it may be seen that the slope of the potentiometric curve and the potential jump change with pH: this may be ascribed to the increasing stability constant of magnesium chelate. Since curves 10 and 11 have a very gentle slope, the best pH for titrating magnesium with EDTA may be considered to lie within the range between these curves. We chose pH = 10.5. This value was obtained by adding concentrated ammonia to the catholyte until the potential at the indicator electrode reached 40 mV against SCE.

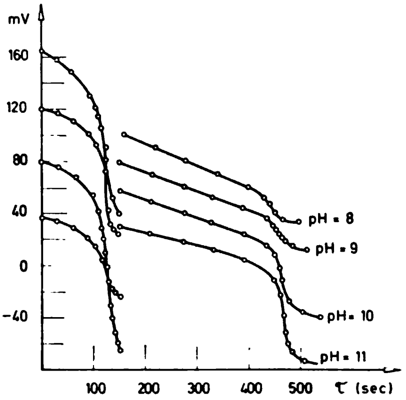

Fig. 4.
Effect of pH on the coulometric-potentiometric curves in titration of Mg^{2+} ion

A standard solution of magnesium was made by dissolving 3 g $Mg(NO_3)_2 \cdot 6H_2O$ in 150 ml water. By titrating this with standard 0.1 N Complexon III at pH 9 using catechol-violet indicator(4), it was found that 1 ml of this solution contained 1.09 mg Mg.

The results of coulometric titration of magnesium with EDTA are given in Table 2.

TABLE 2.
Coulometric Titration of Mg^{2+} with EDTA
at pH = 10.5 and I = 20.0 and 40.0 mA

No.	Taken mg	Found mg	Error		Current mA	Time (theoretical) sec.
			mg	%		
1	0.818	0.808	—0.010	—1.2	20.0	324.0
2		0.820	+0.002	0.2		
3		0.816	—0.002	—0.2		
4	1.636	1.632	—0.004	—0.2	40.0	324.0
5		1.644	+0.008	0.4		
6		1.648	+0.012	0.7		
7	2.725	2.729	+0.004	0.1		540.0
8		2.725	—	—		
9		2.725	—	—		
10	3.270	3.258	—0.012	—0.3		648.0
11		3.270	—	—		
12		3.278	+0.008	0.2		
13	4.360	4.365	+0.005	0.1		864.0
14		4.360	—	—		
15		4.358	—0.002	—0.04		

The titration time of magnesium, defined by the end-point, was determined like that of cobalt, from the potentiometric curves in Fig. 5.

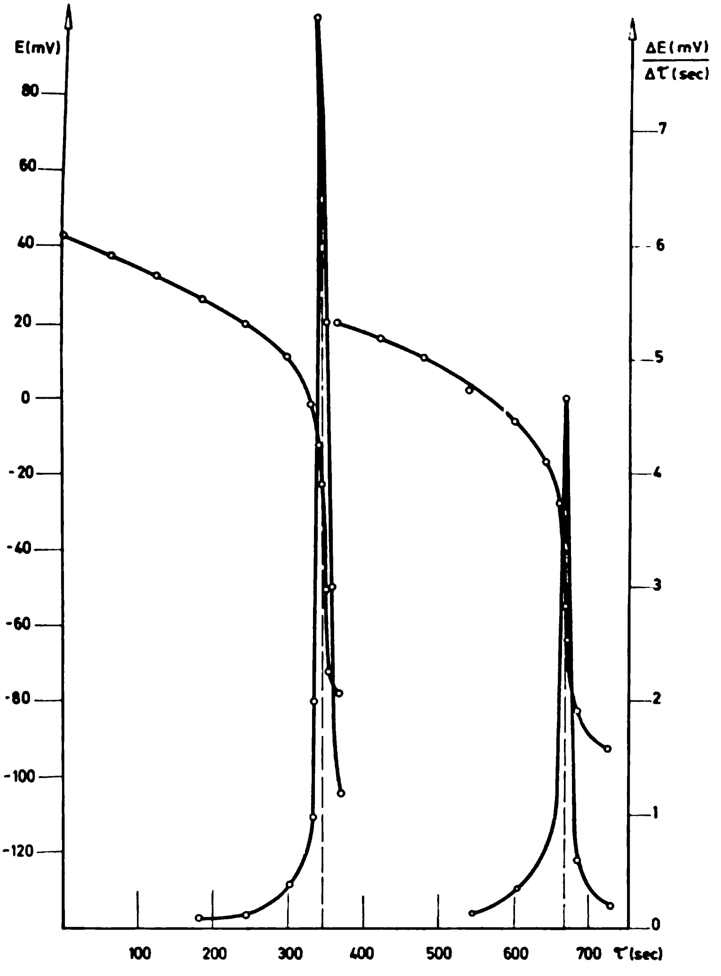

Fig. 5.
Coulometric-potentiometric titration of Mg^{2+} ion

DISCUSSION

The results confirm our hypothesis that constant-current coulometric titration using EDTA ion electrically generated from mercuric chelate can be successfully employed for determination of cobalt and magnesium. Both cations was determined in micro and semimicro quantities, with less than 1% error.

Three tests at every concentration of cobalt or magnesium showed that the potentiometric curves, and therefore also the quantitative results obtained with the mercury indicator and calomel reference electrodes are highly reproducible. However, the time needed for restoring the potential on the mercury electrode (1—2 min.) affects the overall time of determination.

The investigation of the influence of pH on titration of Co^{2+} and Mg^{2+} demonstrates the value of lotting potential-pH curves (1, 2, 3) in theoretical speculations about the prospects for successful titration of a cation with electrically generated Y^{4-}.

From Fig. 2 it may be seen that all potentiometric curves of cobalt (for pH=5, 7, 9 and 11) have the same shape but are vertically displaced, by about 40 mV for pH=9 and 11, and 60 mV for pH=7, and the curve for pH=5 to an even more positive potential. The potential jump at the end-point changes little with pH and it is about 100—110 mV. Both these results and those obtained for magnesium (Fig. 4) are in full agreement with the values expected from the potential-pH curves(1).

Experiments made to try and test the influence of oxygen on the pre-titration and titration curves of Co and Mg with EDTA show that the solution must be freed of oxygen, because by simultaneous reduction at the cathode oxygen decreases η_i at which the titrant (EDTA) is generated. The current utilized to eliminate oxygen in titration of cobalt is $\eta_{iO_2}=7\%$ while with magnesium $\eta_{iO_2}=10\%$, showing that oxygen will have even more detrimental effect in an alkaline solution (in this case that of magnesium). This can be ascribed to the fact that for pH=3—10 the half-wave potential of oxygen reduction varies from —30 to —100 mV. As the potentials for titration of magnesium are more negative than for cobalt, it is clear that the influence of oxygen will be stronger for the former.

In both cases micro quantities were determined with an average relative error below 0.5%, which gives this method the advantage for microdetermination.

Institute of Chemistry, Technology and Metallurgy,
Department of Electrochemistry, Belgrade
School of Technology and Metallurgy, Department of
Physical Chemistry and Electrochemistry, Belgrade University

REFERENCES

1. Reilley, C. N. and W. W. Porterfield. "Coulometric Titrations with Electrically Released Ethylenediaminetetraacetic Acid" — *Analytical Chemistry* 28: 443—447, 1956.

2. Stojković, D. and S. Dravić. "Kulometrijsko-kompleksometrijsko odredjivanje jednog ili više kationa" (Coulometric Complexometric Determination of One or More Cations), in: (*II Jugoslovenski kongres za čistu i primenjenu hemiju, Beograd, juni 1966*), (2nd Yugoslav Congress on Pure and Applied Chemistry, *Yugoslavia*, Belgrade, June 1966).

3. Reilley, C. N. and R. W. Schmid. "Chelatometric Titrations with Potentiometric End-Point Detection" — *Analytical Chemistry* 30: 947—953, 1958.

4. Přibil, R. *Komplexometrie* — Praha: Chemapol, 1955.

5. Schwarzenbach, G. *Die Komplexometrische Titration* (*2nd Ed.*) — Stuttgart: F. Encke, 1956.

GLASNIK HEMIJSKOG DRUŠTVA, Vol. 35, No. 9–10, 1970, pp. 497–504

GHDB-129

543.25:546.48+546.74
Original Scientific Paper

INDIRECT COULOMETRIC DETERMINATION OF CADMIUM AND NICKEL

by

DARINKA J. STOJKOVIĆ

Indirect coulometric titration(1), based on the fact that one substance can be determined indirectly by means of another determined by any of the known coulometric procedures, has found application in the determination of a larger number of cations.

A special case of indirect coulometric titration is that based on hydrolysis:

$$M^{2+}+2H_2O\rightleftarrows M(OH)_2+2H^2.$$

In the above reaction the addition of an acid or base disturbs the equilibrium and the reaction can be directed either way. Thus, if hydrogen ions are eliminated by a base or OH^- ions generated in the catholyte by decomposing water, then at a certain pH quantitative transformation of M^{2+} ions into $M(OH)_2$ becomes feasible.

Indirect coulometric determination employing hydrolysis may be carried out either by calculating the number of cations from the number of coulombs consumed, or from the amount of base consumed in neutralization of the acid formed by hydrolysis, i. e. until a suitable acid-base indicator changes color(4, 5). But if the cation's hydroxide hinders visual end-point detection in titration of the acid(4) then a modified method comprising determination of the acid released in the anolyte is applied, the corresponding hydroxide being eliminated from the system.

For indirect coulometric titration of Cd^{2+} and Ni^{2+} we applied a combined method, considering that nickel forms a colored hydroxide.

In the hydrolysis of cadmium or nickel salts the acid released is equivalent to

$$Cd^{2+}+2H_2O\rightleftarrows Cd(OH)_2+2H^+$$

$$Ni^{2+}+2H_2O\rightleftarrows Ni(OH)_2+2H^+.$$

In the electrolysis of cadmium or nickel salts in a catholyte separated from the anolyte and at suitable pH, the ions of these metals precipitate as hydroxides. In electrolysis of dilute solutions of cadmium or nickel this may be achieved by adding a suitable conducting supporting electrolyte to the solution. We used sodium sulfate for this purpose.

The reactions are as follows:

At the cathode:

$$\begin{array}{l} 2H_2O+2e=H_2+2OH^- \\ \underline{Cd^{2+}+2OH^-=Cd(OH)_2} \\ Cd^{2+}+2H_2O+2e=H_2+Cd(OH)_2 \end{array}$$

At the anode: $H_2O - 2e = 1/2O_2 + 2H^+$.

For nickel the reactions are analogous.

Theoretically possible reactions at the cathode are:

$$Cd^{2+} + 2e = Cd,$$

for $a_{Cd^{2+}} = 1$, and $e_0 = -0.402$ V,

or $Ni^{2+} + 2e = Ni$,

for $a_{Ni^{2+}} = 1$, and $e_0 = -0.203$ V,

and $2H_2O + 2e = H_2 + 2OH^-$,

for $a_{H^+} = 10^{-7}$, and $e_0 = -0414$ V.

It may be assumed that at the cathode the reduction of metal ions and hydrogen takes place simultaneously, but this should not have any effect on the results because an equivalent amount of H^+ ions is generated in the solution at the same time.

Considering that determinations were made in dilute solutions (10^{-3} to 10^{-4} M), and therefore e_0 both for Cd and Ni was shifted to more negative values, the reduction of H^+ ions is most probable, provided the current density at which metal ions are reduced is not exceeded, and this can be monitored visually.

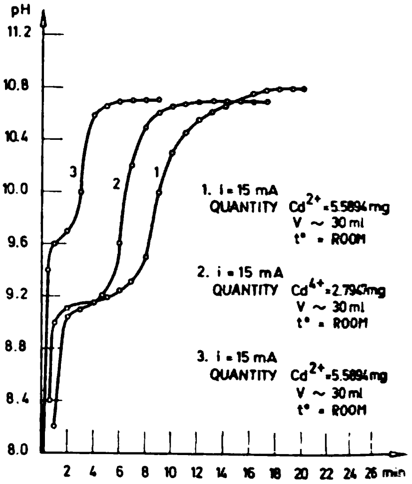

Fig. 1.

Fig. 1. — Electrolytic precipitation of $Cd(OH)_2$

Although the pH at which $Cd(OH)_2$ or $Ni(OH)_2$ in aqueous solutions precipitate quantitatively may be found in the literature(5) as a function of concentration, we found that in the electrolytic precipitation of these hydroxides under the given experimental conditions (i. e. for Na_2SO_4 supporting electrolyte) the function pH=f(t) should be plotted first. From the graphs obtained (Fig. 1) the most suitable pH was assessed.

Figure 1 shows the log-log curves $pH=f(t)$ for Cd. It may be seen that the optimum pH does not depend on concentration. The precipitation time of $Cd(OH)_2$ is a minimum at pH 10.6—10.7, and depends on the absolute amount in the solution and the current density.

Similar graphs were obtained for the precipitation of $Ni(OH)_2$, with the optimum pH at 11.25—11.45. A longer precipitation time produces an excess of OH^- ions, which then adsorb on the already precipitated hydroxide, and this leads to an error in coulometric determination of the acid.

The pH's used were higher than those extrapolated for precipitation of the corresponding hydroxides (obtained by producing the first plateau of the curve to its intesection with the ordinate).

EXPERIMENTAL

The chemicals used were: $3\,CdSO_4 \cdot H_2O$ (Chemapol), $NiSO_4 \cdot H_2O$, $Na_2SO_4 \cdot 10\,H_2O$ (Kemika), KCl (Kemika), and methyl red (Merck), all of *p.a.* quality.

Cadmium sulfate and nickel sulfate were prepared as 0.1 N solutions in double distilled water. Their titer was determined by complexometric titration. Methyl red was prepared as a 1% solution in 60% alcohol.

Apparatus

Cadmium was determined indirectly with the simple apparatus usually employed in constant-current coulometry. The cathodic branch was separated from the anodic, and in the first stage the two compartments were much smaller than in the second. The electrodes were platinum spirals. The salt bridge was as usual, ending with sintered glass discs.

Procedure

In the first stage the aqueous solution of cadmium sulfate is electrolyzed in the sodium sulfate supporting electrolyte of known concentration. The salt bridge connecting the catholyte with the anolyte is also filled with sodium sulfate. With electrolysis at constant current and vigorous stirring of the catholyte cadmium hydroxide precipitates. The precipitate is separated from the electrolyte by decanting at about pH 10. It is then washed several times with a little distilled water and the filtrate pooled with the content of the salt bridge. The residual acid remaining after pooling the two electrolytes is then determined in the second stage by coulometric titration at constant current in the presence of methyl red.

The titrating current is chosen so as to minimize the error for the corresponding quantity of substance taken, but without the titration time becoming too long, otherwise the method would be impractical. The titration is timed with a stopwatch from the switching on of the coulometric circuit and until the indicator changes color.

Cadmium content is calculated from the number of coulombs consumed in neutralizing the acid.

RESULTS AND DISCUSSION

The results for cadmium and nickel are given in Tables 1 and 2.

TABLE 1.

Indirect Coulometric Determination of Cadmium

Precipitation of $Cd(OH)_2$	*Retitration of the acid*
Catholyte: 0.1 N $Na_2SO_4 + Cd^{2+}$ Anolyte: 0.1 N Na_2SO_4	Catholyte: Stage 1 filtrate + + stage 1 anolyte + + content of the salt bridge Anolyte: 0.1 N Na_2SO_4 Indicator: methyl red

Catholyte Na_2SO_4 (N)	Precipitation of $Cd(OH)_2$		Retitration of the acid		Amount of Cd		Error (%)	Theoretical titration time (sec)
	Current (mA)	Time (min)	Current (mA)	Time (sec)	Taken (mg)	Found (mg)		
0.1	10.0	20.0	10.0	438.0	2.795	2.811	0.58	480.1
				432.0		2.806	0.39	
0.5				483.7		2.816	0.75	
				478.1		2.783	—0.44	
0.1			15.0	321.8	2.795	2.809	0.50	320.2
				319.0		2.784	—0.38	
0.5				322.1		2.812	+0.60	
				321.5		2.806	+0.40	
0.1			20.0	238.6	2.795	2.778	—0.62	240.1
				242.0		2.815	0.71	
0.5				241.3		2.809	0.50	
				241.0		2.806	0.41	
0.1			30.0	159.0	2.795	2.778	0.61	160.1
				158.7		2.770	—0.90	
0.5				158.7		2.820	0.90	
				159.2		2.811	0.57	
0.1			40.0	119.0	2.795	2.818	0.83	120.0
				119.0		2.818	0.83	
0.5				118.6		2.819	1.20	
				119.2		2.814	0.67	
0.1			50.0	95.0	2.795	2.824	1.04	96.0
				95.2		2.772	—0.83	
0.5				95.0		2.825	1.04	
				95.0		2.825	1.04	

TABLE 2.

Indirect Coulometric Determination of Nickel

Precipitation of $Ni(OH)_2$

Catholyte: 0.1 N $Na_2SO_4 + Ni^{2+}$

Anolyte: 0.1 N Na_2SO_4

Retitration of the acid

Catholyte: Stage 1 filtrate +
+ stage 1 anolyte +
+ content of the
salt bridge

Anolyte: 0.1 N Na_2SO_4

Indicator: methyl red

Test No.	Precipitation of $Ni(OH)_2$		Retitration of the acid		Amount of Ni		Error (%)	Theoretical titration time (sec)
	Current (mA)	Time (min	Current (mA)	Time (sec)	Taken (mg)	Found (mg)		
1	10.0	20.0	30.0	80.0	0.734	0.729	—0.62	80.5
2				79.0		0.720	—1.86	
3				79.0		0.720	—1.86	
4				78.0		0.711	—3.00	
5				160.0	1.468	1.459	—0.62	161.0
6				159.0		1.450	—1.24	
7				159.0		1.450	—1.24	
8				158.0		1.441	—1.86	
9				321.0	2.936	2.927	—0.31	322.0
10				320.0		2.918	—0.62	
11				320.0		2.918	—0.62	
12				319.0		2.909	—0.93	
13	20.0	15.0		482.0	4.403	4.394	—0.21	483.0
14				481.0		4.385	—0.42	
15				481.0		4.385	—0.42	
16				480.0		4.376	—0.63	
17				643.0	5.871	5.962	—0.16	644.0
18				642.0		5.853	—0.32	
19				642.0		5.853	—0.32	
20	20.0	15.0	30.0	641.0	5.871	8.844	—0.48	644.0
21				965.0	8.806	8.797	—0.10	966.0
22				964.0		8.788	—0.20	
23				964.0		8.788	—0.20	
24				964.0		8.788	—0.30	

From the tables it may be concluded that indirect coulometry is suitable for determination of micro and semimicro quantities of cadmium, the reproducibility is fairly good and the error is well within the usual range for analytical determinations. However, the accuracy of the method is determined by the precision of the instruments used, and may largely depend on subjective error as well.

DETERMINATION OF NICKEL

The results for nickel, determined in quantities from 0.73 to 8.80 mg at 30 mA, are given in Table 3. Quantities of 0.73 mg were determined with an error of 1.3—1.8%, which may well be due to subjective factors in detecting the end-point with an acid-base indicator, although it was hoped to prevent this by titrating until the indicator (methyl red) showed the same color as in pure supporting electrolyte.

As may be seen from the table the amount of acid found was consistently low.

From the slope of the straight line of titration time of the acid formed against ml of 0.1 N $NiSO_4$ taken, the overall titration time per ml was calculated by the least squares method. The titer of the solution calculated from the known time and current of titration was $2.936 \pm 2 \,.\, 10^{-3}$ mg/ml. Its error is determined by the error of time (the slope of the straight line) and titrating current.

The result ($2.936 \pm 2 \,.\, 10^{-3}$ as against 2.9355 mg/ml of the solution taken is quite satisfactory; the discrepancy is in fact far less than the error of determination.

Analysis of the straight line of titration time against number of ml of solution shows a negative intercept of -2.3 ± 0.5 sec., which cannot be neglected. This reveals that in these determinations there was a constant loss of acid of $0.7 \,.\, 10^{-5}$ M/lit. This decrease in the effective amount of acid is most probably due to the OH^- ions generated because of the solubility of the fresh $Ni(OH)_2$ precipitate. The concentration of OH^- calculated from the solubility factor is $1.6 \,.\, 10^{-5}$ M/lit, i. e. of the same order of magnitude as the acid loss.

Judging by the results obtained in the indirect coulometric determination of cadmium(2), ferrous and ferric ion(4), and nickel(5), we consider that the method is applicable for micro and semimicro determination of weakly basic salts and other hydrolyzable cations, provided that the hydroxides formed are not dissolved in the excess OH^- ions generated by electrolysis.

Institute of Chemistry, Technology and Metallurgy,
Department of Electrochemistry, Belgrade
School of Technology and Metallurgy, Department of
Physical Chemistry and Electrochemistry, Belgrade University

Received July 18, 1968.

REFERENCES

1. Tutundžić, P. and S. Mladenović. "Posredna kulometrijska odredjivanja" (Indirect Coulometric Determinations) — *Glasnik hemijskog društva* (Beograd) 19: 562, 1954.
2. Stojković, D. "Posredno kulometrijsko odredjivanje kadmijuma" (Indirect Coulometric Determination of Cadmium) — *Glasnik hemijskog društva*[*] (Beograd) 29: 437—438, 1964.
3. Stojković, D. "Indirektno kulometrijsko odredjivanje nikla" (Indirect Coulometric Determination of Nickel), in: *II Jugoslovenski kongres za čistu i primenjenu hemiju* (2nd Yugoslav Congress on Pure and Applied Chemistry, Belgrade, June, 1966).
4. Stojković, D. "Kulometrijsko odredjivanje natrijumtetraborata i kalijumbiftalata" (Coulometric Determination of Sodium Tetraborate and Potassium Biphthalate) — *Glasnik hemijskog društva* (Beograd) 31:[*] 265—270, 1966.
5. Pavlović, Ž. and S. Mladenović. "Posredne kulometrijske titracije" (Indirect Coulometric Titrations) — *Glasnik hemijskog društva* (Beograd) 31[*]: 265—270, 1966.
6. Pavlović, Ž. and S. Mladenović. "Posredne kulometrijske titracije. II deo. Odredjivanje fero i feri jona" (Indirect Coulometric Titrations. II. Determination of Ferrous and Ferric Ion) — *Glasnik hemijskog društva* (Beograd) 31[*]: 271—277, 1966.
7. Lur'e, Iu. Iu. *Spravochnik po analiticheskoi khimii* (A Manual of Analytical Chemistry) — Moskva: Khimiia, 1967.

---

[*] Available in English translation from National Technical Information Service, Springfield, Virginia, 22151

GLASNIK HEMIJSKOG DRUŠTVA, Vol. 35, No. 9–10, 1970, pp. 505–516

GHDB-130

669.296.4:66.046.5
Original Scientific Paper

A COMPARISON OF THE REFINING EFFECTS OF ARC AND ELECTRON BEAM MELTING OF ZIRCONIUM

by

I. STOJŠIĆ, DJ. CVETANOVIĆ, and N. OBRADOVIĆ

INTRODUCTION

Zirconium sponge obtained by Kroll's method contains a number of impurities, which always include iron, hafnium, magnesium, manganese, nickel, lead, silicon, and titanium.

Owing to its high reactivity with respect both to gases and crucible material, and its high melting point (1852 °C), only arc melting has been economical method for its conversion into the compact form. The relevant handling problems have been treated in several papers(1–3).

During the last few years, however, electron-beam melting has begun to gain ground for the melting not only of zirconium but also of many other metals(4–6). Thanks to certain outstanding characteristics (vacuum of 10^{-4}—10^{-6} torr, good exposure to vacuum of the thin melting film on the rod and the melt, and possibility of keeping the metal liquid as long as required), this method has a considerably better refining effect than arc melting.

The aim of our study was to compare the refining effects of arc and electron-beam melting of zirconium sponge.

Arc melting with permanent or consumable electrodes was carried out in an atmosphere of argon at 400 torr. All meltings with electron-beam were done in a vacuum maintained at less than 10^{-4} torr. Some charges arc-melted with a permanent electrode were later remelted by electron beam.

EXPERIMENTAL

All tests were made with "Degussa" zirconium sponge. The tables give only the lower and upper limits of the impurities found, because the material is unsuitable for taking an average sample.

Arc melting with permanent or consumable electrodes was carried out in a Heraeus VA-L200 furnace. The principle of arc melting using the metal as consumable electrode is shown in Fig. 1.

Melting with a permanent electrode was done with charges of about 80 g. A titanium getter was burned before hand. Zirconium buttons (about 40 mm in diameter and 10 mm high) obtained by melting the sponge with a permanent electrode were turned upside down and remelted at the same arc current, time of keeping the metal liquid and vacuum. Consumable electrodes were made by welding in argon of a number of rods of pressed zirconium sponge. The electrodes were about 350 mm long and 27 mm in diameter; their density was 70% of the theoretical. After characterization, the ingots from the first melting were cut down the vertical axis into four bars. By welding these together in argon, the consumable electrode for remelting was obtained. The water-cooled copper mould was 60 mm in diameter.

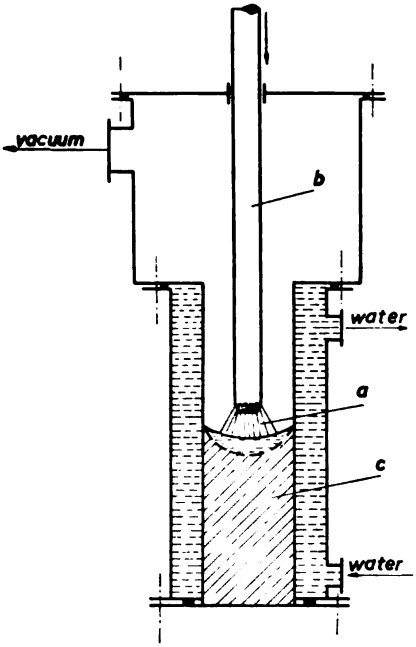

Fig. 1.

Principle of consumable electrode arc-melting
(a) Electric arc
(b) Consumable electrode
(c) Ingot

Electron-beam melting was carried out in a LEW EMO-60 furnace. The principle of this process is illustrated in Fig. 2.

The charges were about 50 g. A titanium getter was used in the same way as in arc melting. The buttons obtained from the first melting were turned upside down and remelted at the same beam energy, consolidation time and vacuum. The rods were prepared for melting in the same way as consumable electrodes for arc melting.

Brinell hardness of the ingots obtained was determined with a 2 mm steel ball, a 40 kg load being applied for 15 seconds. Carbon content was determined by conductometry, to ±5%, on a Leco apparatus. Gases were determined by vacuum melting, using a Ströhlein apparatus: oxygen to

±5%, hydrogen ±10%, and nitrogen ±7%. Metallic impurities were determined by carrier distillation, to within an error of 10—30%, using a Jarrel Ash spectrograph.

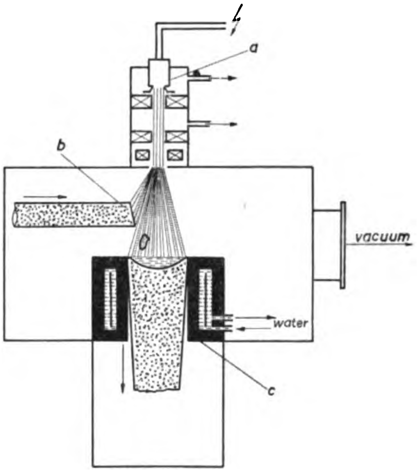

Fig. 2.

Principle of the EMO-60 electron-beam furnace
(a) Electron gun
(b) Melting rod
(c) Crystallizer

Analyses of zirconium buttons obtained by various methods are given in Table 1.

TABLE 1.

Hardness and Interstitial Impurities of Arc and Electron-Beam Melted Zirconium Buttons

Sample	Time (min.	H_B	Interstitial impurities, ppm			
			C	N	O	H
Zr sponge			150—300	80—520	1090—3290	17—73
Arc	2×0	247	214	132	2560	28
El. beam		239	100	73	2115	0.7
Arc	2×3	208	196	580	2400	27
El. beam		173	172	40	1550	0.4
Arc	2×6	247	230	460	1920	36
El. beam		186	200	35	2360	0.5

Arc melting parameters: $I=300$ A, $P_{arc}=400$ torr

El. beam melting parameters: $E=6.8$ kW, $P=a\,.\,10^{-5}$ torr

Zirconium buttons melted by electron-beam were always softer owing to their higher purity and different cooling conditions.

Electron-beam melting reduces interstitial impurities, especially nitrogen and hydrogen. This cannot be said for arc-melting. Owing to the inhomogeneity of the material, the results in Table 1 cannot be analyzed for the refining effects of prolonged consolidation, because the buttons concerned were not remelted but melted together with new sponge charges.

Analyses of metalic impurities in the same buttons as in Table 1 are shown in Table 2. The differences between the two methods are conspicuous, for both consolidation times. Arc-melting removes some aluminum. silicon, magnesium, and probably manganese; the range of metalic impurities removed by electron-beam melting is somewhat wider, including chromium. titanium, and definitely manganese. Only in one result indicates the removal of iron; this was obtained with the longer melting time in the electron beam. Hafnium content, particularly important in nuclear applications of zirconium. is not reduced by either of the two methods.

TABLE 2.

Metalic Impurities of Arc and Electron-Beam Melted Zirconium Buttons

Sample	Time (min)	Metalic impurities, ppm							
		Fe	Mn	Mg	Al	Si	Cr	Ti	Hf
Zr sponge		> 1000	68—72	230—575	270—1000	> 1000	25—406	25	≈100
Arc	2×0	> 1000	112	50	24	230	62	58	
El. beam		> 1000	5	9	24	53	10	11	77
Arc	2×6	> 1000	33	13	71	142	430	44	100
El. beam		≈1000	13	5	8	90	10	10	100

To eliminate any inhomogeneity in the distribution of impurities and compare the refining effects of the two methods, zirconium sponge was first melted and then the buttons obtained were remelted by electron-beam.

TABLE 3.

Weight Loss, Hardness and Interstitial Impurities of Arc-Melted Zirconium Buttons and Those Remelted in Electron-Beam

Sample	Time (min)	Weight loss (%)	H_B	Interstitial impurities, ppm			
				C	N	O	H
Zr sponge				150—300	80—520	1070—3290	17—73
Arc	2×3	0.24	235	196	100	2750	38
El. beam		0.48	208	132	98	2580	38
Arc	2×6	0.35	242	196	110	2120	37
El. beam		0.54	205	86	34	2070	0.3

Arc-melting parameters: $I=300$ A, $P_{arc}=400$ torr

El. beam melting parameters: $E=10$ kW, $P=a.10^{-5}$ torr

Weight losses in melting may be ascribed to: (1) splashing (especially in arc-melting), (2) partial removal of impurities (mainly $MgCl_2$ and moisture in arc-melting), and (3) evaporation of zirconium (especially in electron-beam melting). As would be expected, these losses increased with consolidation time but were greater at the beginning of melting, thus confirming the order of causes suggested above.

Buttons obtained by remelting in the electron beam were softer than those obtained with arc-melting. This suggests better refining by the former method as regards oxygen and nitrogen.

The results in Table 3 also show a poor refining effect of arc-melting as regards interstitial impurities. On the other hand, electron-beam melting reduces hydrogen, nitrogen and oxygen and to some extent carbon.

Metalic impurities in the buttons obtained by arc-melting of zirconium sponge and then remelting them in the electron beam are shown in Table 4.

TABLE 4

Metalic Impurities of Arc-Melted Zirconium Buttons and Those Remelted in Electron-Beam

Sample	Time (min)	Metalic impurities, ppm								
		Fe	Mn	Mg	Al	Si	Cr	Ti	Hf	W
Zr sponge		> 1000	68—72	230—575	270—1000	1000	20—406	25	100	
Arc	2×3	> 1000	35	6.2	22	680	100	13	100	10
El. beam		678	1	4.3	8	13	10	3	100	
Arc	2×6	> 1000	33	13	71	142	430	44	100	10
El. beam		430	1	5.7	23	27	10	33	100	

The results in Table 4 agree with those obtained earlier with arc-melting. Remelting in the electron beam improves purity, which confirms its advantages. The lower content of iron in the buttons remelted in the electron beam shows that this method is highly reliable for its removal. Although contamination with tungsten is a hazard in permanent electrode arc-melting, proved by Dunnworth(2) to be the main reason for increased hardness, in our experiments the phenomenon was not observed.

TABLE 5.

Hardness and Interstitial Impurities of Zirconium Ingots from First and Second Arc-Melting and Those Melted in Electron-Beam

Sample	H_B	Interstitial impurities, ppm			
		C	N	O	H
Zr sponge		150—300	80—520	1090—3290	17—73
1st arc	330	184	771	3725	41
2nd arc	376	160	1650	3990	50
El. beam	270	192	303	2515	0.5

1st arc-melting parameters: $I=1000$ A, $P=400$ torr, $v=15$ kg/h
2nd arc-melting parameters: $I=1000$ A, $P=400$ torr, $v=20$ kg/h
(remelting)
Electron-beam melting parameters: $E=25$ kW, $P=6 . 10^{-5}$ torr, v . 1.5 kg/h

Interstitial and metalic impurities in the ingots obtained by arc- and electron beam melting are shown in Tables 5 and 6.

From the results it may be seen that electron-beam melting produces softer ingots than arc-melting, above all because of the higher purity attained. Arc-melting not only has a poor refining effect but also results in contamination of the zirconium sponge under the given operating conditions. As this is particularly the case with remelted ingots, it follows that the preparation of the consumable electrodes, i. e. cutting and welding, contributes largely to contamination. If contamination due to the preparation of electrodes is assumed to be equal in arc and electron-beam melting, then the latter gives a product with less nitrogen, oxygen, and above all hydrogen. Arc-melting not only shows inferior refining, but has a detrimental effect as regards the final concentration of interstitial impurities.

TABLE 6.

Metalic Impurities of Zirconium Ingots from First and Second Arc-Melting and Those Melted in Electron-Beam

Sample	Metalic impurities, ppm							
	Fe	Mn	Mg	Al	Si	Cr	Ti	Hf
Zr sponge	> 1000	68—72	230—575	270—1000	1000	25—406	25	100
1st arc	> 1000	105	20	28	660	575	17	100
2nd arc	> 1000	76	16	50	320	1000	42	100
El. beam	> 1000	19	7	5	46	85	18	100

For metalic impurities the results for ingots are much the same as those obtained for buttons. In their removal electron-beam melting again showed superior to double remelting in the electric arc.

DISCUSSION

Although solid state solubility of carbon in zirconium was not studied, it must be low because carbides could be seen under the microscope even at as low a carbon content as 0.04%(7).

Arc-melting does not decrease carbon content. The results obtained by remelting the arc-melted buttons in the electron beam suggest that electron-beam melting reduces the carbon content. Great affinity for zirconium ($\Delta F^{\circ}_{298} = -35$ Kcal/mol) should prevent participation of carbon in the reduction of oxides.

ZrO_2 is one of the most stable oxides known ($\Delta F^{\circ}_{298} = -244$ Kcal/mol). According to Lustman(7), up to 29 at% oxygen can be dissolved in zirconium in the form of solid solution, without any ZrO_2 structure being evident. It is considered that 0.2% oxygen causes brittleness. As an interstitial impurity oxygen makes for increased hardness of zirconium. Oxygen content is not reduced under the given conditions of arc-melting, but some reduction is achieved by electron-beam melting. As our study was not aimed at finding a method for the removal of gases, we will only note here some contemporary views on the matter. Schlechton$^{(8)}$ states that the equilibrium pressure of saturated solutions in zirconium is so low that there is no way of removing oxygen by vacuum treatment. Theoretical speculations based on the data given by Brewer$^{(9)}$ indicate that zirconium could be deoxidized via the volatile suboxides; according to Smith$^{(10)}$, at the melting point of zirconium the vapor pressure ratio of $ZrO:Zr=10^2$. Albert and Renucci$^{(11)}$ found that oxygen content was reduced by melting zirconium buttons in an electron beam, and assumed that oxygen evaporated in the form of zirconium suboxide (ZrO). Later they calculated the refining coefficient$^{(12)}$.

As oxygen concentration in our sample was relatively low, it is possible that it was dissolved in the atomic state in liquid zirconium and behaved as a dilute solution with a solubility obeying Sievert's law. We think that a certain contribution of Al and Si cannot be overlooked; in electron-beam melting they are removed in considerable measure, probably partly as Al_2O and SiO.

Up to 20 at% nitrogen forms a solid solution in alpha zirconium, and ZrN above this. This highly stable nitride ($\Delta F^\circ_{298} = -75.3$ Kcal/mol) cannot be dissociated under normal conditions of induction melting in vacuum. Nitrogen has a similar influence on the mechanical properties of zirconium as oxygen, largely affecting its hardness. It is thought that a nitrogen content above 40 ppm causes strong corrosion of zirconium in hot water$^{(13)}$.

The results show that arc-melting does not reduce nitrogen content. Electron-beam melting removes same nitrogen. This is probably nitrogen in solid solution rather than from dissociation of nitride.

Hydrogen, which is easily adsorbed on zirconium, also makes it brittle; a hydride phase appears along with the solid solution (50 at%). Although it does not affect the mechanical properties of zirconium to such an extent as nitrogen or oxygen, hydrogen content is very important for the use of zirconium or its alloys in reactor technology. In thermal cycling its toughness is strongly affected by hydride precipitating from the refined solution.

Under the given conditions hydrogen present in the zirconium sponge was not removed by arc-melting. Electron-beam melting, under all conditions, was highly efficient, and over 95% hydrogen was removed. We consider that in this case dissociation of zirconium hydride does take place, in spite of its relatively high stability ($\Delta F^\circ_{298} = -24.7$ Kcal).

TABLE 7.

Vapor Pressure of Some Metalic Impurities at the Melting Point of Zirconium

Metal	Zr	Fe	Al	Mg	Cr	Si	Mn
P (torr)	$4 \cdot 10^{-4}$	$8 \cdot 10^{0}$	$1 \cdot 10^{2}$	10^{3}	$3 \cdot 10^{1}$	$5 \cdot 10^{0}$	10^{0}

Among the numerous effects of metalic impurities on the properties of zirconium, let us mention only those affecting:

1) hardness,
2) corrosive properties,
3) effective neutron cross-section,
4) solubility of carbon, etc.

Both arc and electron-beam melting reduce a number of impurities, such as magnesium, aluminum, silicon, and chromium. The refining effect of electron-beam melting is nevertheless considerably better and faster. While in arc-melting manganese is probably not removed at all, in electron-beam melting the removal is pronounced. Iron is reliably removed only by electron-beam melting. The better refining effect of electron-beam melting may be ascribed to: (1) high vacuum in the furnace during melting (10^{-5} torr, instead of 400 torr in arc-melting), and (2) slower melting, i. e. possibility of keeping the metal liquid as long as required. Considering the results in Table 7 and the affinity of metalic impurities for zirconium, the advantages of electron-beam melting are obvious. Hafnium, important in the application of zirconium in nuclear technology due to its large neutron cross-section, cannot be removed by vacuum melting.

The vapor pressure of Zn at the melting point (nearly 10^{-5} torr) indicates that evaporation losses are small in both melting methods.

It was found that welding pressed zirconium sponge in preparing the electrodes strongly influenced the final oxygen and nitrogen content of the ingots after melting. The reason for this may be sought in the gettering effect zirconium has for these gases; once formed these oxides or nitrides are difficult to remove by vacuum remelting.

Institute for Technology of Nuclear and Other
Mineral Raw Materials, Belgrade

REFERENCES

1. Gruber, H. and H. Scheidig. "Das Schmelzen von Titan und Zirconium in Vakuum Lichtbogenofen" — *Zeitschrift für Metallkunde* (Stuttgart) 47 (3): 149—159, 1960.
2. Dunnworth, R. S. *Arc Melting of Zirconium* — Lemont: Argonne National Laboratory (No. 5519) 1957.
3. Carver, M. D. and H. Kato. *Evaluating One-Half Million Pounds of Zirconium Sponge, US Bureau of Mines, Report of Investigation* No. 5969 — Washington, 1960.
4. Smith, H. R. and Ch. A. Hunt. "Electron-Bombardment Melting" — *Journal of Metals* (New York) 11 (2): 112—117, 1959.
5. Seagle, S. R. and R. L. Martin. "Electron-Beam Melting — Does It Improve the Properties of Metals and Compounds" — *Journal of Metals* (New York) 14 (11): 812—820, 1962.
6. Stojšić. I. "Naši prvi rezultati u topljenju metala elektronskim snopom" (First Results in Electron-Beam Melting of Metals), in: *IV Jugoslovenski kongres za primenu vakuuma u industriji* (4th Yugoslav Congress on Industrial Applications of Vacuum) — Bled: 1968.
7. Lustman, B. and F. Kerze. *The Metallurgy of Zirconium* — New York: McGraw-Hill Book Co., 1955.
8. Schlechten, A. W. "Zirconium", in: C. A. Hempel (ed.) *Rare Metals Handbook* — New York: Reinhold Publishing Corporation, 1961, Ch. 34.
9. Brewer, L. and G. M. Rosenblatt. "Thermodynamics of Suboxide Vaporization" — *Transactions of the American Institute of Mining, Metallurgical and Petroleum Engeneering* 224 (6): 1268—1271, 1962.
10. Smith, H. R. "Electron Bombardment Melting Techniques", in: R. Bunschah (ed.) *Vacuum Metallurgy* — New York: Reinhold Publishing Corporation, 1957, Ch. 14.
11. Albert, P. and L. Renucci. "Sur la purification du zirconium en oxygene par distillation" — *Bulletin Societe chimique de France* (Paris) 3 (4): 2091—2096, 1962.
12. Ailloud, R., L. Renucci, *et al.* "Sur la purification du zirconium en oxygene par distillation" — *Comptes Rendus Academie de Science* (Paris) 266 (5): 366—368, 1968.
13. Beard, A. R. "Nuclear Power Plant Materials", in: R. Bunschah (ed.) *Vacuum Metallurgy* — New York: Reinhold Publishing Corporation, 1957, Ch. 23.

GLASNIK HEMIJSKOG DRUŠTVA, Vol. 35, No. 9–10, 1970, pp. 517–524

GHDB-131

628.165:546.46:541.8:546.41'264
Original Scientific Paper

PURIFYING BRINE OF Ca^{2+} AND Mg^{2+}. III. SOLUBILITY OF $CaCO_3$ IN BRINE AFTER PURIFICATION

by

SVETOZAR PRIBIĆEVIĆ, BOGDAN STANČIĆ, AND PETAR PETROVSKI

After precipitating Ca^{2+} from a brine some $CaCO_3$ remains dissolved. The solubility of $CaCO_3$ depends on a number of factors. Shortly after precipitation its solubility in the brine may be several times the equilibrium concentration. The concentration of $CaCO_3$ in the brine decreases with time.

A knowledge of the factors affecting the kinetics of $CaCO_3$ solubility decrease in NaCl solution is very important for the purification of brine before evaporation.

Absolute values of the equilibrium solubility of $CaCO_3$ in the brine are not so important, because in a saturated solution they are too small to affect the processes for which the purified brine is used.

METHOD

The solubility of $CaCO_3$ was determined by titrating Ca^{2+} with Complexon III, employing the usual techniques. It was previously determined that NaCl in the solution did not affect the accuracy. However, errors of up to 10% are probable because of the low solubility of $CaCO_3$ in NaCl solution.

Another factor making for poor reproducibility is the need for filtering the brine sample. It is certain that passage of brine through the filter accelerates crystallization of $CaCO_3$, especially if there are already considerable amounts of $CaCO_3$ precipitated in it. Then not only the mechanically suspended but also some of the dissolved $CaCO_3$ is removed by filtration.

However, as the aim of this study was only to determine the qualitative behavior of $CaCO_3$ concentration in supersaturated brines the accuracy attained is more than satisfactory.

EXPERIMENTAL

In all tests the brine composition was 300 g/lit NaCl, 10 gr/lit Na_2SO_4, 0—0.8 g/lit Ca^{2+}, and 0—0.2 g/lit Mg^{2+}. It was softened with soda and potassium hydroxide and then the concentration of $CaCO_3$ determined.

The change of $CaCO_3$ concentration with time was determined in the following way. A 5% solution of Na_2CO_3 was added to the brine (300 g/lit NaCl) in such an amount that there was 0.3 g/lit excess after the reaction had ceased. The brine was then left to stand. From time to time samples were taken, filtered and analyzed. The results are shown in Fig. 1. The curves in the figure represent three typical tests made under identical conditions.

The rate of desaturation, as affected by temperature, was also determined. The results are shown in Fig. 2.

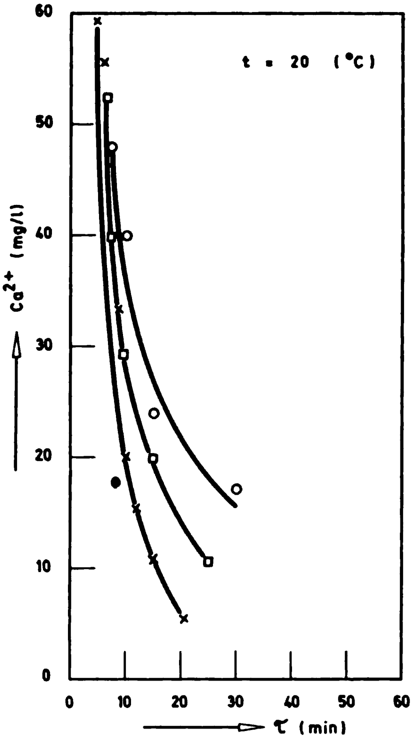

Fig. 1

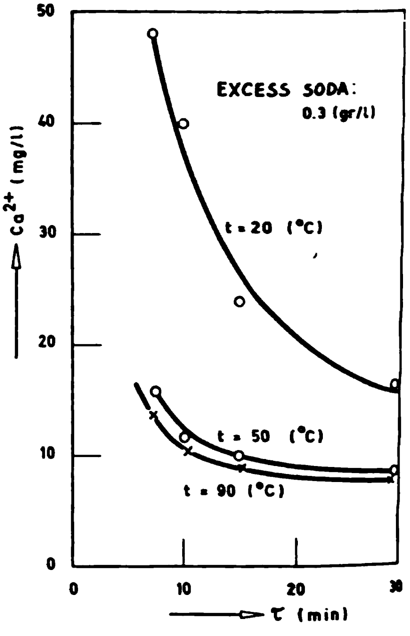

Fig. 2.

Figure 3 shows the dependence of $CaCO_3$ concentration on the excess of soda in the brine.

The rate of desaturation of $CaCO_3$ solution is strongly influenced by impurities in it, especially those that form colloidal solutions or precipitate in the amorphous state.

The effect of the coagulant NALKO-2-1782 on the removal of $CaCO_3$ was studied. $CaCO_3$ was precipitated from a brine containing 0.2 g/lit Ca^{2+}. Precipitation was carried out with 0.3 g/lit excess of soda. Figure 4 shows the change of supersaturation with the addition of the coagulant, curve 1 — one minute after, and curve 2 — one minute before soda was added to the brine.

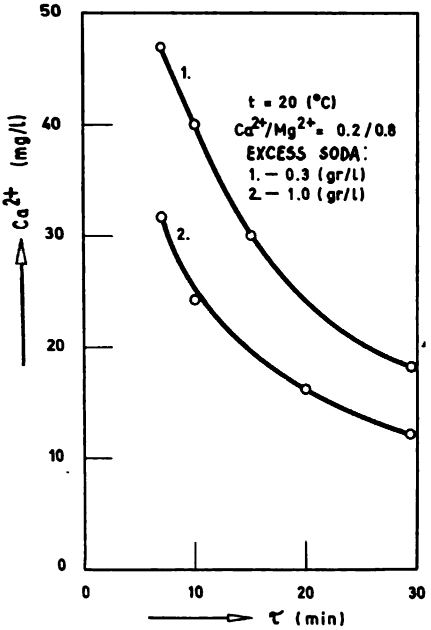

Fig. 3.

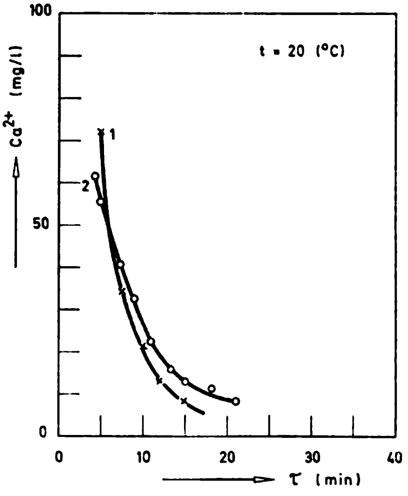

Fig. 4.

The influence of the $Ca^{2+}:Mg^{2+}$ ratio in the brine, when the two ions were precipitated with a mixture of reagents, was also studied. In Fig. 5 this influence is shown for a constant concentration of the two ions (1.0 g/lit) and precipitation with a mixture of reagents (0.3 g/lit excess of soda; pH= =10—12).

It is well known that after precipitation a substance like $Mg(OH)_2$ passes through a series of changes called induction periods(1, 2, 3). It is clear that the influence of $Mg(OH)_2$ on the rate of desaturation of $CaCO_3$ must also vary with the rate of formation of $Mg(OH)_2$ floccules.

These phenomena were studied on a brine containing 0.2 g/lit Ca^{2+} and 0.8 g/lit Mg^{2+}. $Mg(OH)_2$ was first precipitated and the brine left for a while to allow recrystallization of $Mg(OH)_2$. After this, soda was added and $CaCO_3$ precipitated. In this way the fresh $CaCO_3$ precipitate came into the contact with $Mg(OH)_2$ in different degrees of recrystallization. The results are shown in Fig. 6. The concentration of Ca^{2+} (in mg/lit) is plotted on the ordinate, and the time after adding soda to the brine on the abscissa. The curves show the change for a brine to which first NaOH and then Na_2CO_3 were been added. For curve No. 1 the time interval was 0.5 min., for No. 2 — 25 min., for No. 3 — 120 min., and for No. 4 — also 120 min., but the $Mg(OH)_2$ precipitate was eliminated by filtration before adding Na_2CO_3.

The influence of $Mg(OH)_2$ precipitate on previously precipitated $CaCO_3$ was also studied. $CaCO_3$ was precipitated from a brine containing 0.2 g lit Ca^{2+} and 0.8 g/lit Mg^{2+}. After adding soda the brine was left for a while, and then Mg^{2+} precipitated with NaOH. The results are shown in Fig. 7.

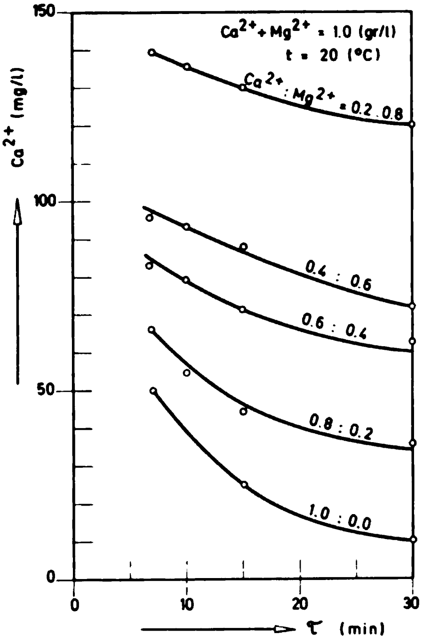

Fig. 5.

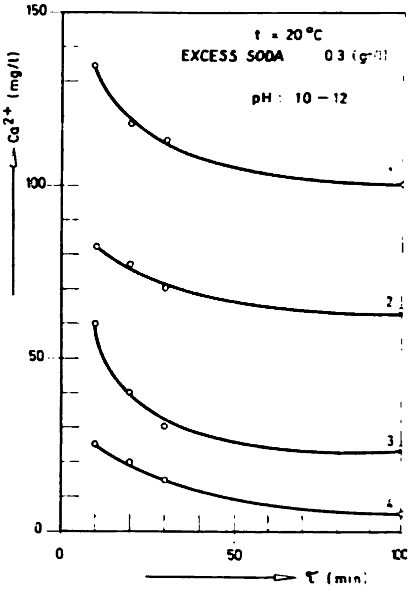

Fig. 6.

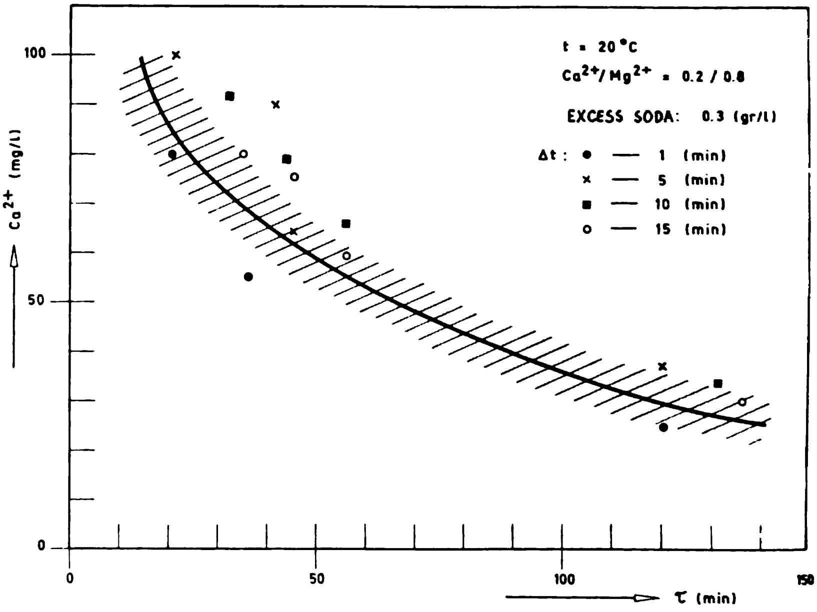

Fig. 7.

DISCUSSION

The results show that the $CaCO_3$ solution is highly supersaturated if it is obtained by precipitating Ca^{2+} with soda. The supersaturation decreases with the time, because dissolved $CaCO_3$ crystallizes. This means that the reagents for purifying the brine must be composed so as to allow enough time for the crystallization of $CaCO_3$.

In a brine containing Ca^{2+} supersaturation disappears in about 30 minutes. The solubility of $CaCO_3$ is decreased by increasing the temperature and the excess of soda in the brine.

According to some data⁽¹⁾, the coagulant NALKO-2-1782 added to the brine can considerably retard the removal of supersaturation, because it gets adsorbed on the seed crystals of $CaCO_3$ and deactivate their surface. However, our results (Fig. 4) show that in quantities of 1—10 mg/lit this coagulant has no effect on supersaturation. The effect of larger quantities was not studied because the use of more than 10 mg/lit is impracticable.

The effect of $Mg(OH)_2$, and to a certain extent of magnesium salts, on the solubility of $CaCO_3$ in a brine is most interesting. In natural brines Mg^{2+} is always present together with Ca^{2+}. The results in Fig. 5 show a remarkable effect of $Mg(OH)_2$ on the solubility of $CaCO_3$. If $Mg(OH)_2$ is precipitated along with $CaCO_3$, it forms a thin film over the crystals of $CaCO_3$⁽¹⁾, thereby causing surface deactivation and preventing their further growth. According to ref. (1), the result of this reaction is that the $CaCO_3$ crystals are 300—400 times smaller than if there was no $Mg(OH)_2$ in the solution.

The effect of $Mg(OH)_2$ was studied under various conditions on a number of brine samples, in order to obtain as much data as possible. The results are shown in Fig. 8. Field I shows how $CaCO_3$ concentration changes if

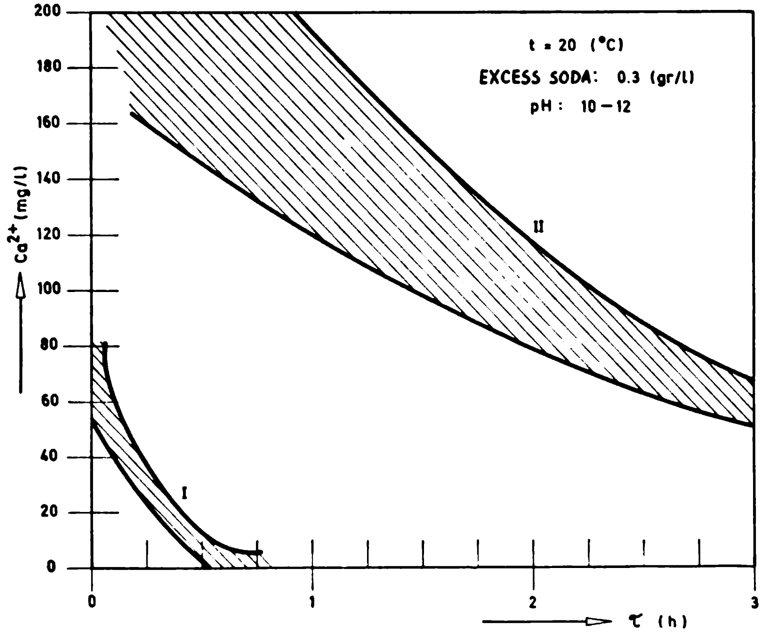

Fig. 8.

Ca^{2+} is precipitated with soda from a pure solution of NaCl. Field 2 shows the same for $CaCO_3$ and $Mg(OH)_2$ precipitated with a mixture of soda and NaOH. The concentration of Ca^{+2} in the brine was 0.5—0.8 g/lit and of Mg^{2+} 0.2—0.5 g/lit. The results obtained by precipitating $CaCO_3$ in the presence of NALKO-2-1782 are also shown in field 1.

The results of the present study may help to solve the problem of the order of adding the reagents to the brine. From Fig. 6 it would appear that the best way to do this is to precipitate $Mg(OH)_2$ first and allow the formation of $Mg(OH)_2$ floccules, which gradually loose their ability to stabilize the $CaCO_3$ solution.

However, Fig. 3 shows that even the fully precipitated $Mg(OH)_2$, if present in the brine during precipitation of $CaCO_3$, still retains some of its stabilizing properties.

On the other hand, if $Mg(OH)_2$ is precipitated first, the advantages of $(CaCO_3+Mg(OH)_2)$ flocculation are lost and clarification takes too long. Hence purification by adding first NaOH and then Na_2CO_3 has little advantage over purification with their mixture. Somewhat better results are obtained if $CaCO_3$ is first precipitated with soda and then NaOH added (Fig. 7), but in this case there is the problem of floccule structure, causing difficulties in the clarification of the brine. Furthermore, $Ca(HCO_3)_2$ is often present in natural brines, for which NaOH has a similar effect as a mixture of NaOH and soda, i. e. it precipitates both $Mg(OH)_2$ and $CaCO_3$. Therefore, a brine is most simply purified by adding a mixture of reagents to it and decreasing the solubility of $CaCO_3$ precipitate by filtering the brine through the layer of precipitate or through powdered marble.

Department of General Chemistry, School of
Technology of Sarajevo University, Tuzla

Laboratory of Tuzla Salt Mines, Tuzla

REFERENCES

1. Furman, A. A. and S.S. Shreĭbman. *Prigotovlenie i ochistka rassola* (Preparation and Purification of Brine) — Moskva: Khimiia, 1966.
2. Chernov, V. F. *Proizvodstvo kal'tsinirovannoi sody* (Production of Calcined Soda) — Moskva: Khimiia, 1956.
3. Boriachek, A. F., E. K. Ovechkin, and S. S. Urazovskii. *K teorii i praktike rassoloochistki* (On the Theory and Practice of Brine Purification) — Kharkov: VSIP, 1949.

BULLETIN OF THE CHEMICAL SOCIETY BELGRADE 30: 1965

CONTENTS

PHYSICAL AND INORGANIC CHEMISTRY

Page

ANALYTICAL CHEMISTRY

ORGANIC CHEMISTRY

BULLETIN OF THE CHEMICAL SOCIETY BELGRADE 30: 1965

AUTHOR INDEX

BULLETIN OF THE CHEMICAL SOCIETY BELGRADE 31: 1966

CONTENTS

PHYSICAL AND INORGANIC CHEMISTRY

ANALYTICAL CHEMISTRY

ORGANIC CHEMISTRY AND BIOCHEMISTRY

BULLETIN OF THE CHEMICAL SOCIETY BELGRADE 31: 1966

AUTHOR INDEX

BULLETIN OF THE CHEMICAL SOCIETY BELGRADE 32: 1967

CONTENTS

PHYSICAL AND INORGANIC CHEMISTRY

ANALYTICAL CHEMISTRY

ORGANIC CHEMISTRY AND BIOCHEMISTRY

BULLETIN OF THE CHEMICAL SOCIETY BELGRADE 32: 1967

AUTHOR INDEX

BULLETIN OF THE CHEMICAL SOCIETY BELGRADE 33: 1968

CONTENTS

PHYSICAL AND INORGANIC CHEMISTRY

ANALYTICAL CHEMISTRY

ORGANIC CHEMISTRY AND BIOCHEMISTRY

BULLETIN OF THE CHEMICAL SOCIETY BELGRADE 33: 1968

AUTHOR INDEX

BULLETIN OF THE CHEMICAL SOCIETY BELGRADE 34: 1969

CONTENTS

PHYSICAL AND INORGANIC CHEMISTRY

ANALYTICAL CHEMISTRY

ORGANIC CHEMISTRY AND BIOCHEMISTRY

BULLETIN OF THE CHEMICAL SOCIETY BELGRADE 34: 1969

AUTHOR INDEX

Izdavač
IZDAVAČKO PREDUZEĆE “NOLIT” — BEOGRAD, TERAZIJE 27

Štampa
“BIROGRAFIKA” — IZDAVAČKO-ŠTAMPARSKO PREDUZEĆE
JUGOSLOVENSKIH ŽELEZNICA, SUBOTICA
TRG LAZARA NEŠIĆA 9